INVESTIGATING THE FOOT-AND-MOUTH DISEASE VIRUS 3A PROTEIN

Emma Louise Howes

A Thesis Submitted for the Degree of PhD
at the
University of St Andrews

2018

Full metadata for this item is available in
St Andrews Research Repository
at:
http://research-repository.st-andrews.ac.uk/

Please use this identifier to cite or link to this item:
http://hdl.handle.net/10023/15521

Investigating the Foot-and-Mouth Disease Virus 3A Protein

Emma Louise Howes

University of
St Andrews

The Pirbright Institute

This thesis is submitted in partial fulfilment for the degree of
PhD at the
University of St Andrews

September 2017

Declarations

1. Candidate's declarations:

I, Emma Louise Howes, hereby certify that this thesis, which is approximately 50, 200 words in length, has been written by me, and that it is the record of work carried out by me, or principally by myself in collaboration with others as acknowledged, and that it has not been submitted in any previous application for a higher degree.

I was admitted as a research student in [month, year] and as a candidate for the degree of Doctor of Philosophy (PhD) in Molecular Virology in September 2013; the higher study for which this is a record was carried out in the University of St Andrews and the Pirbright Institute between 2013 and 2017.

Date 20th September 2017 signature of candidate:

2. Supervisor's declaration:

I hereby certify that the candidate has fulfilled the conditions of the Resolution and Regulations appropriate for the degree of Doctor of Philosophy (PhD) in Molecular Virology in the University of St Andrews and that the candidate is qualified to submit this thesis in application for that degree.

Date 15th September 2017
Signature of supervisor

3. Permission for publication: (*to be signed by both candidate and supervisor*)

In submitting this thesis to the University of St Andrews I understand that I am giving permission for it to be made available for use in accordance with the regulations of the University Library for the time being in force, subject to any copyright vested in the work not being affected thereby. I also understand that the title and the abstract will be published, and that a copy of the work may be made and supplied to any bona fide library or research worker, that my thesis will be electronically accessible for personal or research use unless exempt by award of an embargo as requested below, and that the library has the right to migrate my thesis into new electronic forms as required to ensure continued access to the thesis. I have obtained any third-party copyright permissions that may be required in order to allow such access and migration, or have requested the appropriate embargo below.

The following is an agreed request by candidate and supervisor regarding the publication of this thesis:

PRINTED COPY
a) No embargo on print copy

ELECTRONIC COPY
a) No embargo on electronic copy

Date 20th September 2017 signature of candidate …

Signature of supervisor

Acknowledgements

Firstly I would like to thank my primary supervisor Terry Jackson for your incredible amount of support, encouragement and advice throughout this PhD, and continuing to do so even after you retired. You have helped me to make the most of this opportunity and ensured I stayed on track and helped me become a more independent scientist. I would also like to thank Toby Tuthill for stepping in as a supervisor and being a constant source of advice and knowledge. I'd like to thank my university supervisor Martin Ryan for all of your help, suggestions and for allowing me to become part of your group for a year. Thank you to the collaborators at Dundee and Leeds and Edinburgh for your help with different aspects of this project.

To the members of the Ryan group at St Andrews past and present: John Nicholson, Ashley Pearson, Sean Wilson, Claire Roulston, Katya Minskaia, Garry Luke and Fiona Tulloch thank you for making me feel so welcome, answering my constant questions, helping me out in the lab and for all the fun times away from work, you helped make my year in St Andrews both enjoyable and memorable.

To the residents of both Upper Stanford and Bridgemead past and present thank you for the many fun evenings and weekends over the years it was fantastic living with you all. Special thanks to Madeleine for being an awesome friend and housemate, for putting up with me and for helping keep me sane in my final year!

Grace, Lisa, Sarah, Caroline, Lidia, Joe, Jess, Anusha, Stephen, Amin, Alison, Chris and Jamie you have made working in the Picornavirus Group at Pirbright endlessly entertaining and fun over the years as well as all being a great help to me in the lab. Jenny, Pippa and the other members of the cake club and Bongo Hut thanks for always ensuring that tea breaks were a laugh and good break from the lab work. To the portakabin gang Petra, Lyndsay, Marc and Sophia thank you for making writing up better and easier than it would have been

alone. To Katy, Josie and Marc thanks for the climbing sessions which helped provide me with a distraction from work when I needed it!

Thank you to my fantastic Surrey friends: Lyndsay Cooke for being such a great friend through another degree it has been great to share my PhD experience with you! To Charlotte Batcheldor thank you for all the girly evenings and ensuring I didn't become a complete recluse this last year!

To John Jowitt for being there these last few months and for the constant messages of encouragement and support. Lastly to my family, to the Winson/Klaesson clan: Adrian, Sue, Margaret, Villy, and Granny thanks for the support and ensuring my visits back home were always a laugh and enjoyable, I only wish Grandad was here to see me finally finish this. To my sister Rebecca Howes thanks for the endless encouragement, visits, days out, holidays and always managing to cheer me up when I need it. Finally I would like to thank my parents: Sally and Trevor Howes, I could not have done this without you. From your help with the many house moves, always being on the other end of the phone when I needed you, putting up with the tears moaning and listening to me go on about my project even though you didn't fully understand it, you have always done everything possible to ensure I achieve my best and for that I will be forever grateful.

Abstract

Foot-and-Mouth Disease Virus (FMDV) is a globally important pathogen responsible for causing Foot-and-Mouth Disease (FMD) in wildlife and domestic livestock species and has significant economic impacts. FMD is difficult to control due to its highly infectious nature, wide diversity of host species and the existence of multiple serotypes; therefore, understanding the processes of FMDV infection and viral RNA replication are key to the development of improved diagnostics and vaccines.

This thesis investigates the potential roles of the FMDV 3A non-structural protein using a combination of sub-genomic replicons, recombinant viruses and proteomics techniques. The picornavirus 3A protein has previously been linked with roles in replication complex formation, virulence and determining viral host range. This thesis presents findings showing that a naturally occurring deletion in 3A had differing effects on replication in cells lines derived from different natural hosts thereby supporting the conclusion that 3A has an important role in viral host range.

Proteomic (immunoprecipitation and mass spectroscopy) investigations were carried out to identify potential cellular interaction partners of FMDV 3A, and the impact on infection and replication of reducing expression of two selected cellular proteins Rab7L1 and TBC1D20 was investigated. The 3A protein of FMDV was shown to include a conserved FFAT motif (which bind the ER resident protein VAP) in its N terminal domain. A role for this motif was also investigated with the results suggesting that the 3A FFAT motif is important for efficient viral replication.

Finally, the potential role of 3A to act as the donor of 3B during replication was investigated. Key findings from experiments using FMDV replicons and recombinant viruses showed that full-length P3 and the processing intermediate

3ABBB are not required for viral RNA replication suggesting that the preferred donor of 3B for uridylation is likely a 3BC containing precursor protein.

List of Abbreviations

a.a- amino acid

ACBD3-acyl-coenzyme A [CoA]-binding protein domain 3

AiV-Aichi Virus

Arf1-ADP ribosylation factor 1

BFA-Brefeldin A

BHK-21-Baby hamster kidney cells, clone 21

BRV-Bovine rhinitis virus

BTY-Bovine thyroid cells

CPE-cytopathic effect

cre-cis acting replication element

CV-Coxsackie virus

DMEM- Dulbecco's Modified Essential Medium (DMEM)

DMSO-Dimethylsulphoxide

dH_2O-deionised water

DN-Dominant Negative

DNA-deoxyribonucleic acid

dNTPs- deoxynucleotide triphosphates

DTT-Dithiothreitol

eIF-eukaryotic initiation factor

EMCV- Encephalomyocarditis Virus

ER-endoplasmic reticulum

ERGIC-endoplaspmic reticulcum golgi intermediate compartment

ERAV-Equine rhinitis A virus

EV-enterovirus

FBS-Foetal Bovine Serum

FFAT-two phenylalanines in and acidic tract

FMD-Foot-and-mouth

FMDV-Foot-and-Mouth Disease Virus

FT-Flow through

GAPs- GTPase activator proteins

GEFs- guanine nucleotide exchange factors

GBF1-Golgi-specific Brefeldin A resistance factor 1

GMEM-Glasgow's Minimum Essential Media

GFP-Green Fluorescent protein

HAV-Hepatitis A Virus

HCV-Hepatitis C virus

HEK-Human Embryonic Kidney

HRV-Human Rhinovirus

IP-Immunoprecipitation

IRES-Internal Ribosome entry Site

ITAFs-IRES transacting factors

LB-Luria Broth

Lpro-leader protease

MDBK- Madin Darby Bovine Kidney

MHC-Major Histocompatibility Complex

MOI-multiplicity of infection

MS-Mass spectrometry

OSBP-oxysterol binding protein

O1K-O1Kaufbeuren

O1M-O1 Manisa

PABP-Poly A Binding Protein

PBS-Phosphate Buffered Saline

PCBP2- poly (rC) binding protein 2

PCR-polymerase chain reaction

PFM-Para formaldehyde

Pfu-plaque forming units

PI4P- Phosphatidylinositol 4-phosphate

PI4K- Phosphatidylinositol 4-kinase

P/S-penicillin/streptomycin

Pt.- *Ptilosarcus guernyii*

PTB-cellular factor p57

PV-poliovirus

RC-replication complex

RO-replication organelle

RNA-ribonucleic acid

rNTPs-ribonucleoside triphosphates

rpm-revolutions per minute

RT-reverse transcriptase

SAT-Southern African Territories

SiRNA-small interfering RNA

SDS-Sodium dodecyl sulphate

ss-single stranded

TaV-Thosea Asigna Virus

TBC- Tre-2 Bub2 and Cdc16

TBC1D20-TBC 1 Domain family member 20

TBE-Tris/Borate/EDTA

TCL-Total Cell Lysate

TGN- Trans Golgi Network

TPB-Tryptose Phosphate Broth

TnT- Transcription and Translation coupled reactions

UTR-untranslated region

VAMP-vesicle Associated Membrane Proteins

VAP-VAMP associated proteins

VGM-viral growth media

vRNA-viral RNA

Y2H-yeast-2 -hybrid

Contents

List of Figures

Chapter 1: Introduction

1.1 Foot-and-Mouth Disease

Foot-and-mouth Disease (FMD) is an important notifiable disease that affects both domestic livestock (cattle, pig, sheep and goats) and a large number of wildlife species (including deer and buffalo). FMD is a global problem and outbreaks have occurred in almost every part of the world where livestock are kept and the disease is currently endemic in areas of Africa and Asia (Jamal and Belsham, 2013).

Infected animals often show symptoms of fever and lameness as well as developing lesions on the tongue, snout, and feet, although symptoms in sheep can be very mild and hard to detect. Symptoms are often similar to that of other vesicular diseases including vesicular stomatitis virus and swine vesicular disease (Grubman and Baxt, 2004). Although FMD normally has a low mortality rate, in young animals the infection can spread to the heart and cause myocarditis. FMD also causes reduced milk production and weight loss leading to reduced productivity, particularly as disease can spread rapidly leading to a 100% morbidity rate. In addition some animals may become carriers of FMD, where they are asymptomatic but are persistently infected and continue to shed virus after 28 days (Kitching and Hughes, 2003) although it is still debatable whether or not these animals contribute to the spread of disease.

The aetiological agent of FMD is Foot-and-mouth disease virus (FMDV) which is considered one of the most important pathogens in global agriculture, due to the huge economic burden and impacts on food security that outbreaks of FMD lead to. Outbreaks of FMD cause reduced productivity and loss of stocks as well as trade restrictions on animals and animal products from affected countries leading to economic losses of billions of pounds (Knight-Jones and Rushton, 2013).

Due to the diversity of strains and broad host range of FMDV, outbreaks of FMD tend to spread quickly and are difficult to contain. Transmission routes include

direct contact between infected and naïve animals, mechanical transmission via contaminated vehicles, bedding, and clothing of handlers and by aerosols(Sutmoller et al., 2003, Alexandersen and Donaldson, 2002). Current methods of control vary depending on if a cuntry is classed as disease free or not. Areas of South America use vaccination to prevent disease and are beginning to successfully achieve a "free with vaccination" status (Sutmoller et al., 2003). In Europe vaccination was used until 1992 where following disease free status it was decided vaccination would no longer be used in order to allow trade to be maintained throughout the continent providing a free without vaccination status. The main impact of FMD in Europe is now caused by sporadic outbreaks that occur, the largest most recent one being in 2001 which spread throughout the UK, France and the Netherlands and was caused by a Pan Asia type O virus (Knowles et al., 2005). Control methods implemented during this outbreak included culling of infected animals, restriction of animal movement and trade, and emergency vaccination in the Netherlands (Sutmoller et al., 2003). However despite the implementation of control methods the estimated losses due to loss of stock, tourism and trade was estimated at billions of pounds (Knight-Jones and Rushton, 2013).

Current FMDV vaccines use an inactivated form of the virus grown in BHK-21 cells. However these vaccines do have limitations, firstly as they are made from whole virus antigen and they can contain contaminating amounts of non-structural proteins, inoculated animals develop antibodies to these non-structural proteins making it hard to differentiate between animals that have been infected and those that have been vaccinated (Lee et al., 2006). Secondly production of these vaccines requires large amounts of virus to be grown up which requires high containment bio-secure facilities, and once inoculated animals don't develop a rapid response meaning they are still susceptible to infection for a short period of time following inoculation which is not ideal in an outbreak situation (Doel, 2003). Also due to the large number of circulating strains and a lack of immunological cross protection between the different serotypes control of FMD outbreaks is incredibly difficult (Rodriguez and Gay, 2011). Improved control measures including better vaccines would have large

benefits worldwide; however developing of new methods requires improved understanding of the mechanisms involved during viral infection and replication.

1.2 The *Picornaviridae*

The *Picornaviridae* are a group of small non-enveloped viruses with positive sense single stranded RNA genomes classifying them as type IV viruses according to the Baltimore classification system of viruses. The majority of known picornaviruses have been identified in mammals and birds although recently others have been identified in reptiles and fish (Fichtner et al., 2013, Reuter et al., 2015). There are currently 35 genera of *Picornaviridae* each including at least one or more species (Zell et al., 2017). The most studied genus of *Picornaviridae* is the Enterovirus genus which includes poliovirus (PV) and Coxsackie virus (CV). Since PV is so well studied it is frequently used as a model for how other picornaviruses replicate, meaning it is often compared with FMDV despite the fact there are a number of significant differences between them.

1.2.1 Important members of and major diseases caused by the *Picornaviridae*

PV is the causative agent of poliomyelitis which affects humans and in some cases affects the central nervous system leading to flaccid paralysis. Prior to vaccinations being developed poliomyelitis epidemics used to occur frequently (Racaniello, 2006). Since the introduction of both inactivated and live attenuated PV vaccines and the World Health Organisation initiative to eradicate wild PV, the number of cases has dropped dramatically and cases of wildtype poliomyelitis are currently found in just 3 countries worldwide (Patel and Cochi, 2017).

Another well studied picornavirus is human rhinovirus (HRV), like PV it belongs to the Enterovirus genus. HRV is reported to cause over half of upper respiratory tract infections worldwide, and although normally only causes common colds in healthy individuals, in the elderly and immunocompromised it is linked with more severe disease including pneumonia and increasing severity of asthma (Royston and Tapparel, 2016).

Other examples of important members of the *Picornaviridae* include enterovirus-71 (EV-71), which causes hand-foot-and-mouth disease and enterovirus-68 (EV-68) both of which have recently become more common and widespread. In addition to respiratory illness they can cause neurological problems particularly in children and are a leading cause of viral meningitis (Chang et al., 2016, Messacar et al., 2016). There are currently no vaccines available against these diseases.

1.3 Foot-and-Mouth Disease Virus

FMDV is a member of the *Picornavirdae* family within the order *Picornavirales* and is the type species of the *Aphthovirus* genus The *Aphthovirus* genus currently consists of 4 classified species: *Foot-and-mouth Disease virus* (FMDV), *Equine rhinitis A virus* (ERAV), *Bovine rhinitis A virus (*BRVA*)* and *Bovine rhinitis B virus* (BRVB).

FMDV exists as 7 different serotypes: O, A, C, Asia-1 and Southern African Territories (SAT 1, 2, and 3) and each contains multiple and constantly evolving strains (Domingo et al., 2003). The type O FMDV serotype is the most common and widespread followed by type A, whereas the Asia-1 serotype tends to only found in south East Asia and the SAT viruses are normally restricted to sub-Saharan Africa (Knowles and Samuel, 2003).

The virion consists of a single-stranded (ss) positive-sense RNA genome approximately 8.5 Kb in length packaged inside an icosahedral capsid consisting of 60 identical copies of each of the structural proteins. Unlike the enteroviruses, such as PV, the capsid of FMDV does not have canyon like

depressions upon its surface, a feature believed to be involved in receptor binding of some picornaviruses including the enteroviruses (Hogle et al., 1985, Belnap et al., 2000). Instead FMDV has a pronounced loop on the surface on its capsid, which makes up part of the VP1 protein. This feature known as the G-H loop is more pronounced in FMDV than other picornaviruses and is involved in virus attachment to cells through a conserved RGD motif (see section 1.5.1) (Logan et al., 1993, Burman et al., 2006).

1.4 The FMDV genome and the viral proteins

The FMDV genome is approximately 8.5 KB in length and encodes a single open reading frame. Unlike PV and some other picornavirus genera it encodes for a leader protease and uniquely among the *Picornaviridae* encodes in tandem 3 non-identical copies of the 3B protein. The roles of each component of the genome from 5' to 3' are discussed in the sections below. Figure 1.4 shows the layout of the FMDV genome.
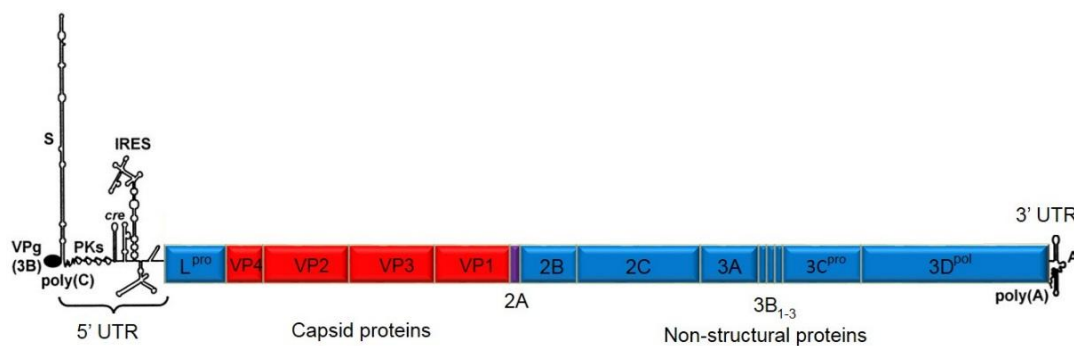
Figure 1.4: Organisation of the FMDV Genome. FMDV has a single stranded positive sense RNA genome encoded as a single open reading frame that is translated to produce a single polyprotein that undergoes further processing to give a variety of intermediate and 14 mature viral proteins. The genome has small protein (VPg) linked to the 5' end and is followed by the 5' Untranslated region (UTR) which contains several different structures and features, the S fragment (S), Pseudoknots (PKs), the cis acting replication element *(cre)*, the IRES, and a long stretch of cytosine residues (polyC). The FMDV genome then encodes the Leader protein, a protein which is not present in all picornavirus

species, followed by the 4 capsid proteins (VP4, VP2, VP3 and VP1 shown in red). The genome then encodes the short 2A peptide (purple) which separates the structural proteins and the remaining non-structural proteins encoded downstream of 2A shown in blue. Finally there is a short 3'UTR followed by the poly A tail (poly A).

1.4.1 VPg

Unlike cellular mRNAs picornavirus genomes are not capped at the 5' end by a 7-methyl guanine cap, instead they have a covalently bound small genome linked protein known as VPg which is encoded by the 3B gene (Grubman, 1980). During replication VPg acts as the primer of the viral polymerase (3D) allowing synthesis of both positive and negative sense RNA strands (Paul and Wimmer, 2015).

1.4.2 The 5' UTR

Following the VPg is the 5 untranslated region (5' UTR) of the genome. This contains a number of different RNA structures and features including the S fragment, poly C tract, pseudoknots, a cis acting replication element (*cre*) in the case of FMDV and the internal ribosome entry site (IRES).

The S fragment is a large stem loop at the 5' end of the genome, which in FMDV is larger than in that of other picornaviruses. PV also has a highly structured region at the end of the 5'UTR known as a cloverleaf, and this has been shown be required for negative strand RNA synthesis and genome stability (Barton et al., 2001) which suggests that the S fragment may play a similar role in FMDV replication. The precise role of the poly C tract is unknown, but it has been shown that virus engineered with varying poly C tract lengths (down to those with just 2 cytosine residues) can be recovered, but those with longer length poly C tracts appear to have an advantage in cell culture (Rieder et al., 1993). Downstream of the poly C tract in FMDV are three or four smaller pseudoknot structures, these structures are also found in EMCV but upstream of the poly C tract but the function of these is also unknown (Duke et al., 1992).

In FMDV the next structure found in the 5 UTR is the cis acting replication element *(cre),* a small stem loop with a conserved loop sequence of AAACA. Alteration of this sequence has been shown to attenuate replication but doesn't appear to affect translation (Mason et al., 2002). FMDV is unusual as all other picornavirus *cre* so far identified are located within the coding regions of the genome. For example, the *cre* of PV is located in the coding region for the 2C protein (Goodfellow et al., 2000, Paul et al., 2000) and in HRV 14 the *cre* is in the VP1 coding region (McKnight and Lemon, 1998). The *cre* acts as a template for uridylation of VPg to produce VPgpUpU by the viral polymerase 3D. VPgpUpU then in turn acts as a primer for the polymerase in viral replication (Nayak et al., 2006, Paul et al., 2000).

The final element of the 5' UTR is the IRES which directs translation of the genome by a cap independent mechanism. Different picornaviruses use different types of IRES, with the IRES of PV belonging to group 1 and that of FMDV belonging to group 2. The FMDV IRES is approximately 450 nucleotides in length (Belsham and Brangwyn, 1990). These highly conserved structures are responsible for recruitment of the 40S ribosomal subunit as opposed to relying on scanning of the genome from the 5' end.

1.4.3 Leader protein

The first protein encoded within the FMDV genome coding region is the leader protein which in FMDV is a papain like cysteine protease and is involved in shutting off host cell translation. The L protein is only found in some picornavirus species (including members of the aphthoviruses, kobuviruses and cardioviruses) and plays varying roles in the different genera including aiding RNA replication and encapsidation in kobuviruses, and acting as a viral protease in members of the aphthovirus and erbovirus genera (Belsham, 2013, Romanova et al., 2009, Sasaki et al., 2003). The FMDV L protein has two initiation codons separated by 84 nucleotides; consequently, the protein can be produced in two forms Lab and Lb. Deletion of the Lab region appears to be lethal but viruses which have Lb removed can still replicate (Belsham, 2013).

The FMDV L protein has been shown to cleave the cellular translation initiation factor eIF4G to inhibit host cell translation and is responsible for cleaving itself from the end of the P1 region of the genome (Belsham, 2013, Devaney et al., 1988).

1.4.4 The Capsid proteins

Following L is the P1 region of the genome that encodes the structural (or capsid) proteins VP4, VP2, VP3 and VP1. Initially, the capsid proteins are formed as P1-2A, and VP4 and VP2 are made as a single protein known as VP0. Single copies of VP0, VP3 and VP1 assemble to form promoters, and 5 protomers then combine to form a pentamer. Subsequently, 12 pentamers associate, to form a provirion into which RNA is packaged. Finally the maturation cleavage of VP0 to VP2 and VP4 occurs producing a complete virion.

In addition to protecting the viral RNA (vRNA), the structural proteins play a variety of roles, for example, VP1 has a large extended G-H loop that includes an RGD motif which has been shown to mediate integrin binding (Burman et al., 2006, Logan et al., 1993). Clusters of histidine residues at the interface between VP2 and VP3 in the assembled capsid have been suggested to be the possible reason for FMDV dissociation at acidic pH (Curry et al., 1995). Finally the VP4 protein is a small myristolated protein located on the inner face of the capsid and for HRV has been linked with formation of a multimeric pore predicted to allow release of the RNA genome into the cytoplasm (Panjwani et al., 2014) it is possible a similar role may be played by that of FMDV VP4.

1.4.5 The 2A protein

Separating the structural and non-structural regions of the genome is the 2A protein. In FMDV, 2A is shorter than in other picornaviruses and is only 18 a.a in length. For FMDV, it is thought that 2A, rather than cleaving itself at the C terminus or being cleaved by another viral protease, promotes hydrolysis of the linkage between P1-2A and 2B effectively simultaneously separating P1-2A

from the rest of the polyprotein and allowing the ribosome to continue to process the downstream proteins during translation (Donnelly et al., 2001b). The FMDV 2A peptide and first a.a residue of 2B have been shown to be able to mediate cleavage in multiple artificial systems (Ryan and Drew, 1994, Minskaia et al., 2013).

1.4.6 The 2B protein

The next part of the genome encodes the 2B protein. The 2B proteins of picornaviruses are predicted viroporins. The structure and characteristics of FMDV 2B agrees with this hypothesis as it exhibits intracellular localisation at the ER and has two predicted trans-membrane domains both of which are characteristics of class IIB viroporins (Ao et al., 2015). Viroporins alter membrane permeability and monomers of these can also assemble within cell membranes, leading to the formation of pores which promotes virus budding from the cell. In PV, 2B has also been shown to disrupt calcium balance within the cell inducing apoptosis (Aldabe et al., 1997).

1.4.7 The 2C protein

The next part of the genome encodes the 2C protein. The 2C proteins of picornaviridae appear to have ATPase and GTPase activity (Sweeney et al., 2010, Klein et al., 1999). PV 2C has been shown to be involved in the initiation of negative strands synthesis (Barton and Flanegan, 1997). All the 2C proteins of the picornaviruses also contain helicase domains (Klein et al., 1999, Pfister et al., 2000) with the EV-71 2C protein having been shown to have helicase activity (Xia et al., 2015). Additionally an interaction between the structural protein VP3 and the nonstructural 2C protein of PV has been linked with a possible role in aiding genome encapsidation (Wang 2014). The exact role of FMDV 2C is as yet undetermined although the intermediate 2BC protein has been linked with inhibition of protein secretion (Moffat et al., 2005, Moffat et al., 2007), a role which is carried out by 3A in PV (Doedens et al., 1997).

1.4.8 The 3A protein

Following 2C, the genome encodes the proteins that make up the P3 region of the genome, which are responsible for playing key roles in viral replication. The first of these is 3A. The 3A protein of picornaviruses has been linked with virulence, replication and host range and is discussed in more detail in sections 1.6 and 1.7.

1.4.9 The 3B proteins

3B encodes the VPg protein which acts as the primer for the viral polymerase (3D) and is found linked to the 5' end of the genome. FMDV is unusual in that it encodes 3 non-identical copies, all of which are found linked to viral RNA (King et al., 1980) and can be uridylated by the 3D polymerase *in vitro* (Nayak et al., 2005).The majority of Picornaviruses encode a single 3B protein although some members of the Picornavirdae have been shown to encode multiple copies of the 3B protein within their genomes (including aquamavirus A and mosavirus A) (Boros et al., 2013, Reuter et al., 2014). FMDV 3B3 has been found to be the most efficient substrate for this reaction followed by 3B2 and 3B1 respectively (Nayak et al., 2005). Despite encoding multiple copies FMDV is still able to replicate without 3B1 and 3B2 although a reduction in replication is observed (Falk et al., 1992, Pacheco et al., 2010, Pacheco et al., 2003). Until recently no naturally isolated strains of FMDV encoding less than 3 copies of 3B have been identified, however a type O virus has recently been identified from an outbreak in South Korea that contains a 23 a.a nucleotide deletion that removes the last 5 a.a of 3A and first 18 residues of 3B1, which effectively removes the first copy of 3B (3B1). This virus appeared to have a low pathogenicity in pigs under experimental conditions which could imply that 3B copy number may be an important determinant of virulence in pigs (Park et al., 2016). However this study used limited animals and only investigated effects in

pigs and did not test effects of infection in other FMDV natural hosts such as cattle.

1.4.10 The 3C viral protease

The genome then encodes 3C. The picornavirus 3C protein has been shown to be a viral protease and is responsible for most of the cleavages of the viral polyprotein. Aside from processing of the L protease from P1-2A, and the final maturation cleavage of VP0 to VP2 and VP4, FMDV 3Cpro is thought to carry out all other processing events. However, for some picornaviruses 3CD containing precursors have also been shown to be responsible for processing the capsid proteins (Spear et al., 2015).

Like Lpro the 3C protease (3Cpro) is also involved in shutting off host cell translation. It is able to cleave eIF4G late in the replication cycle, but is also able to cleave eIF4A which is part of the cap binding complex (Belsham et al., 2000). FMDV 3C has also been shown to cause fragmentation of the Golgi apparatus (Zhou et al., 2013) during replication.

1.4.11 The 3D polymerase

The 3D protein is the last protein encoded by the genome. The 3D protein of picornaviruses (3Dpol) is the viral encoded polymerase (an RNA-dependent RNA polymerase) responsible for replication of the viral genome. Like other viral RNA-dependent RNA polymerases, that of FMDV has a right hand shaped structure consisting of thumb, fingers and palm domains The active site of the polymerase contains a conserved YGDD motif (Hansen et al., 1997, Ferrer-Orta et al., 2004). FMDV 3Dpol is likely to interact with a number of viral and cellular proteins during the synthesis of new genome copies, and studies using PV have suggested interactions with PABP (Barton et al., 2001) as well as with 3AB (Hope et al., 1997) and, it is therefore possible similar interactions may occur with FMDV 3Dpol.

1.4.12 The 3' UTR

Following the 3D polymerase is the 3' UTR, which is shorter than the 5' UTR and contains fewer structures with just two predicted stem loops (SL1 and SL2) that are followed by a poly A tail. These structures are predicted to interact with stem loops and RNA structures in the 5' UTR, namely the IRES and S-fragment (Serrano et al., 2006) and are required for replication as deletion of the entire 3' UTR inhibits replication (Sáiz et al., 2001). There is also some evidence to suggest the 3'UTR of PV may interact with the 3AB protein of PV (Harris et al., 1994).

1.5 The Viral life cycle

The infection cycle of FMDV is shown in the top panel of Figure 1.5 (adapted from Whitton et al, 2013). Key steps are summarised in the table in the lower panel and described in more detail in the following sections.
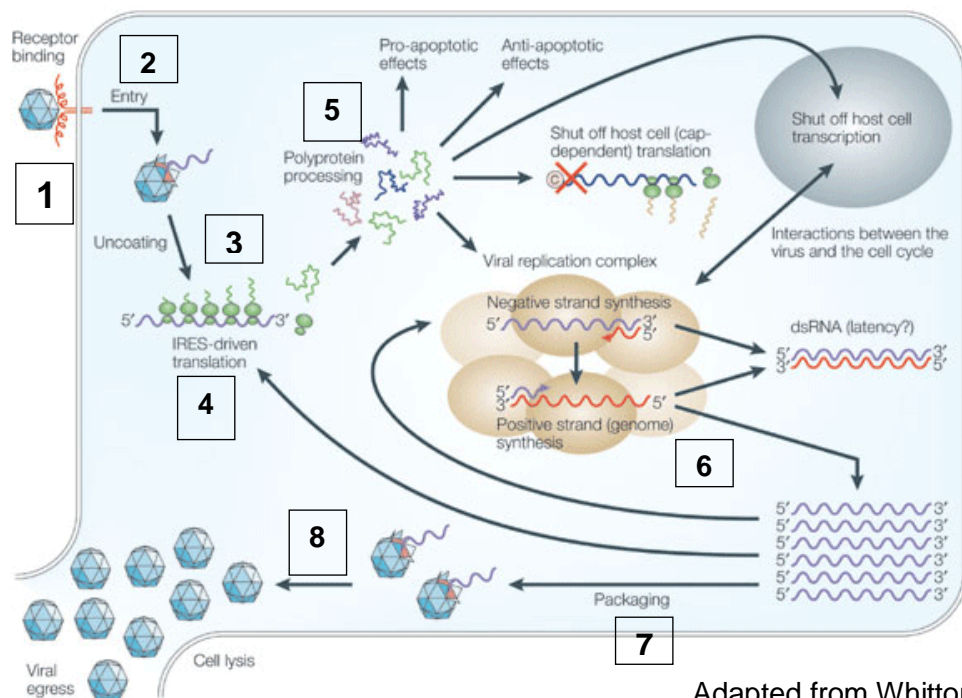
Adapted from Whitton et al ,2013

| **1.Attatchment** |
| Virus binds receptor: This is either integrins or/ and heparan sulfate glycan |

| **2. Entry** |
| Virus enters cell using clathrin dependent endocytosis |

| **3. Uncoating** |
| (i) Virion particle dissociates in early endosome due to acidic pH of early endosome |
| (ii) Viral genome released into cytoplasm |

| **4. Translation** |
| Viral genome is translated by cap independent mechanism to produce a single polyprotein |

| **5.Polyprotein Processing** |
| Polyprotein is processed by viral proteases (Lpro and 3Cpro) to produce intermediates and mature viral proteins |

| **6. Replication** |
| (i) Positive sense genome used to make negative sense RNA template |
| (ii) Synthesis of new positive sense RNA genome copies for translation or new virion synthesis |

| **7. Genome Packaging and Assembly** |
| Viral genome is packaged into assembled (exact mechanism is unknown) |

| **8. Maturation Cleavage** |
| Following viral genome packaging and assembly of the capsid VP0 is cleaved to produce VP2 and VP4 |

Figure 1.5. The FMDV viral infection cycle: The main stages of the infection cycle of FMDV are shown and numbered in the diagram (top, adaped from Whitton *et al*, 2013), with explanations of key events including translation genome replication and assembly are described in the table (bottom).

1.5.1 Attachment and Entry

Picornaviruses have been shown to utilise various cellular receptors for attachment to the cell surface. For PV the main receptor has been identified as CD155 (Mendelsohn et al., 1989) whereas major type rhinoviruses use ICAM-1 (Greve et al., 1989). Both these viruses have canyons on their surface which act as the interaction point between virus and receptor (He et al., 2000). FMDV has been found to use two main groups of receptors, integrins and heparan sulfate. Integrins are a group of cell surface receptors made up of different alpha and beta subunits forming heterodimeric glycoproteins. Heparan sulfate is a glycosaminoglycan and highly sulphated and hence negatively charged (Meneghetti et al., 2015).

Field isolates of FMDV use RGD binding integrins including αvβ3, αvβ6, αvβ8 and αvβ1 integrins as receptors (Baranowski et al., 2000, Jackson et al., 2000, Jackson et al., 2002, Berryman et al., 2005, Neff et al., 1998). The presence of an RGD motif located on the GH loop of VP1 allows the virus to interact with the integrin receptor (Burman et al., 2006). Tissue culture adapted strains of FMDV have been shown to have an increased affinity for heparan sulfate, which is thought to be due to accumulations of mutations that lead to an increase in positive charge on the outer capsid surface (Chamberlain et al., 2015, Jackson et al., 1996).

Entry of FMDV into the cell has been shown to occur through clathrin mediated endocytosis for isolates that bind to the αvβ6 integrin, this pathway has also been shown to be utilised by a second *Aphthovirus*, equine rhinitis A virus (ERAV) (Berryman et al., 2005, Groppelli et al., 2010). In comparison heparan sulfate binding virus isolates were found to use caveolae mediated endocytosis suggesting the receptor used can influence the entry pathway (O'Donnell et al.,

2008). Following uptake by either mechanism the virus is trafficked to early endosome where a change to acidic pH is believed to trigger particle dissociation and genome uncoating and membrane penetration (see below).

1.5.2 Uncoating of the viral particle

Two mechanisms of uncoating appear to be utilised by picornaviruses. Following binding to its receptor PV has been shown to undergo a conformational change to produce an A type or infectious particle, which leads to exposure of VP4 and the N terminal of VP1 (Belnap et al., 2000). FMDV which differs from the enteroviruses in both its receptors and lack of canyon on the cell surface is predicted to have a simpler mechanism of uncoating in that it doesn't appear to produce intermediate particles. Instead the uncoating mechanism of FMDV seems to be pH triggered with particle dissociation occurring in intracellular acidic endosomes following a pH change (Caridi et al., 2015, O'Donnell et al., 2005).

Following uncoating the capsid protein VP4 is released and interacts with the cell membrane forming a multimeric pore, which likely allows the vRNA to be released into the cytoplasm (Panjwani et al., 2014). Once the vRNA has been released translation and replication is able to take place within the cytoplasm.

1.5.3 Translation of the Genome

Picornaviruses rely on a cap-independent mechanism to translate their genomes where the ribosomal subunit binds directly to the IRES located in the 5' UTR of the genome. As is the case for cap-dependent translation, a number of cellular proteins are required to form a complex at the IRES, including a group known as IRES transacting factors (ITAFs). The binding of cellular protein PCBP2 to a stem loop within the IRES has been shown to be essential in translation of PV (Sean et al., 2008). The cellular factor p57 (also known as PTB) has been shown to interact with the IRES of several picornaviruses including FMDV, Encephalomyocarditis virus (EMCV) and PV, having varying

effects (Kafasla et al., 2011, Wang et al., 2013). PTB is believed to be a splicing factor (Belsham and Sonenberg, 1996). The protein G3BP1 has recently been found to bind RNA sequences within the IRES of FMDV, this event has been suggetsed to have a regulatory effect on translation of the genome (Galan et al., 2017).

In addition to utilising the cellular machinery to translate its genome viral proteins have also been shown to be involved in shutting down cap dependent translation. The initiation factor eIF4G, which usually forms part of the cap binding complex and helps initiate translation, is cleaved by the L protein of FMDV and the 2A protease of PV leading to inhibition of host cell cap-dependent translation. This is thought to aid the translation of the viral genome by reducing competition with host cell translation (Etchison et al., 1982, Gradi et al., 1998, Devaney et al., 1988). The genome is translated as a single polyprotein which then undergoes a cascade of proteolytic processing to produce a number of intermediate processing products prior to further cleavage producing the mature viral proteins.

The FMDV polyprotein is cleaved by the viral proteases the L protein and 3Cpro and the 2A peptide to produce initial precursor proteins of L, P1-2A, 2BC and 3ABCD. These precursors undergo subsequent series of cleavages by the 3C protease to produce a number of processing intermediates (e.g. VP0 and 3CD) in addition to the 14 mature viral proteins (Mason et al., 2003).

Following translation and production of viral proteins the viral RNA is then replicated. The exact mechanism that cause the switch between translation and replication remains poorly understood. One theory suggested for PV is that 3CD cleaves PCBP2 thereby disrupting its ability to interact with SRp20 and recruit ribosomes to the IRES and allowing the synthesis of a negative strand template by the 3D polymerase (Chase et al., 2014, Perera et al., 2007).

1.5.4 Genome Replication

To allow RNA synthesis the vRNA is thought to circularise. For PV this is thought to occur due to an interaction of the cloverleaf and the PCBP2 complex at the 5'UTR with PABP that is bound to the poly A tail (Herold and Andino, 2000). The following step in viral RNA replication is the uridylation of 3B, thought to occur at the *cre* (located in the 5'UTR of FMDV and 2C in PV (Mason et al., 2002, Goodfellow et al., 2000). Uridylated 3B is then transferred to the 3' end of the genome (likely as part of a complex by 3D or 3CD) to act as primer for the 3D polymerase allowing synthesis of negative-sense strands. This leads to production of an intermediate double stranded RNA product known as the replicative form, which is then unwound and acts as a template for further positive strand synthesis (Paul and Wimmer, 2015, Daijogo and Semler, 2011).

Replication of many positive strand RNA viruses, including hepatitis C virus (HCV), Zika and Dengue as well as the picornaviruses is associated with cellular membranes. This association with membranes is thought to provide a structural scaffold for the formation of the replication complex (RC) thereby allowing RNA replication. These enclosed membrane structures have been defined as replication organelles (Hsu et al., 2010) and are often enriched with PI4P and cholesterol. Formation of these organelles requires the virus to trigger rearrangement of cellular membranes through diverting different cellular pathways and viral proteins including 3A are thought to play a key role in this process (this process is described in further detail in sections 1.6.2 and 1.6.3).

1.5.5 Genome Packaging and virion assembly

The exact mechanism of packaging for FMDV is not fully understood. It is believed that specific sequences may exist within the genome that act as signal to aid genome packaging. Studies with Aichi virus (AiV) have found possible roles for the leader protein in RNA encapsidation (Sasaki et al., 2003) and the current theory is that viral genomes contain specific packaging signals that trigger packaging of the genome prior to the maturation cleavage of VP0. It is

however known that processing of the polyprotein produces capsid proteins VP1, VP3 and VP0, single copies of which form a protomer. Five of these protomer units then combine to form pentameric subunits, 12 of which form the fully assembled icosahedral capsid structure. Following genome packaging a final maturation cleavage of VP0 occurs resulting in VP2 and VP4 mature proteins.

1.6 The Picornavirus 3A protein

The 3A protein is the first protein encoded by the P3 region of the picornavirus genome and has been shown to play a number of roles during viral replication, with the majority of studies using PV 3A as a model protein. The 3A protein is a membrane-associated protein and therefore thought to play a key role in virus replication and formation of the viral replication complex and organelles (see section 1.6.2) as well as being linked with virulence and host range. For example, studies have found that changes to the 3A proteins of Hepatitis A virus (HAV) may be involved in adaptation to cell culture (Graff et al., 1994) and for PV a single amino acid (a.a) change of isoleucine to threonine at a.a 46 of 3A impaired the viruses ability to cause CPE in Vero cells (the virus retained its ability to cause CPE in HeLa cells) (Lama et al., 1998). Additionally Harris *et al.* identified residues in 3A which when combined with mutations in 2B led to improved replication of HRV in murine cells (Harris and Racaniello, 2005). Furthermore mutations in the 3A protein of Coxsackie virus B3 (CVB3) have been linked with reduced myocardiogenicity when tested *in vivo* in mice (Massilamany et al., 2015). FMDV 3A also appears to play similar roles in viral host range and virulence as discussed in section 1.7.2.

1.6.1 Picornavirus 3A and the early secretory pathway

PV 3A has been shown to inhibit protein secretion from cells (Doedens et al., 1997), however for FMDV this process is carried out by the processing

intermediate protein 2BC or co-expression of 2B and 2C (Moffat et al., 2005, Moffat et al., 2007). This suggests there are likely potential differences between FMDV and the enteroviruses in their interactions with the early secretory pathway. Furthermore, expression of PV 3A has also been found to lead to a reduction in the expression of the major histocompatibility complex 1 and inhibit the secretion of some pro-inflammatory cytokines including IL-6 and IL-8(Dodd et al., 2001). This ability is considered beneficial for the virus, providing a mechanism by which to avoid the innate immune response.

1.6.2 Host cell membranes remodeling; the role of 3A in forming the replication complex and replication organelles

During infection the *Picornaviridae* (like many RNA viruses) cause reorganisation of intracellular membranes generating structures termed replication organelles (RO). These membrane structures are specialized sites dedicated to vRNA replication and are thought to provide membranes with unique protein and lipid compositions and provide a structural scaffold for the formation of replication complexes (Miller and Krijnse-Locker, 2008) through providing an environment where the viral proteins e.g. 3Dpol (Hsu et al., 2010) and cellular factors e.g. OSBP required for replication concentrate (Arita et al., 2013, Roulin et al., 2014, Strating et al., 2015).

The exact role of viral non-structural proteins in RO formation is unclear but studies have found that expression of some viral non-structural proteins is enough to lead to rearrangement of the intracellular membranes and trigger formation of ROs (Teterina et al., 1997). The PV 3A, 2C, and 2BC can each induce ER modifications but co-expression of 3A and 2BC together is required to induce membrane structures that are similar to those observed in naturally infected cells (Suhy et al., 2000).

Recent evidence has established that enteroviruses, cardioviruses and kobuviruses (e.g. PV, CV, EMCV and AiV) utilise components of both vesicular (e.g. GBF1) and non-vesicular (e.g. PI4K, OSBP, PI4P and cholesterol) lipid

trafficking to generate RO. Interestingly, formation of RO by viruses form different genera appear to require different cellular proteins and PI4KIIIβ (phosphatidylinositol 4-kinase IIIβ), PI4KIIIα, Arf1 (ADP-ribosylation factor 1), GBF1 (Golgi brefeldin A resistant guanine nucleotide exchange factor 1), Sar1 (secretion-associated and Ras-related 1), ACBD3 (acyl-coenzyme A [CoA]-binding protein domain 3) and OSBP (oxysterol-binding protein) have all been implicated in facilitating virus replication (Arita et al., 2013, Belov et al., 2008, Greninger et al., 2012, Hsu et al., 2010, Lanke et al., 2009, Midgley et al., 2013, Roulin et al., 2014, Wessels et al., 2006).

The 3A protein has a central role in formation of ROs and studies of RO formation support a model where the picornavirus 3A protein subverts lipid homeostasis, including phospholipid biosynthesis and cholesterol trafficking to generate membranes required for developing an RO. During RO formation it is thought that enterovirus 3A binding to GBF1 leads to the recruitment of phosphatidylinositol 4-kinase III β (PI4KIIIβ) which in turn generates PI4P (phosphatidylinositol 4-phosphate) which then accumulates at the RO. The accumulation of PI4P leads to the recruitment of OSBP which in turn leads to an accumulation of cholesterol at RO that is driven by the OSBP-mediated PI4P/cholesterol counter flow system. A direct interaction between the 3A protein of PV, CVB3 and HRV14 and GBF1 has been found providing supporting evidence for this theory (Wessels et al., 2006, Greninger et al., 2012, Viktorova et al., 2015). GBF1 has also been found to be present in the ROs generated during CVB3 and PV infection and depletion of GBF1 causes inhibition of vRNA synthesis, implying it is required for enterovirus replication (Belov et al., 2007, Belov et al., 2008, Mossessova et al., 2003).

Interestingly, expression of CVB3 non-structural protein 3A on its own leads to membrane enrichment of both PI4KIIIβ and PI4P suggesting that 3A is responsible for the active recruitment of the kinase to RO (Dorobantu et al., 2014). Other picornaviruses such as EMCV and AiV also generate PI4P-enriched RO. Similarly to the enteroviruses, PI4KIIIβ is also essential for AiV (genus Kobuvirus) replication but is recruited to RO by a different strategy from that used by enteroviruses. Multiple non-structural proteins, (2B, 2BC, 2C, 3A,

and 3AB) of AiV have been shown to interact with the Golgi protein acyl-coenzyme A binding domain containing 3 (ACBD3). In uninfected cells, ACBD3 and PI4KIIIβ interact which is thought to contribute to localisation of PI4KIIIβ at the Golgi. Therefore, binding of the AiV non-structural proteins to ACBD3 appears to mediate the recruitment of PI4KIIIβ to RO (Greninger et al., 2012, Greninger et al., 2013, Klima et al., 2017, Sasaki et al., 2012).

In comparison, the cardiovirus EMCV replicates independently of PI4KIIIβ and, instead, subverts PI4KIIIα (phosphatidylinositol 4-kinase III alpha) to generate PI4P at ROs and siRNA-mediated knockdown and pharmacological inhibition of PI4KIIIα inhibits EMCV genome replication. Furthermore, EMCV as the 3A protein interacts directly with and PI4KIIIα, which appears to be responsible for PI4KIIIα recruitment to RO. However, similar to the enteroviruses, PI4P produced at RO recruits OSBP to RO and inhibition of OSBP shuttling inhibits EMCV RNA replication. Additionally Dorubantu *et al* found that mutations in the 3A of EMCV overcame the requirement of PI4KIIIα for replication, providing further evidence of a direct interaction between EMCV 3A and PI4KIIIα (Dorobantu et al., 2016).

1.6.3 Formation of FMDV ROs

FMDV replication differs from that of the enteroviruses in a number of ways. For example enterovirus replication has been shown to be inhibited by the fungal metabolite Brefeldin A (BFA) whereas FMDV (and also the cardioviruses) are insensitive to its effects. This is potentially due the fact that enteroviruses require an intact Golgi for infection and replication (Gazina et al., 2002, Lanke et al., 2009, Cuconati et al., 1998), while FMDV in comparison appears to be able to replicate even when the Golgi is disrupted due to the action of BFA (Gazina et al., 2002, Martin-Acebes et al., 2008, Midgley et al., 2013, Monaghan et al., 2004, O'Donnell et al., 2001).

Formation of RO has also been studied for FMDV. Initial investigations showed that consistent with other picornaviruses, FMDV infection generates large numbers of single- and double-membrane structures that are likely to be RO

(Martin-Acebes et al., 2008, Monaghan et al., 2004). Early after infection, the ER-Golgi intermediate compartment (ERGIC) and Golgi are disrupted by FMDV before major changes are detected in the ER (Zhou et al., 2013, Midgley et al., 2013), suggesting FMDV may inhibit vesicular traffic through the early secretory pathway and that FMDV replication membranes are likely derived from the ER or pre-Golgi membranes. Enteroviruses on the other hand are predicted to utilise Golgi derived membranes (Gazina et al., 2002, Lanke et al., 2009).

The viral components of FMDV RO have been investigated in detail (Berryman et al., 2016) using IBRS2 cells at the mid-phase of the replication cycle and labelling for double stranded RNA, which is produced during infection and considered to be a marker for RO (Sasaki et al., 2012, Richards et al., 2014). Double stranded RNA did not co-localise with FMDV 2C or 3D, both of which are markers of ROs, it also showed little co-localisation with positive strand RNA. However, there was extensive co-localisation of the positive strand RNA with both 2C and 3D. FMDV 3A also co-localised with positive strand RNA but was also found distributed throughout the cytoplasm (Berryman et al., 2016) suggesting 3A may be present in more than one location and have multiple roles in replication.

Despite the apparent differences in how RO form, common themes to emerge are that picornavirus replication requires PI4P and cholesterol (Harak and Lohmann, 2015, Dorobantu et al., 2015a). Cells infected with various picornaviruses show elevated PI4P levels, with PI4P being thought to localise to ROs (Dorobantu et al., 2015a, Greninger et al., 2012, Sasaki et al., 2012). In FMDV infected cells however this is not the case, PI4P levels are not elevated nor does PI4P localise to ROs (Berryman), therefore FMDV appears to utilise a novel mechanism to generate ROs. As described above, the enteroviruses and kobuviruses both use PI4KIIIβ, and EMCV utilises PI4KIIIα to increase levels of PI4P at ROs. In comparison FMDV doesn't require activity of either of these enzymes, and replication is unaffected when they are inhibited by the selective inhibitors of PIK93 and AL-9 (Berryman et al., 2016).

The observation that FMDV replication is independent of PI4KIIIα is consistent with a study by Dorobantu *et al* (Dorobantu et al., 2015a) who reported that infection by ERAV (also an *Aphthovirus*) is was not inhibited by AL-9. In addition a study using CVB3 found that a 3A point mutation resulted in virus able to replicate independently of PI4KIIIβ (van der Schaar et al., 2012) therefore drug-resistant variants of CVB3 appear to behave similarly to FMDV as they can replicate independently of PI4KIIIβ. This implies that picornaviruses from multiple genera may have evolved to replicate independently of type III PI4Ks. Taken together these results suggest the RO membranes generated by FMDV lack PI4P and therefore have a different lipid composition to those found in other picornavirus-infected cells. FMDV has also been found to be able to replicate independently of OSBP, this is consistent with findings described above as PI4P is required to recruit OSBP to the RO. Studies utilizing the OSBP inhibitor 25-HC have found not all picornaviruses require OSBP for replication including ERAV (another member of the *Aphthovirus* genus) and Human Parechovirus in addition to FMDV (Strating et al., 2015, Berryman et al., 2016). Due to the potential differences in how FMDV generates RO in comparison to other picornaviruses, it is possible that FMDV 3A may recruit alternative host factors that enable virus replication.

1.7 FMDV 3A

1.7.1 General characteristics of the FMDV 3A protein

FMDV 3A differs from that of other members of the picornaviridae in that it is much longer due to an extension of its C terminal domain. The 3A protein of FMDV is 153 a.a in length whereas PV 3A is just 87 a.a. All other picornaviruses have a 3A protein of less than 100 a.a with the exception of equine rhinitis virus B (ERBV) (Wutz et al., 1996) and BRBV (Hollister et al., 2008). Figure 1.7.1 shows the alignment of 3A protein sequences from the 4 currently classified members of the *Aphthovirus genus* (panel A), each of which are longer than the majority of picornaviruses that belong to other genera of the

picornaviridae. This includes the kobuviruses and enteroviruses as shown in Figure 1.7.1 panel B which shows the alignment of FMDV 3A with other members of the picornaviruses belonging to different genera. Sequences are aligned based on the predicted transmembrane regions of the proteins. Table 1.7.1 shows the genus and length of each of the viruses included in the alignments (both panels A and B) in Figure 1.7.1. These alignments show that FMDV has a much longer C terminal domain in comparison to other picornaviruses.

A.

```
FMDV                                            ISIPSQKSVLYFLIEKGQHEAAIEFFEGMVHDSIKEELRPLIQQTSFVKRAFKRLKENFEIVALCLTLL
BRBV MGKYMTLDDIKKRKPVVIPFTGRSYQAGRDINASPEMQEKLLKYLVKNEHLDAALNFYNEECDEDVRDKWGPSIGKYLEVKTLWMKVKKYSHLFLTGLMLIGNM
BRAV        VKTLHDKLKASLPKGRGYRCDREVNLKTDEAERMFRYLLNRDPALAGEFLEKECDPELADKYLPLLREHTGKSKLWAMLTKHCDLFLHGLLLVANLV
ERAV              PIFKQSWSDLFKKCTTDEEQKMLQFLIDNKDSEILRAFVSERSILLHEEYVKWESYMTRRAKFHRLAADFAMFLSILTSLIVIFCLVY
Continued:
FMDV ANIVIMIRETRKRQKMVDDAVNEYIEKANITTDDKTLDEAEKSPLETSGASTVGFRERTLPGQKACDDVNSEPAQPVEEQPQAE
BRBV LLLYLNNRAPEEKKKKKKNKTEEDNTTKE
BRAV TLYFQNRKPKRQ
ERAV SMYQLFKTPDEH
```

B.

```
FMDV          ISIPSQKSVLYFLIEKGQHEAAIEFFEGMVHDSIKEELRPLIQQTSFVKRAFKRLKENFEIVALCLTLLANIVIMIRETRKRQKMVDDAVNEYIEK
Aichi  GNRVIDAEPREIPLEYADDLLEAMAHHRPVPCSL GLSQAIANNTPIQQISETFWKYRKPIFTCTTFLAVLGFLCSSVIPLARSLWKSKQDTPQEPQ
CVB3   GPPVYREIKISVAPETPPPPAIADLLKSVDSEAVREYCKEKGWLVPEINSTLQIEKHVSRAFICLQALTTFVSVAGIIYIIYKLFAGFQ
EMCV                APVDEVSFHSVVQQLKARQEATDEQLEELQEAFAKVQERNSVFSDWLKISAMLCAATLALSQVVKMAKDLVRVQLDEQEQ
PV     GPLQYKDLKIDIKTSPPPECINDLLQAVDSQEVRDYCEKKGWIVNITSQVQ TERNINRAMTILQAVTTFAAVAGVVYVMYKLFAGHQ
EV-71   GPPKFRPIKICLEEKPAPDAISDLLASVDSEEVRQYCRDQGWIIPETPTNVERHLNRAVLVMQSIATVVAVVSLVYVIYKLFAGFQ
HRV     GPVYKDLEIDVCNTPPSECINDLLKSVDSEEIREYCKKKKWIIPEIPTNIERAMNQASMIINTILMFVSTLGIVYVIYKLFAQT
Continued
FMDV  ANITTDDKTLDEAEKSPLETSGASTVGFRERTLPGQKACDDVNSEPAQPVEEQPQAE
```

Figure 1.7.1.1 Sequence alignments of Picornavirus 3A proteins: The 3A a.a sequences of selected 3A proteins, aligned based upon the sequence of their predicted trans-membrane domains, are shown. The top alignment (A) shows FMDV 3A in comparison to the other members of the aphthoviruses and the lower panel (B) shows the FMDV 3A sequence in relation to picornavirus 3A from other genera, all of which are shorter in length, predicted transmembrane domains of each virus are shown in blue. The genera of the viruses shown and the lengths of the 3A sequences are shown in Table 1.7.1.1

Table 1.7.1.1: Comparison of Picornavirus 3A proteins: The length (in a.a) of selected picornavirus 3A proteins from various genera is shown. FMDV is the longest followed by BRBV, another member of the Aphthovirus genus, whereas the 3A protein of enteroviruses is typically shorter in length (less than 100 a.a).

Virus	Genera	3A length (a.a)
FMDV	Aphthovirus	153
BRBV	Aphthovirus	133
BRAV	Aphthovirus	109
ERAV	Aphthovirus	100
Aichi	Kobuvirus	95
CVB3	Human enterovirus B	89
EMCV	Cardiovirus	88
PV	Human enterovirus C	87
EV71	Human enterovirus A	86
HRV14	Rhinovirus A	85

The N terminal domain of FMDV 3A is highly conserved across serotypes despite being one of the most variable proteins of FMDV (Knowles et al., 2001). The protein itself contains the N terminal domain which has two predicted alpha helices that are thought to be involved in dimerization of 3A (Gonzalez-Magaldi et al., 2012). FMDV 3A also has a predicted hydrophobic transmembrane domain spanning residues 59-76, the flanking N and C termini are predicted to point towards the cytosol (González-Magaldi et al., 2014). Downstream of the transmembrane domain is the much more variable C terminal domain, this domain is considerably longer in FMDV in comparison with other members of the picornaviridae. This region has also been found to be a hotspot for deletions and substitutions (Carrillo et al., 2005). Figure 1.7.1.2 shows the predicted features found within 3A including the alpha helices within the N terminal domain, predicted to be involved in dimerization of FMDV 3A (Gonzalez-Magaldi et al., 2012) and the predicted hydrophobic transmembrane domain of the protein. Like other picornavirus 3A proteins that of FMDV is membrane associated and is thought to interact with membranes via its predicted

hydrophobic transmembrane domain, as shown in Figure 1.7.1.2, lower panel. (González-Magaldi et al., 2014)

```
WT O1K 3A

123456789*123456789*123456789*123456789*123456789*123456789*123456789*123456
ISIPSQKSVLYFLIEKGQHEAAIEFFEGMVHDSIKEELRPLIQQTSFVKRAFKRLKENFEIVALCLTLLANIVIMI


789*123456789*123456789*123456789*123456789*123456789*123456789*123456789*123
RETRKRQKMVDDAVNEYIEKANITTDDKTLDEAEKSPLETSGASTVGFRERTLPGQKACDDVNSEPAQPVEEQPQAE
```


Figure 1.7.1.2 Predicted features of FMDV 3A: The top panel shows the location of both predicted alpha helicies within the N terminal domain (residues 25 to 33 and 37 to 44) shown in green and the position of the hydrophobic transmembrane domain (residues 59 to 76) shown in blue. The lower panel shows the predicted interaction of FMDV 3A with intracelluar membranes via its transmembrane domain (as described by González-Magaldi et al., 2014), where both the N and C protein termini point towards the cytosol.

1.7.2 FMDV 3A and links with viral host range

FMDV 3A has been linked with determining viral host range. Virus isolates with deletions in the C terminal domain (ranging in size from 10-20 a.a) have previously been identified in vaccine strains passaged in eggs and in outbreak strains (Beard and Mason, 2000, Giraudo et al., 1990, Knowles et al., 2001). The strain responsible for the 1997 FMD outbreak in Taiwan contained the same deletion of a.a 93-102 as identified in the vaccines strains passaged through eggs (Beard and Mason, 2000, Giraudo et al., 1990). During this outbreak, pigs were severely affected with approximately 4 million pigs from

affected farms being slaughtered, there was however no reported cases in cattle during the outbreak (Dunn and Donaldson, 1997, Beard and Mason, 2000). A second deletion of a.a residues 133-143 has also been identified in viruses that affected pigs; however, this virus was also found in cattle and studies that used these viruses to infect keratinocytes from both cattle and pigs showed the that viruses with this deletion grew equally well in either cell type (Knowles et al., 2001). Interestingly, such deletions have been identified in a number of viruses that have been circulating in Asia since at least the 1970s (Knowles et al., 2001).

Deletions in 3A have been associated with an attenuated phenotype in cattle and bovine cells but viruses with theses deletions appear to be highly infectious in pigs (often referred to as porcinophillic) (Beard and Mason, 2000, Dunn and Donaldson, 1997). Further work showed a recombinant virus containing a much larger deletion had a similar phenotype and was attenuated for cattle but remained virulent for pigs (Pacheco et al., 2013, Pacheco et al., 2003). In addition, it has also been shown that removing the entirety of 3A downstream from a.a residue 81 does not affect replication in BHK-21 cells (Behura et al., 2016). Furthermore a single a.a change within 3A led to adaptation of the virus to a guinea pig host supporting the idea that 3A plays a role in viral host range (Nunez et al., 2001). Although recently Ma *et al* have suggested other regions of the FMDV genome could also be responsible for determining viral host range in addition to that of 3A (Ma et al., 2014, Ma et al., 2016).

Recent evidence has shown that the attenuation of replication caused by deletions within 3A appears to be able to overcome following accumulation of mutations upstream in the genome. In particular a threonine to isoleucine change at residue 135 in 2C was identified as causing enhanced growth in BHK-21and IBRS2 cells of a virus that had a deletion of a.a 84 to 143 in 3A. This change occurred following passaging of the virus, which initially exhibited a reduced growth rate and smaller plaques than that of a virus with full-length 3A (Yuan et al., 2017).

FMDV 3A has also been linked with virulence, Rosas et al have shown that viral replication levels increased in cells that stably expressed FMDV 3A or 3AB whereas viral susceptibility was lower in cells transiently expressing 3A (Rosas et al., 2008).

1.7.3 Cellular Interacting partners of 3A

A number of cellular proteins have been reported to interact with the 3A protein of picornaviruses. As discussed above in sections 1.6.2 and 1.6.3, the 3A protein of EMCV has been shown to bind the lipid kinase, PI4KIIIα (Dorobantu et al., 2016), the 3A proteins of enteroviruses (e.g., PV and CV) bind GBF1 (Wessels et al., 2006) and several viruses of both the enterovirus and kobuvirus genera (e.g. AiV) directly bind ACBD3 (Greninger et al., 2012, Klima et al., 2017, Sasaki et al., 2012). As these proteins are required for formation of viral RCs and ROs, the above observations support a key for 3A in picornavirus replication. For FMDV, a Y-2-H screen identified DCTN3 (Dynactin 3) as a cellular interacting partner of 3A (Gladue et al., 2014) . DCTN3 is a subunit of a dynactin complex, which serves as a cofactor for the dynein motor. However, a direct interaction between 3A and DCNT3 was not demonstrated and the functional significance of this interaction for FMDV replication is unknown. However, it was shown that over expression of DCTN3 or proteins predicted to disrupt the dynactin complex decreased FMDV infection (Gladue et al., 2014).

1.7.4 Other potential roles of 3A in genome replication

The 3A protein is believed to play an important role in replication, as described above. There is also the likely probability that 3A containing intermediates (e.g. 3AB), produced during post translational processing of the polyprotein, may play key roles in replication. The VPg (3B) protein has been shown to be a substrate for uridylation when a free peptide, however this may not be the only form to undergo this reaction in infected cells and it has been suggested that 3B containing precursors (both 3AB and 3BC) or the entirety of P3 may be the

functional source of 3B for uridylation (Nayak et al., 2005, Paul and Wimmer, 2015).

For PV, 3BC, 3BCD and P3 have been shown to serve as substrates for uridylylation in vitro although the reaction is less efficient for the larger 3B containing precursors (3BCD and P3) (Pathak et al., 2008), suggesting that 3BC may be the VPg donor for replication. This conclusion has been supported by the observation that (in contrast to 3C-containing precursors) attempts to uridylate PV 3AB in vitro were unsuccessful (Paul and Wimmer, 2015). This could also be the case for FMDV, however, since FMDV encodes multiple copies of 3B within its genome a wider range of 3A or 3C-containing processing intermediates e.g. $3A3B_1$, $3AB_{12}$, $3AB_{123}$ or $3B_{123}3C$ could potentially be the source of VPg for uridylation.

1.7.5 Possible Chaperone activity of 3A

The 3A of picornaviruses have been reported to have chaperone activity. 3AB of EV71 is reported to be a nucleic acid chaperone protein and to have nucleic acid helix-destabilizing and strand annealing activity. This activity is dependent on 3B and the last 7 a.a at the C-terminal of 3A, of which 5 a.a were identified as critical for RNA chaperone activity (Tang et al., 2014). Furthermore 3AB of PV has been suggested as having a chaperone effect promoting hybridization of complementary nucleic acids and destabilizing secondary structure (DeStefano and Titilope, 2006). It is therefore possible that FMDV 3A may also play roles as a chaperone.

1.8 Aims

This project utilised a combination of sub-genomic replicons, reverse genetics and proteomics techniques with the aim of gaining further understanding of the roles played by the non-structural viral protein 3A during FMDV replication.

Project Aims:

1. FMDV 3A has been implicated as a factor of host specificity. Aim 1 is to investigate the effects of a novel naturally occurring large deletion in 3A and deletion of 3B1 on replication in different host derived cell lines

2. Picornavirus 3A binds cellular proteins and plays a central role in formation of replication organelles. Aim 2 is to utilise proteomics techniques to identify potential cellular protein interaction partners of 3A and investigate effects of reducing expression levels of these partners on infection and viral replication

3. 3A is membrane associated. VAP proteins bind proteins with a FFAT motif. Aim 3 is to investigate the role of a potential FFAT-like domain in 3A in FMDV replication

4. 3A and 3C have the potential to deliver VPg (3B) to a replication complex. Aim 4 is to investigate the role of 3A as the chaperone for delivery of VPg to the viral replication complex.

Chapter 2: Materials and Methods

2.1 Materials

2.1.1 Cell lines:

Baby Hamster Kidney-21 clone 13 cells (BHK-21), and Madin Darby Bovine Kidney (MDBK) and Human Embryonic Kidney293 (HEK 293) cells were obtained from the central service unit at Pirbright and maintained in Glasgow's minimum essential media (GMEM) with 10% Foetal Bovine Serum (FBS) (Sigma) 1% L-glutamine (Sigma) and 1% penicillin/streptomycin (P/S) (Sigma).

Porcine kidney IBRS2 cells were obtained from the central service unit at Pirbright and maintained in GMEM with 10% Adult Bovine Serum and P/S. A second porcine kidney cell line, SK-RST cells were obtained from the American Type Culture Collection and maintained in Dulbecco's Modified Essential Medium (DMEM), supplemented with 10% FBS and P/S.

Primary bovine thyroid (BTY) cells were provided by the central service unit at the Pirbright Institute growing in GMEM supplemented with 10% FBS and 1%Field Antibiotics (Pirbright Institute).

Parental and TBC1D20 knockout HeLa cell lines were kindly provided by Dr M.Handley (The Roslin Institute) and maintained in DMEM supplemented with 10% FBS and P/S.

2.1.2 Viruses and sub-genomic FMDV replicons:

FMD viruses in this study were based on the full length infectious clone of O1 Kaufbeuren (O1K) strain (Zibert et al., 1990, Ellard et al., 1999).

A schematic representation of the FMDV genome and wildtype FMDV replicons based on FMDV O1K is shown in Figure 2.1.2. Replicons contained *Ptilosarcus guernyi* Green Fluorescent Protein (Pt.GFP or mCherry reporter genes in place of majority of the capsid proteins are referred to as O1K Pt.GFP or O1K mCherry respectively. Negative control replicons that had 2 a.a mutations within

the polymerase active site (GDD motif mutated to GNN), of the viral polymerase (3D) were used to measure background signal from non-replicative input RNA (referred to as O1K Pt.GFP GNN and O1K mCherry GNN). Replicons were all kindly provided by Dr F. Tulloch (University of St Andrews) and modified from the GFP-PAC replicon system developed by Tulloch *et al* (Tulloch et al., 2014). In the course of this project O1K Pt.GFP was modified to produce various mutations or deletions to the P3 proteins in order to test effects on replication.

The full length FMDV O1K cDNA clone plasmid (pT7S3) was used as template DNA to PCR amplify the capsid coding region required to restore sub-genomic replicons to full length infectious clones which were used to recover recombinant viruses.
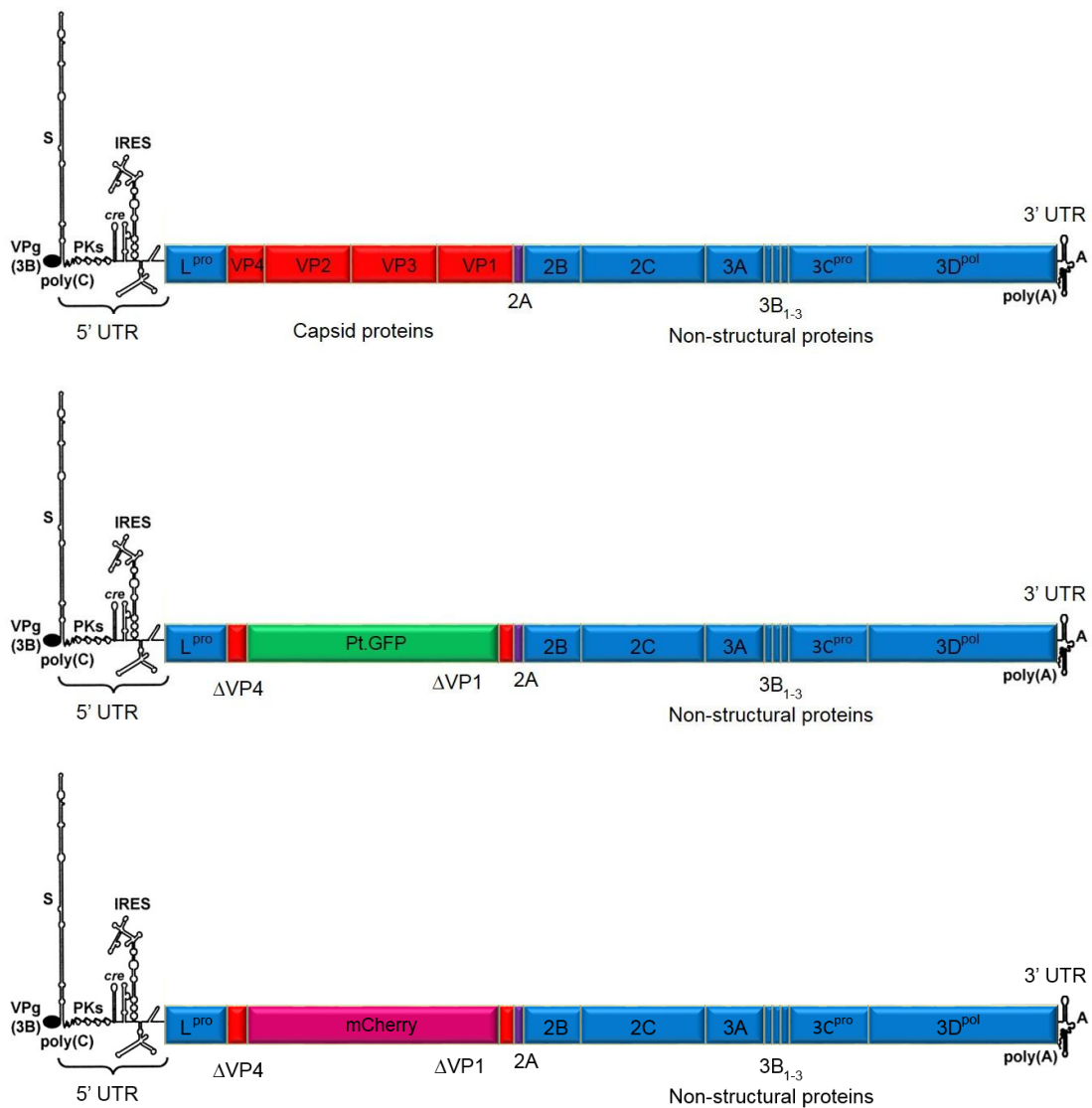
Figure 2.1.2 Genome organisation of FMDV and Design of sub-genomic FMDV replicons: The full length genome of FMDV (top panel) and with the majority of the capsid coding region replaced with either a Pt.GFP reporter gene (middle panel) or an mCherry reporter (bottom panel) were used to study effects of changes to the P3 region by using fluorescent reporter gene expression as an indirect measure of replication.

2.1.4 Fusion protein expression plasmids

3A and 3ABBB-GFP fusion protein expression plasmids were developed by cloning in PCR products encoding 3A or 3ABBB into the multiple cloning site region of the pEGFP-N1 expression plasmid (Clonetech).

2.1.5 DNA Gene Blocks

DNA sequences synthesised in plasmid backbones used to make the Δ3A81-137 deletion and the 3A, 3C and No Donor replicons were obtained from Gene Art (Life technologies). Gene blocks used to create the Δ3A93-143, SKRΔ3B1, SKR+3B1, O1KΔ3B1, OSBP and Protrudin replicons were obtained from Eurofins.

2.1.6 Oligonucleotides

All primers used in this study were ordered from Integrated DNA Technologies and Sigma, and suspended to 100 µM stock solutions in dH2O before further dilution for working stock concentrations as required.

2.1.7 Antibodies

2.1.7.1 Primary Antibodies

The monoclonal antibody to FMDV protein 3A (2C2) was kindly gifted to the Picornavirus group by Emiliana Brocchi (IZS, Brescia, Italy) and the polyclonal Rabbit antibody TC27, raised against FMDV 3D, was generated in house at the Pirbright Institute. The primary antibodies to PDI (ER marker) and GM130 (Golgi marker) were kindly provided by the Bioimaging group at Pirbright. Primary antibodies to β-actin and GFP were obtained from Roche and Sigma respectively

2.1.7.2 Secondary Antibodies

Alexa fluor conjugated secondary antibodies: goat anti-mouse (IgG H+L) 488, goat anti-mouse (IgG2a) 568, goat anti mouse (IgG1) 488 and goat anti-mouse (IgG H+L) 568 were all obtained from Invitrogen Molecular probes.

Goat Anti-Rabbit and Rabbit-anti mouse horse radish peroxidase conjugated secondary antibodies were acquired from Biorad and Dako respectively.

2.2 Methods

2.2.1 Tissue culture

2.2.1.1 Maintaining of cell lines

All cell lines were maintained through regular passage when cells reached confluence. Media was removed and monolayers washed with PBSa (without Ca^{2+} and Mg^{2+} ions). Cells were removed from flasks by incubation with Trypsin-EDTA (life technologies), detached cells in trypsin were transferred into universals and growth medium added to inactivate the trypsin. The cell suspension was centrifuged for 3 minutes at 1000 rpm to pellet cells. The supernatant was removed and the cell pellet re-suspended in 5ml complete growth media and seeded into T175 flasks (Greiner).

2.2.1.2 Freezing and resuscitation of cells

Frozen cell stocks were made by detaching confluent cell monolayers and pelleting as described in section 2.2.1.1, re-suspending in FBS with 10% DMSO (Sigma), dividing into 1 ml aliquots and storing at -80°C or in liquid nitrogen for long term storage.

2.2.1.3 Transfection of cells

Plasmid DNA and *in vitro* transcribed RNA was transfected using Lipofectamine 2000 (Invitrogen). Plasmid DNA or *in vitro* transcribed RNA were diluted in Optimem serum free media (Gibco) and incubated for 5 minutes at room temperature. Lipofectamine 2000 was diluted in optimum in a separate tube and incubated for 5 minutes. The contents of the two tubes were mixed and incubated for 15 minutes at room temperature. Growth medium was removed from cells and transfection mix pipetted on, fresh complete growth media was then added to cells. For plates going onto the IncuCyte zoom for live cell analysis clear FluoroBrite media (Gibco) with 10% FBS was added in place of standard growth media. Table 2.2.1.3 summarises transfection ratios used.

Experiment type	Plate /Flask size	Amount of DNA/RNA	Amount of lipofectamine	Total volume of media (after transfection)
Replicon assay	24 well plate	500 ng RNA	2 µl	500 µl
GFP fusion transfection for IPs	20 cm dish	20 µg DNA	45µl	950 µl
Transfection of infectious copy RNA	T25 flask	3 µg	8 µl	500 µl

Table 2.2.1.3 Conditions used for transfection of DNA and RNA using Lipofectamine 2000: Cells seeded into various size tissue culture vessels were transfected using the ratios of lipofectamine to DNA and RNA shown in the table above. DNA, RNA and lipofectamine were diluted into Optimem serum free media and mixed to total volume shown and transfection mix added to cells.

siRNA was transfected into cells using Dharmafect 4 transfection reagent (Dharmacon). siRNA in a 5 µM solution was diluted in a 10 µl volume of Optimem, in a separate tube Dharmafect 4 was diluted in 10 µl volume of Optimem. The contents of each tube were gently pipetted to mix and incubated for 5 minutes. The contents of the two tubes were then mixed together and incubated for a further 20 minutes. 80 µl of antibiotic free GMEM with 10% FBS was then added to transfection mix, complete media was removed from cells in a 96 well plate and replaced with the 100 µl mix of transfection mix and media per well.

2.2.1.4 Treatment of cells with BFA

Cells (BHK-21 or SK-RST) cells were seeded into 24 well plates and incubated overnight until 80% confluent. Prior to transfections cells were pre-treated for 15

minutes with either DMSO (the solvent carrier) or BFA (5mg/µl) diluted in fluorobrite media with 10% FBS at 37°C. BFA containing media was left on cells for the duration of the experiment.

2.2.2 Infection of cells with FMDV

Cells seeded in T25 flasks or multi well plates at approximately 80% confluency were infected with supernatant from previous viral passages using MOIs calculated based on viral titre. Infectious supernatant was diluted to correct multiplicity of infection (MOI) in Viral Growth Medium (VGM), complete growth medium was removed from cells and replaced with infectious supernatant. Flasks and plates were incubated and frozen at different time points post infection.

2.2.3 DNA work and Generation of constructs

2.2.3.1 Bacterial transformation

JM109 (Promega), DH5α (Invitrogen) or XL 10 Ultra competent cells (Agilent) were transformed (according to manufactures protocols). DNA was added to competent cells, incubated on ice before heat shocking for 30 seconds at 42°C and incubating on ice for a further 2 minutes. Cells were left to recover in SOC media for an hour at 37°C before plating on plates containing ampicillin or kanamycin dependent on antibiotic resistance gene in plasmid. Plates were incubated at 30°C for 20-24 hours.

2.2.3.2 Small and large scale preparation of plasmid DNA

Colonies from transformed bacteria were picked and used to inoculate 5 or 10 ml of LB broth containing antibiotics (ampicillin (100µg/ml) or kanamycin (50µg/ml) depending on sensitivity of plasmid). Cultures were incubated overnight at 30 or 37°C, shaking at 200 rpm. Between 1 and 3 ml of culture for small scale preps were spun at 13300 rpm for 3 minutes, to pellet bacteria. Pellets were subjected to alkaline lysis and neutralisation, and plasmid DNA purified through columns containing affinity matrixes. In order to prepare larger

amounts of plasmid DNA the 5 or 10 ml cultures described above were diluted into 250 ml LB broth with antibiotics and grown overnight as described above, before pelleting bacteria from the entire volume by centrifugation at 5000 rpm for 10 minutes. Plasmid DNA was prepared using Qiagen plasmid maxi prep spin kit (Qiagen) as per manufacturer's instructions.

2.2.3.3 Restriction digestion of DNA

Restriction digest of DNA was carried out according to manufactures protocol (Promega and New England Biolabs). Typically reactions were set up in a total volume of 20 µl, consisting of: DNA (100ng-1µg), 2µl 10X reaction buffer, 5u/µg of DNA of enzyme and dH20 to 20µl. Reactions were incubated at 37°C (unless a different temperature was stated by manufacturer) for 2 hours to ensure complete digestion of the DNA. Reactions were run on a Tris/Borate/EDTA (TBE) agarose gel to check for complete digestion before being used in further downstream processes.

2.2.3.4 Agarose gel electrophoresis

DNA and RNA samples were run on 1% TBE gels for analysis unless otherwise stated. For a 1% gel 1g of Agarose was dissolved in 100ml of 1X Ultrapure TBE buffer (diluted 10X stock in dH2O) through heating. Once cooled 2.5 µl of ethidium bromide was added to agarose prior to pouring. DNA samples were mixed with 6X purple loading dye (New England Biolabs) and loaded onto gel, Quick load 1Kb DNA marker (New England Biolabs) was used unless otherwise stated. Gels were run in 1X TBE buffer at 120V until the dye front reached the end of gel. Gels were imaged using a Biorad gel documentation system and image lab software.

2.2.3.5 Extraction of DNA from agarose gels

Gels were placed on a UV light box to visualise DNA bands and cut out. Capture buffer was added to gel slices and melted at 65°C. DNA was then extracted through column purification using GE healthcare illustra GFX PCR DNA and Gel extraction kit and eluted into 20 µl dH2O.

2.2.3.6 Ligation of DNA

DNA that had been prepared by restriction digest and gel extraction was used as vector and insert fragments for ligations to create new constructs. Vector DNA was phosphatase treated prior to ligation with recombinant shrimp alkaline phosphatase (New England Biolabs) for 30 minutes at 37°C and enzyme heat inactivated for 5 minutes at 65°C. Ligations, including vector only control reactions, were set up at varying ratios in 10µl volumes with T4 DNA ligase and ligase buffer containing ATP (New England Biolabs). Reactions were incubated overnight at 16°C and 2-5 µl transformed into competent cells (See section 2.2.3.1).

2.2.3.7 Quikchange mutagenesis

Quikchange mutagenesis reactions were carried using a Quikchange lightening mutagenesis kit (Agilent) as per manufacturer's instructions. Mutagenic primers were designed to fit specifications using Agilent's online design tool and purchased from Sigma. Following Quikchange reaction DNA was transformed into XL 10 Gold Ultracompetent cells (See section 2.2.3.1).

Colonies from transformed bacteria were used to inoculate Lb broth mini prep cultures, mini prep DNA was prepared (Section 2.2.3.2) from these and clones screened by either restriction digest (Section 2.2.3.3) or by Sanger sequencing (2.2.8.1).

2.2.3.8 Polymerase Chain Reaction

Fragments of DNA were amplified using Polymerase Chain Reaction. Standard PCR reactions were carried out using Taq DNA polymerase (NEB) and consisted of template DNA, 1µl Forward primer (10µM), 1µl Reverse primer (10µM), 1µl dNTPs, 5µl 10X standard Taq polymerase buffer, 1µl Taq polymerase and dH2O to 50µl.

Typical cycling conditions are shown in Table 2.2.3.8 Annealing temperatures were normally set to approximately 4°C below the lowest primer Tm and tended

to range between 55°C and 60°C. Reactions were run on an Eppendorf Mastercycler Thermocycler.

Stage	Temperature	Duration	
Initial denaturation	95°C	30 seconds	
Denaturing	95°C	15 seconds	X 30 cycles
Annealing	55-60°C	30 seconds	
Extension	68°C	1 minute/kb DNA	
Final Extension	68°C	5 minutes	

Table 2.2.3.8 Standard PCR cycling conditions: PCR amplification of DNA was carried out using conditions shown in the table above with Taq DNA polymerase. Primer annealing temperatures and extension times were adjusted accordingly with regard to primer melting temperatures and product length.

2.2.4 RNA work

2.2.4.1 In vitro transcription of RNA

All RNA work was carried out in areas and with equipment that had been treated with RNAse zap (Sigma). DNA from replicon or infectious clone plasmids was linearized by restriction digest using AscI (New England Biolabs) as described in section 2.2.3.3. Linearized DNA was used as a template for *in vitro* transcription reactions set up as follows: Template DNA (up to 5µl), 5x transcription reaction buffer (4µl), DTT (2µl), rNTPs (8µl), RNAsin (0.5µl (40U/µl)), DNA dependent RNA T7 polymerase (1µl (10U/µl)), dH20 to 20µl (Promega) Reactions were incubated for 2-4 hours at 37°C, and treated with RNAse free DNAse (2µl) (Promega) for 15 minutes at 37°C. RNA integrity was analysed using gel electrophoresis and quantified using a Qubit fluorimeter (Section 2.2.4.2).

2.2.4.2 Quantification of RNA with Qubit fluorimeter

RNA was quantified using a fluorimeter (Qubit (Invitrogen) or Quantus (Promega)) using the broad range RNA assay kit as per manufacturers protocol. Briefly 1µl of sample was mixed with 199 µl of fluorescent RNA binding dye (molecular probes) and read against prepared standards.

2.2.4.3 siRNA assays

Three different SiRNAs were designed against different points in the porcine Rab7L1 sequences using the Dharmacon design tool. The SiRNAs were re-suspended in nuclease free dH2O and diluted to 5µM then pooled together and transfected into IBRS2 cells (porcine kidney cells) in 96 well plates to a final amount of 5pg per well (See section 2.2.4.3). At 48 hours post transfection cells were infected with O1K FMDV for 4 hours , fixed with 4% PFM (see section 2.2.7.1) and labelled for FMDV 3A using the 2C2 primary monoclonal antibody and a secondary antibody conjugated to a fluorophore (goat anti-mouse alexa fluor 488 (molecular probes)). Cell nuclei were labelled with ToPro 3 dye according to manufacturer's protocol (Molecular probes). The total number of cells and number of infected cells were then counted using the Spectramax I3 minimax plate reader (Molecular Devices) to determine if knockdown of Rab7L1 expression impacted on FMDV infection in porcine cells. Cellular GFP intensity was also measured to see if the siRNA was impacting in any way on replication.

2.2.5 Virus assays

2.2.5.1 Virus passage and recovery

BHK-21 cells were seeded into T25 flasks to be 80% confluent the following day. Cells were then transfected with *in vitro* transcribed RNA from infectious FMDV clones using method described in section 2.2.1.3. Following the addition of transfection mix, 5ml viral growth media (VGM) consisting of GMEM with P/S and 1%FBS was added to cells. Cell monolayers were monitored for up to 48

hours and flask frozen at observation of total CPE compared to non-transfected flasks or at 48 hours post transfection.

Frozen flasks were thawed and supernatant collected and spun down to pellet cellular debris and split into 1 ml aliquots. One of these 1 ml aliquots was passaged onto fresh BHK-21 cells in T25 flasks containing 5ml of VGM and appearance of CPE monitored before passaging again as described above.

2.2.5.2 Virus titrations

Viral titre was calculated by plaque assay. Briefly cells were seeded into 6 well plates and allowed to adhere overnight. Virus samples were serially diluted ten-fold into PBS, cells were washed with PBS and viral dilution series added to wells. Plates were incubated at 37°C for 15 minutes and wells overlaid with Eagles Overlay (containing tryptose phosphate broth, FBS and P/S) mixed with melted indubiose agarose. Plates were left at room temperature to allow overlay to set then incubated at 37°C for 48 hours. Cells were then fixed and stained using formaldehyde containing Methyl blue cell stain and left overnight at room temperature. Overlays were removed and plaques counted to determine viral titre. Titrations were carried out in duplicate for each sample therefore plaque counts from each sample at the same dilution were averaged and multiplied by ten to give final viral titre in plaque forming units per ml (pfu/ml).

2.2.5.3 Viral RNA extraction

Extraction of RNA from clarified supernatant was performed using the Qiamp Viral RNA Mini Kit from Qiagen. Briefly 140µl of viral supernatant was added to 560µl of lysis buffer mixed and incubated for ten minutes. 560µl of 100% ethanol was added to samples and tubes vortexed briefly before being affinity matrix column purified according to kit protocol and RNA eluted into 60µl elution buffer and stored at -80˚C.

2.2.5.4 Reverse transcription (RT) PCR reactions

RT reactions were carried out on extracted viral RNA or *in vitro* transcribed RNA to produce cDNA. Reactions were carried out as follows: 15µl of RNA, 3µl

10mM DNTPs (Promega), 3µl of primer (UK FMDV Rev6), were mixed and heated for 3 minutes at 70°C. Tubes were cooled on ice before adding: 5 x first strand synthesis buffer 8µl (Invitrogen), nuclease free H2O 5µl (Ambion), 2µl 0.1µM DTT (Invitrogen) and 1µl Superscript III RT enzyme (Invitrogen). Reactions were incubated at 45°C for 60 minutes and 85°C for 5 minutes followed by 4°C indefinitely. cDNA was purified using illustra GFX GE healthcare kit before being used in PCR reactions.

2.2.6 Protein Analysis

2.2.6.1 Preparation of samples for SDS PAGE

Cells (BHK-21, MDBK) were seeded into multi-well plates and left to adhere overnight at 37°C before being transfected with plasmid DNA, or RNA from replicons or infectious clones or infected with FMDV virus and incubated for 37°C for time required. Media from transfected or infected cells was then removed and replaced with 3X lysis buffer (3X SDS loading dye, with DTT in PBS). Lysed samples were scraped from wells into 1ml screw cap tubes and heated at 96°C for 5 minutes to denature proteins.

2.2.6.2 Analysis of proteins by SDS PAGE

Samples were prepared as described in section 2..2.6.1 and loaded onto 12% SDS (unless otherwise stated) prepared polyacrylamide gels alongside a 10-250 KDa pre-stained protein ladder (Biorad). Gels were run in 1X Tris-Glycine Buffer with SDS at 100V until dye front just ran off the end.

2.2.6.3 Western Blotting

Proteins were transferred from SDS polyacrylamide gels onto nitrocellulose membranes as follows: Gels were removed from plates and placed in a blotting cassette with dH2O pre-soaked sponges, membrane and filter paper. Cassettes (Biorad) were place in tank with an ice block and 1X transfer buffer (1X Tris-glycine buffer with 20% methanol) and transfer reaction run at 100V for 90 minutes.

Membranes were blocked for 1 hour at room temperature or overnight at 4°C in 5% Marvel milk block buffer (5% Marvel milk in PBS-Tween) in falcon tubes rotating on a spiramix. Primary antibodies were diluted as required in block buffer (primary antibodies were use at 1 in 100 dilution and secondary antibodies at a 1 in 250 dilution unless otherwise stated, and membranes incubated with them for 1 hour on rotating then washed in PBS-Tween for 15 minutes, changing buffer at 5 minute intervals. Secondary antibodies were diluted in block buffer 1 in 2000 and incubated with membranes in falcon tubes for 1 hour on rotating. Washing step was repeated as above. Membranes were placed in a clean white tray and West Pico Supersignal Chemiluminescent substrate added (Thermo scientific) and imaged using the Syngene G: box.

2.2.6.4 Immunoprecipitations

BHK-21 cells were seeded into 20cm diameter tissue culture dishes and allowed to adhere overnight. Cells were transfected with 20µg of fusion protein DNA (3AGFP or 3AB GFP) or a pEGFP-N1 control and incubated for 12 and 24 hours (see section 2.2.1.3 for transfection method). Cells were checked for GFP expression prior to removal using an Evos cell imaging system microscope. Immunoprecipitation (IP) buffer was added to monolayers and cells harvested and aliquoted into 1 ml tubes. Following harvesting samples were sonicated and 50µl of sample retained as total cell lysate (TCL). Remaining lysate was centrifuged at 18,0000g for 10 minutes at 4°C, a further 50µl was removed as starting material. Magnetic anti GFP beads (Dundee cell products) were re-suspended in 100µl of RIPA buffer and split into 1.5ml tubes. Remaining lysates were added to the tubes with beads, mixed and incubated for 2 hours on a rotating wheel at 4°C. Beads were pelleted by centrifugation and the entire supernatant kept as flow through (TCL). Anti GFP beads were re-suspended in IP Buffer, and washed three times before finally being re-suspended in elution buffer and heated to detach complexes. Tubes were placed against a magnetic rack and eluted liquid separated from beads (IP sample). TCL, FT and IP samples were run on a 4 to 20 % gradient gel (Biorad) SDS gel and western blotted (as described in sections 2.2.6.2 and 2.2.6.3) using a GFP antibody to

ensure IPs had worked before further preparation of samples for mass spectrometry was conducted (section 2.2.6.5).

2.2.6.5 Preparation of samples for Mass spectrometry

IP samples from section 2.2.6.4 were run on a 4-12% gradient gel (Biorad), and stained with Sypro Ruby red to visualise bands. Bands were cut out, dehydrated using Carbon Nitrile, washed and in gel digested with Trypsin. Following digestion peptide samples were cleaned up using a tC18 Sep-Pak Plate and eluted into low protein binding eppendorfs. Finally they were dried by centrifugation overnight and re-suspended in 5% Formic acid and run on the mass spectrometer. All steps in this preparation and final running of samples was carried out according to protocols adapted by and with help of Dr Armel Nicolas (University of Dundee).

2.2.6.6 Transcription and translation coupled reactions

TnT reactions were carried out using a TnT T7 Quick for PCR DNA kit (Promega) using PCR products that were produced by amplifying the 3A to mid 3C region of each of the donor constructs. The forward primer was designed to include a T7 promoter and Kozak sequence followed by a start codon directly upstream of the N terminus of 3A. The reverse primer was situated in the middle region of 3C meaning that 3C was truncated to approximately 10KDa and inactive as it was truncated to upstream of the predicted active site.

Reactions were set up as per manufacturer's instructions, and following incubation half of the samples were treated with exogenously expressed 3C protease (kindly provided by Dr J.Newman). Samples run on 4-20% gradient gels (Biorad) which were then soaked in salicylic acid dried and exposed to film for varying durations prior to developing.

2.2.7 Microscopy and fluorescence assays

2.2.7.1 Fixation of cells

Media covering infected cells was aspirated off and replaced with 4% paraformaldehyde in PBS for 1 hour. The PFM was removed and cells washed 3 times with PBS. Fixed cells were placed in fresh PBS and stored at 4°C.

2.2.7.2 Preparation of slides for confocal microscopy

Cells on coverslips were fixed as described in section 2.2.7.1 and treated with 0.1% Triton X100 in PBS. Coverslips were washed 3 times with PBS (Sigma), followed by blocking with fish skin gelatin block buffer for 1 hour. Primary antibody diluted in block buffer was added for 1 hour and cells washed 3 times with PBS. Secondary antibody conjugated to an Alexafluor (either 488 or 561, for red or green fluorescence respectively), was diluted 1 in 200 in block buffer and added to cells that were incubated for 45 minutes in the dark, then washed 3 times with PBS. Finally cell nuclei were stained with DAPI, 1 in 10000 in dH2O for 10 minutes followed by washing with PBS. Coverslips were mounted onto cells using vector and sealed with clear nail varnish.

2.2.7.3 Confocal Microscopy

Fluorescently labelled cells on coverslips were visualised using the Leica TCS/SP2 or Leica TCS/SP8 confocal laser scanning microscope. Further image analysis and preparation was done using the Leica LAS software.

2.2.7.4 Replicon assays using the IncuCyte Zoom

During this work a number of replicon based assays were carried out using expression of a fluorescent reporter gene (Pt.GFP or mCherry) as an indirect measurement of viral RNA replication and a method adapted from Tulloch et al (Tulloch et al., 2014).: *In vitro* transcribed RNA from FMDV replicons was transfected into cells in 24 well plates using the method described in section 2.2.1.3. GFP or mCherry expression was measured at hourly intervals using an IncuCyte zoom cell imaging system (Essen Bioscience) housed inside an incubator at 37°C with 5% CO_2 allowing measurement of replication in real time.

Expression was measured at 4 sites within each well and combined to give single measurements for each well of levels of intensity and numbers of cells expressing GFP or mCherry and an image per site at each time point. Analysis of data was carried out using the IncuCyte software with processing definitions developed to correct for object size and intensity levels. All data shown is expressed as Green Object Average mean calculated using size and pixel intensity of objects, or as the Green object count per image calculated by averaging the total number of objects counted across all 4 images within the well. Values from triplicate wells were combined and averaged and the standard deviations calculated.

2.2.7.5 Minimax assays

Assays to measure infection in SiRNA treated cells and replicon assays in TBC1D20 knockout cell lines, were carried out using a Minimax i3 Spectramax imaging plate reader (Molecular devices). For both types of assay, cells were in black sided clear bottomed plates. In the replicon assays a single site in each was chosen to image at an hourly interval. In the SiRNA assays 4 sites per well were imaged at a single time point and intensity and count data combined and divided by 4 by the softmax pro 6 software (Molecular devices). Data was exported and upper and lower thresholds of intensity set and any outlying results removed to allow accurate averages of triplicate (siRNA assays) or quadruplets (replicon assays) to be calculated.

2.2.8 Sequence analysis

2.2.8.1 Sanger Sequencing of plasmids and PCR products

Sanger sequencing was carried out by University of Dundee sequencing or GATC Biotech as per manufacturer's protocol, on samples from St Andrews or in house on samples from Pirbright. Plasmid DNA or PCR products from samples at Pirbright were prepared using ABI Big dye terminator v3.1 (Applied Biosystems) as per manufacturer's instructions. Following PCR step samples

were ethanol precipitated, vacuum dried for 15 minutes and re-suspended in 20µl Hi-Di Formamide (Applied Biosystems).

2.2.8.2 Deep sequencing of plasmid DNA

Infectious copy plasmid DNA was linearized using AscI, column purified and re-suspended to the concentration of 0.2 ng/µl. Library preparation and running of samples on Miseq (Illumina) was kindly carried out at Pirbright by Dr Caroline Wright according to manufacturer's protocol.

2.2.8.3 Sequence data analysis

Sequence analysis was carried out using DNASTAR Lasergene programs Seqman pro 14 and Seqman NGen 14 to produce consensus sequences. Alignments of consensus sequences were carried out using BioEdit and plasmid maps created and analysed using A plasmid Editor (ApE) and DNASTAR SeqBuilder 14.

2.2.9 Statistical Analysis

Statistical analysis was carried out using Minitab 17, General Linear Model, and One way-ANOVA with Tukey's correction. Graphs were plotted using Graph Pad prism 7 software.

Chapter 3: Investigating effects of deletions within FMDV 3A on replication

3.1 Introduction

The FMDV 3A protein has an extended C terminal domain compared to other picornaviruses (See Chapter 1 figure 1.7.1.1). Naturally occurring deletions of 10-20 a.a within this region of the protein have been found, both in viruses passaged through eggs for vaccines used in South America (Giraudo et al., 1990), and in outbreaks strains including the type O virus responsible for the 1997 FMDV outbreak in Taiwan (See Chapter 1 section 1.7.2). The 1997 Taiwan virus had a 10 a.a deletion in the C terminal domain of 3A (residues 93-102), which appeared to impact on viral host range as this virus was highly virulent in pigs but attenuated in cattle. A similar pattern of virus growth was seen when propagating these strains in bovine and porcine cells *in vitro* (Beard and Mason, 2000, Pacheco et al., 2003, Pacheco et al., 2013).

Another deletion of 11 a.a in 3A (residues 133-143) has also been identified in a number of field viruses also isolated during FMD outbreaks in Asia, however viruses with this deletion were found in both cattle and pigs and appeared to replicate normally in both porcine and bovine keratinocytes (Knowles et al., 2001). In addition, recombinant viruses with this deletion replicated normally in BHK-21 and both bovine and porcine kidney cells (Ma et al., 2014). Furthermore, a recombinant virus with a large internal deletion (so-called "super deleted" virus) in 3A that spanned a region containing both of the above deletions (residues 93-143) was shown to remain infectious in porcine cells but was also attenuated in bovine cells (Pacheco et al., 2003) and Behura *et al.* showed that the entire C terminal domain of 3A in an Asia-1 type isolate can be removed without impacting on replication in BHK-21 cells (Behura et al., 2016).

Here I have investigated the effects of a large naturally occurring deletion in 3A of 57 a.a (residues 81-137) on replication in cells derived from different natural hosts of FMDV. The deletion was discovered during sequencing of an FMDV O1 Manisa vaccine isolate and appeared to exist as part of a mixed viral

population that included viruses that also contained the full length 3A protein. Initially, the ability of the 3A deleted virus (FMDV O1Man Δ3A81-137) to replicate independently as opposed to requiring "help" from other wildtype viruses in the mixed population was tested using sub-genomic replicons.

FMDV is unusual among the picornaviridae as it is insensitive to Brefeldin A (BFA) (Martin-Acebes et al., 2008, O'Donnell et al., 2001, Midgley et al., 2013). To investigate whether the C terminal domain of the FMDV 3A is required for BFA resistance, the effect of BFA on replication of the replicon with the 81-137 deletion was also investigated. BFA inhibits activation of the cellular factor ARF1 by inhibiting the GEF activity of GBF1 and thereby inhibits COP-I vesicle formation and disrupts the Golgi apparatus (Niu et al., 2005). The 3A of the enteroviruses binds directly to GBF1 (Wessels et al., 2006) and thus BFA also inhibits their replication (Lanke et al., 2009). Furthermore it has been found that mutations in PV 3A confer resistance to BFA. Since FMDV differs to the enteroviruses in its resistance to BFA and FMDV 3A has a longer C terminal domain compared to other picornaviruses, it was thought that this extended region may provide another way to interact with GBF1 thus allowing FMDV to evade the effects of BFA. Therefore the effects on replication of replicons with large deletion in this region were tested in BFA treated BHK-21 cells.

The effects on FMDV replication of a second deletion, of 23 a.a that included the last 5 a.a of 3A and most of 3B1 except for the last 5 a.a was also investigated. This deletion was identified in a novel outbreak strain in South Korea that was discovered in pigs (Park et al, 2014). The FMDV genome is unusual as it encodes three non-identical copies of 3B (3B1, 3B2 and 3B3) (chapter 1 section 1.4.9) and the above deletion effectively removes the first copy (3B1). Studies with recombinant viruses have shown that FMDV remains replication competent when 3B1 or 3B2 are removed (Falk et al., 1992) or when only one copy of 3B is encoded as long as it is not 3B1 alone (Arias et al., 2010). In contrast, Pacheco *et al* found that a virus with only one copy of 3B (3B3) was able to replicate in porcine cells but not in bovine cells *in vitro*, suggesting that multiple copies of 3B are required for efficient virus replication in bovine cells (Pacheco et al., 2003). Here the effect of the 23 a.a deletion on

replication in porcine and bovine cells using replicons was investigated. The undeleted region of 3A was left as O1K (i.e. the sequence in our O1K Pt.GFP replicon) or changed to match that of the Korean virus (i.e. the virus identified with the 23 a.a deletion) and replicons with the deletion in each variation made (see section 3.6, figure 3.6.1).

Finally each of the deletions described above (the 57a.a deletion in 3A and the 23 a.a spanning 3A and 3B1) were introduced into infectious clones and recombinant viruses recovered using an established reverse genetics system. The recovered viruses were characterised to see if they exhibited the same replication characteristics as the replicons.

3.2 Effects of deletions in 3A on replication of FMDV replicons in different host cell lines.

To investigate whether an O1 Manisa virus with a large internal deletion in the C terminal region of 3A (FMDV O1Man Δ3A81-137) that was found within a mixed population of viruses with and without the deletion (see above), was able to replicate independently, the same deletion was made in the C-terminal coding region of 3A in an FMDV O1K replicon (FMDV O1K Pt.GFP). This replicon has Pt.GFP encoded in place of the majority of the FMDV capsid region and allows GFP expression to be used as an indirect measure of replication (Tulloch et al., 2014), (See chapter 2 section 2.2.1.2). In addition, all of the a.a that were different in the remaining part of 3A were also changed so that the 3A sequence in the replicon matched exactly that of the Δ3A deleted O1 Manisa virus (FMDV O1Man Δ3A81-137). In addition, a second deletion in 3A of a.a 93-143 (previously investigated by Pacheco *et al*) was also made in the FMDV O1K Pt.GFP replicon for use as an additional control (Pacheco et al., 2003). An alignment showing the differences in each of the 3A sequences compared to the sequence of O1K 3A (the 3A sequence found in the O1K Pt.GFP replicon) is shown in Figure 3.2.1.

```
WT O1K               ISIPSQKSVLYFLIEKGQHEAAIEFFEGMVHDSIKEELRPLIQQTSFVKRAFKRLKENFEIVALCLTLLANIVI
O1Man Δ3A81-137      ISIPSQKSVLYFLIEKGQHEAAIEFFEGMVHDSIKEELRPLIQQTSFVKRAFKRLKENFETVALCLTLLANIVI
O1K Δ3A81-137        ISIPSQKSVLYFLIEKGQHEAAIEFFEGMVHDSIKEELRPLIQQTSFVKRAFKRLKENFETVALCLTLLANIVI
O1K Δ3A93-143        ISIPSQKSVLYFLIEKGQHEAAIEFFEGMVHDSIKEELRPLIQQTSFVKRAFKRLKENFEIVALCLTLLANIVI


                     MIRETRKRQKMVDDAVNEYIEKANITTDDKTLDEAEKSPLETSGASTVGFRERTLPGQKACDDVNSEPAQPVEEQPQAE
                     MIRETR------------------------------------------------------------VSSEPAKPVEDRPQAE
                     MIRETR------------------------------------------------------------VSSEPAKPVEDRPQAE
                     MIRETRKRQKMVDDAVNE----------------------------------------------------QPVEEQPQAE
```

Figure 3.2.1: Alignment of 3A sequences from FMDV O1K and replicons and viruses with deletions in 3A. The alignment shows the 3A a.a sequences of (i) the WT O1K virus on which the O1K Pt.GFP replicon is based (blue), (ii) the virus with a large deletion in 3A that was isolated from a mixed population (O1Man Δ3A81-137) (purple), (iii) the sequence of 3A within the replicon after making the deletion found in O1Man Δ3A81-137 (red) and (iv) the 3A sequence of the replicon with the 93-143 deletion (O1K Δ3A93-143) (green). The predicted trans-membrane domain region of 3A is shown in black and residues differing between the O1K and O1Man Δ3A81-137 sequences are highlighted (yellow). These residues were changed in a version of the 81-137 deletion Pt.GFP replicon so the 3A sequence matched exactly that of the O1Man Δ3A81-137 sequence (the virus in which the deletion was found).

Equal amounts of *in vitro* transcribed RNA (500ng, quantified using a Qubit, (see chapter 2 section 2.2.4.2) from the WT replicon (O1K Pt.GFP) and the ∆3A replicons (O1K Pt.GFP ∆3A81-137 and O1K Pt.GFP ∆3A93-143) were transfected into BHK-21, SK-RST (porcine) and MDBK (bovine) cells. RNA from a fourth replicon, (O1K Pt.GFP GNN) with an inactive 3D polymerase was included and served as a control for GFP expression levels from non-replicating RNA. The natural fluorescence of GFP (GFP expression) was measured at hourly intervals and used as an indirect measure of RNA replication. Results from 3 independent experiments are shown in Figure 3.2.2.

I

II

III

A

BHK-21

BHK-21

BHK-21

B

SK-RST

SK-RST

SK-RST

C

MDBK

MDBK

MDBK

O1K Pt.GFP
O1K Pt.GFP GNN
O1K Pt.GFP Δ3A81-137
O1K Pt.GFP Δ3A93-143

55
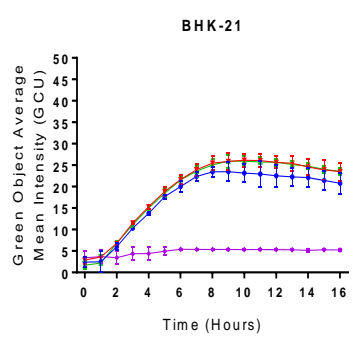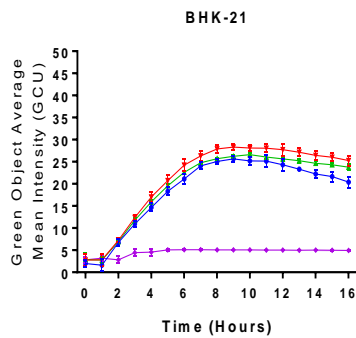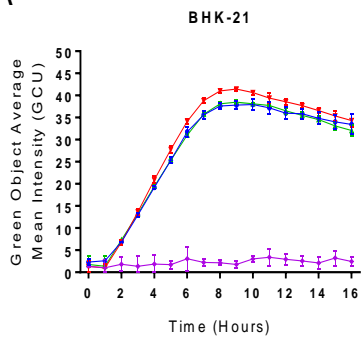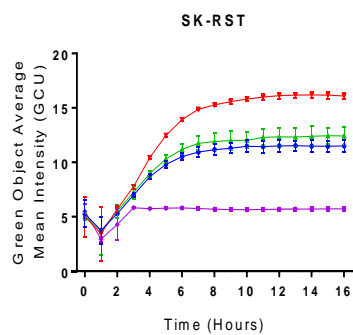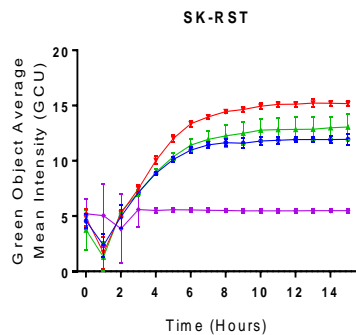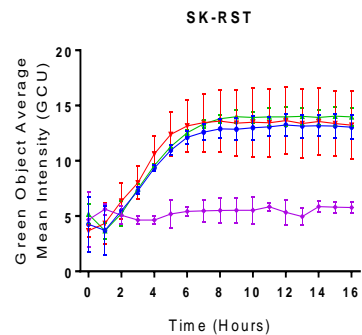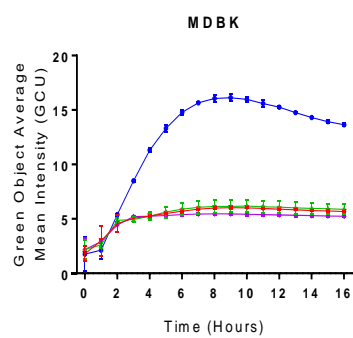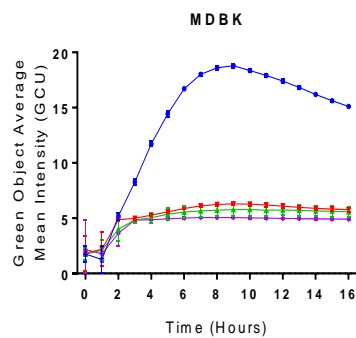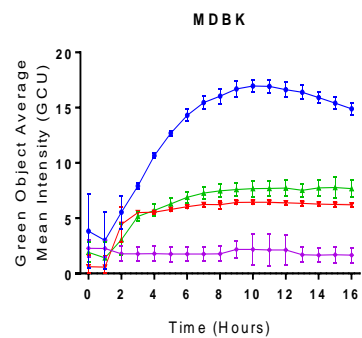
Figure 3.2.2: Effects of large deletions in 3A on replication in different host cell lines using GFP replicons. Triplicate wells of BHK-21, SK-RST and MDBK cells were transfected with 500ng of *in vitro* transcribed replicon RNA from 4 different replicons and average GFP intensity of the cells measured at hourly intervals to give an indirect measure of replication. Cells were transfected with either a wildtype (O1K Pt.GFP (blue)), 3D polymerase mutation control (O1K Pt.GFP GNN) (purple), or one of two replicons containing a deletion in 3A (O1K Pt.GFP Δ3A81-137 (red) and O1K Pt.GFP Δ3A93-143 (green). Graphs show results from 3 independent experiments each with triplicate samples (wells). Data points and error bars show mean +/- SD.

In BHK-21 cells (Fig 3.2.2 Panel A), the GFP intensity levels for the replicons with deletions in 3A (O1K Pt.GFP Δ3A81-137 and O1K Pt.GFP Δ3A93-143) were slightly higher than for the WT replicon (O1K Pt.GFP) in all 3 experiments. Similar results were seen in porcine SK-RST cells (Fig 3.2.2 Panel B), where GFP expression for the Δ3A replicons was again higher than for the WT replicon. The overall average GFP intensity for each replicon was lower in SK-RST cells compared to BHK-21 cells, suggesting that BHK-21 cells support higher levels of FMDV replication. In contrast, in the bovine MDBK cells (Figure 3.2.2 Panels C) only the WT replicon appeared to replicate efficiently as the signal from both O1K Pt.GFP Δ3A81-137 (red) and O1K Pt.GFP Δ3A93-143 (green) were reduced to the level of the O1K Pt.GFP GNN (purple) control in 2 of the experiments (Panels CII and CIII) suggesting that the GFP signal was the result of translation of the input RNA. In the other experiment (panel CI) the GFP signal for the Δ3A replicons was higher than that from the O1K Pt.GFP GNN control but in this experiment the signal from the O1K Pt.GFP GNN control was noticeably lower than in the other experiments. Nevertheless, the replicons with deletions in 3A were strongly attenuated in MDBK cells. In MDBK cells, the levels of the GFP signal (intensity) for O1K Pt.GFP were similar to that of SK-RST cells, but were reduced in comparison to that seen for BHK-21 cells.

A statistical analysis (One way ANOVA multiple comparisons with Tukey's correction) was carried out on the GFP intensity levels seen at the time (between 9 and 11 hours post-transfection) of peak GFP intensity of O1K Pt.

GFP (Figure 3.2.3). This analysis used combined data for each cell line from all 3 experiments, (Note in Figure 3.2.3, only significant differences are shown).
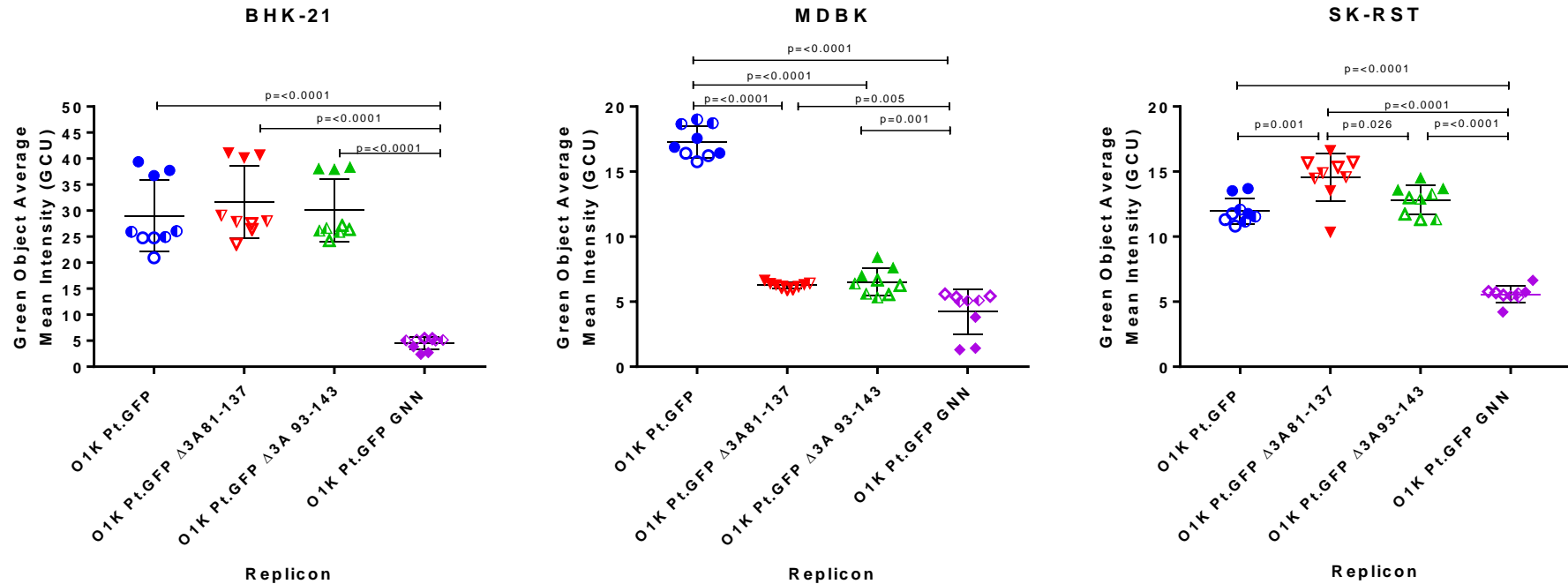
Figure 3.2.3: Effects on peak fluorescence and replication of deletions in 3A in different cell lines. Cellular GFP intensity data from the time point of peak fluorescence during the replicon time course assays (Figure 3.2.2) was used to compare replication in MDBK and SK-RST cells (One-way ANOVA with Tukey's correction). Data from 3 independent experiments each with triplicate samples was compared, solid symbols are replicates from experiment 1, half-filled symbols show replicates from experiment 2 and empty symbols show replicates from experiment 3. Lines and error bars show mean +/- SD. The p-value indicates statistical significance.

In BHK-21 cells significant differences in the GFP intensity levels were seen for the wildtype replicon (O1K Pt.GFP) and for the Δ3A replicons (O1K Pt.GFPΔ3A81-137 or O1K Pt.GFPΔ3A93-143) compared to the replication deficient O1K Pt.GFP GNN control. In contrast, there were no significant differences between the GFP intensity levels for the wildtype (O1K Pt.GFP) and the Δ3A replicons (O1K Pt.GFPΔ3A81-137 or O1K Pt.GFPΔ3A93-143) or between the two Δ3A replicons themselves (Figure 3.2.3 BHK-21) suggesting that all 3 replicons (with and without 3A deletions) replicate similarly in BHK-21 cells.

As seen in BHK-21, in SK-RST cells (Figure 3.2.3 SK-RST) all 3 replicons (O1K Pt.GFP, O1K Pt.GFP Δ3A81-137 and O1K Pt.GFP Δ3A93-143) showed significantly higher GFP intensity levels compared to the O1K Pt.GFP GNN control. In addition, a significant difference (p=0.001) was seen between O1K Pt.GFP and O1K Pt.GFP Δ3A81-137 and there was a small significant difference between the two replicons with Δ3A deletions (p=0.026). However, no significant difference was observed between O1K Pt.GFP and O1K Pt.GFP Δ3A93-143. This suggests that the 81-137 deletion in 3A may enhance replication in porcine cells.

In MDBK cells, the GFP signal intensity for the WT replicon (O1K Pt.GFP) was significantly higher than for Pt.GFP Δ3A81-137 or O1K Pt.GFP Δ3A93-143, which is consistent with the apparent attenuation of the Δ3A deleted replicons in these cells (Fig 3.2.2 MDBK). However, statistical significant differences in GFP intensity were also seen for each of the Δ3A deletion replicons compared to the GNN control (O1K Pt.GFP GNN) (p=0.005 and p=0.001 respectively), suggesting that although they are severely attenuated in MDBK cells, both Δ3A deleted replicons were replication competent in these cells.

The above observations show that both Δ3A deleted replicons can replicate efficiently in BHK-21 and porcine SK-RST cells but not in bovine MDBK cells. In addition, although the O1K Pt.GFP Δ3A93-143 replicon showed an apparent replication similar to the WT replicon (O1K Pt.GFP), the 3A deletion of a.a 81-137 appeared to result in enhanced replication in SK-RST cells. These

observations suggest viruses with the 81-137 a.a deletion in 3A would be capable of independent replication and furthermore that this deletion may enhance replication in pig cells while leading to severe attenuation of replication on bovine cells and therefore that full-length 3A may be required for FMDV replication in bovine cells.

3.3 Providing full length 3A in *trans* does not restore replication of replicons with deletions in 3A in MDBK cells

Previously it has been shown that certain mutations and deletions in Picornavirus genomes that cause attenuation can be overcome by providing the altered element in *trans* in the form of a helper virus or replicon. These include the *cre* of FMDV (Tiley et al., 2003) and also the 3AB protein of PV (Towner et al., 1998). Furthermore, other studies have shown that FMDV replicons containing insertions in 3A, that are lethal to replication, can be complemented and replication restored by supplying wildtype 3A in *trans* (Herod et al., 2015). In addition, Rosas *et al.* showed that infection of BHK-21 cell lines that stably expressed 3A led to an increase in virus yield and percentage of infected cells compared to infection of parental BHK-21 cells (Rosas et al., 2008).

Since the above deletions in 3A appear to negatively impact on FMDV replication in bovine (MDBK) cells it was decided to see if replication of the Δ3A deleted replicons could be restored by providing full length 3A in *trans*. RNA for each of the Δ3A-deleted replicons was co-transfected with either *in vitro* transcribed RNA from a "helper" replicon (O1K mCherry), containing full length 3A and an mCherry reporter gene in place of Pt.GFP, or yeast tRNA to ensure the same amount of RNA was transfected into each cell. A co-transfection using wildtype O1K mCherry and wildtype O1K Pt.GFP replicons was also included. Transfections were carried out in parallel in both MDBK cells and BHK-21 cells (BHK-21 cells were used as a positive control for replication of the Δ3A deletion replicons). The average cellular intensity levels of both GFP and mCherry were measured at hourly intervals.

I

II

III

A
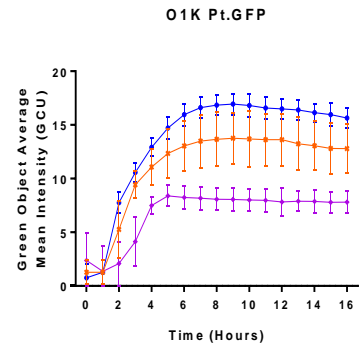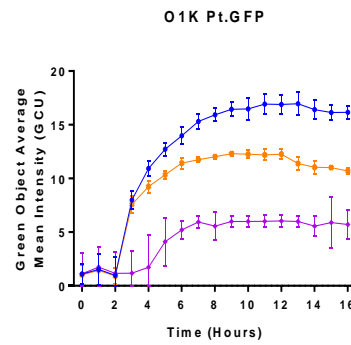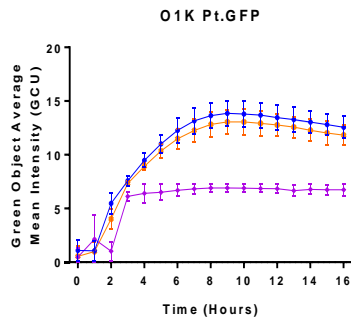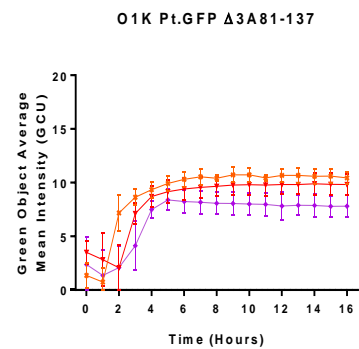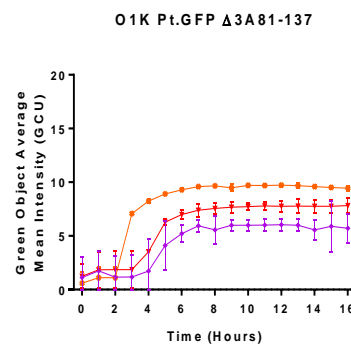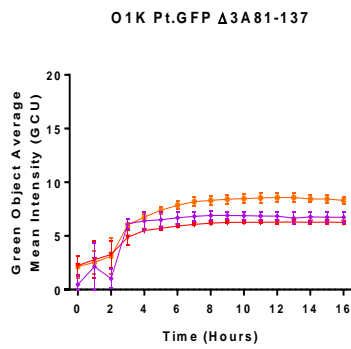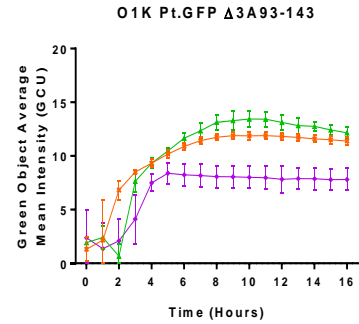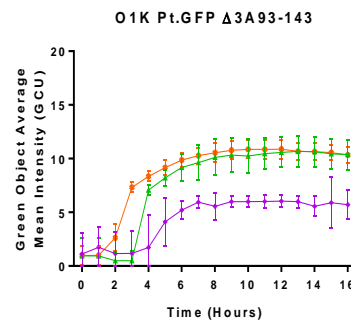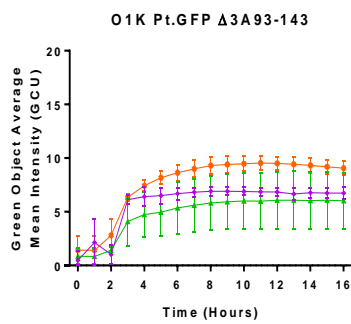
O1K Pt.GFP

O1K Pt.GFP

O1K Pt.GFP

B

O1K Pt.GFP Δ3A81-137

O1K Pt.GFP Δ3A81-137

O1K Pt.GFP Δ3A81-137

C

O1K Pt.GFP Δ3A93-143

O1K Pt.GFP Δ3A93-143

O1K Pt.GFP Δ3A93-143

Replicon	+yeast tRNA	+O1K mCherry (WT)
O1K Pt.GFP		
O1K Pt.GFPΔ3A81-137		
O1K Pt.GFPΔ3A93-143		
O1K Pt.GFP GNN		
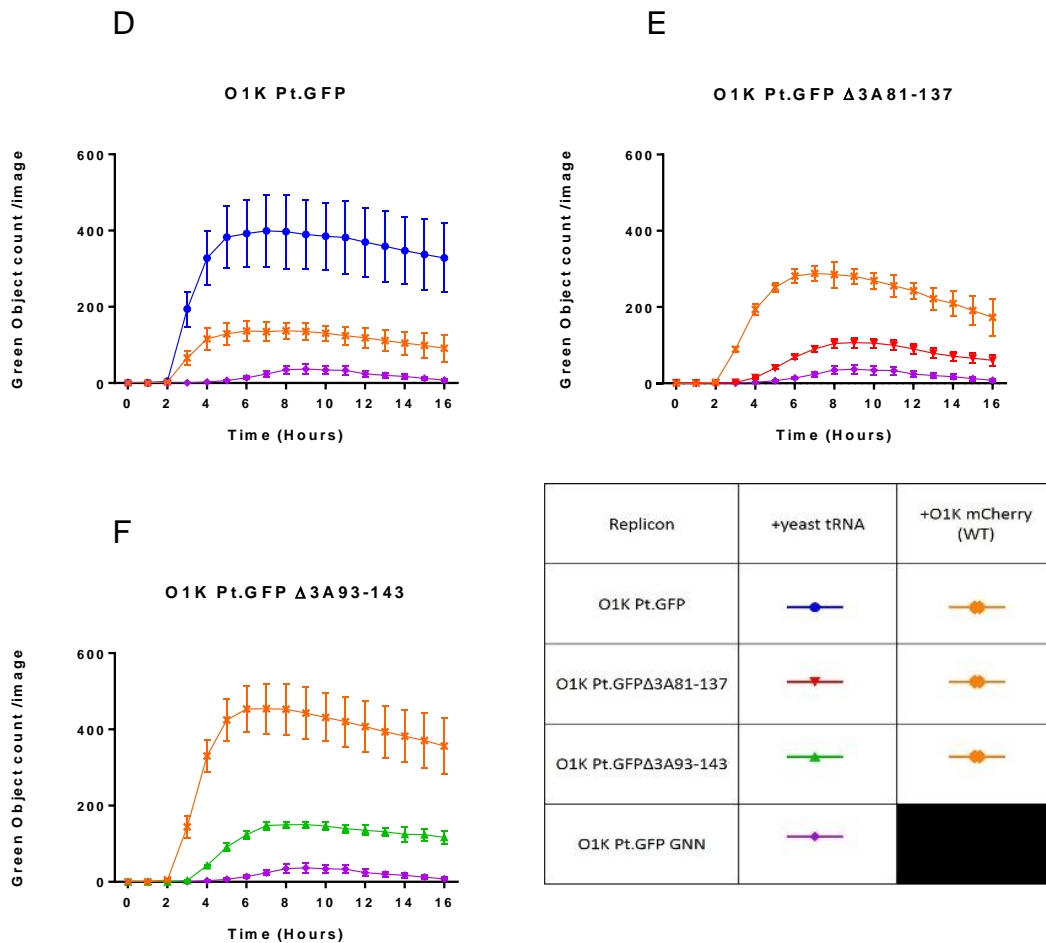
Figure 3.3.1: Effects of providing full length 3A in trans on replication of ∆3A replicons in MDBK cells. RNA from O1K Pt.GFP panels AI, AII and AIII, and ∆3A deletion replicons (indicated on panels BI, BII, BIII and CI, CII and CIII) were co-transfected with either yeast tRNA (blue (panel A), red (panel B) and green (panel C) or RNA from the wildtype O1K mCherry replicon containing full length 3A and an mCherry reporter gene in place of Pt.GFP (orange) (panels A, B and C) into MDBK cells. O1K Pt.GFP GNN (purple) (panels A, B and C) was transfected with yeast tRNA as a negative control for signal produced from translation of input RNA. Average cellular GFP intensity (Panels A, B and C) was measured at hourly intervals for 16 hours, in 3 independent experiments each with triplicate samples. Data points and error bars show the mean +/- SD. The number of Pt. GFP expressing cells per image was also calculated (panels D, E and F) and the results shown for one representative experiment of the three experimental repeats. Data points and error bars show mean +/- SD.

Figure 3.3.1 shows results from 3 independent experiments carried out with triplicate wells for each condition using MDBK cells. Panels AII and AIII showed

a clear decrease in GFP intensity levels when the O1K Pt.GFP replicon was co-transfected with the O1K mCherry replicon when compared to when co-transfection with yeast tRNA, possibly due a competition effect for limited cellular resources and factors required for FMDV replication. A similar but smaller decrease in GFP intensity was seen in experiment 1 (panel AI).

Figure 3.3.1 panel B shows results for co-transfection using O1K Pt.GFP Δ3A81-137. In all 3 experiments (BI, B II and BIII) the GFP intensity signal showed a slight improvement when co-transfected with the O1K mCherry replicon over co-transfection with yeast tRNA). The results from co-transfection using O1K Pt.GFP Δ3A93-143 were inconsistent and difficult to interpret, as the GFP intensity level showed an increase when co-transfected with O1K mCherry in experiment 1 (panel CI), was similar in experiment 2 (panel CII) and a decrease in experiment 3 (panel CIII) when compared to the level seen when co-transfected with yeast tRNA. The number of GFP expressing cells was also investigated to see if an increase in the number of green objects was observed when the Δ3A deletion replicons were co-transfected with O1K mCherry, as this could also indicate possible trans-complementation. Figure 3.3.1 panels D, E and F show the data for one experiment as the number of GFP expressing cells per image counted at hourly intervals for O1K Pt.GFP, O1K Pt.GFPΔ3A81-137, and O1K Pt.GFP Δ3A93-143 respectively. Similarly to what was seen with GFP intensity levels (in panels AII and AIII), panel D shows the number of GFP expressing cells decreased when O1K Pt.GFP was co-transfected with O1K mCherry replicon compared to when co-transfected with yeast tRNA, which fits with the theory that two replication competent replicons are competing for cellular resources. Panels E and F show that there was an increase in the number of GFP expressing cells when each of the Δ3A deletion replicons were co-transfected with O1K mCherry (orange lines) suggesting that there could be a possible "helper" effect from the O1K mCherry 3A that results in improved replication, as more GFP positive cells are seen, but the effects on replication is still likely to be relative small as there was not a major effect on GFP intensity levels.

The above experiments were also carried out in parallel with BHK-21 cells, to test if any effects on replication were seen when co-transfecting replicons in a cell line where the ∆3A deletion replicons were replication competent. Figure 3.3.2 shows that for all 3 replicons (O1K Pt.GFP, O1K Pt.GFP∆3A81-137, and O1K Pt.GFP ∆3A93-143) a drop in GFP intensity levels was seen when co-transfected with the O1K mCherry replicon compared to yeast tRNA. This is similar to the results seen for the two wildtype replicons (O1K Pt.GFP with O1K mCherry) in MDBK cells (Figure 3.3.1, panels AII and AIII) and is potentially due to a competition effect, as all the replicons are replication competent in BHK cells and there is likely competition for cellular factors required for replication leading to a drop in GFP intensity levels produced from cells transfected with both replicons

.

I

II

III

A

O1K Pt.GFP

O1K Pt.GFP

O1K Pt.GFP (WT)

B

O1K Pt.GFP Δ3A81-137

O1K Pt.GFP Δ3A81-137

O1K Pt.GFP Δ3A81-137

C

O1K Pt.GFP Δ3A93-143

O1K Pt.GFP Δ3A93-143

O1K Pt.GFP Δ3A93-143

Replicon	+yeast tRNA	+O1K mCherry (WT)
O1K Pt.GFP		
O1K Pt.GFPΔ3A81-137		
O1K Pt.GFPΔ3A93-143		
O1K Pt.GFP GNN		

Figure 3.3.2: Effects of providing full length 3A in *trans* on replication of ∆3A replicons in BHK-21 cells. RNA transcribed from O1K Pt.GFP (panels AI, AII and AIII), and the indicated ∆3A deletion replicons (panels BI, BII, BIII and CI, CII and CIII) were co-transfected into BHK-21 cells with either yeast tRNA (blue (panel A), red (panel B) and green (panel C) lines) or RNA from an mCherry replicon containing full length 3A (orange lines panels A, B and C). The O1K Pt.GFP GNN (purple) (Panels A, B and C) was transfected with yeast tRNA as a negative control for signal produced from translation of input RNA. Average cellular GFP intensity was measured at hourly intervals for 16 hours, in 3 independent experiments each with triplicate samples. Data points and error bars show mean +/- SD

A statistical analysis (One way ANOVA multiple comparisons with Tukey's correction) was carried out on the data for the time point (9 to 11 hours post transfection dependent on experiment) when the GFP intensity levels peaked for co-transfection of O1K Pt.GFP with yeast tRNA (Note on Figure 3.3.3, only significant differences between each replicon when co-transfected with yeast or O1K mCherry are shown). In MDBK cells, there was a significant difference ($p=0.001$) between the GFP intensity levels for the O1K Pt.GFP replicon when co-transfected with yeast tRNA(blue symbols) or O1K mCherry replicon RNA (orange symbols), indicating a significant reduction in replication when the two wildtype replicons are co-transfected. However there was no significant difference for either of the ∆3A deletion replicons when co-transfected with yeast tRNA compared to when co-transfected with O1K mCherry replicon RNA.
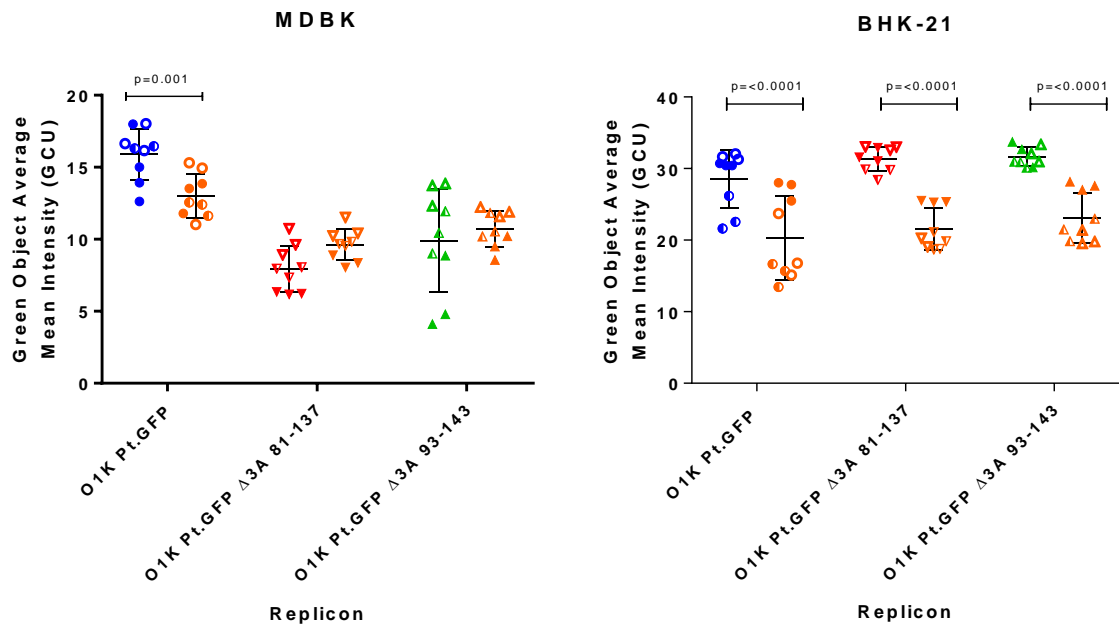
Figure 3.3.3: Effects on peak GFP intensity levels of supplying full length 3A in trans within a helper mCherry replicon. O1K Pt.GFP or the replicons with deletions in 3A were co-transfected into MDBK or BHK-21 cells with the wildtype O1K mCherry replicon (orange symbols) or with yeast tRNA (blue, red and green symbols). GFP intensity levels at time point of peak GFP intensity (between 9 and 11 hours depending on experiment) of O1K Pt.GFP co-transfected with yeast tRNA from 3 independent experiments (each with triplicate samples) were compared (One-way ANOVA, Tukey's correction). Filled symbols show replicates from experiment 1, half-filled symbols show replicates from experiment 2 and empty symbols show replicates from experiment 2 and empty symbols show replicates from experiment 3

In BHK-21 cells there was a significant difference between intensity levels of each of the GFP replicons when they were co-transfected with yeast (blue, red and green symbols) in comparison to when co-transfected with the wildtype O1K mCherry replicon (orange symbols).

Overall these results show that large deletions (a.a 81-137 and a.a 93-143) in the C terminal domain of 3A cannot be complemented efficiently by full-length 3A provided in *trans* by a helper replicon.

3.4 Effects of Brefeldin A (BFA) on replication of FMDV replicons with deletions in 3A

FMDV has previously been reported to be resistant to BFA (Midgley et al., 2013, Martin-Acebes et al., 2008, O'Donnell et al., 2001). To test if the 81-137 and 93-143 a.a deletions in 3A, (shown in Figure 3.2.1), led to sensitivity to BFA, BHK-21 cells were pre-treated with BFA (5 μg/ml) or, DMSO (the solvent carrier) for 15 minutes at 37°C or were left untreated before being transfected with RNA from O1K Pt.GFP, O1K Pt.GFP GNN, O1K Pt.GFP Δ3A81-137 or O1K Pt.GFP Δ3A93-143 replicons. The average GFP intensity of cells was measured hourly for a period of 16 hours (Figure 3.4.1).
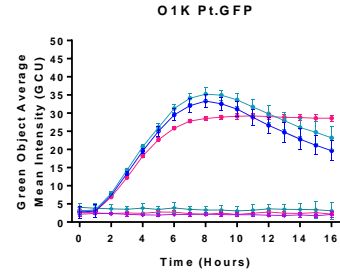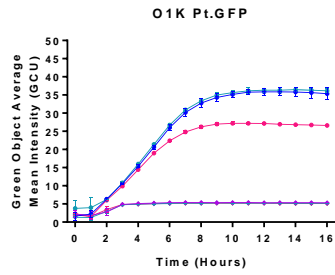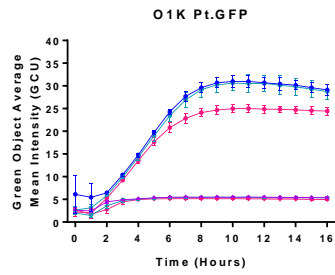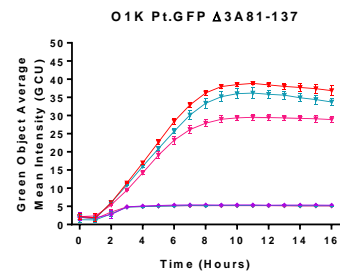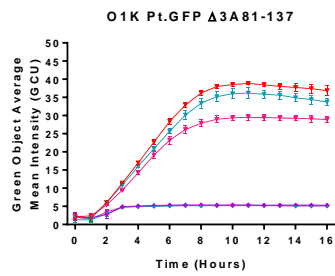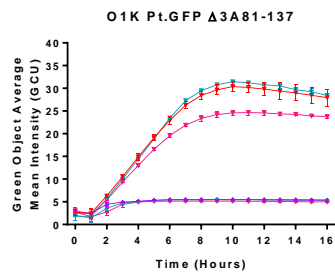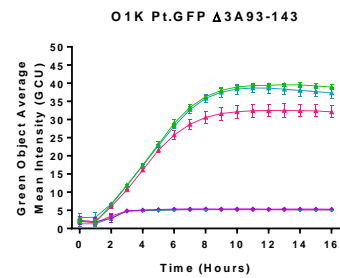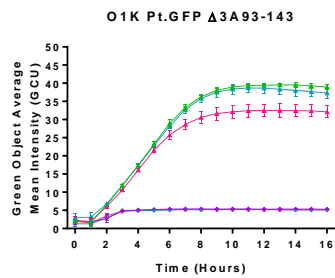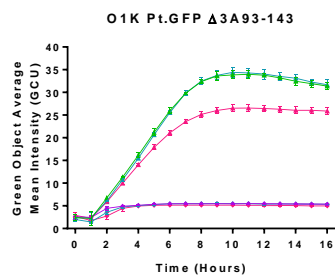
Replicon	Untreated	+DMSO	+BFA
O1K Pt.GFP	●	●	●
O1K Pt.GFPΔ3A81-137	▼	▼	▼
O1K Pt.GFPΔ3A93-143	▲	▲	▲
O1K Pt.GFP GNN	◆	◆	◆
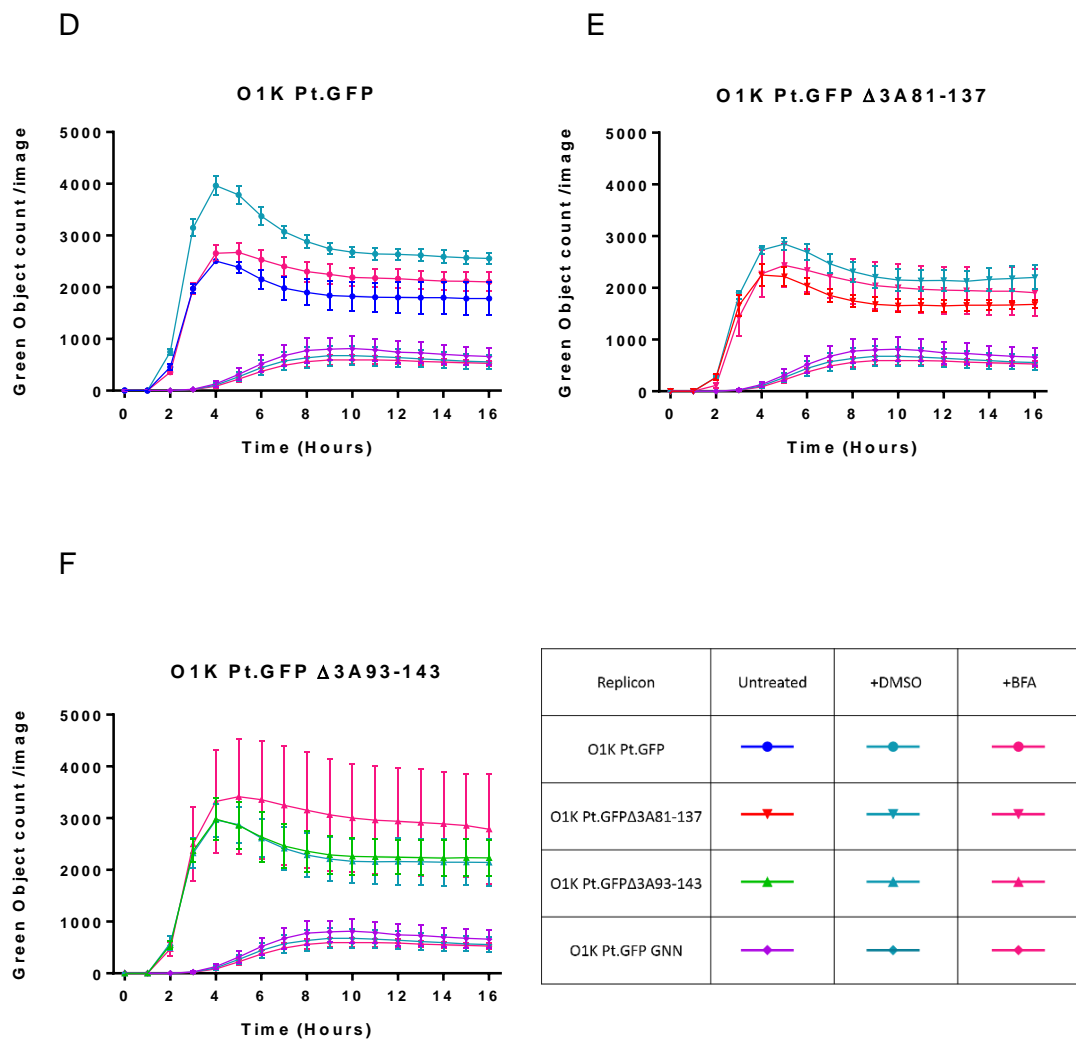
Figure 3.4.1: Effects of BFA on replication of FMDV replicons with deletions in 3A. BHK-21 cells were pre-treated with BFA (5μg/ml), DMSO or left untreated for 15 minutes prior to transfection with *in vitro* transcribed RNA from the O1K Pt.GFP (panel A), Δ3A deleted replicons (panels B and C) or the O1K Pt.GFP GNN replicons (panels A, B and C). Shown are the results from 3 independent experiments each with triplicate samples. Intensity levels for cells treated with DMSO are shown in pale blue and for cells treated with BFA in pink. Intensity levels for cells left untreated are shown in dark blue, red, green and purple for O1K Pt.GFP, O1K Pt.GFPΔ3A81-137, O1K Pt.GFPΔ3A93-143 and O1K Pt.GFP GNN respectively. The number of GFP expressing cells per image was also quantified (panels D-F) to determine the effects of treatment with DMSO and BFA on transfection efficiency. Results from one representative experiment are shown in panels D (O1K Pt.GFP), E (O1K Pt.GFPΔ3A81-137) and F (O1K Pt.GFPΔ3A93-143). Data points and error bars show the mean +/- SD.

Results from 3 independent experiments are shown in Figure 3.4.1. For all 3 replicons, (Panel A, O1K Pt.GFP, panel B, O1K Pt.GFP Δ3A81-137 and panel C O1K Pt.GFP Δ3A93-143) and for each experiment, there was a noticeable decrease in GFP intensity levels, (indicating an inhibitory effect on replication) when the cells were pre-treated with BFA. There was little differences seen in GFP intensity between cells pre-treated with DMSO or cells left untreated in any of the experiments suggesting the apparent inhibitory effects on replication seen with BFA were not due to the solvent carrier. No effect of BFA treatment was observed on the GFP intensity levels of cells transfected with RNA from O1K Pt.GFP GNN replicon suggesting that BFA did not affect replicon RNA translation. As FMDV has been reported to be insensitive to BFA the results for the wildtype O1K Pt.GFP replicon was unexpected (see section 3.8, Discussion).

It is possible that the apparent inhibitory effect of BFA on replication could result from BFA having an effect on the transfection efficiency. Therefore the number of GFP expressing cells per image was also quantified to check if the pre-treatment conditions (DMSO or BFA) had an effect on transfection efficiency. Figure 3.4.1 panels D, E and F show representative results from one experiment. The number of GFP expressing cells transfected with O1K Pt.GFP GNN was similar regardless of the pre-treatment showing translation was not affected. The number of GFP expressing cells for O1K Pt.GFP, and the Δ3A deleted replicons were all higher in cells pre-treated with BFA than cells which were untreated. In DMSO treated cells, the number of GFP expressing cells was higher than both the BFA treated and untreated cells for the O1K Pt.GFP and O1K Pt.GFP Δ3A81-137 replicons (panels D and E) and was similar to the untreated cells for O1K Pt.GFP Δ3A93-143 (panel F). Together, these observations suggest that pre-treatment with BFA was not having a negative effect on transfection efficiency of replicon RNA.

A statistical analysis (One way ANOVA multiple comparisons with Tukey's correction) was carried out using the data from the time point (9 to 10 hours post transfection dependent on experiment) where the GFP intensity levels from

untreated cells transfected with O1K Pt.GFP replicon RNA were at their peak Figure 3.4.2).
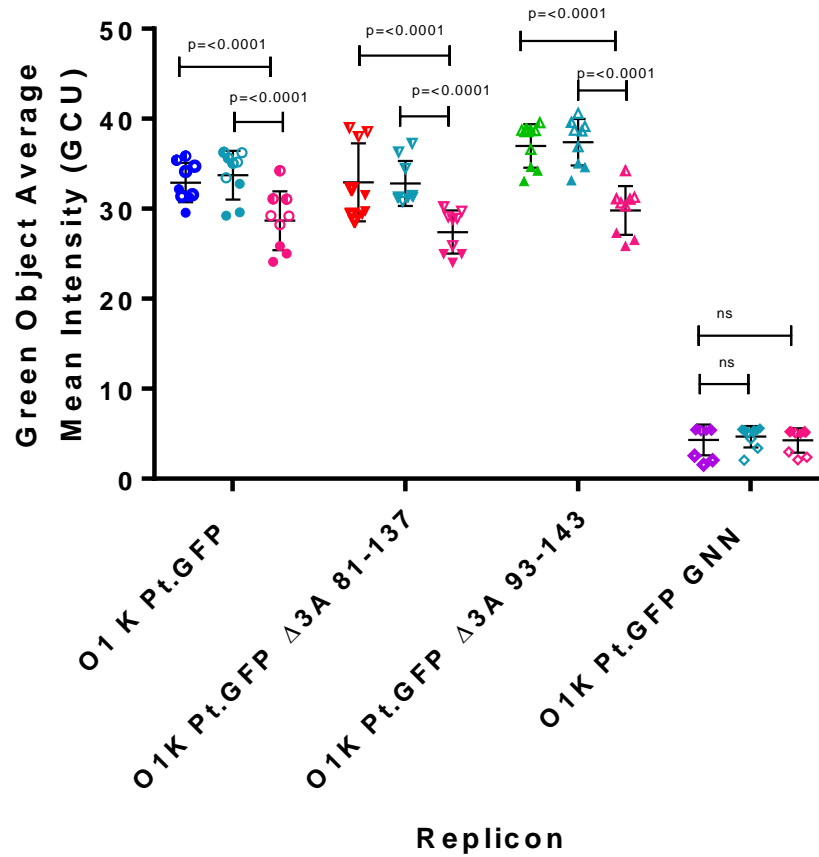
Figure 3.4.2: Effects of BFA on replication of FMDV replicons with deletions in 3A: Cells were pre-treated with DMSO or BFA or left untreated and transfected with RNA from the O1K Pt.GFP, the Δ3A deleted replicons or O1K Pt.GFP GNN replicons and GFP intensity measured over time. Data from the time point at which the GFP intensity levels of the untreated cells transfected with O1K Pt.GFP peaked was compared (One way ANOVA,

Tukey's correction). Significant differences were seen for each replicon between replication (apart from O1K Pt.GFP GNN) in the cells pre-treated with BFA compare to the untreated cells or cells pre-treated with DMSO. No significant difference in replication was seen between cells pre-treated with DMSO or those left untreated. Shown are results from 3 independent experiments each with triplicate samples. Data for cells treated with DMSO are shown in pale blue and for cells treated with BFA in pink. Filled symbols show replicates from experiment 1, half-filled symbols show replicate from experiment 2 and empty symbols show replicates from experiment 3.

Figure 3.4.2 shows there was a significant decrease (p=<0.0001) between GFP intensity levels for each of the replicons between untreated cells (blue, red and green symbols) or DMSO treated cells (pale blue symbols) with cells pre-treated with BFA (pink symbols) for O1K Pt.GFP and the Δ3A deletion replicons. As expected significant differences were not seen between untreated and DMSO pre-treated cells confirming that the inhibitory effects on replication is due to BFA and not the solvent carrier (DMSO). No significant effect was seen between the GFP intensity levels for the O1K Pt.GFP GNN replicon regardless of cell treatment suggesting that pre-treatment with BFA does not affect translation.

3.5 Virus recovery and characterisation of viruses with deletions in 3A on different cell lines

The above results report the effect on FMDV replication of deletions involving 3A in cells derived for the porcine and bovine hosts of FMDV by using sub-genomic replicons. To further test if the virus containing the 3A deletion (a.a 81-137) could replicate independently, and if it has the same replication characteristics as the replicon in different host cell lines, replicons O1K Pt.GFP, Pt.GFP Δ3A81-137 and O1K Pt.GFP Δ3A93-143 were converted into full length infectious genomes. This was done by replacing the region encoding the Pt.GFP reporter gene in the replicon plasmids with the capsid coding region from the FMDV O1K infectious clone. The resulting infectious copy plasmids were used as a template to transcribe vRNA *in vitro,* which was then transfected into T25 flasks of BHK-21 cells and the flasks monitored for up to 48 hours for

the appearance of CPE. At CPE (or at 48 hours post transfection), the cells were freeze-thawed and clarified cell supernatants passaged onto fresh BHK-21 cells. Following 2 passages (BHKp2), RNA was extracted from the infected cell lysate, reverse transcribed to make ss cDNA and used as the template in a PCR reaction using primers that annealed in the 2C and 3C coding regions. The PCR products were gel extracted and sequenced using primers internal to the PCR product. All 3 viruses (O1K WT, O1KΔ3A81-137 and O1KΔ3A93-143) were successfully recovered, and the sequence data showed that the 3A region (including the deletions) was stably maintained.

The recovered viruses (O1K WT, O1KΔ3A81-137 and O1KΔ3A93-143) at (BHKp2) were titrated by plaque assay on BHK-21, MDBK and IBRS2 (a porcine kidney cell line, known to be infected efficiently by FMDV) cells and the virus titres are shown in Table 3.5.1. Consistent with previous reports showing that the 93-143 deletion in 3A attenuates replication in bovine cells (Pacheco et al., 2003), the O1KΔ3A93-143 virus gave no visible plaques in MDBK cells, whereas plaques caused by the O1KΔ3A81-137 virus were small, indistinct, and difficult to quantify. Nevertheless, the MDBK titre for the O1KΔ3A81-137 virus was much lower than for the wildtype virus. In contrast, all 3 viruses showed similar titres in BHK-21 and IBRS2 cells. These results are consistent with those seen using GFP replicons (section 3.2) and confirm that the deletions in 3A attenuate replication in MDBK cells but not in porcine or BHK-21 cells.

Virus	Virus Titre (log10 pfu/ml)		
	BHK-21	IBRS2	MDBK
O1K WT	1.3×10^7	6.5×10^7	1.3×10^6
O1K Δ3A81-137	1.5×10^7	3.2×10^6	8×10^2
O1K Δ3A93-143	1×10^7	2.2×10^7	No plaques

Table 3.5.1: Viral titres of passage 2 (BHKp2) viruses on different cell lines. Viral supernatants from infected BHK-21 (BHKp2) cells were titrated by plaque

assay on BHK-21, IBRS2 and MDBK cells in duplicate and an average titre calculated.

The reason for the apparent attenuation of the 3A-deleted viruses in bovine cells is unclear and it is possible that the reduced replication could be due to a difference in the innate immune response between cell lines used allowing viruses to grow to a higher titre in BHK-21 and IBRS2 cells. Therefore, to confirm the attenuation in bovine cells it was decided to further investigate replication using primary bovine thyroid cells (BTY), which are highly sensitive to FMDV infection and routinely used in FMD diagnosis (Ferris et al., 2002). Triplicate wells of IBRS2 and BTY cells were infected at an MOI of 1 (based on original end point titres from BHK-21 cells, see Table 3.5), with each of the viruses, O1K WT, O1KΔ3A81-137 or O1KΔ3A93-143 (BHKp2) for 8 hours. The cells were freeze thawed and cell supernatants collected. Figure 3.5.1 shows viral titres (using BHK-21 cell monolayers) for each virus prepared in IBRS2 or BTY cells.
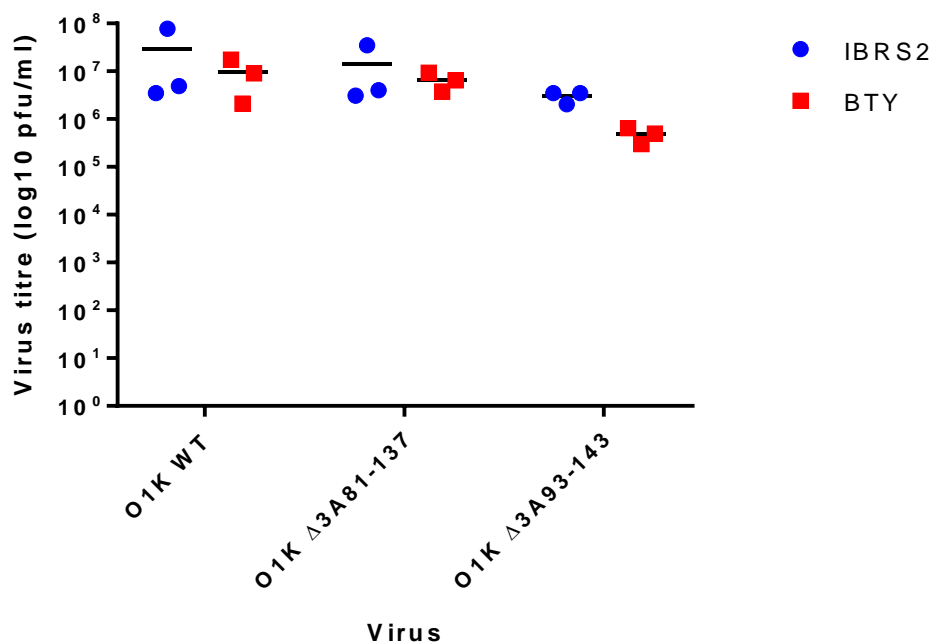
Figure 3.5.1: Effects of deletions in FMDV 3A on viral growth in different host cells. Infectious viruses with deletions in 3A (residues 81-137 or 93-143) were recovered in BHK-21 cells to passage 2 (BHKp2) and used to infect triplicate wells of IBRS2 and BTY cells at an MOI of 1 for 8 hours. Infected supernatant was collected and viral titre calculated by plaque assay for each sample on BHK-21 cells. Comparison of means (One way ANOVA with Tukey's correction) showed no significance between viral titres for FMDV O1K WT or either of the Δ3A deleted viruses between cell types.

This experiment showed the end point titres (i.e. at 8h post infection) for O1K WT and O1KΔ3A81-137 were similar when the viruses were passed through IBRS2 or BTY cells while the titres of the O1KΔ3A93-143 were slightly reduced in both cell types when compared to the other viruses. Furthermore, although for each virus the titre on BTY cells was lower that on IBRS2 cells there was no significant difference seen (when analysed by one way ANOVA, Tukey's correction) (Figure 3.5.1).

Together, the above experiments show that the viruses with 3A deletions could be recovered and appear to grow well in one bovine cell type (BTY) but are

potentially attenuated in another (MDBK). Presently it is not clear why this should be so; however, it could suggest that the innate immune status of the cells themselves rather than what host species they are derived form could be contributing to the attenuation of the replicons and viruses with deletions in 3A seen in MDBK cells. However, the results shown in Figure 3.5.1 are based on end point titres (the virus titre is calculated on BTY and IBRS2 cells at 8 h post-transfection) and therefore can only be interpreted to show that the viruses with 3A deletions are competent for replication in porcine and bovine cells and do not inform on the relative fitness of the viruses in porcine and bovine cells (see Discussion).

3.6 Effects of a deletion spanning the end of 3A and majority of 3B1 on replication of FMDV replicons in different host cell lines

FMDV is unusual among picornaviruses in that it encodes three copies of VPg (or 3B) yet recombinant viruses with one copy removed remain replication competent (Falk et al., 1992, Pacheco et al., 2003, Pacheco et al., 2010). Here the effects on FMDV replication of a 23 a.a deletion spanning the C terminal end of 3A and most of 3B1 was investigated (Figure 3.6.1). This deletion removes the last 5 a.a. of 3A and all of 3B1 except for the last 5a.a at the carboxyl terminal end and therefore, effectively removes the first copy of VPg (3B1) and was identified in a virus (O/SKR/6/2014) isolated from pigs in South Korea. Interestingly, the outbreak affected both cattle and pigs but when tested the virus appeared to have a low pathogenicity in pigs (Park et al., 2016).

This deletion was made in the O1K Pt.GFP replicon (Figure 3.6.1) creating O1K Pt.GFPΔ3B1. A second replicon (Pt.GFP SKRΔ3B1) with this deletion was also made that had further a.a changes in the remaining part of 3A so that it matched exactly the sequence of the South Korean virus in 3A. A third replicon was made that had full-length 3A using the 3A sequence (O1K Pt.GFP SKR+3B1) from a closely related strain to the South Korean virus (O/HKN15/2010). The sequence of 3A for each of the above replicons is shown in Figure 3.6.1.

```
O1K WT:    I S I P S Q K S V L Y F L I E K G Q H E A A I E F F E G M V H D S I K E E L R P L I Q Q T S F V K R A
SKRΔ3B1:   I S I P S Q K S V L Y F L I E K G Q H E A A I E F F E G M V H D S V K E E L R P L I Q Q T S F V K R A
SKR+3B1:   I S I P S Q K S V L Y F L I E K G Q H E A A I E F F E G M V H D S V K E E L R P L I Q Q T S F V K R A
O1KΔ3B1:   I S I P S Q K S V L Y F L I E K G Q H E A A I E F F E G M V H D S I K E E L R P L I Q Q T S F V K R A


F K R L K E N F E I V A L C L T L L A N I V I M I R E T R K R Q K M V D D A V N E Y I E K A N I T T D D K T L
F K R L K E N F E V V A L C L T L M A N I V I M I R E T R K R Q Q M V D D A V N E Y I E R A N I T T D D K T L
F K R L K E N F E V V A L C L T L M A N I V I M I R E T R K R Q Q M V D D A V N E Y I E R A N I T T D D K T L
F K R L K E N F E I V A L C L T L L A N I V I M I R E T R K R Q K M V D D A V N E Y I E K A N I T T D D K T L


D E A E K S P L E T S G A S T V G F R E R T L P G Q K A C D D V N S E P A Q P V E E Q P Q A E G P Y A G P L
D E A E K N P L E T S G A S T V G F R E R T L P G R K V G D D V S Y E P A H P G D E - - - - - - - - -- -- -
D E A E K N P L E T S G A S T V G F R E R T L P G R K V G D D V S Y E P A H P G D E Q P Q A E G P Y A G P L
D E A E K S P L E T S G A S T V G F R E R T L P G Q K A C D D V N S E P A Q P V E E - - -- - -- - - - - - -


  E R Q K P L K V R A K L P Q Q E
  - - - - - - - - - - - - L P Q Q E
  E R Q K P L K V R A K L P Q Q E
  - - - - - - - - - - - - L P Q Q E
```

Figure 3.6.1: Sequence alignment showing 3A and 3B1 region of replicons with a 23 a.a deletion in the C terminal end of 3A and majority of 3B1. The deletion identified in the O/SKR/6/2014 virus isolate was made in 2 different replicons. O1KΔ3B1 (shown in orange) where the 23 a.a deletion was made in the existing FMDV O1K Pt.GFP replicon (which is based on O1K), and SKRΔ3B1 (shown in green) which had both the deletion and the residues that differed between the O1K and O/SKR/6/2014 sequences in the remaining region of 3A altered to match those of the O/SKR/6/2014 virus. SKR+3B1 is shown in grey and, has the same sequence as SKRΔ3B1 but with the deletion repaired using the sequence of a closely related virus O/HKN15/2010. The 3B1 region is shown outlined in red.

RNA from each of the 3 replicons Pt.GFP O1KΔ3B1, Pt.GFP SKRΔ3B1 and Pt.GFP-SKR+3B1 was transfected into BHK-21, MDBK, and SK-RST cells. In addition the wildtype O1K Pt.GFP and polymerase knockout (O1K Pt.GFP GNN) replicons were included as controls. The GFP intensity was measured at hourly intervals over a 16 hour period and the results from 3 independent experiments are shown in Figure 3.6.2.

I

II

III

A

BHK-21

BHK-21

BHK-21

B

SK-RST

SK-RST

SK-RST

C

MDBK

MDBK

MDBK
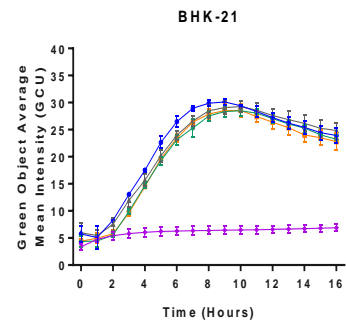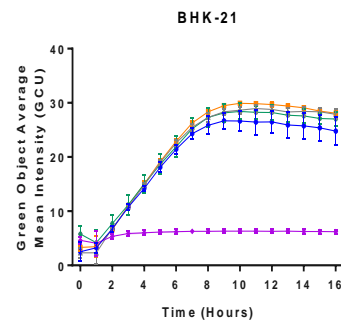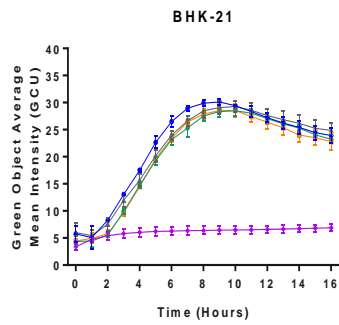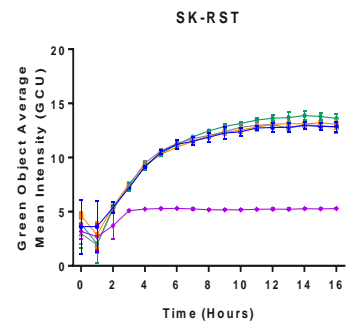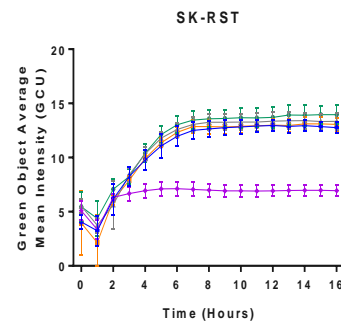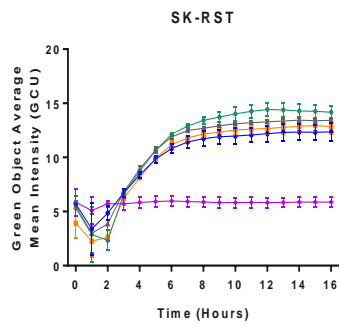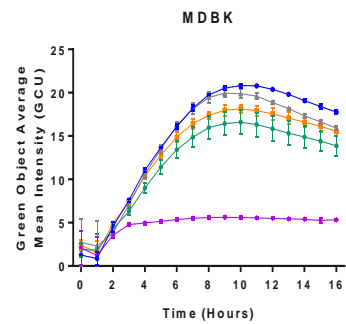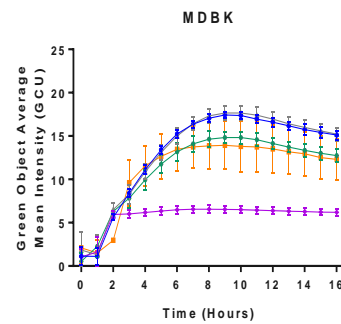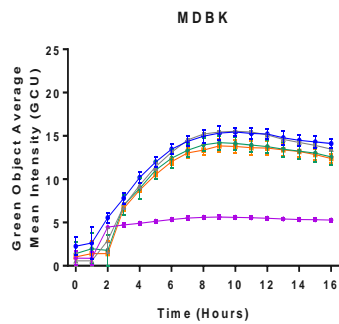
- ● O1K Pt.GFP WT
- ● O1K Pt.GFP GNN (3D pol mut)
- ▲ Pt.GFP SKR+3B1
- ● Pt.GFP SKRΔ3B1
- ■ O1K Pt.GFP Δ3B1

Figure 3.6.2: Effects of a 23 a.a deletion in the C terminal domain of 3A and 3B1 on replication in different cell lines. RNA from 5 replicons, 2 with full length 3A and 3B1 (O1K Pt.GFP and Pt.GFP SKR+3B1), and two variants with a 23 a.a deletion in 3A and 3B1 (O1K Pt.GFP Δ3B1 and Pt.GFP SKRΔ3B1) and the translation only control O1K Pt.GFP GNN was transfected into either BHK-21, SK-RST or MDBK cells. The average GFP intensity levels were measured at hourly intervals as an indirect measure of replication. Shown are the results from 3 independent experiments with triplicate sample. Data points and error bars show the mean +/- SD.

In BHK-21 and porcine SK-RST cells, each of the replicons with the deletion (O1K Pt.GFP Δ3B1, O1K Pt.GFP SKRΔ3B1) showed little difference in replication (i.e. the GFP intensity) to their matched wildtype replicons (O1KPt.GFP and Pt.GFP SKR+3B1) suggesting that this deletion was not detrimental for replication in these cell lines. In contrast, in two of the experiments (panels CII and CIII) with MDBK, the replicons with the deletion showed a lower level of GFP intensity compared to the respective matched wildtype replicons (O1K Pt.GFP and Pt.GFP SKR+3B1) whereas in experiment 1 (panel CI) the GFP intensity levels were more similar to the replicons without the deletion.

Data from the time of peak GFP intensity levels (9 to 10 hours post transfection) of O1K Pt.GFP for each cell line was compared (One way ANOVA, Tukey's correction) and is shown in Figure 3.6.3. In BHK-21 cells the only significant differences seen were between each of the 4 replicons and the Pt.GFP GNN translation control. This was also seen in SK-RST and MDBK cells (not shown on the figure).
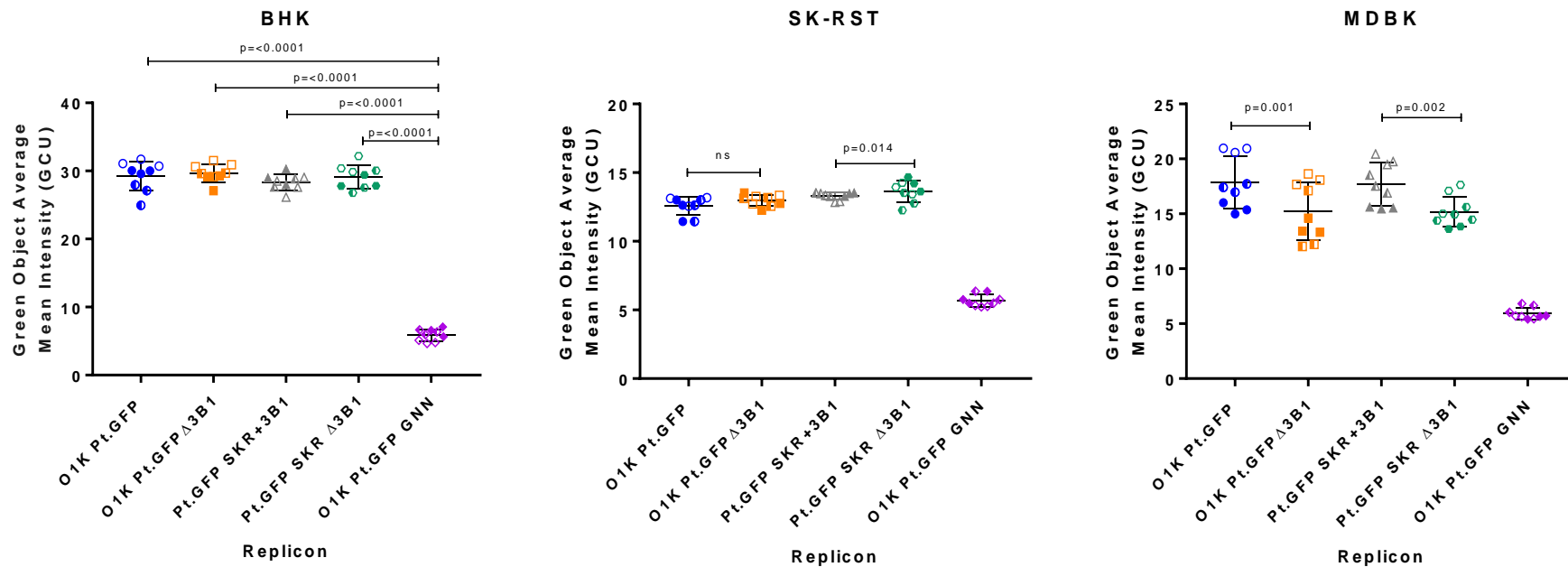
Figure 3.6.3: Effects on replication of a 23 a.a deletion in 3A and 3B1 in different cell lines. Average GFP intensity data from the time point (9 or 10 hours post transfection dependent on experiment) of peak fluorescence of Pt.GFP (WT) during replicon time course assays (see Figure 3.6.2) was used to compare differences between GFP intensity levels of the different replicons with each other (One-way ANOVA, Tukey's correction). All data from 3 independent experiments, each with triplicate samples was compared. Solid symbols are replicates from experiment 1, half-filled symbols show replicates from experiment 2 and empty symbols show replicates from experiment 3. Lines and error bars show mean +/- SD. For clarity only significant differences between matched pairs of replicons are shown on the MDBK and SK-RST graphs.

In SK-RST there was also a relatively small but significant difference in GFP intensity levels between the Pt.GFP SKR+3B1 replicon and its deleted counterpart, Pt.GFP SKRΔ3B1 (p=<0.014), which suggested that the deleted replicon was replicating better than the wildtype replicon (Pt.GFP SKR+3B1) in porcine cells. However, this difference was not seen for the O1K Pt.GFP replicon compared to O1K Pt.GFPΔ3B1, as they appeared to replicate similarly. In contrast, in MDBK cells both of the replicons with the deletion showed a significant reduction in Pt.GFP levels compared to their wildtype counterparts suggesting that replication was reduced in bovine cells.

3.7 Recovery of viruses with 3B1 deletion

The Pt.GFP O1KΔ3B1, Pt.GFP SKRΔ3B1 and Pt.GFP SKR+3B1 replicons were made into infectious clones and viruses recovered in BHK-21 cells using the same method as described in section 3.5. The recovered viruses were further passaged twice through BHK-21 cells to produce working stocks (BHKp2). The BHKp2 viruses were then titrated on BHK-21 cells (Figure 3.7.1).
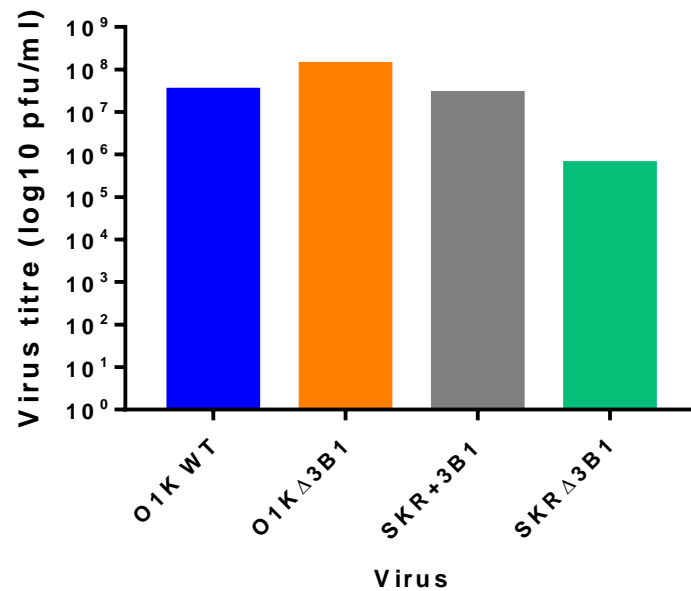
Figure 3.7.1: Growth of viruses with a 23 a.a deletion spanning end of 3A and 3B1 in BHK-21 cells. Passage 2 (BHKp2) viruses with a deletion of 23 a.a spanning the last 5 a.a of the C terminal domain of 3A and covering the majority of 3B1 were titrated by plaque assay on BHK-21 cells. All viruses produced similar titres apart from SKRΔ3B1 (green), which was slightly less (approximately 1.5 log) than its wildtype counterpart (SKR+3B1) (grey) and the O1K variant containing the deletion (orange).

This analysis showed that both viruses with deletions were replication competent in BHK-21 cells. The titres for the O1K WT virus and its deleted counterpart (O1KΔ3B1) were similar whereas the titre of the SKRΔ3B1 virus was approximately 1.5 log less than its wildtype counterpart (SKR+3B1) suggesting that the SKRΔ3B1 virus has a reduced ability to replicate. However, as the data are end point titres (the infection time between BHKp1 and BHKp2 was over 24h) from a single experiment they should be treated with caution. However, due to time constraints it was not possible to analyses these viruses further in bovine and porcine cells.

3.8 Discussion

Deletions in 3A have previously been identified in a number of FMDV isolates from both outbreak and vaccine strains. These deletions are relatively short (10-20 a.a), in the C terminal domain of 3A (Beard and Mason, 2000, Pacheco et al., 2003, Giraudo et al., 1990) and have been linked to changes in host range and attenuated replication in cattle and bovine cells *in vitro*. The work in this Chapter has investigated a larger natural deletion of 57 a.a (residues 81-137) also in the C terminal domain that was identified within a vaccine isolate of a type O virus. Unusually, this deletion existed in a virus as part of a mixed population where some of the viruses also had a full-length 3A. Replicon assays showed that a replicon with this deletion was able to replicate as well as a wildtype replicon in BHK-21 and porcine (SK-RST) cells but was severely attenuated in bovine (MDBK) cells. These results confirm that the deletion does not compromise replication in all cell lines and are similar to previously studies in natural hosts of FMDV which showed that viruses with smaller deletions in 3A remain highly infectious for pigs and replicated well in porcine cells but had limited replication in bovine cells and were less virulent for cattle (Beard and Mason, 2000, Pacheco et al., 2003, Pacheco et al., 2013). A study by Knowles *et al.* determined that the 93-102 deletion in 3A had been present in field viruses that were circulating in pigs in Asia since at least 1970. In addition, this analysis also showed that viruses with this deletion that were isolated before 1983 appeared to grow equally well in bovine and porcine cells suggesting that this deletion on its own does not fully account for the inability of the deleted viruses to replicate in bovine cells (Knowles et al., 2001).The results from this study (Chapter 3) show that the larger deletion in 3A also attenuates replication in bovine cells, which suggest that the additional changes that lead to attenuation for bovine cells may also reside within the C terminal domain of 3A.

A strategy for the production of safer FMDV vaccines currently under consideration is to grow replication-defective viruses in so-called "helper" cell lines that supply the defective viral protein in *trans*. Previous reports with defective replicons have concluded that 3A can be supplied in trans by a "helper" replicon (Herod et al., 2015) and that infection of cells stably expressing

3A led to an increase in viral yield (Rosas et al., 2008). In this study (Chapter 3), supplying full length 3A form a second wildtype helper replicon (O1K mCherry) in trans-complementation assays showed that supplying 3A in *trans* did not significantly restore replication of the replicon with the 81-137 deletion in 3A. However, there was a noticeable increase in the number of Pt.GFP positive cells when the replicon with the 81-137 deletion was co-transfected with the wildtype O1K mCherry replicon over when co-transfected with yeast RNA suggested that some rescue of replication may have occurred. This rescue was at best inefficient and suggests that "helper" cells to rescue 3A deleted viruses may not be a viable option. Another option under consideration is to produce pig specific vaccines that could not replicate in bovines. The experiments present here suggest that vaccine viruses with large deletions in 3A have the potential to be developed as such pig specific vaccines, as if these isolates were attenuated to a level safe to act as a live attenuated vaccine in pigs they would pose less risk to bovine species if they were to infect.

Recombinant viruses with deletions in 3A of a.a 81-137 and 93-143 were also studied. Previously viruses with deletions in 3A have been described as 'porcinophillic' as they cause severe disease in pigs, so it was thought that an 81-137 3A deleted virus may show a preference for porcine cells. However, recovered viruses with this deletion were infectious for both IBRS2 and BTY cells. These observations appear not to fit with the replicon assay results as the 81-137 deletion attenuated replication in a different bovine cell line, MDBK cells suggesting that effects on replication seen with replicons may differ to those seen with infectious viruses.

During my studies, and as part of a BBSRC funded sLoLa investigating FMDV replication, a post doc in the lab (Dr Caroline Wright) carried out a mixed infection experiment in IBRS2 and BTY cells using equal amounts (infectious viruses) of the 3A 81-137 deleted and wildtype isolated viruses. Using PCR through the 3A region, this showed that for BTY cells the wildtype virus rapidly dominated the infection and by passage 5 the 3A deletion was lost. In contrast, in IBRS2 cells the opposite was seen and by passage 5 only the virus with the

3A deletion could be detected. These observations appear to agree with the results of the replicon experiments in MDBK cells and confirm that the deletion in 3A results in a virus that is more fit for replication in pig cells but weakens replication in bovine cells.

Replicon experiments on a smaller deletion that spanned from the C terminal end of 3A, which removed the last 5 a.a of 3A and most of 3B1 except for the last 5 a.a, showed there was no effect of this deletion on replication in BHK-21 cells compared to a wildtype replicon. Interestingly, the deletion resulted in a small improvement in replication in SK-RST cells and a small but statistically significant reduction in replication in MDBK cells. Infectious virus based on an existing infectious clone (FMDV O1K) containing this deletion grew to similar titres to the wildtype virus in BHK-21 cells suggesting this deletion was not detrimental to replication. However, a recombinant virus with a 3A sequence and deletion that matched the original isolate (SKRΔ3B1) in which the deletion was first identified appeared to show reduced replication compared to its counterpart with full-length 3A and 3B1 suggesting that within the context of the SK isolate this deletion may affect replication. However due to time constraints this was only tested in BHK-21 cells using an end point titration and further work is required to fully characterise replication of this virus in porcine and bovine cells.

Experiments investigating the effects of BFA on replication of replicons containing deletions in 3A (figure 3.4.1) showed that BFA inhibited replication of FMDV replicons with the 81-137 or 93-143 a.a deletions in the C terminal domain of 3A. However, unexpectedly BFA also had a similar inhibitory effect on the wildtype O1K Pt.GFP replicon. This was unexpected, as previous publications have reported that BFA has little or no effect on FMDV yield (O'Donnell et al., 2001, Martin-Acebes et al., 2008, Monaghan et al., 2004) suggesting that FMDV replication is insensitive to BFA. However, the study by Martín-Acebes *et al.*, noted an increase in the number of infected cells following BFA treatment (Martin-Acebes et al., 2008). Similarly, another study by Midgley *et al.*, also reported an increase (~40%) in the number of infected cells following

BFA treatment (Midgley et al., 2013). Closer inspection of the experimental conditions of the above experiments shows that the studies by Martín-Acebes *et al.*, and Midgley *et al.*, used a low MOI (0.5 and 0.3 respectively) whereas O'Donnell *et al.*, and Monaghan *et al.*, used higher MOI's (10 and 1.0 respectively). No effect of BFA on virus yield was reported by Monaghan *et al.*, but the study by O'Donnell *et al.*, showed a 2-fold reduction in FMDV yield on BFA treatment. Together these observations (plus the results shown in Figure 3.41. and 3.4.2) suggest BFA could have multiple effects on FMDV replication and the outcome of the experiment could be influenced by the MOI. When carried out at a high MOI, inhibitory effects of BFA on FMDV vRNA replication may be masked by other beneficial effects on infection which could account for the small reduction in virus yield seen by O'Donnell *et al.*, and no difference in virus yield reported by Monaghan *et al.* In contrast, when carried out at low MOI stimulation of infection may predominate as reported by Martín-Acebes *et al.,* and Midgley *et al.,* (Midgley et al., 2013, Martin-Acebes et al., 2008) who observed an increase in the number of infected cells after BFA treatment. The results shown in Fig 3.4.1 are consistent with this as BFA had an apparent inhibitory effect on replication. This would also suggest that the apparent enhancement in the number of infected cells seen by Martín-Acebes *et al.,* and Midgely et al., results from an effect before intracellular replication, most likely cell-entry. The above observations suggest the possibility that BFA has a relatively small and previously uncharacterised inhibitory effect on post-entry FMDV replication while possibly stimulating FMDV cell-entry. Similar inhibitory effects of BFA were seen in the replicon assays for wildtype and 3A-deleted replicons with BHK-21 and SK-RST cells suggesting that the mechanisms of resistance to BFA is/are not provided by the extended C terminal of 3A. These observations also show that, in some cases results seen with replicons may be different to those with infectious virus, since studies with FMDV have concluded that replication does not appear to be effected by BFA treatment whereas in the replicon experiments a significant drop in replication was seen.

Overall the results of this Chapter have shown that a naturally occurring, large deletion in the C terminal domain of 3A (found as part of a mixed viral

population) did not compromise replication and viruses with this deletion were able to replicate independently in BHK-21 and SK-RST but was attenuated in MDBK cells. It was also shown that viruses with this deletion were able to grow in both porcine and bovine cells, with only small differences in end-point viral titre when compared to the wildtype virus. However other studies suggest that the deletion results in a virus that has a strong preference for porcine cells (C Wright personal communication). My study also showed a smaller deletion across 3A and 3B1 may affect replication in cell lines derived from different FMDV hosts. This suggests that 3A may play a role in viral host range but it is likely that multiple other factors are also involved.

Chapter 4: Identifying Potential Cellular Interaction partners of FMDV 3A

4.1 Introduction

It has been suggested that picornavirus 3A interacts with a number of cellular and viral proteins during the replication cycle (Chapter 1 section 1.7.3). However most of the proteins identified at present have been found to interact with the 3A of kobuviruses and enteroviruses, in particular PV 3A. Very few interaction partners for FMDV 3A have been identified. Since FMDV 3A is structurally different to the 3A proteins of other picornaviruses and appears to have varying roles during replication it is likely it will interact with different proteins when compared to that of other picornaviruses.

Known interaction partners for both enteroviruses and kobuviruses include PI4KIIIβ, GBF1 and ACBD3 (Dorobantu et al., 2015b, Greninger et al., 2012, Klima et al., 2017, Sasaki et al., 2012, Wessels et al., 2006) (see Chapter 1 section 1.7.3). However these have not been linked with interactions with FMDV viral proteins. One proposed interaction partner for FMDV 3A is DCTN3 (Dynactin 3), a subunit of the dynactin complex that serves as a co-factor for the dynein motor protein and has been linked with intracellular transport between organelles (Gladue et al., 2014). PV 3A has also been reported to bind a component of the dynein complex, but it interacts with LIS1 rather than DCTN3 (Kondratova et al., 2005). Furthermore it is thought that it is likely FMDV 3A may interact with proteins involved in the innate immune response pathway. Li *et al* suggested that FMDV 3A expression resulted in reduced expression of some proteins within this pathway including RIG-I and MDA5 (Li et al., 2016).

In this chapter 3A-GFP fusion proteins have been used with the proteomics techniques of immunoprecipitation and mass spectrometry to identify additional interaction partners of FMDV 3A.

Mass spectrometry (MS) is an analytical technique that can be used to identify different proteins in a sample according to their mass. The most widely used MS method of analysis of protein-protein interactions involves affinity pull-down

(immunoprecipitation (IP)) methods prior to analysis on a mass spectrometer to identify specific proteins that interact with the target protein. Protein complexes are isolated either using antibodies specific to the target protein or by expressing tagged variants of the target protein within cells and isolating the target protein (and interaction partners) using antibodies to the tag. Once isolated the eluted proteins are digested before undergoing LC/MS-MS where spectra are produced based on protein size and abundance (Georges and Frappier, 2015, ten Have et al., 2011, Trinkle-Mulcahy et al., 2008). A key factor that can influence results when using this technique is the potential for non-specific interactions, particularly during the IP step where non-specific proteins may bind to the isolation beads, which could lead to sample contamination and a high number of non-specific hits. In this work, GFP tagged 3A was expressed (i.e. 3A-GFP fusion proteins) to allow the isolation of 3A and bound cellular proteins by IP using a GFP antibody conjugated to magnetic beads. GFP was selected to use as a tag as it has been shown to bind to few contaminant proteins and or bead matrices (Trinkle-Mulcahy et al., 2008), making it ideal for use in mass spectrometry. Furthermore, protein expression of the tagged 3A proteins was easily monitored through expression of the GFP detected by fluorescence microscopy.

Following analysis of data from the mass spectrometry two potential interaction partners were identified as good candidates to carry out further experiments with, and effects of reducing expression levels on FMDV infection was investigated. These proteins were the Rab GTPase Rab7L1 and the Tre-2 Bub2 Cdc16 (TBC) protein TBC1D20.

4.2 Development of 3A-GFP fusion proteins for use in IP and Mass Spectrometry experiments

To identify possible interaction partners of 3A using IPs and mass spectrometry, expression plasmids were generated for 3A-GFP (i.e. GFP fused to the C terminus of 3A) and 3ABBB-GFP (i.e. GFP fused to the C terminus of 3B3) .The 3A and 3ABBB regions were amplified by PCR from a replicon template using

primers that introduced restriction sites on either end. The restriction sites were then used to clone the PCR products into the multiple cloning site of the expression plasmid pEGFP-N1 to create plasmids in which the EGFP coding region was located downstream of that coding for 3A (referred to as 3A-GFP) or 3ABBB (referred to as 3ABBB-GFP) creating C terminal fusion proteins (Chapter 2 section 2.1.4)). Plasmid maps of the fusion protein expression plasmids are shown in Figure 4.2.1.Sequencing of the plasmids (data not shown) revealed that in 3A-GFP full length 3A and GFP were present and joined in frame, while in 3ABBB-GFP part of the coding sequence for the 3BBB region was missing, full length 3B1 and 3B2 were encoded but only the first 7 a.a of the 3B3 region were coded for. However, as full-length 3A and the remaining part of 3BBB were still encoded in frame with GFP it was decided to continue working with this construct.
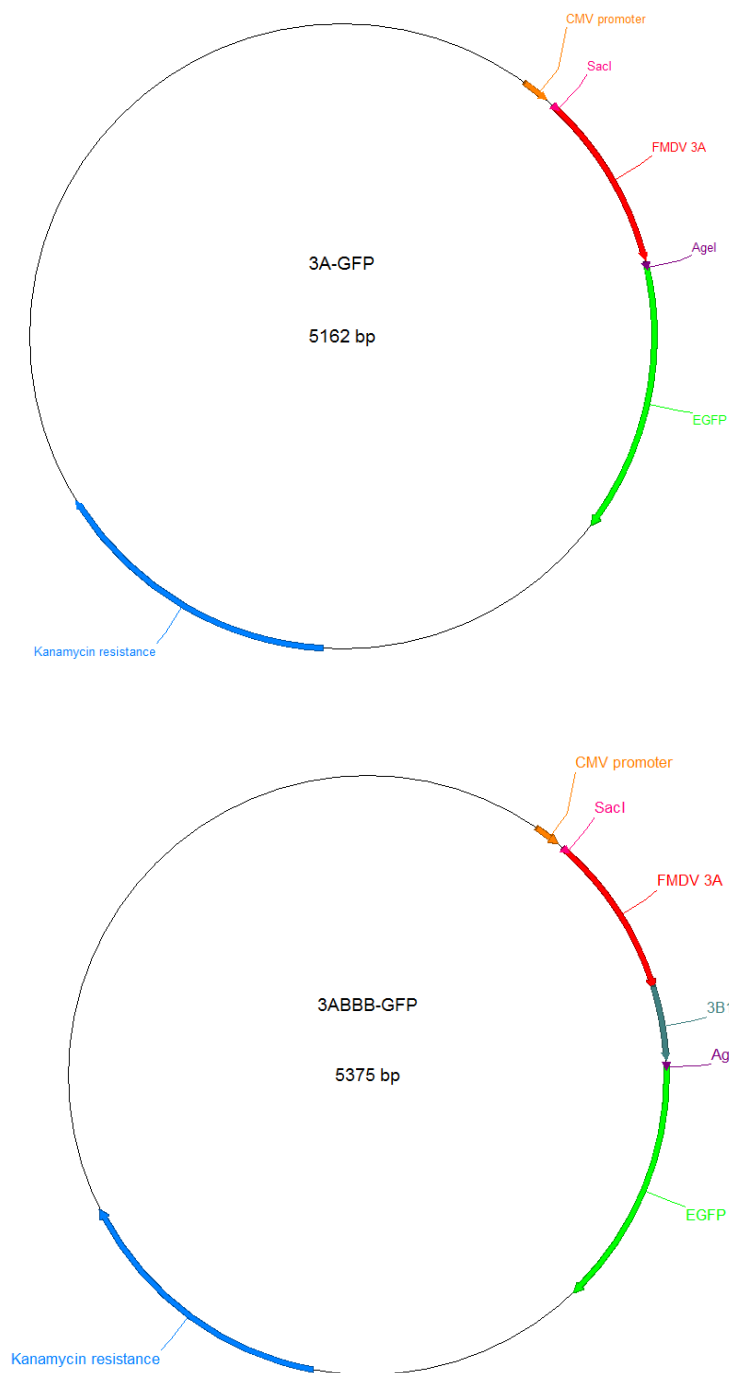
Figure 4.2.1 3A-GFP and 3ABBB-GFP fusion protein expression plasmids: Fusion protein plasmids which would allow expression off GFP tagged 3A or 3ABBB in cells were developed by PCR amplifying the corresponding regions of the FMDV genome and cloning the PCR products into the pEGFP-N1

expression plasmid to produce plasmids where GFP was fused to the C terminal of 3A or 3ABBB as shown in the plasmid maps above.

To test if the GFP fusion proteins were being expressed correctly, plasmid DNA from 3A-GFP, 3ABBB-GFP and pEGFP-N1 (the vector control) was transfected into HEK-293 cells. Transfected cells were fixed and labelled for 3A expression (for analysis by confocal microscopy), or samples were lysed and analysed by western blot for both 3A and GFP expression. Confocal microscopy images, see Figure 4.2.2, show that GFP expression from pEGFP-N1 occurred throughout the cell, including in the nucleus (top panels), whereas GFP expression from the fusion proteins (middle and bottom panels for 3A-GFP and 3ABBB-GFP respectively) was localised to the perinuclear region and cytoplasm but not seen in the nucleus. This suggests that most of the fusion protein was still intact as GFP alone appears to accumulate in the nucleus. Furthermore 3A expression (shown in red) was localised with the GFP expression in the cytosol, suggesting it remained fused to GFP.

	DAPI	GFP	FMDV 3A	Merge
pEGFP-N1				
3A-GFP				
3ABBB-GFP				
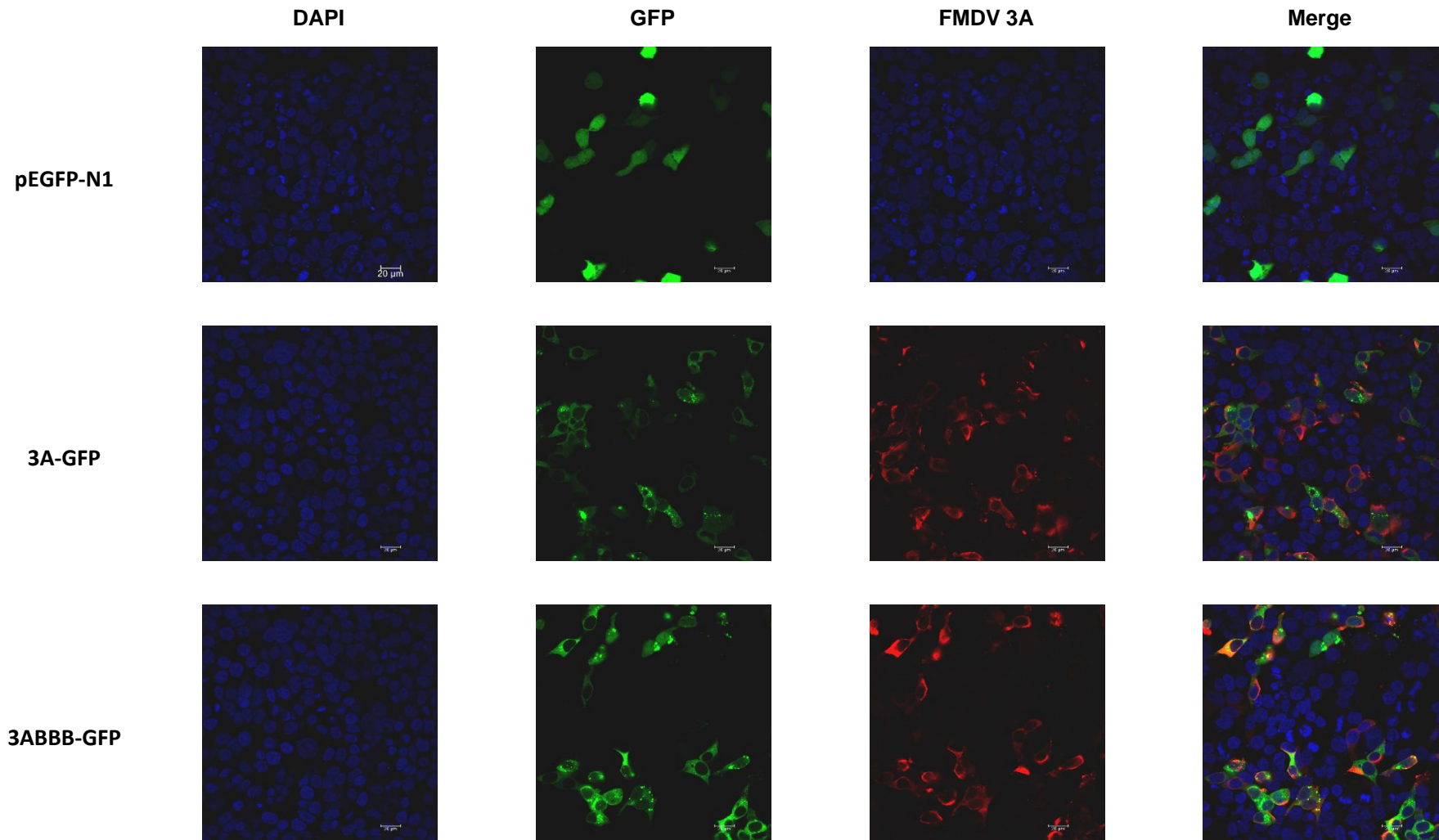
Figure 4.2.2: FMDV 3A-GFP fusion proteins show different cellular localisation to GFP expressed on its own (in form of pEGFP-N1). GFP fusion proteins were transfected into HEK 293 cells, at 12 hours post transfection cells were fixed and labelled for FMDV 3A (using Mab 2C2) and nuclei stained with DAPI (blue) and imaged using confocal microscopy. Images show GFP expression (green) FMDV 3A expression (red) and a merge image for each expression plasmid including the pEGFP-N1 control.

Further analysis by western blot (Figure 4.2.3) showed that 3A remained fused to GFP in the 3A-GFP construct at both 12 and 16 hours post transfection. A band at the expected size (44 KDa) of the fusion protein was seen, in blots for both 3A (with antibody 2C2, panels A and C) and GFP (with antibody ab290, panels B and D). The 3ABBB-GFP construct also gave bands of the correct size (52KDa) showing that the fusion protein was intact at 12 hours (panels A and B). However when the GFP fusion proteins were expressed in cells for 16 hours it was found that 2 bands were detected for 3ABBB-GFP when blotting using an antibody for 3A (panel C) and the band detected when blotting using an antibody for GFP was a similar size to that seen with the vector plasmid control pEGFP-N1 of 27 KDa (panel D). These results suggest that while the 3A-GFP fusion protein is stably expressed and remains intact over 16 hours the 3ABB-GFP fusion protein appears to be "cleaved" after prolonged expression. Therefore it was decided to only express the 3ABBB-GFP fusion protein in cells for 12 hours prior to the IP reactions, whereas the 3A-GFP fusion protein was expressed in cells for both 12 and 24 hours before harvesting cells for IP reactions.

A

pEGFP-N1 3A-GFP 3ABBB GFP

50 —
37 —

FMDV 3A

pEGFP-N1 3A-GFP 3ABBB-GFP

50 —
37 —
25 —

GFP

12 Hours
Post
Transfection

C

3ABBB-GFP 3A-GFP pEGFP-N1

50 —
37 —
25 —
20 —

FMDV 3A

3ABBB-GFP 3A-GFP pEGFP-N1

50 —
37 —
25 —
20 —

GFP

16 Hours
Post
Transfection
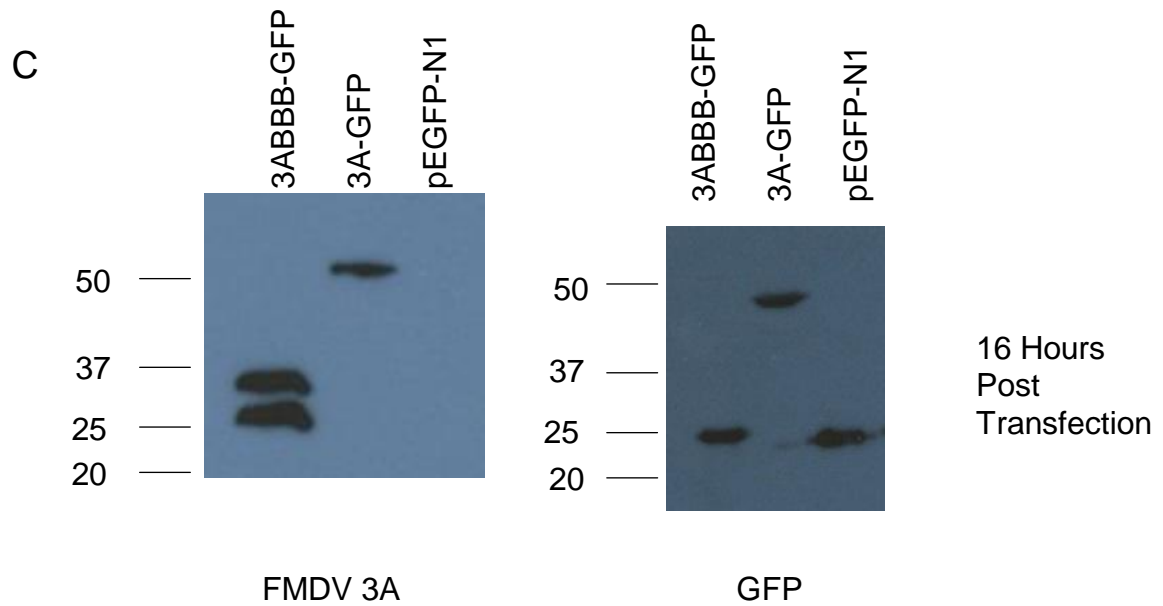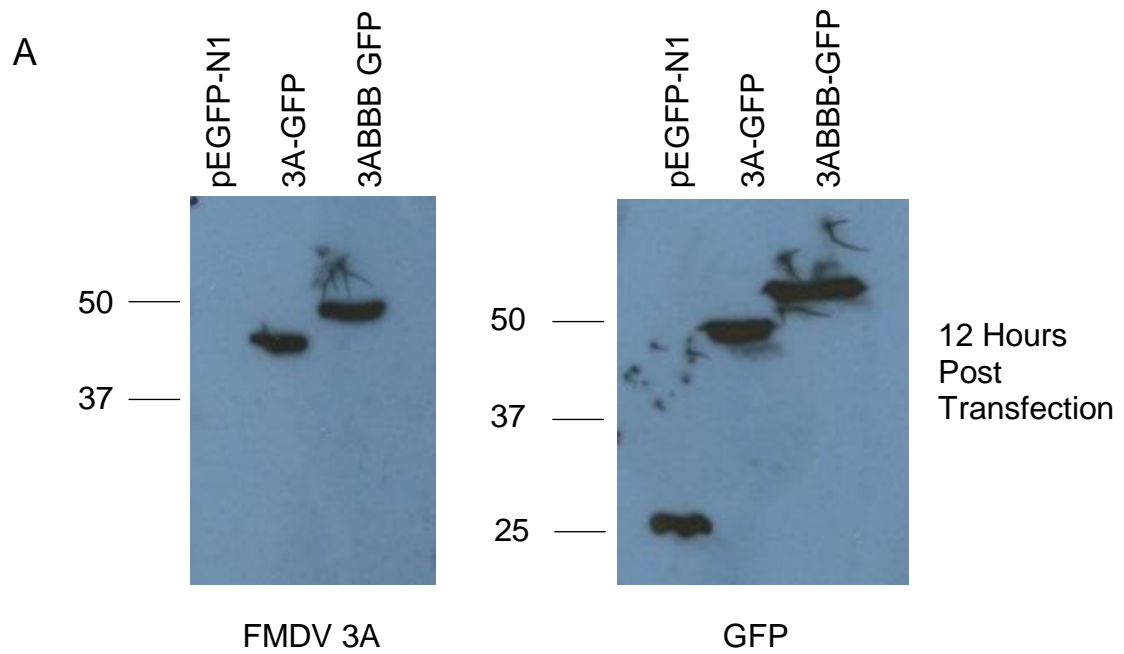
Fusion Protein	Predicted size (KDa)
GFP	27
3A	17
3ABBB	25
3A-GFP	44
3ABBB-GFP	52

Figure 4.2.3: Western blots showing expression of fusion proteins 3A-GFP and 3ABBB-GFP. HEK 293 cells were transfected for 12 (panel A and B) or 16 hours (panels C and D) with plasmid DNA of 3A-GFP, 3ABBB-GFP and GFP only control (pEGFP-N1). Transfected cells were lysed, and the lysates run on SDS PAGE gels and western blotted for expression of both FMDV 3A and GFP. Size markers are shown on the left hand side of the blots

4.3 Using Immunoprecipitation and mass spectrometry to identify potential interaction partners of FMDV 3A

4.3.1 Isolating 3A interaction complexes using IP reactions

To identify potential cellular proteins that interact with FMDV 3A, IPs followed by mass spectrometry were carried out. BHK-21 and MDBK cells were transfected with DNA from 3A-GFP or 3ABBB-GFP expression plasmids (see section 4.2.1) and incubated for 12 or 24 hours, then checked for GFP expression using a fluorescent microscope.

After observation of GFP expression cells were either fixed with 4% PFA (see Chapter 2 section 2.2.7.1) or left unfixed, t,hen harvested into IP buffer (see Chapter 2, section 2.2.6.4). Samples were then sonicated and incubated with a GFP specific antibody bound to magnetic beads. Following incubation beads were washed three times and protein complexes eluted. Samples of the original cell lysate (TCL), the washes (FT) and the final elution (IP) were western blotted using a GFP antibody to check IPs had worked. Figure 4.3.1 shows representative blots of samples from IPs conducted on cell lysates from cells transfected with 3A-GFP at 24 hour post transfection and those from cells transfected with 3ABBB-GFP and harvested at 12 hours post transfection.

A. BHK-21

B. MDBK
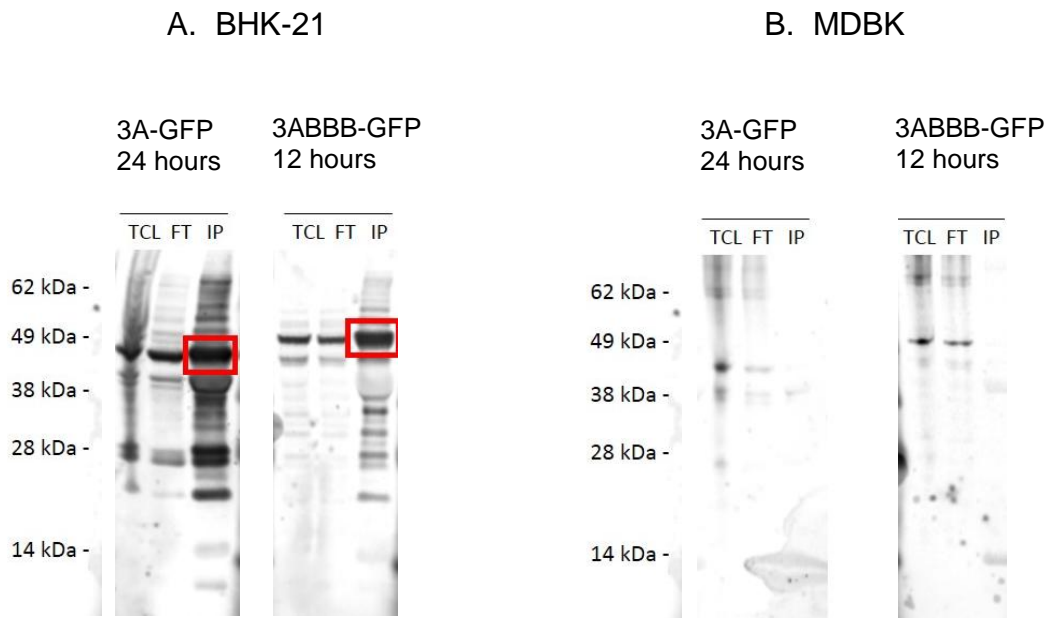
Figure 4.3.1: Western blots of IP samples using antibody to GFP. 20µl samples of total cell lysate, flow through (from the wash steps) and IPs, (final elutions) from experiments done in BHK-21 (panel A) or MDBK cells (panel B), were run on a 4-20% gradient SDS-PAGE gel and western blotted using an antibody to GFP. Bands shown in red are the correct size for 3A-GFP and 3ABBB-GFP and show that they had been successfully pulled down in BHK-21 cells (panel A) as they are present in the final IP sample. Sample preparations and blots were carried out with the help of Dr Armel Nicolas (University of Dundee).

As shown in Figure 4.3.1 panel B the IPs with samples from MDBK cells had not worked well as no bands at correct size (corresponding to the 3A-GFP fusion proteins) were seen in the eluted samples. However in BHK-21 cells, bands of the correct size (44 and 52 KDa) were seen and were more intense in the IP than in the flow through (wash) samples. (Figure 4.3.1 panel A) suggesting that for BHK the IP step was successful for both fusion proteins. Data from samples that were fixed prior to harvesting from cells is not shown in figure 4.3.1, to help with clarity but again the IPs from this set of samples in MDBK were unsuccessful whilst those in BHK-21 did show bands that were more intense in eluted IPs samples and at the correct sizes, suggesting that the IP had worked correctly.

4.3.2 Mass spectrometry of IP samples

The BHK-21 IP samples were further prepared for mass spectrometry using in gel digestion and fractionation (see Chapter 2 section 2.2.6.5). They were then run on the mass spectrometer. IPs, preparation and running of samples on Mass Spectrometry was carried out with the help of Dr Armel Nicolas (University of Dundee). Initial analysis of mass spectrometry data (kindly conducted by Dr Armel Nicolas) produced a large number of potential hits therefore further analysis was required.

4.3.2.1 Results from Initial Mass Spectrometry Analysis

This PhD was closely aligned with a BBSRC sLoLa grant to investigate FMDV replication. This included a yeast-2-hybrid (Y-2-H) investigation (carried out at Edinburgh University) of cellular interacting partners of FMDV 3A and 3A precursors (3AB, 3ABB and 3ABBB) in addition to other non-structural proteins of FMDV. The results of the mass spectrometry-based experiment from this study are considered in conjunction with the Y-2-H study.

None of the major cellular proteins (GBF1, ACBD3, PI4KIIIa) that bind picornavirus 3A proteins or have previously been implicated in RO formation (PI4KIIIβ) by other picornaviruses were identified in the extensive list produced by initial analysis of the MS data (from the experiment using 3A or 3ABBB as the target proteins). In addition, LIS1, or RIGI and MDA5 were also not identified. DCTN3 (dynactin 3) has been proposed as a cellular interacting protein for FMDV 3A. In the mass spec analysis, a number of dynactin proteins were identified including DCTN1, DCTN2, DCTN3, DCTN4 and DCTN6. As the role of DCTN3 in FMDV infection has already been explored (Gladue et al., 2014) and given that a number of other DCTN subunits were identified as potential FMDV 3A interacting partners, suggesting they may not bind 3A directly, it was decided not to pursue this interaction further. Other proteins of interest identified included VAP-B (see chapter 5), Rab7L1 and TBC1D20 (see below). Similarly, GBF1, ACBD3, PI4KIIIα and PI4KIIIβ) were not identified in the Y-2-H screen (using 3A, 3AB1, 3AB1B2 and 3AB1B2B3 as the target proteins). In addition, DCTN3 and LIS1, and RIGI and MDA5 were also not

identified. In addition, VAP- B and TBC1D20 were not identified while Rab7L1 was identified but only with 3ABB as the target protein

Based on results of initial analysis two proteins were selected to investigate further as discussed in sections 4.4 and 4.5. However to gain more useful insights from the data set additional and more extensive analysis is required, to establish potential impacts on cellular pathways and gene expression.

4.4 Investigating effects of knocking down Rab7L1 expression on FMDV infection

Rab7L1 was identified as a possible interacting partner for FMDV 3A in the initial mass spectrometry analysis and was also identified in a Y2H screen using 3ABB as the target protein (the Y2H screen was carried out by collaborators at Edinburgh University). Therefore, as Rab7L1 was identified in two independent screens, using different methods, it was thought to be a good candidate to investigate further.

Rab7L1 (also known as Rab29) is a member of the Rab GTPase family, a group of small proteins that have been shown to play multiple roles in intracellular vesicular transport. There are at least 70 Rab family members and many have been investigated in detail. However, the cellular functions of others including Rab7L1 are not well known.

Rab7L1 was originally considered a close homologue of Rab7; however, sequence alignments have demonstrated that Rab7L1 is more closely related to Rab32 (46% a.a identity) and Rab38 (49% a.a identity), which regulate post-Golgi trafficking events (Wasmeier et al., 2006). Recently Rab7L1 has been shown to be involved in maintenance of the integrity of the Golgi, and the retrograde trafficking of M6P receptors from endosomes to the Trans Golgi network (TGN) (Wang et al., 2014). In addition, Rab7L1 has been found to mediate Salmonella infection (Spanò et al., 2011) and modify intraneuronal protein sorting through interacting with LRRK2 and has been shown to be linked with Parkinson's disease risk (MacLeod et al., 2013, Tang, 2017). In the

experiments below, siRNA was designed against target sequences of the porcine Rab7L1 gene and used to investigate effects of knocking down expression of Rab7L1 on FMDV infection in IBRS2 cells.

Three separate siRNA's were designed (using Dharmacon custom siRNA design tool) and equal amounts pooled together prior to transfection. The target sequences of each siRNA are shown in the table of Figure 4.4.1, along with their locations (highlighted in red) within one of the full transcript sequence of porcine Rab7L1 (Figure 4.4.1). All three of the Rab7L1 target sequences are an exact match for all currently identified transcript variants of the porcine Rab7L1 gene available by NCBI.

siRNA to porcine Rab7L1	Target Sequence
siRNA 1	GAGCAATTCCAAAGAAGAA
siRNA 2	GGACAGAAACATCAGTCAA
siRNA 3	CAACAGCCAGAGATGGAAA

Sus scrofa RAB29, member RAS oncogene family (RAB29), transcript variant X1, mRNA XM_003357400.2 Coding sequence:

ATGAGCAGCCGCGATCACCTGTTCAAAGTGCTGGTGGTGGGGGATGCCGCAGTG
GGCAAGACGTCCCTGGTGCAGCGGTATTCCCAGGACAGCTTCAGCAAACACTAC
AAGTCCACGGTGGGAGTGGATTTCGCTCTGAAGGTGCTCCAGTGGTCTGACTCA
GAGGTGGTGCGCCTCCAGCTGTGGGATATTGCAGGCCAGGAGCGCTTCACCTCT
ATGACCAGACTTTACTATCGGGATGCCTCTGCCTGTGTTATCATGTTTGATGTTAC
CAACGCCACTACCTTCAGCAACAGCCAGAGATGGAAACAGGACCTGGACAGCAA
GCTCACACTGCCTAATGGAGGGCCAGTGCCCTGCCTGCTCTTAGCCAATAAGTGT
GATCTATCCCCTTGGGCGGTGAGCCGAGACCAGGTTGACCGGTTCAGTAAAGAG
AACGGCTTCACAGGTTGGACAGAAACATCAGTCAAGGAGAACAAAAATATTAACG
AGGCGATGAGAGTCCTCATTGAAAAGATGATGAGCAATTCCAAAGAAGAAATGTC
TTTGTCCACCCAAGGGAACTACATTAACCTGCACACCAAGCCCACCTCCAGCTGG
ACCTGCTGCTAATAGCATTTGGCTTGTGTTTGCTCACAGTCCTAGGAGG

Figure 4.4.1: Design of siRNA sequences targeting expression of porcine Rab7L1. Three different siRNAs were designed using the Dharmacon custom design tool. Three target sequences (as shown in the table) were selected based on highest scoring targets that required no modifications and whose locations didn't overlap. The target sequences are present in all transcript variants available to date and location within one of the transcript variants are shown in red.

IBRS2 cells were transfected with various amounts of the three pooled siRNAs (5pg, 10pg or 20pg) or a non-targeting control siRNA (5 pg, 10 pg or 20 pg) using Dharmafect 4 or left untreated (Chapter 2 section 2.2.1.3). At 48 hours post transfection cells were infected with O1K FMDV for 4 hours. Cells were then fixed, labelled for FMDV 3A (using 2C2 monoclonal antibody), and the nuclei stained with Topro 3 dye (allowing for quantification of the total number of cells per well). Infection was then quantified using 3A (here detected by GFP expression) as a marker of infection using a fluorescent imaging plate reader (Chapter 2 section 2.2.7.5). Results from 2 independent experimental repeats are shown in Figure 4.4.2

.
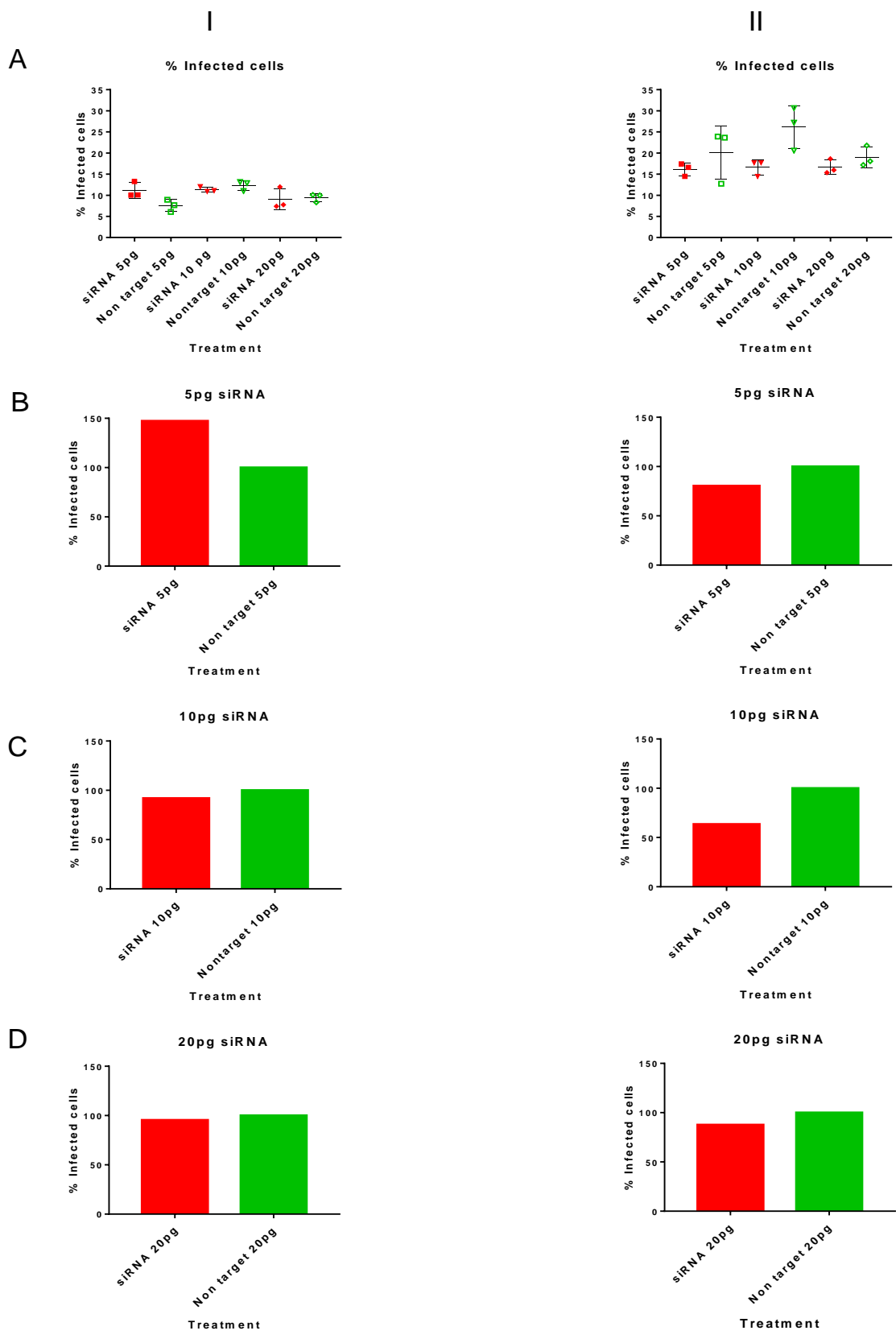
Figure 4.4.2 Effects of knocking down Rab7L1 expression on FMDV replication. IBRS2 cells were transfected with varying amounts of siRNA to target Rab7L1 or with a non-targeting control. At 48 hours post transfection cells were infected with FMDV O1K for 4 hours then fixed and labelled for infection using a primary antibody against FMDV 3A (mAb 2C2) and secondary antibody Alexa fluor 488. Cell nuclei were stained with Topro 3 dye and the total number of cells per well and number of infected cells per well counted using the Spectramax i3 plate reader. Panels AI and AII show the percentage of infected cells in cells treated with siRNA to Rab7L1 (red symbols) or the non-targeting control (green symbols). Error bars show mean +/-SD. Untreated cells were also infected for use as a positive control of infection (data not shown). Panels in rows B, C and D show the percentage of infected cells with each amount of siRNA used normalised to the non-targeting control. Two independent experiments (I and II) were carried out each with triplicate samples per condition

The percentage of infected cells was determined and is shown in Figure 4.4.2 (panels AI and AII), and showed little or no difference for infection of the Rab7L1 siRNA treated cells in comparison to the cells treated with non-targeting SiRNA control (green) for both experiments, and for each amount of siRNA (5, 10 or 20 pg). Figure 4.4.2 panels B, C and D show the percentage of infected cells in siRNA treated cells (red) when normalised to the percentage of infected cells treated with the non-targeting siRNA control (green), following treatment with 5, 10 or 20 pg of siRNA (panels B, C and D respectively). With the exception of experiment 1 where cells were treated with 5 pg of siRNA, (panel BI), the differences in infection levels between siRNA treated and non-target treated cells was less than 20% in both experiments for all siRNA amounts. This suggests that any effect solely due to the siRNA directly knocking down Rab7L1 was likely to be very small and that there may have been non-targeting effects from the Rab7L1 siRNA or transfection effecting infection levels. Therefore it is possible the decrease in infection may not solely be due to knock down of Rab7L1 expression.

4.5 Investigating effects of knocking out TBC1D20 on FMDV Infection and replication

Initial analysis of the mass spectrometry data (Section 4.3.2.1) showed that a number of TBC-domain proteins were detected as potential interacting partners for 3A, including TBC1 Domain Family Member 20 (TBC1D20). TBC-domain proteins belong to a family of GTPase activator proteins (GAPs) of Rab-like small GTPases and contain Tre-2 Bub2 and Cdc16 (TBC) domains (Bernards and Settleman, 2004, Frasa et al., 2012). Rab proteins regulate many aspects of membrane trafficking and are essential for the coordination of budding, transport and fusion of vesicles (Stenmark, 2009). The Rab proteins cycle between inactive and active states, which regulates their binding to specific effector proteins. Rab proteins are activated by guanine nucleotide exchange factors (GEFs) that promote the formation of active, GTP-bound states, while GAPs promote Rab inactivation by stimulating GTP-hydrolysis activity.

TBC1D20 has been identified as a GAP for the Rab 1 protein (Sklan et al., 2007a) which plays a key role in Golgi biogenesis and ER-to-Golgi trafficking (Plutner et al., 1991, Tisdale et al., 1992). Therefore TBC1D20 has an indirect role in regulation of the early secretory pathway through regulating Rab-1-mediated vesicular traffic between the ER and Golgi. Over-expression of TBC1D20 has been shown to have a dominant negative (DN) effect and causes loss of structure of the Golgi complex and inhibits vesicle transport from the ER (Haas et al., 2007, Sklan et al., 2007a).

A study by Midgley *et al* (Midgley et al., 2013) showed that expression of DN Rab1 appeared to make FMDV infection more favourable. Midgley also investigated the effect of over expression of TBC1D20 on FMDV infection of IBRS2 cells (Midgley, 2011). Agreeing with previous studies (Haas et al., 2007, Sklan et al., 2007a) the over expression of TBC1D20 was shown to disrupt the ER, ERGIC and the Golgi suggesting that membrane flow through the early secretory pathway was inhibited (Midgley, 2011). In addition, this study showed that over expression of a catalytically inactive mutant of TBC1D20 (TBC1D20 R105A) also appeared have a similar effect, as in cells expressing this mutant

the ER, ERGIC and Golgi were similarly affected. As TBC1D20 is a GAP for Rab1 and over expression of TBC1D20 acts as a DN protein, it would be thought that expression of TBC1D20 may reduce the amount of Rab1 activation and therefore have a similar inhibitory effect as DN Rab1 on FMDV infection. However over expression of TBC1D20 had an inhibitory effect on infection. Furthermore, over expression of the catalytic inactive mutant TBC1D20 R105A also inhibited infection showing that this effect was independent of Rab1 GAP activity. As a result it is possible that TBC1D20 is required for FMDV infection and that over expression of the wildtype or inactive TBC1D20 mutant could aid movement of FMDV non-structural proteins (including 3A) to a different cellular environment that is not favourable for replication.

4.5 1 Investigating effects of knocking out TBC1D20 on FMDV Infection

Parental and TBC1D20 knockout HeLa cell lines (in which different guide RNAs targeted different Exons to completely knockout the expression of TBC1D20 using CRISPR methods) referred to as Exon 5 or Exon 7 (based on the exon targeted), were kindly provided by Dr Mark Handley (The Roslin Institute, Edinburgh University). Infection assays were carried out by seeding cover slips with each cell line, infecting with FMDV O1K WT for 4 hours, then fixing, and labelling the cells for infection using an antibody (2C2) to FMDV 3A. Ten fields of view per cover slip were imaged, each using three varying red laser settings (high, medium and low) to allow for easier discrimination between background fluorescence and infected cells (see figure 4.5.1 1 for example images). Levels of infection looked to be higher in the parent cells compared to the knockout cells although the labelling for FMDV 3A appeared to be strongest in intensity in the Exon 5 knockout cell line in comparison to the parent and Exon 7 cell lines.

	Parent	Exon 5	Exon 7
DAPI			
Low			
Medium			
High			
Merge			
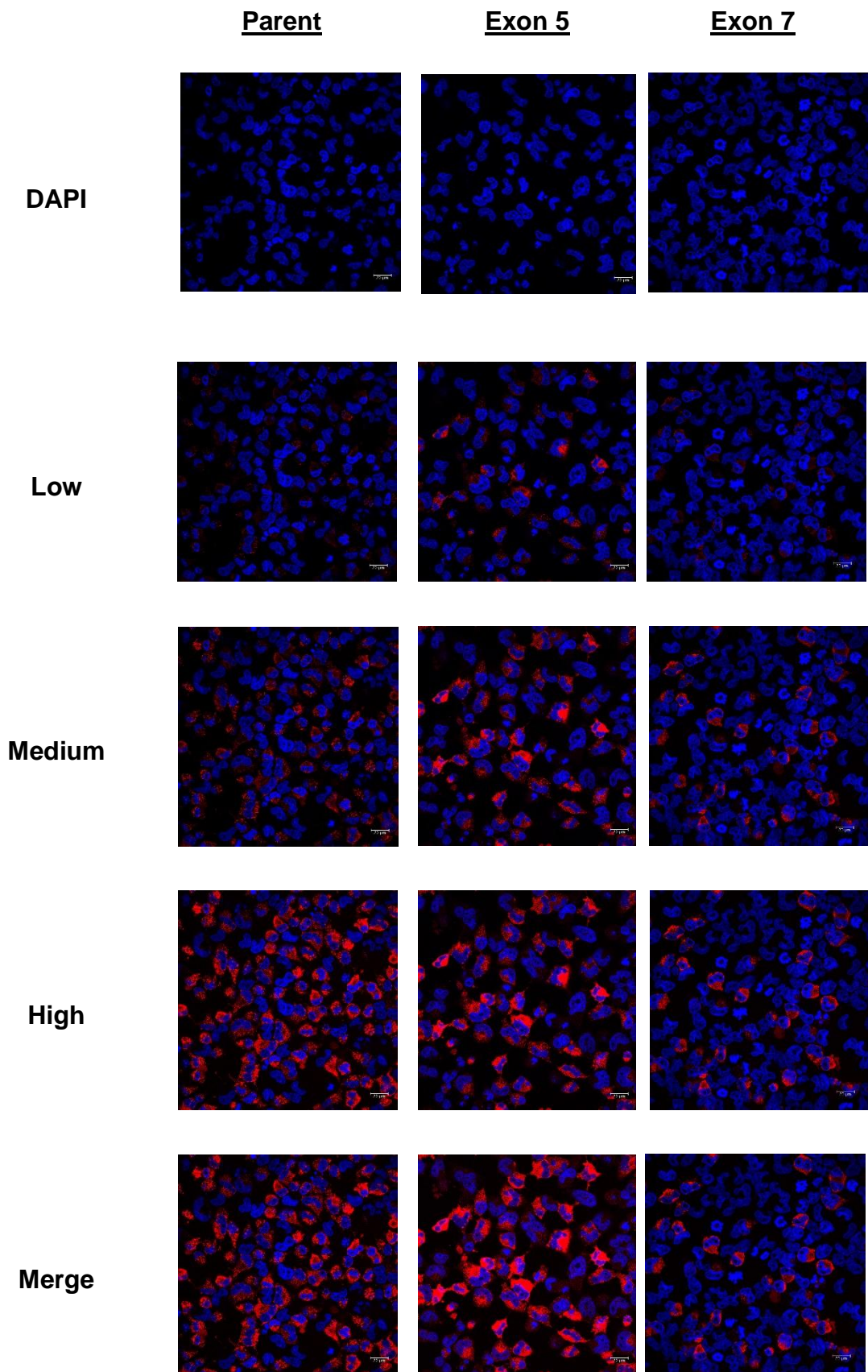
Figure 4.5.1.1: FMDV infection of parent and TBC1D20 knockout HeLa cell lines. Parent and knockout cell lines (Exon 5 and Exon 7) were seeded onto cover slips and infected with FMDV O1K virus for 4 hours. Cells were fixed, and labelled with a monoclonal antibody against FMDV 3A (red), nuclei were stained using DAPI. To allow infected cells to be easily distinguished from background cells were imaged using three different laser intensities; high, medium and low and the images merged. Infected cells were then much brighter and easier to identify. The number of nuclei (blue) and number of infected cells from ten fields of view per cover slip were counted to quantify infection levels. Images above show a single field of view example.

The total number of cells (based on the number of DAPI (blue) stained nuclei) and the number of infected cells (based on detection with an antibody to FMDV 3A (red) as a marker of infection) were counted for each field of view. Ten fields of view per cover slip were counted with 3 cover slips being used for the parent and Exon 5 cell lines (30 fields of view in total) and 2 for the exon 7 cell line (20 fields of view in total).

Figure 4.5.1.2 (panel A) shows the total number of cells (blue) and the number of infected cells (red) from all fields of view counted per cell line. The total number of cells counted overall was similar between cell lines but the number of infected cells was slightly less in the knockout cells. The percentage of infected cells was calculated for each cell line (shown in Figure 4.5.1.2 panel B) and normalised data (normalised to the parental cell line) is shown in Figure 4.5.1.2 panel C. The percentage of infected cells was lower in each of the knockout cell lines compared to the level of infection seen in the parental cell line (24.2% reduction in Exon 5 and 30.1% reduction in Exon 7, panel C). However, a one way ANOVA carried on data found these differences between the percentage infected cells in each cell line was non-significant. Nevertheless, there was a small decrease in the level of infection for the knockout cells suggesting that TBC1D20 may enhance FMDV replication but does not appear to be essential.

A

B

C
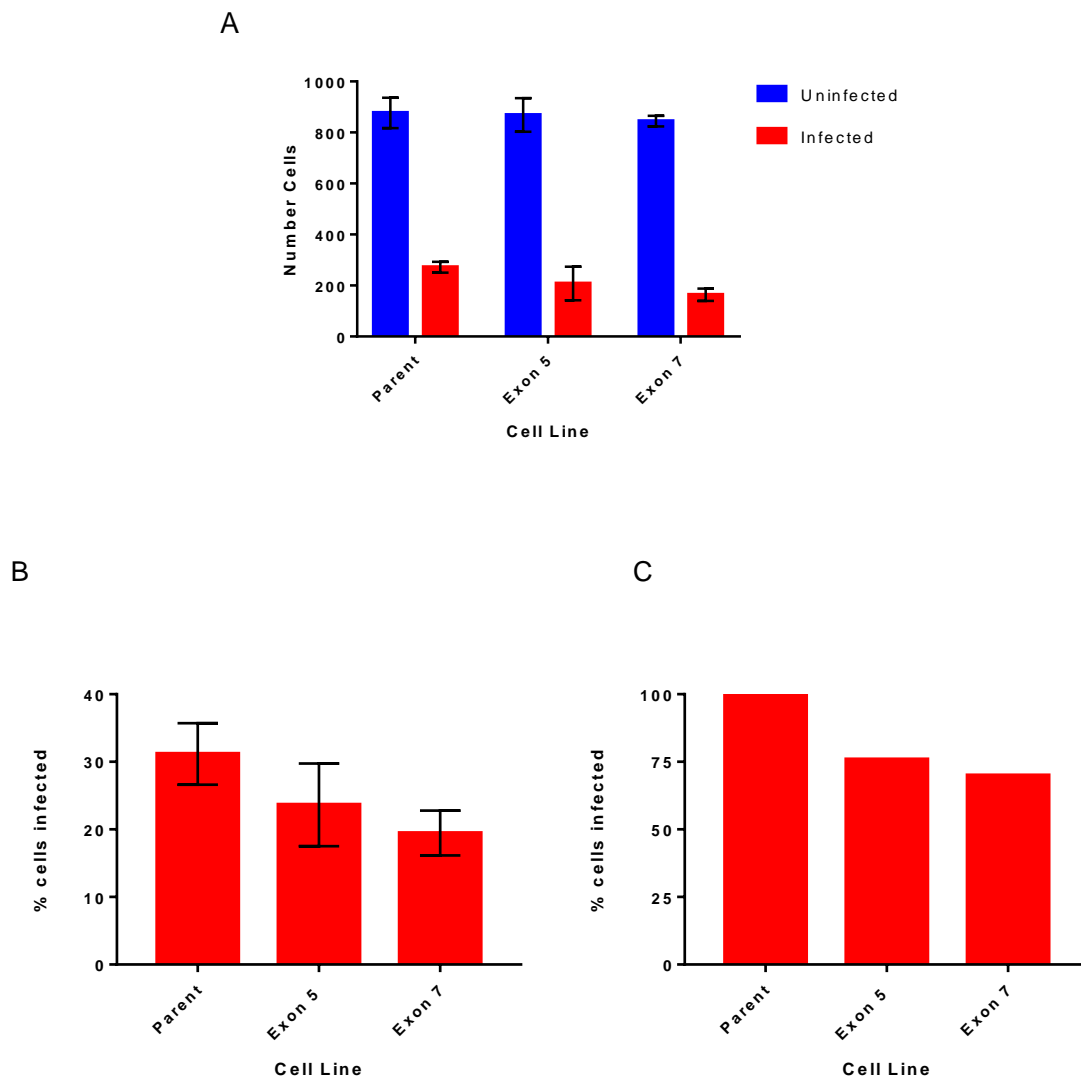
Figure 4.5.1.2: Effects of knocking out TBC1D20 on FMDV infection: Parental and TBC1D20 knockout cell lines (Exon 5 and Exon 7) on cover slips were infected with O1K FMDV for 4 hours, fixed and labelled with antibody to FMDV 3A as an indicator of infection. Ten fields of view per cover slip with 2 or 3 cover slips per cell line were imaged. Total number of cells was counted based on DAPI staining of nuclei (blue bars, panel A), and infected cells were counted based on detection of FMDV 3A (red bars, panel A). Cell counts were used to calculate the percentage of infected cells, shown in panel B. These percentages were normalised and are shown in panel C. Error bars show mean +/-SD of the counts or percentage from ten fields of view from 2 cover slips (Exon 7) or 3 cover slips (Exon 5 and parent).

4.5.2 Comparing intracellular structures of the parent and TBC1D20 knockout cell lines

To determine if changes in the ER and Golgi resulted from TBC1D20 depletion, uninfected parental and knockout cells (Exon 5 and 7), were labelled for confocal microscopy, using antibodies to the Golgi marker, GM130, and the ER (PDI). Representative images are shown in Figures 4.5.2.1 and 4.5.2.2 respectively.

	DAPI	Golgi	Merge
Parent			
Exon 5			
Exon 7			
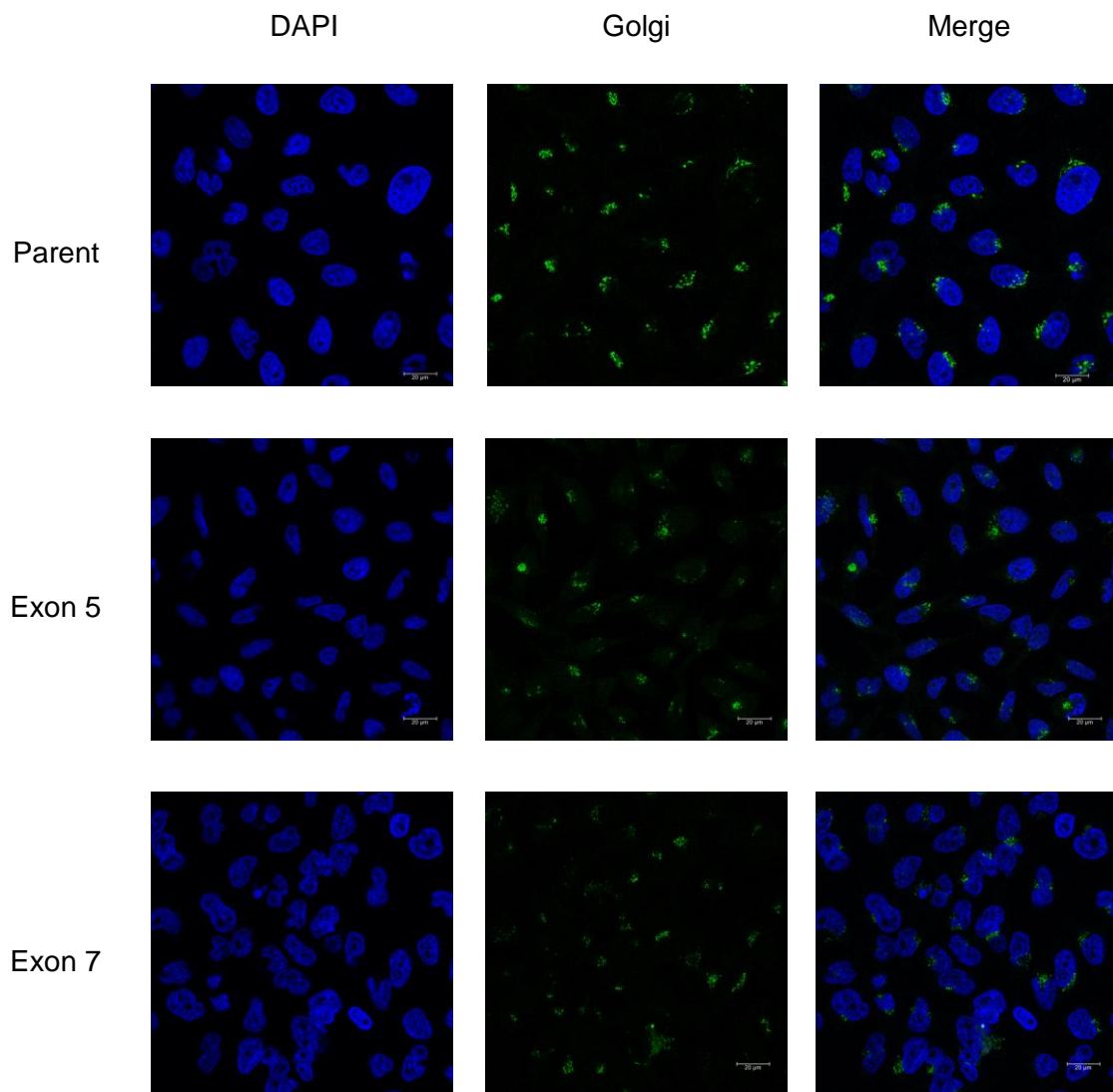
Figure 4.5.2.1: Comparison of Golgi structure in parent and TBC1D20 knockout cell lines. Parent and TBC1D20 knockout Hela cells were seeded onto cover slips, fixed Golgi apparatus labelled (using antibody to GM130 (green)), cell nuclei were stained using DAPI (blue). Labelled cells were imaged by confocal to allow comparison between the cell lines and see if knocking out TBC1D20 had affected the Golgi structure.

| | DAPI | ER | Merge |
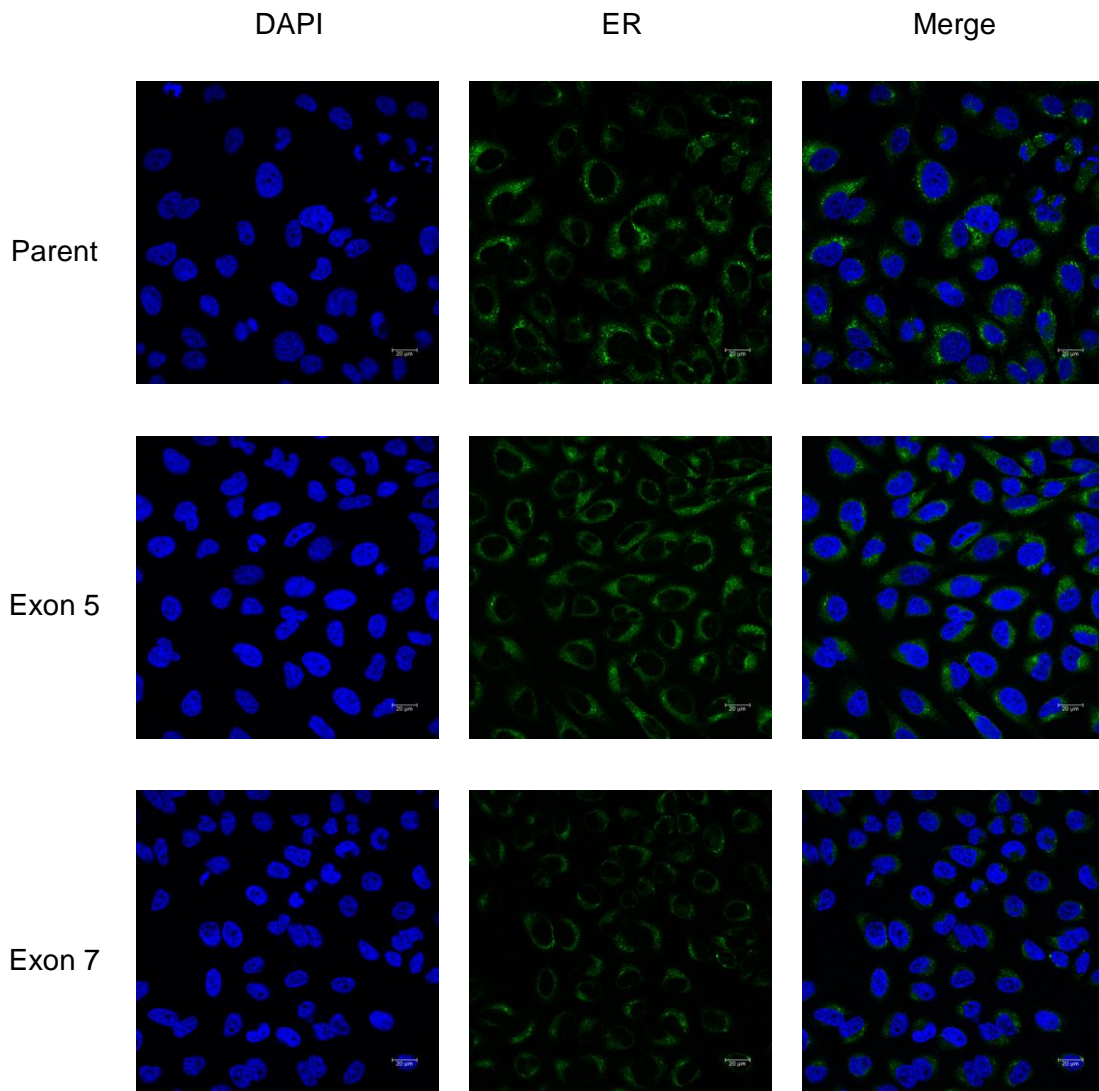
Figure 4.5.2.2: Comparison of ER structure in parent and TBC1D20 knockout cell lines. Parent and TBC1D20 knockout Hela cells were seeded on cover slips, fixed and the ER labelled (using antibody to PDI, shown in green). Nuclei were stained using DAPI (blue) and cells imaged by confocal microscopy to look for structural differences in the ER between the parental and knockout cell lines (Exon 5 and Exon 7).

Labelling for GM130 (green), Figure 4.5.2.1, showed that the Golgi was extensively disrupted in the knockout cell lines when compared to the knockout

cells with the most disruption being observed in the Exon 5 cell line. The middle panels show that the labelling for GM130 was far more dispersed in each of the knockout cell lines (middle panels, middle and bottom rows) compared to in the parent cell line which did express TBC1D20 (middle panel, top row).In the parent cell line labelling was more consistent and showed clear structures. Labelling of the ER protein PDI (green) (Figure 4.5.2.2) on the other hand showed little difference in ER structure between the parent and knockout cell lines, although fluorescence was fainter in one of the knockout cell lines (Exon 7).

4.5.3 Effects of knocking out TBC1D20 expression on FMDV replication

To determine the ability of the TBC1D20 knockout cell lines to support replication each cell line (parent, Exon 5 and Exon 7) was transfected with the wildtype FMDV O1K Pt.GFP and O1K Pt.GFP GNN replicons (see Chapter 2 section 2.2.1.3) and GFP intensity measured (as an indirect measure of replication) at hourly intervals on the Spectramax i3 minimax imaging cytometer (Figure 4.5.3).
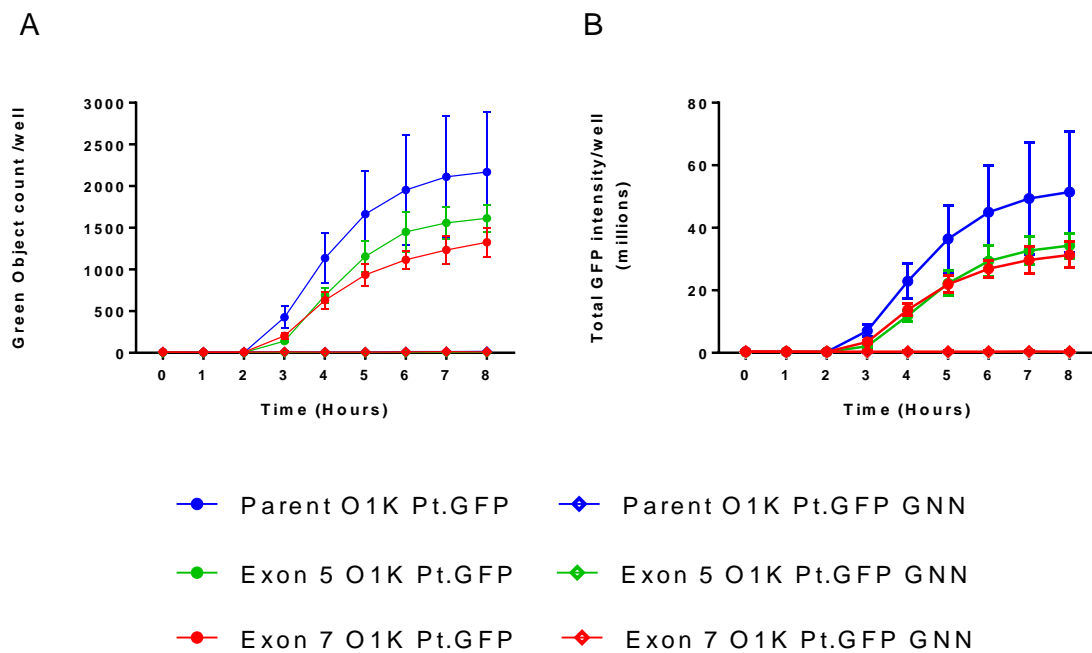
Figure 4.5.3: Effects of knocking out TBC1D20 on FMDV replication. Parent and knockout HeLa cell lines (Exon 5 and Exon 7) were seeded into 96 well plates and transfected with O1K Pt.GFP or O1K Pt.GFP GNN replicon RNA. Plates were read at hourly intervals on the minimax Spectramax i3 plate reader and the number of GFP expressing cells (A) and total GFP intensity of wells (B) was measured as indirect measures of FMDV replication. One experiment was carried out with 4 replicate wells per condition, data points and error bars show mean +/- SD.

This experiment showed a similar reduction in the level of infected cells for the knock out cells compared to the parental cells as was found using infectious virus (section as the number of GFP expressing cells (Panel A) was reduced. In addition, the overall GFP intensity per well (Panel B) in the knockout cell lines was also decreased when compared to the parent cell line. This suggests that FMDV replication is reduced in both the knockout cell lines implying that TBC1D20 may be required for optimum vRNA replication.

4.6 Discussion

Experiments carried out in this chapter used proteomic techniques to identify novel cellular interaction partners of FMDV 3A and investigate effects of changing expression levels of possible partners on infection. FMDV 3A likely

interacts with a wide range of proteins, a great number of which have yet to be identified and which could likely help increase understanding of the roles it plays in replication.

The 3A protein of picornaviruses plays a major role in formation of a viral RC and RO (as described in Chapter 1). However, none of the major cellular proteins (GBF1, ACBD3, PI4KIIIα) that bind picornavirus 3A proteins were identified in the initial FMDV 3A mass spectrometry analysis (carried out at University of Dundee) or in the Y2H screen (carried out by collaborators at Edinburgh University). This is consistent with studies by Berryman *et al* (Berryman et al., 2016) who showed that FMDV replication was independent of PI4K and, therefore, unlikely to depend on GBF1 or ACBD3. However DCTN3 (dynactin 3), which has been proposed as a cellular interacting protein for FMDV 3A (Gladue et al., 2014), and TBC1D20 (which had been identified by a previous PhD student at Pirbright as a potential cellular factor required for FMDV infection (Midgley, 2011) were identified in the mass spectrometry data analysis. Furthermore Rab7L1 was identified as a potential interacting partner, for FMDV 3A, in both the mass spectrometry and Y2H screens.

A previous study carried out on FMDV, identified DCTN3 (Dynactin 3) as a cellular interacting partner of 3A using a Y2H screen (Gladue et al., 2014). DCTN3 is also a subunit of a dynactin complex, which serves as a cofactor for the dynein motor. In addition, it was reported that over expression of DCTN3 or proteins that have been shown to disrupt the dynactin complex decreased FMDV infection. The region of 3A proposed to bind DCTN3 lies with the C terminal region of 3A (Gladue et al., 2014) that is proposed to influence host range specificity of FMDV (see Chapter 3) which suggests that DCNT3 may be a requirement for FMDV infection of bovine but not porcine cells. However, deletions in this region do not affect FMDV infection of BHK cells suggesting that if FMDV 3A binds DCTN3 then this interaction is may influence pathogenesis in certain hosts but is not necessarily a requirement for replication. The 3A protein of PV has been reported to bind LIS1 which belongs to the same complex as DCTN3. However, the relevance of this interaction was not studied in infected cells (Kondratova et al., 2005). Furthermore a study by

Teterina *et al* did not identify LIS1 as an interaction partner in pull-down experiments using epitope tagged PV 3A. Neither did they detect PI4K as an interaction partner of 3A but did confirm binding of GBF1 supporting the theory that PV 3A may not bind LIS1 directly (Teterina et al., 2011). However it was decided not to pursue further the potential role of DCTN proteins in FMDV infection, instead other proteins were selected to carry out additional studies on.

As mentioned above Rab7L1 was identified as a possible interacting partner for FMDV 3A in both the mass spectrometry analysis and the Y2H screen, suggesting that Rab7L1 may be required for FMDV infection. The cellular functions of Rab7L1 are largely unknown, although there is some evidence that HCV NS5 may partially localise with Rab7L1 during infection (Sklan et al., 2007a, Sklan et al., 2007b), and Rab7L1 has previously been linked with maintenance of the structure of the trans-Golgi network (Wang et al., 2014). However, in siRNA experiments conducted in IBRS2 cells no effect on FMDV infection was seen, suggesting that Rab7L1 is not required by FMDV. This observation should be considered a preliminary one, as due to a lack of Rab7L1 specific antibodies it was not possible to confirm the effect of the siRNA on the protein expression levels. If time had been permitting, it would have been useful to develop an RTqPCR to determine the effectiveness of the siRNA at the RNA level.

TBC1D20 was also identified as a potential interacting partner for FMDV 3A. The TBC1D20 protein is a known GAP for Rab1, a Rab GTPase that is involved in protein trafficking between the ER and Golgi and is required for Golgi structure maintenance (Haas et al., 2007). Direct interactions between TBC1D20 and viral proteins have been identified. The NS5A protein of Hepatitis C virus (HCV) binds TBC1D20 and TBC1D20 was shown to be essential for HCV infection and its depletion leads to inhibition of viral replication and infection (Sklan et al., 2007a, Sklan et al., 2007b). The TBC1D20 protein has also been identified as a host factor required for HIV as over expression of TBC1D20 arrests trafficking of the HIV-1 envelope protein through the secretory pathway and hampered envelope processing (Nachmias et al., 2012). Deficiencies in the Rab GAPs, such as TBC1D20 are associated with a number

of disorders, and mutations in TBC1D20 have been associated with Warburg micro syndrome an autosomal recessive disorder characterized by severe eye and brain abnormalities (Handley et al., 2015).

A previous PhD student in our laboratory has also studied the role of TBC1D20 in FMDV infection. For FMDV, it was observed that over expression of TBC1D20 reduces the number of infected cells by ~40% whereas TBC1D20-R105A appeared to have a greater inhibitory effect and reduced infection by ~60%. The reduction in infection caused by TBC1D20-R105A (a catalytically inactive variant of TBC1D20) was attributed to a possible a dominant-negative effect on the cells endogenous TBC1D20, blocking an essential interaction with down-stream effectors (Midgley, 2011). However, these observations could be interpreted to show that TBC1D20 has a role in FMDV infection that does not depend on its GAP activity.

Experiments using TBC1D20 knockout cell lines in this work showed there was a slight drop in FMDV infection levels in the knockout cell lines compared to in the parent cell line. However this drop was not enough to be significant suggesting TBC1D20 is not essential for FMDV infection but may have an enhancing effect. Furthermore it was found that the knockout cell lines appeared to have some disruption to the Golgi even when not infected, however as full disruption to the Golgi was observed in the parent cell line this difference in structure of the Golgi is likely not the only factor responsible for the drop in infection levels observed.

Together, the observations by Midgley and the results of this Chapter confirm that an intact Golgi is not required for FMDV replication, and, suggest a role for TBC1D20 in FMDV infection. This conclusion is based on the observations that depletion of TBC1D20 appears to inhibit genome replication and infection (section 4.5), whereas a previous study found expression of DN mutants of TBC1D20 inhibited FMDV infection (Midgley, 2011). These observations appear to somewhat contradict the observation that DN Rab1 inhibits FMDV infection (Midgley et al., 2013), as TBC1D20 has been identified as the GAP for Rab1. However, Midgley *et al* also showed that DN Arf1 also appeared to enhance

infection (Midgley et al., 2013). Therefore it is possible that the effect of blocking membrane flow through the secretory pathway by expression of DN Arf1 or DN Rab1 is independent, and not linked to, the role of TBC1D20 in infection. Although not proven, this conclusion is supported by the apparent inhibition seen with the catalytically inactive mutant of TBC1D20 (TBC1D20-R105A) (Midgley, 2011), which shows that inhibitory effect on FMDV infection is independent of GAP activity. Nevertheless, it seems that TBC1D20 is not an absolute requirement for FMDV infection and may instead serve as a co-factor that improves the efficiency of replication. Further studies will be required to determine the TBC1D20 proteins precise role in infection.

In summary this chapter has investigated effects of altering expression levels of two selected proteins, predicted to be possible interaction partners from mass spectrometry experiments, on FMDV infection and replication. However results from the mass spectrometry data produced an extensive range of possible hits that have yet to be identified and further analysis is required confirm how many of these are true interaction partners, and work on this data is ongoing.

Chapter 5: Investigating a potential FFAT-like motif in FMDV 3A

5.1 Introduction

FMDV replication occurs on intracellular membranes and requires interactions between viral proteins and intracellular organelles, and the proteins expressed on their surfaces (See chapter 1 sections 1.62 and 1.6.3). The ER and ERGIC resident proteins: **V**esicle associated membrane proteins (VAMP) **A**ssociated **P**roteins (VAP) are known to interact with several proteins via a specific motif known as an FFAT motif (Wyles and Ridgway, 2004, Loewen and Levine, 2005, Loewen et al., 2003).

Vertebrates have two VAP proteins: VAP-A and VAP-B while in yeast the main VAP-like protein is Scs2P (Loewen et al., 2003, Murphy and Levine, 2016). A splice variant of VAP-B known as VAP-C has also been identified but is not well characterised, although it has been shown to interact with HCV NS5B and over expression of VAP-C had a negative effect on viral replication (Kukihara et al., 2009). The VAP proteins are type II integral membrane proteins that act as receptors for cytoplasmic proteins at membrane contact sites (Skehel et al., 2000) and have been linked with roles in maintenance of the Golgi structure (Peretti et al., 2008) and intracellular protein trafficking (Peretti et al., 2008, Prosser et al., 2008, Wyles and Ridgway, 2004).

Dysfunction of VAP proteins has been shown to have negative effects; dysfunction of VAP-B has been linked with motor neurone diseases, and a single mutation within VAP-B has been linked with late onset amyotrophic lateral sclerosis as it leads to large aggregates forming in the ER (Nishimura et al., 2004). Over expression of oxysterol binding protein (OSBP: which has a FFAT motif; see below) was able to reduce these aggregates (Prosser et al., 2008).

A number of VAP interacting proteins have been identified, some of which contain a FFAT motif (i.e. two phenylalanine (FF) in an acidic tract (FFAT)). The FFAT sequence acts as an ER targeting motif that directly interacts with VAP proteins located on the ER or ERGIC (Prosser et al., 2008). They are described

as having the canonical sequence of 7 residues: E^1-F^2-F^3-D^4-A^5-x-E^7 (using the single letter a.a code, where x is any a.a) and a flanking region with multiple acidic residues and few basic residues (Loewen and Levine, 2005). These FFAT motif containing proteins target a number of membrane contact sites across many organelles and have been found in a large number of proteins, although not all VAP interacting proteins have a FFAT motif.

The majority of FFAT-motifs identified have been found in proteins involved in lipid transfer including the lipid transfer proteins OSBP and OSBP-related proteins (ORPs), and the ceramide transport protein (CERT) (Loewen et al., 2003, Kawano et al., 2006). Other FFAT motif containing proteins include the Rab18 GEF, Rab3GAP1, which regulates the morphology of the ER (Gerondopoulos et al., 2014), the AKAP220 and AKAP110 proteins (Mikitova and Levine, 2012) and the retinal degeneration B proteins Nir1, 2 and 3 (Amarilio et al., 2005). FFAT motifs have also been identified in yeast, e.g. the transcription factor Opi1p, which interacts with Scs2 (the yeast VAP homologue) via an FFAT motif (Loewen et al., 2003, Loewen and Levine, 2005) and some plant lipid transfer proteins (Mikitova and Levine, 2012).

Each of the elements of FFAT motifs (the core motif residues and the acidic flanking sequence) have sequence flexibility and a number of proteins have been identified with one or more differences to the canonical sequence; these are known as FFAT-like motifs (Saita et al., 2009, Mikitova and Levine, 2012). Such motifs have been found in proteins such as Protrudin, which has the FFAT-like motif EFKDAIE (Saita et al., 2009). However it has also been shown that an acidic residue cannot replace a small neutral residue at position 5 (Mikitova and Levine, 2012) and that substituting the aspartic acid (D) residue with alanine at position 4 of the FATT-like motif of Protrudin inhibited interactions with VAP (Saita et al., 2009). Furthermore many VAP proteins with a FFAT motif tend to contain an additional FFAT or FFAT-like motif and sometimes up to three such motifs have been identified in a single protein (Murphy and Levine, 2016). FFAT-like motifs may have differing strengths of interaction with the ER, which has been used as an estimate of VAP binding. Murphy and Levine developed a scoring system based on the 6 N terminal

residues of the acidic tract, and the 7 core motif residues whereby each variation to the canonical sequence was classed as a suboptimal element. In this system a canonical FFAT motif scores 0, and it is used to predict potential interactions between FFAT-motif containing proteins and VAP-A or VAP-B (Murphy and Levine, 2016).

It has been shown that viral proteins of hepatitis C virus (HCV), in particular NS5A and NS5B, also interact with VAP proteins. NS5B interacts with VAP-B, although not through a FFAT motif, but through binding to the VAP-B MSP domain and it has been found knocking down expression of VAP-B can be detrimental to HCV replication (Gupta and Song, 2016, Hamamoto et al., 2005). It has also been shown NS5A of HCV interacts with VAP-A as long as GPS2 is present (Gupta et al., 2012, Xu et al., 2013). NS5A and NS5B are key components of the HCV replication complex, and the interactions with VAP-A and VAP-B appears to anchor the RNA replication complex to the ER, which is required for HCV genome replication (Gao et al., 2004). This shows that viral proteins are able to interact with VAP-A and VAP-B and that this is required to replicate efficiently. Other viral proteins have been shown to interact with VAP proteins including the p48 protein of Norwalk virus (Ettayebi and Hardy, 2003), which interacts with VAP-A, and p33 of tombusvirus, which interacts with the OpiI and Scs2 proteins in yeast (Barajas et al., 2014).

Analysis of FMDV 3A sequences revealed a conserved region within the N terminal domain (residues 24-30) containing a possible FFAT-like motif with the core motif sequence E^1-F^2-F^3-E^4-G^5-M^6-V^7, and flanking region with acidic residues and few basic residues (Figure 5.1.1). This predicted FFAT-like motif sequence was found to be conserved in strains from each of the seven FMDV serotypes and is located close to a predicted dimerization domain of 3A (spanning residues 25-44) (Gonzalez-Magaldi et al., 2012). Furthermore VAP-B was identified as a potential interaction partner of 3A, in the mass spectrometry experiments using a 3A-GFP fusion protein (Chapter 4 section 4.3.2). A secondary possible FFAT-like sequence in FMDV 3A was also identified but likely has too many basic residues in the 5' flanking region to be considered a true FFAT-like motif. The lower panel of Figure 5.1.1 shows the sequences of

the FFAT and FFAT-like motifs of OSBP and Protrudin as well as that of the predicted first motif in FMDV 3A and the potential FFAT (although this is most likely not an FFAT domain, see above). The top panel shows the a.a sequence of O1K FMDV with the prediction of the likely FMDV-like domain in red and the secondary possible FFAT-like domain in green.

```
WT O1K 3A
ISIPSQKSVLYFLIEKGQHEAAIEFFEGMVHDSIKEELRPLIQQTSFVKRAFKRLKENFEIVALCLTLLANIVIMIRETR
KRQKMVDDAVNEYIEKANITTDDKTLDEAEKSPLETSGASTVGFRERTLPGQKACDDVNSEPAQPVEEQPQAE
```

```
                       1234567
Canonical    ------/EFFDAXE/--
OSBP         DEDDEN/EFFDAPE/II

Protrudin    EAEPDE/EFKDAIE/ET
FMDV 3A      QHEAAI/EFFEGMV/HD
FMDV 3A (2)  AFKRLK/ENFEIVA/LC
```
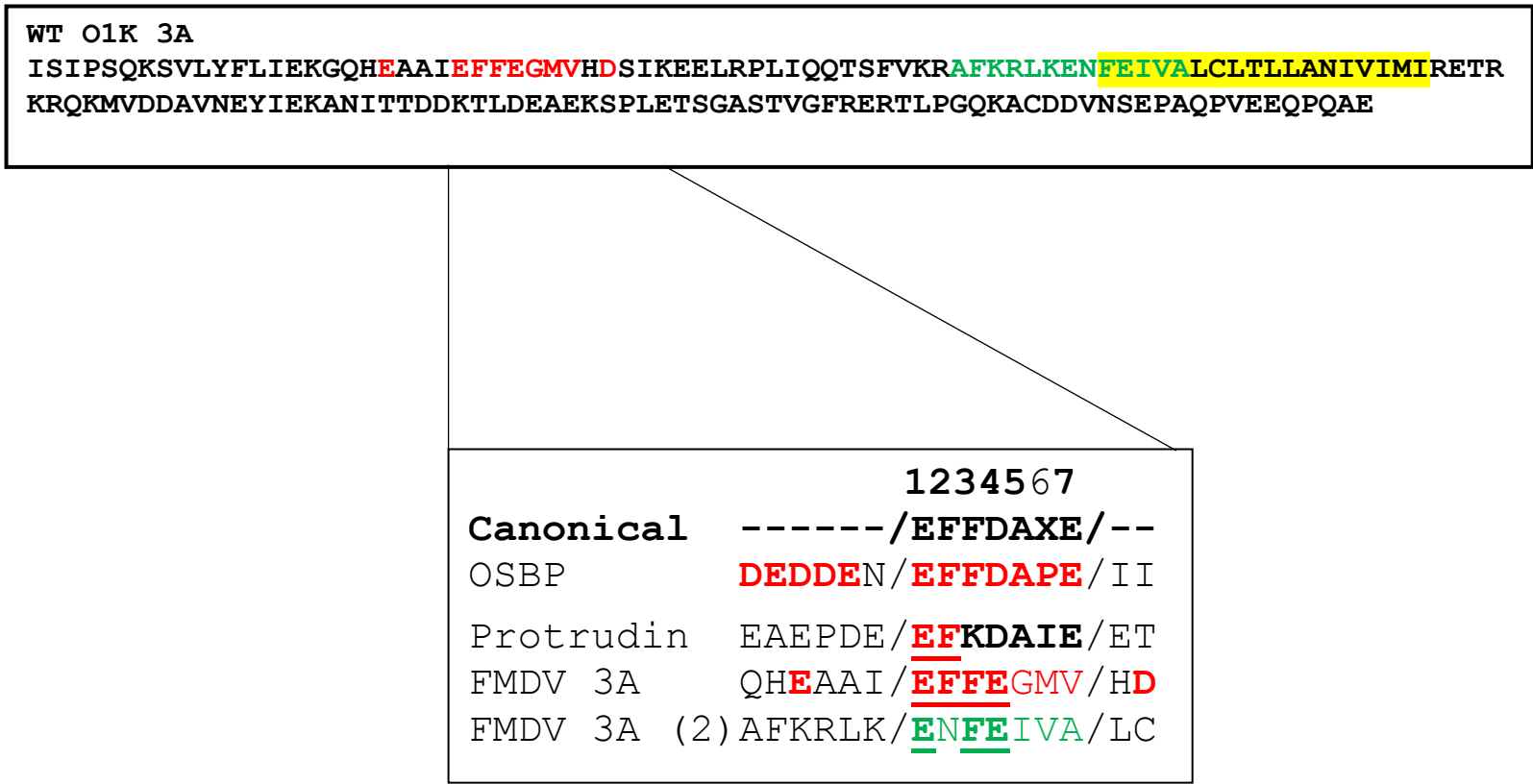
Figure 5.1.1: Location of a predicted FFAT-like motif in FMDV 3A: Analysis of FMDV 3A sequences found a region potentially fitting the characteristics of an FFAT-like motif located in the N terminal domain of 3A. The top panel shows the location of the predicted FFAT-like motif within the 3A. The FFAT-like motif is shown in red, with the secondary predicted FFAT motif in green, yellow highlights the predicted transmembrane domain of 3A. Lower panel shows sequence comparison between known FFAT and FFAT-like motifs of OSBP and Protrudin and the predicted motifs within FMDV 3A (FMDV 3A sequence was investigated in this work where as FMDV 3A (2) was determined to likely have too many basic residues upstream to be a true FFAT domain), and the canonical sequence of a FFAT motif.

This Chapter investigates the possible roles that the predicted FFAT-like motif in 3A may play in FMDV replication. The experiments used the FMDV GFP replicon system to measure effects on replication of introduction of various mutations within the core FFAT-like motif. Infectious recombinant viruses containing some of the mutations (which were used to test stability of viruses with mutations in this region of FMDV 3A) were also generated. Work carried out includes the substitution of multiple residues within the core motif, and replacing the core motif residues with those of other known FFAT motifs from different cellular proteins.

5.2 Effects on replication of changing multiple residues within the predicted FFAT-like motif of FMDV 3A

The N terminal domain of FMDV 3A is much more conserved than the C terminal domain. Therefore, as the predicted FFAT-like motif is located close to the N terminus and conserved across all seven serotypes of FMDV it could play an important role in replication through interactions with VAP proteins, similar to that proposed for HCV (Gupta et al., 2012, Gupta and Song, 2016, Hamamoto et al., 2005). Previous studies have shown that substituting various residues within the FFAT motif of several cellular proteins prevents binding to VAP proteins and ER localisation (Loewen et al., 2003, Mikitova and Levine, 2012).

To investigate if the predicted FFAT-like motif is required for FMDV replication a range of a.a substitutions were made in the 3A coding region within the O1K Pt.GFP replicon using quikchange mutagenesis (Chapter 2 section 2.2.3.7). These mutations altered two (EFFE to **AA**FE or EF**AA**) or four (EFFE to **ALLA**) a.a residues within the core motif creating replicons (i) O1K Pt.GFP AAFE, (ii) O1K Pt.GFP EFAA and (iii) O1K Pt.GFP ALLA respectively. Table 5.2 shows the mutations made in each replicon at both the a.a (top lines) and nucleotide (bottom lines) levels.

Replicon	FFAT-like motif Sequence						
O1K Pt.GFP	E	F	F	E	G	M	V
	GAA	TTC	TTT	GAG	GGC	ATG	GTC
O1K Pt.GFP GNN	E	F	F	E	G	M	V
	GAA	TTC	TTT	GCG	GGC	ATG	GTC
O1K Pt.GFP AAFE	**A**	**A**	F	E	G	M	V
	GCA	**GC**C	TTT	GAG	GGC	ATG	GTC
O1K Pt.GFP EFAA	E	F	**A**	**A**	G	M	V
	GAA	TTC	**GC**T	G**C**G	GGC	ATG	GTC
O1K Pt.GFP ALLA	**A**	**L**	**L**	**A**	G	M	V
	GC**A**	TT**A**	**C**TT	G**C**G	GGC	ATG	GTC

Table 5.2: Mutations made in the predicted FFAT-like motif of FMDV 3A.
Different mutations were made in the predicted FFAT-like motif in the 3A coding region of the O1K Pt.GFP replicon. These included changing the first 2 residues to alanine (O1K Pt.GFP AAFE), the third and fourth residues to alanine (O1K Pt.GFP EFAA) or residues 1 to 4 to alanine or leucine (O1K Pt.GFP ALLA). The changes to the a.a sequence for each replicon are shown with the nucleotide base changes shown below. The O1K Pt.GFP GNN replicon has a wildtype FFAT-like motif.

In vitro transcribed RNA from each replicon with mutations (O1K Pt.GFP AAFE, O1K Pt.GFP EFAA and O1K Pt.GFP ALLA), the parental wildtype replicon O1K Pt.GFP and O1K Pt.GFP GNN (a translation control) was transfected into BHK-21 cells (as described in Chapter 2 section 2.2.1.3) and GFP intensity levels measured over time on the IncuCyte zoom to determine the effects of the mutations on replication (Figure 5.2.1)

.
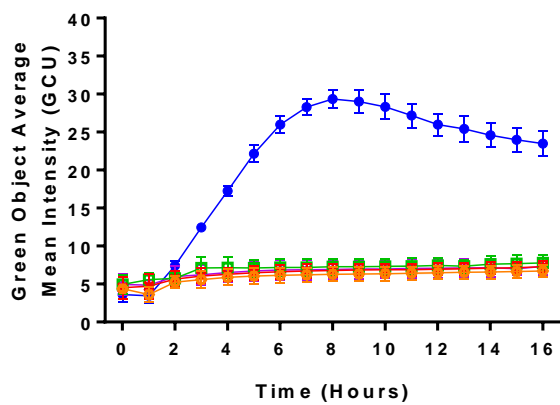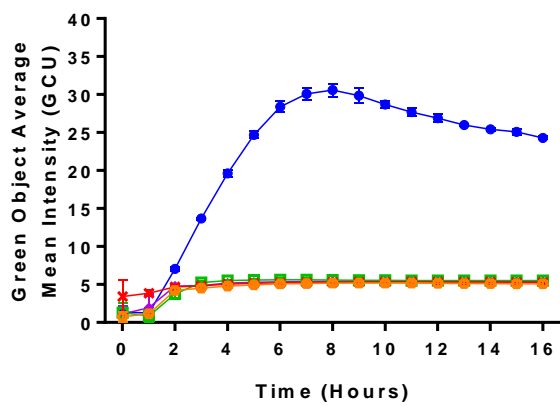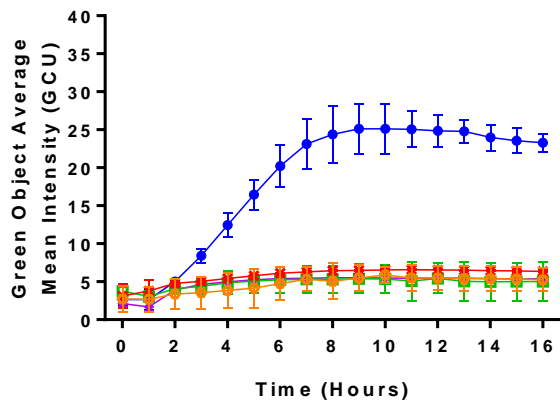
Figure 5.2.1: Effects of mutating two or more residues within a predicted FFAT-like domain of FMDV 3A. BHK-21 cells were transfected with replicon RNA from each of the replicons containing mutations within the predicted FFAT-

like motif of FMDV 3A along with RNA for the O1K Pt.GFP wildtype and O1K Pt.GFP GNN replicons to act as positive and negative controls of replication. GFP intensity levels were measured at hourly intervals as an indirect measure of replication. Results are shown for 3 independent experiments each with 3 replicate samples per replicon. Data points and error bars show mean +/- SD.

Results from 3 independent experiments showed (Figure 5.2.1) that each of the replicons with mutations in the predicted FMDV 3A FFAT-like motif gave similar GFP intensities as the replication defective O1K Pt.GFP GNN replicon. This suggests that the mutations had no effect on translation of the input RNA (for which O1K Pt.GFP GNN is a control) but prevented replicon RNA replication. Experiments carried out in parallel using cell lines derived from natural hosts of FMDV (MDBK (bovine) and SK-RST (porcine) cells) showed a similar effect on replication levels as none of the replicons containing mutations in the FFAT-like motif had GFP intensity levels above that of the translation only control (O1K Pt.GFP GNN) (data not shown). This suggests that the N terminal domain with FMDV 3A is potentially conserved due to having an essential function in replication and does not tolerate multiple a.a substitutions.

5.3 Effects of mutation of the glycine residue at position 5 of the predicted FFA-like motif in FMDV 3A on replication

Substitutions at position 5 of the canonical FFAT motif sequence have previously been found to have varying effects on VAP binding and can either enhance or prevent ER targeting, dependent on the a.a changes (Mikitova and Levine, 2012). Therefore, a second set of mutations were made that changed the glycine residue at position 5 within the predicted FFAT-like motif of FMDV 3A. This residue was changed to alanine (O1K Pt.GFP EFFE**A**), glutamic acid (O1K Pt.GFP EFFE**E**) or serine (O1K Pt.GFP EFFE**S**) in O1K Pt.GFP. The mutations at the a.a and nucleotide level are shown in Table 5.3.

Replicon	FFAT-like motif Sequence						
O1K Pt.GFP	E	F	F	E	G	M	V
	GAA	TTC	TTT	GAG	GGC	ATG	GTC
O1K Pt.GFP GNN	E	F	F	E	G	M	V
	GAA	TTC	TTT	GAG	GGC	ATG	GTC
O1K Pt.GFP EFFEA	E	F	F	E	**A**	M	V
	GAA	TTC	TTT	GAG	G**CT**	ATG	GTC
O1K Pt.GFP EFFEE	E	F	F	E	**E**	M	V
	GAA	TTC	TTT	GAG	G**AG**	ATG	GTC
O1K Pt.GFP EFFES	E	F	F	E	**S**	M	V
	GAA	TTC	TTT	GAG	**TC**C	ATG	GTC

Table 5.3: Mutations made at position 5 of the predicted FFAT-like motif in FMDV 3A. The glycine residue at position 5 of the FFAT-like motif of FMDV 3A was changed to alanine (O1K Pt.GFP EFFE**A**), glutamic acid (O1K Pt.GFP EFFE**E**) or serine (O1K Pt.GFP EFFE**S**) in the O1K Pt.GFP replicon. Amino acid sequence (top) and nucleic acid sequences (bottom) are shown for each of the replicons developed.

Replicon RNA from each of the replicons with a mutation at residue 5 of the FFAT-like motif, along with RNA from O1K Pt.GFP and O1K Pt.GFP GNN controls was transfected into BHK-21 cells and GFP intensity measured at hourly intervals using the IncuCyte zoom, as described for the previous set of mutations (Section 5.2). Figure 5.3.1 shows that mutating the glycine residue at position 5 had varying effects on replication.

.
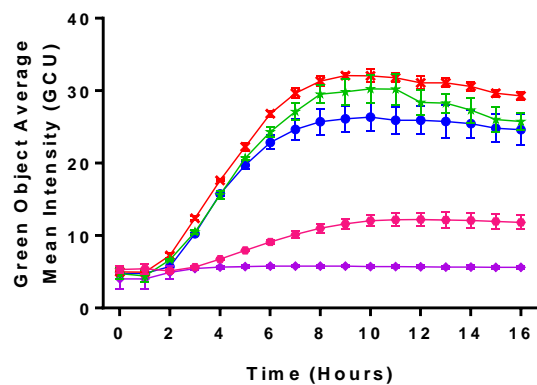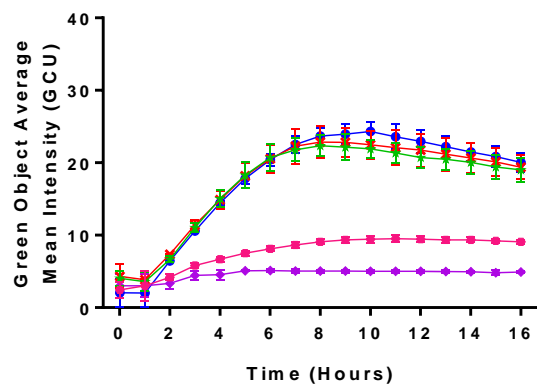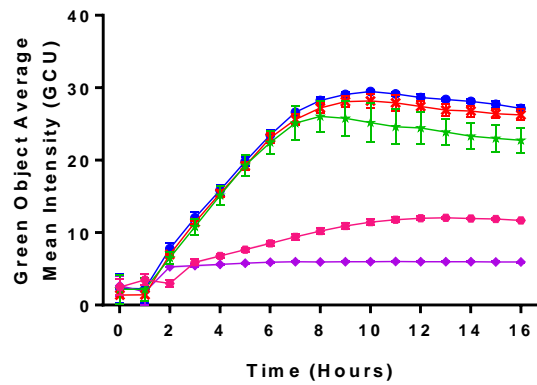
Figure 5.3.1: Effects of mutating the glycine residue at position 5 of the predicted FFAT-like domain in 3A. RNA transcribed *in vitro* from replicons containing mutations at the glycine residue at position 5 of the predicted FFAT-

like motif in FMDV 3A (O1K Pt.GFP EFFE**E**, O1K Pt.GFP EFFFE**A** and O1K Pt.GFP EFFE**S**) was transfected into BHK-21 cells in addition to RNA from the positive (O1K Pt.GFP) and negative (O1K Pt.GFP GNN) controls. GFP intensity was measured at hourly intervals as an indirect measure of replication. Three independent experiments with triplicate samples were carried out, data points and error bars represent mean +/- SD

The replicons where the glycine was mutated to alanine (O1K Pt.GFP EFFEA, shown in green) or glutamic acid (O1K Pt.GFP EFFEE, shown in red) gave similar GFP intensity levels to that of O1K Pt.GFP (shown in blue) suggesting they were able to replicate as efficiently as the wildtype replicon and that these mutations did not affect replication. However when the glycine residue was mutated to a serine (shown in pink) the GFP intensity levels were lower than those seen for O1K Pt.GFP, although levels were still higher than those observed with the translation only control (O1K Pt.GFP GNN), showing that the replicon was replication competent but partially attenuated compared to the wildtype and other mutated replicons. This was the case in each of the experimental repeats (Figure 5.3.1). Parallel experiments were carried out in MDBK and SK-RST cells (data not shown) for all three glycine substituted replicons and the results showed that the O1K Pt.GFP EFFEE and O1K Pt.GFP EFFEA replicons gave similar replication to the wildtype replicon as in BHK-21 cells. However, the O1K Pt.GFP EFFES appeared more severely attenuated in MDBK and SK-RST cells in comparison to in BHK-21 cells, with GFP intensity levels similar to O1K Pt.GFP GNN.

5.4 Changing the FMDV 3A predicted FFAT-like motif sequence to that of known FFAT motifs of cellular proteins

To further test the sequence flexibility of the potential FFAT-like motif in FMDV 3A, the sequence within O1K Pt.GFP was replaced with the sequence of the FFAT motif of OSBP, which has a canonical FFAT sequence of EFFDAPE (Loewen et al., 2003, Loewen et al., 2004), or to the FFAT-like motif of Protrudin, which varies from most other FFAT-like motifs as it only contains one

phenylalanine residue (EFKAIDE) (Saita et al., 2009). Table 5.4 shows the mutations made at both a.a and nucleotide levels. Replicon RNA was transfected in BHK-21 cells and GFP intensity levels measured as in sections 5.2 and 5.3 to generate a measure of vRNA replication.

Replicon	FFAT-like motif Sequence						
O1K Pt.GFP	E	F	F	E	G	M	V
	GAA	TTC	TTT	GAG	GGC	ATG	GTC
O1K Pt.GFP GNN	E	F	F	E	G	M	V
	GAA	TTC	GCT	GCG	GGC	ATG	GTC
O1K Pt.GFP OSBP	E	F	F	**D**	**A**	**P**	**E**
	GAA	TTC	TTT	GA**C**	G**CC**	**CC**G	G**AG**
O1K Pt.GFP Protrudin	E	F	**K**	**D**	**A**	**I**	**E**
	GAA	TTC	**AAG**	GAC	G**CC**	AT**C**	G**AG**

Table 5.4: Changing the predicted FFAT-like motif of FMDV 3A to that of cellular proteins with known FFAT motifs. The sequence of the predicted FFAT-like motif in FMDV 3A was swapped with the sequences of the known FFAT motif of OSBP, which has the canonical sequence of EFFDAPE, or to that of the previously published FFAT-like motif of Protrudin, which has the sequence EFKDAIE. The changes shown in the table were introduced into the 3A coding region of the O1K Pt.GFP replicon.

Figure 5.4.1 shows that both replicons in which the predicted FFAT motif was changed for the sequence of that of a previously identified FFAT motif of OSBP or the FFAT-like motif of Protrudin showed reduced levels of replication as the GFP intensity signals were similar to the O1K Pt.GFP GNN replicon. This was the case in all three independent experimental repeats, and suggests that although FFAT-like domains themselves can tolerate a certain amount of variation this is not the case for the FFAT-like motif in 3A. However, it is possible that changing multiple residues in the N terminal domain of FMDV 3A affects other possible functions of the protein (e.g. dimerization).
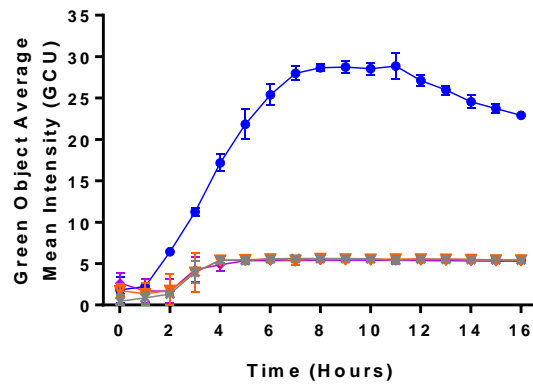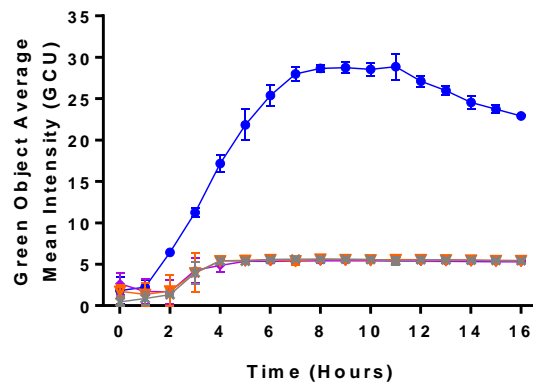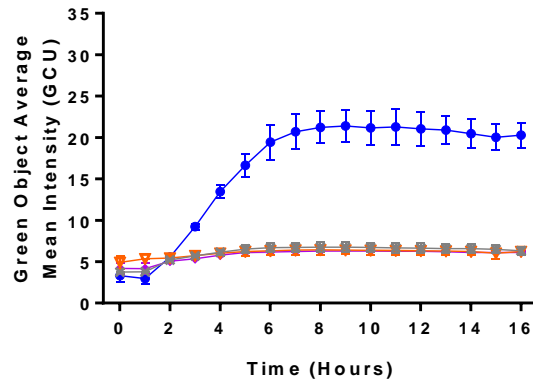
Figure 5.4.1: Changing the predicted FFAT-like motif sequence in FMDV 3A to that of known FFAT motifs and its effects on replication. RNA from O1K Pt.GFP OSBP and O1K Pt.GFP Protrudin replicons, in which the predicted

FFAT-like motif in FMDV 3A had been changed to match that of OSBP or protrudin respectively, was transfected into BHK-21 cells alongside RNA from O1K Pt.GFP and O1K Pt.GFP GNN. The GFP intensity was measured at hourly intervals as an indirect measure of replication. Three independent experiments each with triplicate samples were carried out. Data points and error bars show mean +/-SD.

5.5 Recovery of infectious FMDV containing mutations within the predicted FFAT-like motif in 3A

Three of the replicons generated in sections 5.2 and 5.3 were selected to generate infectious cDNA clones (i.e. recombinant viruses). The replicons selected were O1K Pt.GFP AAFE, O1K Pt.GFP ALLA (both appeared unable to replicate as replicons) and O1K Pt.GFP EFFES (reduced replication as a replicon). Scores of the strengths of these FFAT-like motifs were also calculated using the system developed by Murphy and Levine that predicts the strength of possible FFAT motifs by assigning each element with a score and combining them (see section 5.1) (Murphy and Levine, 2016). The calculations and scores for O1K WT, O1K AAFE, O1K ALLA and O1K EFFES are shown in Figure 5.5.1 (panels A, B, C and D respectively). The score of the predicted wildtype sequence the (i.e. FFAT-like motif) of FMDV 3A was calculated to be 6.5 (panel A), whereas the mutation of multiple residues to create the AAFE and ALLA mutations increased the scores (thereby weakening the motif) to 11.5 and 12.5 respectively (panels B and C). In the virus where a single a.a substitution of glycine to serine (O1K EFFES) had been made however, it actually improved the score reducing it to 3.5 (thereby making it closer to the optimum score of 0) as shown in panel D.

Panel A (wildtype FMDV)

Position	A	C	D	E	F	G	H	I	K	L	M	N	P	Q	R	S	T	V	W	Y	Score
1	1	1	0	0	1	1	1	1	2	1	1	1	1	1	2	1	1	1	1	1	0
2	4	4	4	4	0	4	4	4	4	4	4	4	4	4	4	4	4	4	2	1	0
3	1	1	1	1	0	1	1	1	1	1	1	1	1	1	1	1	1	1	1	0	0
4	2	2	0	2	2	2	2	2	2	2	2	2	2	2	2	1	1	2	2	2	2
5	0	0	4	2	2	2	2	2	2	2	2	2	2	2	3	1	1	2	2	2	2
7	1	1	0	1	1	1	2	1	2	1	1	1	1	1	2	1	1	1	1	1	1
Flankx6		1	1						-1						-1	1	1				1.5
Overall	Add all flank scores ≥4=0, ≥3=0.5, ≥2=1, <2=1.5																				6.5

Panel B

Position	A	C	D	E	F	G	H	I	K	L	M	N	P	Q	R	S	T	V	W	Y	Score
1	1	1	0	0	1	1	1	1	2	1	1	1	1	1	2	1	1	1	1	1	1
2	4	4	4	4	0	4	4	4	4	4	4	4	4	4	4	4	4	4	2	1	4
3	1	1	1	1	0	1	1	1	1	1	1	1	1	1	1	1	1	1	1	0	0
4	2	2	0	2	2	2	2	2	2	2	2	2	2	2	2	1	1	2	2	2	2
5	0	0	4	2	2	2	2	2	2	2	2	2	2	2	3	1	1	2	2	2	2
7	1	1	0	1	1	1	2	1	2	1	1	1	1	1	2	1	1	1	1	1	1
Flankx6		1	1						-1						-1	1	1				1.5
Overall	Add all flank scores ≥4=0, ≥3=0.5, ≥2=1, <2=1.5																				11.5

Panel C

Position	A	C	D	E	F	G	H	I	K	L	M	N	P	Q	R	S	T	V	W	Y	Score
1	1	1	0	0	1	1	1	1	2	1	1	1	1	1	2	1	1	1	1	1	1
2	4	4	4	4	0	4	4	4	4	4	4	4	4	4	4	4	4	4	2	1	4
3	1	1	1	1	0	1	1	1	1	1	1	1	1	1	1	1	1	1	1	0	1
4	2	2	0	2	2	2	2	2	2	2	2	2	2	2	2	1	1	2	2	2	2
5	0	0	4	2	2	2	2	2	2	2	2	2	2	2	3	1	1	2	2	2	2
7	1	1	0	1	1	1	2	1	2	1	1	1	1	1	2	1	1	1	1	1	1
Flankx6		1	1						-1						-1	1	1				1.5
Overall	Add all flank scores ≥4=0, ≥3=0.5, ≥2=1, <2=1.5																				12.5

Panel D

Position	A	C	D	E	F	G	H	I	K	L	M	N	P	Q	R	S	T	V	W	Y	Score
1	1	1	0	0	1	1	1	1	2	1	1	1	1	1	2	1	1	1	1	1	0
2	4	4	4	4	0	4	4	4	4	4	4	4	4	4	4	4	4	4	2	1	0
3	1	1	1	1	0	1	1	1	1	1	1	1	1	1	1	1	1	1	1	0	0
4	2	2	0	2	2	2	2	2	2	2	2	2	2	2	2	1	1	2	2	2	2
5	0	0	4	2	2	2	2	2	2	2	2	2	2	2	3	1	1	2	2	2	0.5
7	1	1	0	1	1	1	2	1	2	1	1	1	1	1	2	1	1	1	1	1	1
Flankx6		1	1						-1						-1	1	1				1.5
Overall	Add all flank scores ≥4=0, ≥3=0.5, ≥2=1, <2=1.5																				3.5

Figure 5.5.1: Scoring of strength of predicted FFAT-like motif in FMDV 3A. The strength of the potential FFAT-like motif in 3A was calculated using a scoring system developed by Murphy *et al* in which suboptimal elements of the core residues of the motif and the upstream 6 N terminal flanking residues were each assigned a score with that of an optimal FFAT domain scoring 0. The scores calculated for the wildtype FMDV (panel A), and 3 of the different mutations created (panels B, C and D) are shown with the residues that were used to calculate the binding score highlighted in blue.

Infectious clones were generated as described previously in Chapter 3 section 3.5 by replacing the Pt.GFP coding region with the O1K WT capsid-encoding region from the pT7S3 infectious clone. Infectious copy RNA was transfected into BHK-21 cells and cells monitored for appearance of CPE. At total CPE, or 48 hours post transfection, cells were freeze-thawed and lysate clarified and passaged onto new BHK-21 cells, and this process was repeated until viruses reached passage 2 or 3 (BHKp2 and BHKp3).

Infectious virus was recovered from all three of the infectious copies (O1K AAFE, O1K ALLA and O1K EFFES) with CPE being observed from 20 hours post infection at passage 1 (BHKp1), with little difference in CPE levels observed in comparison to the wildtype O1K positive control (derived from Pt.GFP O1K) apart from O1K AAFE, which showed less CPE. By passage 2 however viruses with mutations were achieving full CPE at times similar to the wildtype virus. Images showing CPE at passage 1 for each of the FFAT-like motif mutant viruses (from set 1) are shown in Figure 5.5.2. Similar observations were made in 3 independent experiments (referred to as experiment 1, 2 and 3 below).

Virus	Passage 1	Time post Infection
O1K WT		18 hours
O1K AAFE		46 hours
O1K ALLA		46 hours
O1K EFFES		46 hours
Cell only		46 hours

Figure 5.5.2 Recovery of FFAT-like motif mutant viruses. In vitro transcribed RNA from the 3 infectious clones with FFAT motif mutations in 3A (O1K AAFE, O1K ALLA and O1K EFFES) was transfected into BHK-21 cells, after 48 hours cells were freeze thawed and supernatant passaged onto new BHK-21 cells. Cell monolayers were checked regularly for appearance of CPE. The images show the time point post infection for passage 1. At the time shown, 2 of the 3 mutated viruses gave almost complete CPE. Positive and negative controls (O1K WT and cell only) were also included.

As the experiments using replicons with the mutations at the FFAT-like motif showed reductions in replication (O1K Pt.GFP EFFES), or complete attenuation to the level of the translation only control (O1K Pt.GFP AAFE and O1K Pt.GFP ALLA), it was thought that viruses with the AAFE and ALLA mutations may not be recoverable or would show reduced growth rate in comparison with the wildtype O1K virus. However, the rapid recovery of the mutant viruses and the observations that they appeared to cause CPE with similar kinetics at passage 2 to the wildtype FMDV control (which was seen in three independent experiments, each carried out using newly transcribed RNA) suggested that the recovered viruses could show reversion of the a.a sequence to restore the wildtype FFAT-like motif. Therefore, RNA from each of the recovered viruses was extracted and sequenced by Sanger sequencing to see if the mutations were stably maintained or if reversion of the mutations had led to the viruses being recoverable (see Section 5.6).

5.6 Sequencing recovered viruses for evidence of reversion of mutations made within the predicted FFAT-like motif of FMDV 3A

Viral RNA from lysates of a selection of the recovered viruses for experiments 1 and 2, at passage 1, 2 and 3 (BHKp1, BHKp2 and BHKp3) was extracted as described in Chapter 2 section 2.2.5.3. Single-stranded cDNA was made using reverse transcription (Chapter 2 section 2.2.5.4) and the 3A region amplified by PCR using primers that bind within 2C and 3B2. PCR products were purified by

gel extraction and sequenced using Sanger sequencing (as described in Chapter 2 section 2.2.8.1).

The O1K EFFES virus, which as a replicon had remained replication competent but was partially attenuated in comparison to the wildtype (section 5.2), maintained the mutations within the predicted FFAT-like motif at passage 2 and 3 in experiment 2. However, for experiment 1, by passage 1 the recovered virus appeared to have reverted back to wildtype sequence. These observations suggest that this mutation may be stably maintained and allow recovery of infectious virus containing the G to S a.a substitution at position 5 of the FFAT-like motif within 3A. Further support for this outcome was seen following a third experiment (discussed below) that yielded similar results.

The results of the sequence analysis also showed there appeared to be a reversion of the O1K ALLA virus (which contained the most nucleotide changes across the motif; 4 in total) back to the wildtype FFAT-like motif sequence for experiments 1 and 2. This occurred rapidly and could account for why little difference in the time taken for complete CPE to develop was seen in comparison to the O1K WT virus at passage 1 as the mutations had already been reverted. The other mutant virus (O1K AAFE) also reverted to wildtype but more slowly as in experiment 1, the consensus sequence at the first passage (BHKp1) appeared to be AFFDG before reverting fully to the wildtype sequence by passage 2 (BHKp2). However this slower change was not seen in the other experiment (experiment 2), where BHKp1 appeared to have the sequence EFFEA, which then changed to the wildtype sequence at passage 2 (BHKp2).

The recovered viruses from experiment 2 were passaged once more (BHKp3) and sequenced, which showed that the EFFES sequence was faithfully maintained while the sequence of the other 2 viruses (with AAFE and ALLA mutations) gave the consensus wildtype sequences as expected, since they had already given wildtype consensus sequences at a prior passage (See Table 5.6 for a summary of sequence results for each passage).

Experiment 1:

Virus	Transfected cells	Passage 1	Passage 2
O1K AAFE	-	AFFDG	EFFEG
O1K ALLA	EFFEG	-	-
O1K EFFES	-	EFFEG	-

Experiment 2:

Virus	Transfected cells	Passage 1	Passage 2	Passage 3
O1K AAFE	-	EFFEA	EFFEG	-
O1K ALLA	EFFEG	-	-	-
O1K EFFES	-	-	-	EFFES

Experiment 3:

Virus	Transfected cells	Passage 1	Passage 2
O1K AAFE	EFFEG	-	-
O1K ALLA	EFFEG	-	-
O1K EFFES	-	-	EFFES

Table 5.6: Sanger sequencing results from viral passages of viruses with FFAT-like motif mutations: Viruses with various mutations in the predicted FFAT-like motif in 3A were recovered and passaged in BHK-21 cells. RNA was extracted, used to make single stranded cDNA and the 2C to 3B2 region PCR amplified and sequenced by Sanger sequencing to look for reversions. For simplicity tables show consensus sequence results at each passage where a change from expected sequence was observed only. Results from 3 independent experiments using different input RNA preparations are shown.

The rapid appearance of the wildtype sequence for the AAFE and ALLA viruses suggested the possibility for contamination with the O1K WT, parental virus, particularly as the same apparent speed of reversion was observed in a subsequent "test" experiment where the positive control virus (O1K WT) was not included (data not shown). To address this issue further, each of the infectious copy plasmids (O1K AAFE, O1K ALLA and O1K EFFES) were re-transformed in bacteria (DH5 α *E.coli*), and grown at a lower temperature of (30°C) and new plasmid stocks prepared from a single, isolated colony. The

new plasmid DNA was then linearised and used to produce new *in vitro* transcribed RNA that was subsequently transfected into BHK-21 cells to recover virus and repeat the viral passage and Sanger sequencing (referred to as experiment 3).

In addition, the transcribed RNA was used as a template to obtain the sequence of the 3A FFAT motif for each of the infectious copy plasmids which showed the presence of the mutations that had been introduced to the FFAT-like motif.

In experiment 3 sequencing RNA extracted from transfected cells showed that the O1K AAFE virus appeared to have the complete wildtype consensus sequence at the nucleotide level. In comparison the O1K EFFES virus appeared to have maintained the mutations at BHKp2, which supports the results from experiment 2 that this virus is recoverable with the mutation. In contrast to the EFFES virus, but similar to the AAFE virus, the O1K ALLA virus again had the consensus wildtype sequence. This was seen following sequencing of RNA extracted from the transfected cells despite sequencing of the transcribed RNA suggesting the mutations were present. The sequencing results from experiment 3 are shown in table 5.6.

To further address the possibility of contamination by the wildtype virus, the O1K ALLA infectious copy plasmid (selected as it had the most mutations present but still appeared to change rapidly to wildtype) was deep sequenced to see if there was evidence of mixed populations at the plasmid level, and if the DNA was potentially contaminated. DNA was prepared and deep sequenced using an Illumina Miseq (Chapter 2 section2.2.8.2). Deep sequencing revealed that not a single run had a complete wildtype FFAT-like motif and the majority (and hence consensus) had the complete ALLA FFAT motif sequence. With an error rate of 0.5% for the process, this showed that >99.5% of infectious copy plasmid had the ALLA sequence and that the level of contamination, if any, was below the detection threshold of the software. *In vitro* transcribed viral RNA derived from this plasmid was also sequenced over the 3A region (as described above for previous viral passage experiment), which also showed that the

consensus sequence of the FFAT-like motif was ALLA. This RNA was then used in a subsequent transfection.

A transfection time course using the vRNA from above was carried out using BHK-21 cells. RNA samples were collected from the transfected cells at 2, 4, 6, 8 and 10 hours post transfection. RNA was extracted from the samples and reverse transcribed to make single stranded cDNA, which was then used as a template to amplify the 3A region by PCR as described previously. Aliquots (5µl) of the PCR products were analysed by gel electrophoresis and the remainder column purified and sequenced by Sanger sequencing.

The region containing the predicted FFAT-like motif was sequenced using 3 different primers, and each sequence obtained showed potential mixed populations, with major and minor peaks occurring at the nucleotides that had been mutated to create the ALLA sequence, suggesting potential contamination with a wild type virus. Importantly, two peaks were not observed in the input RNA at the mutated nucleotides and the traces either side of the mutations (i.e. outside of the region encoding the FFAT motif) showed only one clear peak at every position. Figure 5.6.1 shows the detailed chromatogram obtained for one sequencing primer for each sample.
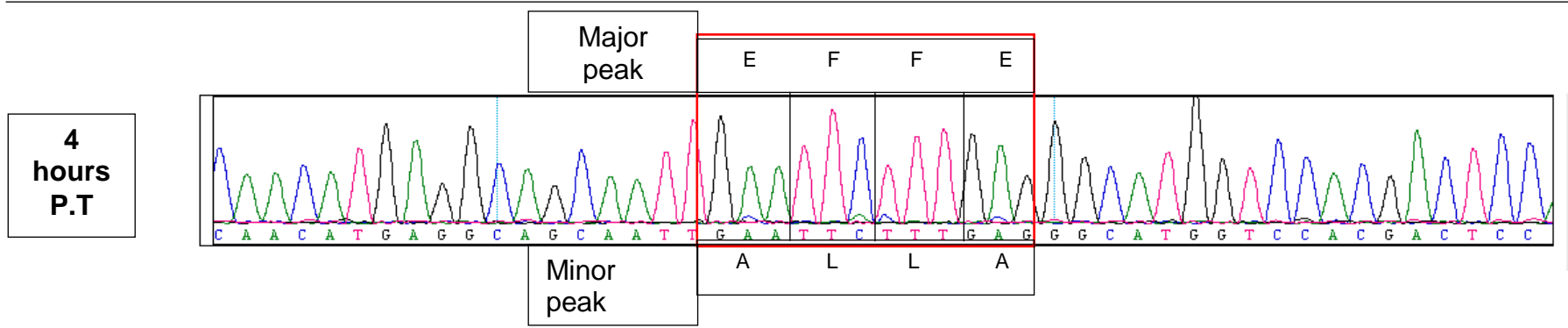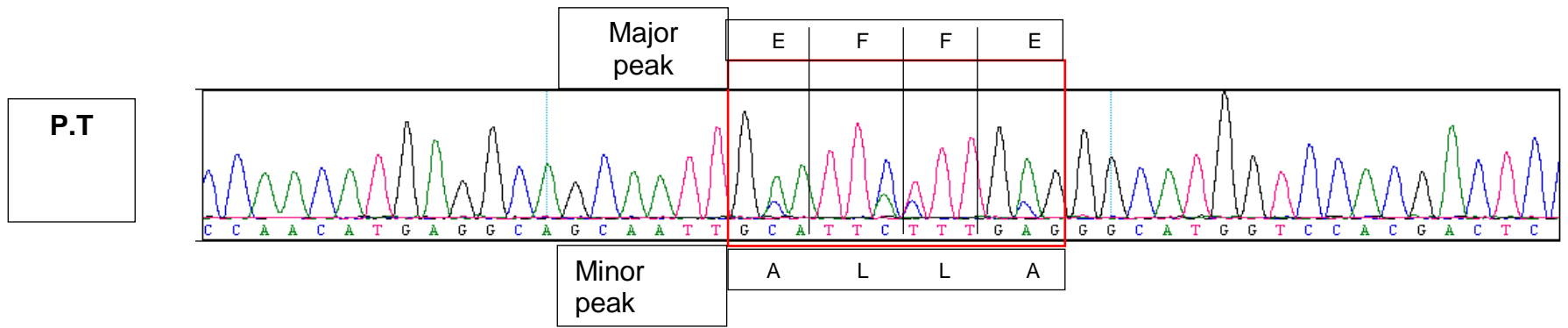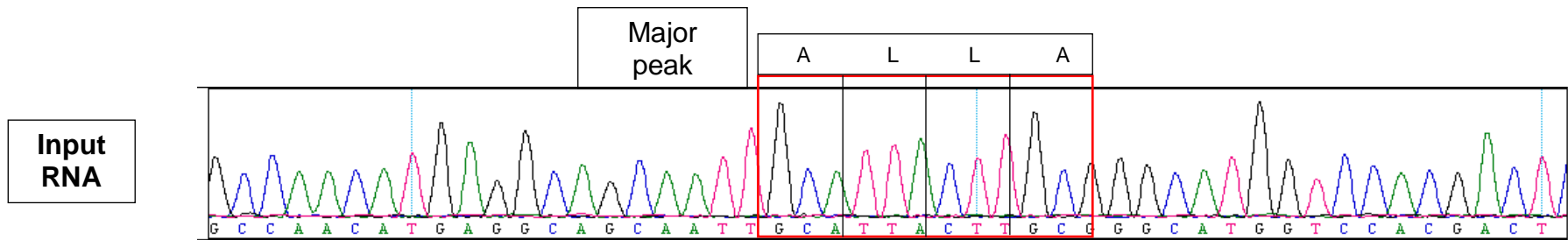
Figure 5.6.1: Chromatogram traces showing sequencing of RNA extracted from cells transfected with O1K ALLA RNA over time. Sanger sequencing of PCR products derived from single stranded cDNA of RNA extracted from transfected cells or from *in vitro* transcribed RNA prior to transfection. This showed that from 2 hours post transfection mixed peaks were seen at positions where the mutations had been made. One representative trace is shown from a single primer (in total 3 primers were used to obtain sequencing data). Consensus sequence data and sequences based on both the larger (major peak) and smaller (minor peaks) is summarised in table 5.6.2.

Analysis of the sequences showed that the chromatogram for the input RNA had single peaks across the entire region sequenced and that each of the 4 nucleotide changes made was present (Figure 5.6.2 panel A). However, by 2 hours (panel B) the chromatogram showed duplicate peaks at each of the 4 mutation sites; the larger peaks (major) showed that the nucleotide sequence for the EFFE wildtype motif had become the dominant sequence present, whereas smaller peaks (minor) showed the nucleotide sequence for the ALLA mutation virus. A similar pattern was observed in the chromatogram for the samples from 4 hours post transfection (panel C) although at this time point the minor peaks appeared smaller. This pattern of minor peaks for the ALLA sequence decreasing in size continued across the remaining time points (6 and 8 hours post transfection, data not shown) until by 10 hours post transfection where the smaller peaks were barely visible and the predominating peaks were the nucleotide sequence for the wildtype FFAT-like motif (data not shown). Sequence data for the first 4 hours is summarised in table 5.6.2 showing the sequence observed from the larger (major peaks), the smaller (minor peaks) and the overall consensus sequence provided by the software. A further observation made was that no double peaks were present throughout the sequences flanking the FFAT-like motif residues, which could indicate compensatory mutations from reversion. Although reversion to the wildtype sequence cannot be completely ruled out, the almost immediate replacement of the ALLA mutations by the wildtype sequence, and the observation that the change at each mutation site appeared simultaneously suggests the O1K ALLA

virus was likely outcompeted by a wildtype virus suggesting the presence of a contaminating replication competent virus.

Time point	Major peak sequence	Minor peak sequence	Consensus
Input RNA	–	–	GCA TTA CTTGCG A L L A
2 hours post transfection	GAA TTC TTT GAG E F F E	GCA TTA CTT GCG A L L A	GMA TTC TTT GAG A/E F F E
4 hours post transfection	GAA TTC TTT GGC E F F E	GCA TTA CTT GCG A L L A	GAA TTC TTT GAG E F F E

Table 5.6.2 Results of sequencing samples from transfection time course of O1K ALLA: In vitro transcribed RNA from O1K ALLA was transfected into BHK-21 cells and samples frozen at 2 hourly intervals. RNA was extracted from samples, single stranded cDNA made and the 3A region amplified by PCR. PCR products were sequenced by Sanger sequencing using 3 primers (one forward and 2 reverse). Table shows the nucleotide and a.a sequences for both the larger peaks (major sequence) and smaller peaks (minor peaks), as well as the consensus sequence output from the software following alignment of sequences from each of the primers used (3 in total).

5.7 Discussion

Proteins with FFAT motifs have been shown to interact with VAP proteins (Furuita et al., 2010, Kaiser et al., 2005). However, the ability of proteins with FFAT and FAAT-like motifs to bind VAP has been determined mostly by determining the ability of cytosolic proteins to interact with the ER. Although these studies have defined an optimal sequence of EFFDAxE for interaction with VAP proteins, they have also shown that some of the positions within the core motif tolerate variations and that FFAT binding can be retained when more that one of the core residues are mutated (Kaiser et al., 2005, Mikitova and Levine, 2012). This means that FFAT binding motifs are noted for their flexibility

and a large number of FFAT and FFAT-like binding motifs have been described (Murphy and Levine, 2016).

FMDV replication complexes (RC) form on cellular membranes and 3A is a membrane-associated protein that is likely to contribute to RC formation (Se Chapter 1 sections 1.6.2 and 1.6.3). Therefore it is possible that 3A requires a host factor or protein to tether to membranes, to initiate RC formation. Analysis of FMDV 3A identified a region near the N terminus of the protein, at residues 24 to 30, which fits the profile of a potential FFAT-like motif having the sequence EFFEGMV, as well as multiple acidic residues located in the N terminal flanking region. As FAAT motifs bind to VAP this suggested the intriguing possibility that FMDV 3A could use VAP proteins as a membrane tether. With this in mind, VAP A has been implicated as a host factor required for replication of HRV (Roulin et al., 2014). Testing the effects of a range of different mutations made within the 3A FFAT-like motif on viral replication using the FMDV replicon showed that substitution of 2 or more residues within the FFAT motif (EFFE to AAFE, EFAA or ALLA) led to a decrease in replication with GFP intensity levels similar to that of the translation only control, which would be consistent with these mutations abrogating VAP binding (Mikitova and Levine, 2012, Loewen and Levine, 2005).

Similar observations were made when the entire 3A FFAT-like motif was changed to that of previously identified FFAT motifs of OSBP and Protrudin. This shows that if the FMDV 3A sequence is a functional FFAT-like motif then changing it to other FFAT motifs was not tolerated. In addition, major changes to the FMDV sequence could impact on other processes mediated by 3A that are required FMDV replication. For example, the EFFEGMV sequence is located in the N terminal domain of FMDV 3A, an area which is more highly conserved than the C terminal domain of 3A, suggesting it may play an important role in viral replication that may or may not be due to an interaction with the VAP proteins. The fact it is conserved could also suggest there could be potential RNA structures in that region that may be disrupted in the mutant replicons/viruses although this explanation requires further exploration potentially using replicons and viruses with silent mutations as opposed to those

which change the a.a sequence. In addition, it is possible that changes at the FFAT-like motif could adversely affect 3A dimerization, which has been proposed to be required for FMDV infection as the predicted FFAT-like sequence within 3A is located adjacent to the predicted dimerization domain region (Gonzalez-Magaldi et al., 2012).

Changing the a.a at position 5 within the core motif in FMDV 3A was also studied and was found to have varying effects on replication; no effect on replication was seen upon changing the wildtype glycine residue to alanine or glutamic acid but replication dropped to around half the levels of the wildtype O1K Pt.GFP replicon when the glycine was replaced by a serine residue. This was seen in BHK-21, MDBK and IBRS2 cells although attenuation of O1K Pt.GFP EFFES was more severe in MDBK and IBRS2 cells. The observation that the introduction of alanine (A) at position 5 does not appear to affect FMDV replication is consistent with the effect of this change for other VAP binding proteins as previously observed by Mikitova *et al* (Mikitova and Levine, 2012). The introduction of serine (S) at position 5 appears to partially inhibit replication of the FMDV replicon. This is also consistent with the study by Mikitova *et al* who showed that the FFAT-like motif found in the AKAP 220 protein, has an S residue at position 5 (EFFDSxD) and shows only moderate ER binding (Mikitova and Levine, 2012). Therefore it is possible this change may have negatively impacted on the ability of the predicted FMDV 3A motif to interact with VAP causing the observation of reduced FMDV replication.

The results from studies on the glycine to alanine, and glycine to serine mutations are consistent with the expected outcome of previous studies introducing these mutations into other proteins known to bind VAP. However, this study also showed that the introduction of an acidic residue (e.g. glutamic acid (E)) at position 5 leads to a major reduction in VAP binding (Mikitova and Levine, 2012). Here my results show that changing the residue at position 5 from a glycine residue (G) to an acidic residue, glutamic acid (E) in the predicted FMDV 3A FFAT-like motif did not affect replication of the replicon (O1K Pt.GFP EFFEE), which could be interpreted to indicate that it does not function as a VAP binding site. However, as stated above there is considerable

flexibility in FFAT binding motifs and the inclusion of an E residue at position 5 may be tolerated within the context of different surrounding core sequences and the apparent viability of the EFFEE replicon does not completely rule out VAP binding.

Attempts to recover infectious viruses with FFAT mutations (AAFE and ALLA) appeared to suggest that viruses with mutations that inhibited replication completely (based on results from replicon assays) were unrecoverable as they consistently were found to have wildtype FFAT domains at early passage. Despite showing that the ALLA infectious copy plasmid (sequenced by both Sanger and deep sequencing) and *in vitro* transcribed RNA (sequenced by Sanger sequencing) derived from this plasmid had the ALLA sequence, it appears that the most likely explanation for recovery of viruses with the wildtype 3A sequence was a very low level of contamination with the wildtype virus (O1K WT) that was able to outcompete the non-replicative O1K ALLA virus. The one virus that was recoverable and retained the FFAT motif mutations was that with the glycine to serine substitution at position 5 (O1K EFFES). Experiments using GFP-based replicons showed this mutation led to a decrease in replication of the replicon, however this virus could be recovered, and the mutation was maintained. This was the one mutation that was selected to make into a virus in which the mutation led to the FFAT-like sequence being more similar to that of the predicted canonical sequence and hence was predicted to be a stronger FFAT-like domain than the wildtype based on the system derived by Murphy and Levine 2016 (Murphy and Levine, 2016). A retained ability to bind VAP may explain why the EFFES replicon appeared to be replication competent (although reduced compared to the wildtype) but also why the mutation was retained within the recovered viruses. In contrast, the other mutations (AAFE and ALLA) greatly reduce the FFAT-motif score and are predicted to abrogate VAP binding. Consistent with the above, if a low level of a contaminating wildtype virus was present in the EFFES virus then, as the mutant virus was replication competent and able to grow, it could outcompete the wildtype virus. One way to avoid this problem in future work would be to include marker mutations into the infectious clone, located somewhere upstream of the changes made that could

be used to differentiate between reverted virus and a contaminating wildtype virus. Nevertheless, the problems caused by this apparent contamination were time consuming and prevented further attempts to recover and characterise mutant viruses.

The predicted FFAT-like motif overlaps a region within the N terminal domain of FMDV 3A that is predicted to form one of two alpha helices and to serve as a 3A dimerization domain and mutations within this region had a negative effect on viral infectivity (Gonzalez-Magaldi et al., 2012). In addition, peptides corresponding in sequence to this region were reported to interfere with dimerization of 3A and decrease in FMDV infection (Gonzalez-Magaldi et al., 2015). Therefore it is possible that creating mutations within the FFAT-like motif could also be affecting protein structure and having an impact on regions downstream that are responsible for other functions required for viral replication, such as dimerization. Therefore, further work is required to identify if there is a direct interaction between FMDV 3A and VAP-A and VAP-B before it can be confirmed that this region within 3A does act as an FFAT-like domain.

Overall the results of this Chapter have shown that FMDV 3A has a potential FFAT-like motif located at the N terminal region of the protein that is conserved across the seven FMDV serotypes. Using a GFP-based replicon showed that mutations within this motif have varying effects on replication. In addition, a virus with mutations in this motif that did not completely inhibit replication of the replicon appears to be recoverable and the mutations stably maintained. These studies also suggest that results of experiments with recombinant viruses with mutations need to be treated with caution when reversions to wildtype sequences are seen, and suggest that the introduction of additional silent mutations distant to the sequence under investigation, that effectively act as markers of the recovered viruses as having truly reverted (and not having been outcompeted by a contaminating virus), should be included in the recombinant virus design.

Chapter 6: Investigating the potential role of 3A as the chaperone for delivery of VPg to the viral replication complex

6.1 Introduction

The proteins encoded by the P3 region of the genome of picornaviruses and the intermediate products generated during P3 processing have been shown to play a variety of roles in viral replication. One potentially important role of the P3 precursors is acting as the source of VPg (3B) for uridylation. VPg is uridylated on its third a.a residue (a tyrosine) to form VPg-pUpU, which serves as the primer for initiation of viral RNA replication (See Chapter 1 introduction section 1.4.9).

The initial models of picornavirus RNA replication (see Chapter 1 section 1.5.6) predicted that the intermediate precursor 3AB was the template for VPg uridylation (Liu et al., 2007, Murray and Barton, 2003). However, more recently a study by Pathak *et al* using PV suggested that a P3 intermediate processing product with 3B at its amino terminus (3BC or 3BCD) is the more likely precursors that act as the VPg donor as they showed that 3BC and 3BCD can bind more efficiently to the *cre* than VPg alone and be uridylated (Pathak et al., 2008). In addition to full length P3 ($3AB_1B_2B_3CD$), FMDV has the potential to produce several 3A-containing (e.g. $3AB_1B_2B_3$, $3AB_1B_2$, $3AB_1$) or 3C-containing precursors (e.g. $3B_1B_2B_33C$, $3B_2B_33C$, $3B_33C$, or each of these with 3CD) of VPg. However, it is not yet known which of these (or 3B alone) is uridylated in infected cells and used for viral genome replication. However, the recombinant FMDV 3C precursor proteins $3B_1B_2B_33C$ and $3B_33C$ have each been shown to be uridylated *in vitro* although neither was as efficient as "free" 3B3 (Nayak et al., 2006).

This Chapter investigates the donor of VPg for FMDV replication, using sub-genomic replicons and recombinant viruses. The P3 coding region was modified by inserting the '2A-like' sequence from the insect virus, Thosea Asigna virus (TaV) so that VPg (3B) could only be covalently linked to either 3A (referred to as 3A Donor) or 3C (referred to as 3C Donor). A third construct was created

with 2 copies of the TaV 2A in which 3B would only be produced as the 'free' 3B peptide(s) and not covalently linked to 3A or 3C (known as the No Donor).

The 2A peptide of many viruses, including FMDV, has been shown to allow co-translational "cleavage" of polyproteins, as they prevent formation of a covalent bond at their C terminal residue (Donnelly et al., 2001b, Ryan and Drew, 1994). Therefore, inclusion of a TaV "2A-like" peptide sequence provided a method of preventing a covalent linkage forming between 3A and 3B1, or between 3B3 and 3C that would still allow ongoing translation of downstream proteins. The TaV 2A sequence was chosen as it has previously been shown to be as active as the FMDV 2A peptide sequence in its ability to "cleave" itself at the C terminus (Donnelly et al., 2001a). In the Donor constructs (3A Donor, 3C Donor and the No Donor), to ensure that the processed P3 proteins had authentic N and C termini following cleavage at the TaV 2A sites, additional a.a (6 in total) were included (these are shown in Figure 6.1.1) to generate artificial cleavage sites. In the 3A Donor, the first 6 a.a of FMDV 3C were inserted between $3B_3$ and TaV2A to generate an artificial 3C site that would (when processed) give an authentic C terminus to $3B_3$. Similarly, the last 6 a.a of FMDV $3B_3$ were included before 3C to create an artificial 3C site, to generate an authentic N terminus for 3C.

For the 3C Donor, the first 6 a.a of $3B_1$ were inserted between 3A and TaV 2A to generate an artificial 3C site that would (when processed) give an authentic C terminus to 3A. Similarly, the last 6 a.a of 3A were included before $3B_1$ to create an artificial 3C site to generate an authentic N terminus for $3B_1$. In addition, the first 6 a.a of $3B_1$ included a Y3F mutation to prevent this sequence for functioning as a primer for vRNA replication.

In the No Donor cassette, 4 artificial 3C cleavage sites were included as follows:

1. The first 6 a.a of $3B_1$ were inserted between 3A and the first copy of TaV 2A to generate an artificial 3C site that would (when processed) give an authentic C terminus to 3A. In addition, a Y3F mutation was included to prevent this sequence for functioning as a primer for vRNA replication.

2. The last 6 a.a of 3A were included before $3B_1$ to create an artificial 3C site to generate an authentic N terminus for $3B_1$.

3. The first 6 a.a of 3C were inserted between 3B3 and the second copy of TaV 2A to generate an artificial 3C site that would (when processed) give an authentic C terminus to $3B_3$.

4. The last 6 a.a of $3B_3$ were included before 3C to create an artificial 3C site to generate an authentic N terminus for 3C.

The nucleotide sequence for these additional short a.a sequences (each 6 residues) were changed by introducing silent mutations in an attempt to limit recombination and distinguish revertant viruses from potential contaminating wildtype viruses. In addition, where the artificial cleavage site included the first 6 a.a of 3B1 the tyrosine at position 3 was substituted for a phenylalanine to prevent this sequence acting as primer for replication. Furthermore, a proline was added after each of the TaV sequences in order to facilitate cleavage. Silent mutations (8 in total) were also introduced into the second TaV 2A sequence of the No Donor construct in order to limit recombination.

The design of the P3 Donor cassettes is shown in figure 6.1.1. In the 3A Donor, only 3A is linked to $3B_{1-3}$ and 3B (VPg) can only be supplied to the replication complex by 3A. In the 3C Donor, $3B_{1-3}$ is only covalently linked to 3C therefore only 3C can supply VPg to a replication complex. In the No Donor, neither 3A nor 3C were linked to $3B_{1-3}$ so 3B would only ever be generated as "free" 3B peptide. However free 3B could also be generated by both of the other constructs (i.e. the 3A and 3C Donors) in addition to 3B intermediates. Natural 3C cleavage sites are indicated by the black arrows whereas the additional artificial cleavage sites are shown by blue arrows. The full sequence of the donor cassettes are shown in appendix 2 (A2).

Construct	P3 Region	Primary processing products

3A Donor

| 3A | 3B$_{1-3}$ | 3C a.a 1-6 | TaV 2A | P | 3B3 a.a 19-24 | 3CD |

Products:
| 3A | 3B$_{1-3}$ | 3C a.a 1-6 | Tav 2A |

| P | 3B3 a.a 19-24 | 3CD |

3C Donor

| 3A | 3B1 a.a1-6 | TaV 2A | P | 3A a.a 148-153 | 3B$_{1-3}$ | 3CD |

Products:
| 3A | 3B1 a.a1-6 | Tav 2A |

| P | 3A a.a 148-153 | 3B$_{1-3}$ | 3CD |

No Donor

| 3A | 3B1 a.a 1-6 | TaV 2A | P | 3A a.a 148-153 | 3B$_{1-3}$ | 3C a.a 1-6 | TaV 2A | P | 3B3 a.a 19-24 | 3CD |

Products:
| 3A | 3B1 a.a 1-6 | Tav 2A |

| P | 3A a.a 148-153 | 3B$_{1-3}$ | 3C a.a 1-6 | Tav 2A |

| P | 3B3 a.a 19-24 | 3CD |

Key:
P= Proline
Dashed lines indicate TaV 2A cleavage site, blue arrows indicate artificial 3C cleavage site, black arrows show natural 3C cleavage sites
Y3F=Tyrosine at position 3 of 3B1 has been changed to phenylalanine

Figure 6.1.1 Design of P3 region of Donor Cassettes: 3B donor constructs were designed where 3B could only ever be covalently linked to 3A (3A Donor), 3C (3C Donor) or free 3B produced (No Donor) through addition of a TaV 2A sequence between 3A and 3B1, or 3B3 and 3C or both. Proline residues (P) were added after the TaV 2A sequences to aid the 2A mediated cleavage. Additional a.a were included (3B1 a.a 1-6, 3C a.a 1-6, 3B3 a.a 19-24 or 3A 148-153) between the copies of TaV 2A and P3 proteins to act as artificial 3C cleavage sites and ensure authentic N and C termini were produced during processing. The predicted primary processing products produced following TaV 2A mediated cleavage (occurring at the site indicated by dashed lines) are also shown.

Each Donor cassette was cloned into the O1K Pt.GFP replicon generating 3B Donor replicons (referred to as O1K Pt.GFP 3A Donor, O1K Pt.GFP 3C Donor and O1K Pt.GFP No Donor) that were used to assess replication in BHK-21 and natural host-derived cell lines (porcine and bovine). Infectious clones based on each of the replicons were also constructed and viruses recovered, passaged and sequenced. Finally processing experiments (western blots and TnT reactions) were carried out to ensure that each construct was processing as expected and that any unwanted changes in processing were not responsible for differences seen in replication and growth between the different replicons and viruses.

6.2 Determining the effects on FMDV replication of the addition of TaV 2A sequences using replicons in different cell lines

DNA gene blocks for FMDV P3 which encoded the additional copies of TaV 2A and the other a.a changes described above (Table 6.1.1) were cloned in to the O1K Pt.GFP replicon plasmid replacing the existing P3 region. This led to the development of 3 new replicons, O1K Pt.GFP 3A Donor, O1K Pt.GFP 3C Donor and O1K Pt.GFP No Donor. RNA was transcribed *in vitro* from each of these replicons and transfected into BHK-21 cells. Replicons, O1K Pt.GFP and O1K Pt.GFP GNN were included as controls for normal replication and the background signal from translation of input RNA. GFP intensity was measured at regular intervals using the IncuCyte zoom as described previously.

Results (as shown in Figure 6.2.1) showed that both the O1K Pt.GFP 3A Donor and O1K Pt.GFP No Donor replicons appeared unable to replicate and gave GFP intensity signals that were similar to the O1K Pt.GFP GNN control. The O1K Pt.GFP 3C Donor, in comparison, appeared to be replication competent, giving a higher intensity signal than O1K Pt.GFP GNN. However, the O1K Pt.GFP 3C Donor was attenuated as the GFP signal was approximately 57% lower than the positive control wildtype replicon (O1K Pt.GFP).
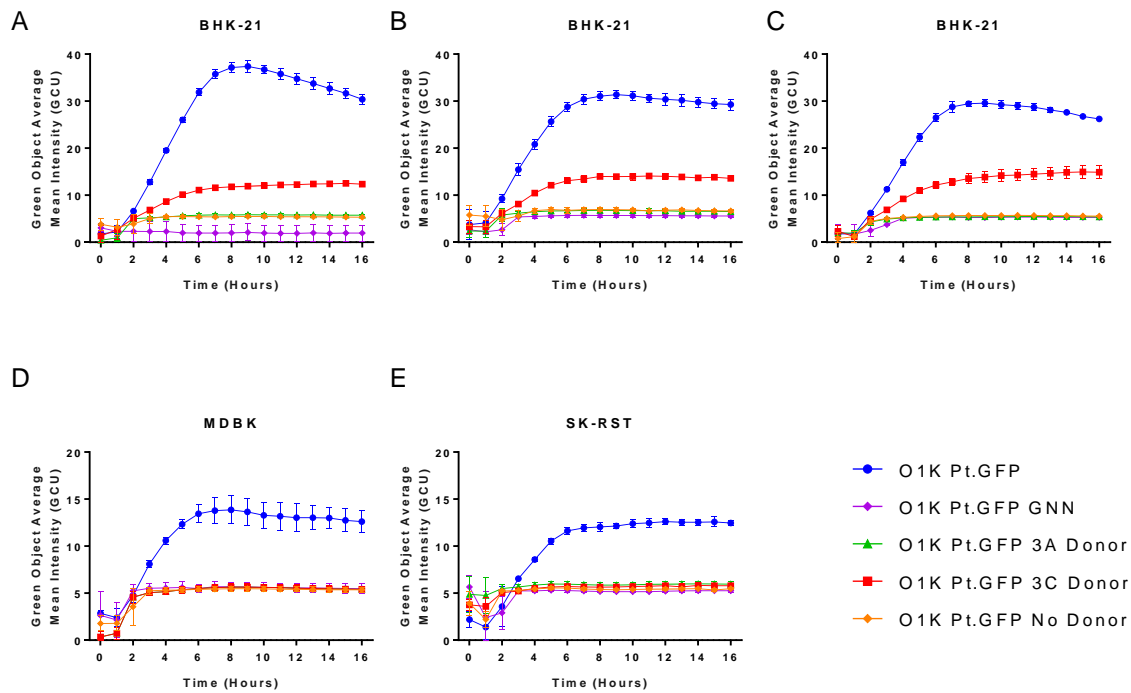
Figure 6.2.1 Replication of the 3A, 3C and No donor replicons in BHK-21, MDBK and SK-RST cells: RNA for the Donor replicons (O1K Pt.GFP 3A Donor, O1K Pt.GFP 3C Donor and the O1K Pt.GFP No Donor) were transfected into the indicated cell line (BHK-21, MDBK or SK-RST). In parallel cells were also transfected with RNA from the wildtype O1K Pt.GFP and the translation control O1K Pt.GFP GNN replicons. GFP intensity was measured at hourly intervals as an indirect measure of replication. Three independent experiments were carried out for each cell line each with triplicate samples. Panels A, B and C show all 3 experiments for BHK-21 cells. Panels D and E show one representative experiment for MDBK and SK-RST cells. Data points and error bars show mean +/- SD.
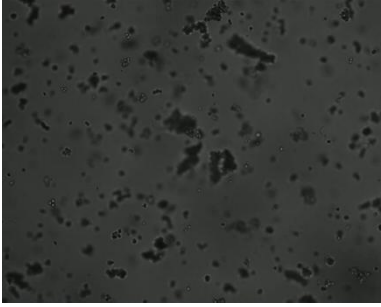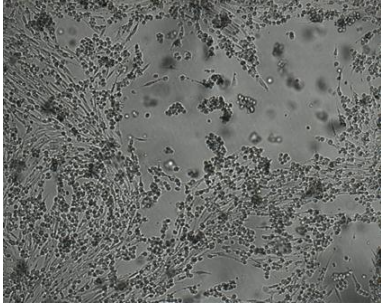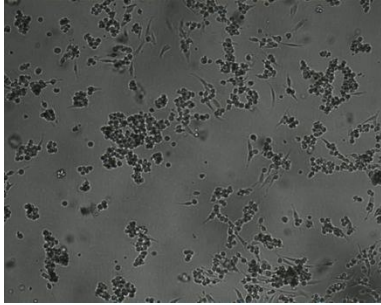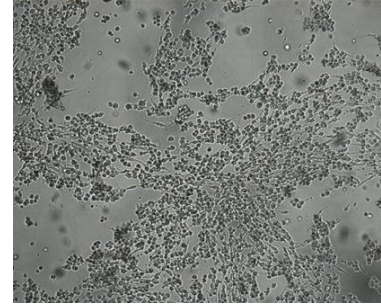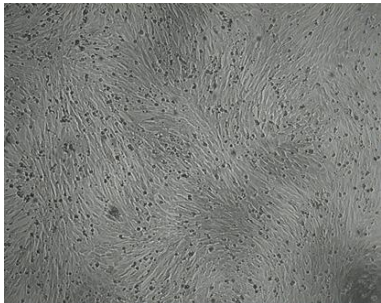
These results suggest that 3B needs to be covalently linked to 3C for efficient replication of FMDV in BHK-21 cells. The donor replicon experiments were also carried out (in parallel, using the same replicon RNA preparations) in cell lines derived from the natural hosts of FMDV, i.e. MDBK (bovine) and SK-RST (porcine) cells. Figure 6.2.1 panels B and C show results from one representative experiment (in MDBK and SK-RST cells respectively) of three independent repeats, each with triplicate samples. In both MDBK and SK-RST cells each of the 'donor' replicons (O1K Pt.GFP 3A Donor, O1K Pt.GFP 3C

Donor and O1K Pt.GFP No Donor) gave similar GFP intensities to the O1K Pt.GFP GNN replicon suggesting that the changes made to the P3 region had not impacted on translation but had affected replication in these cell lines.
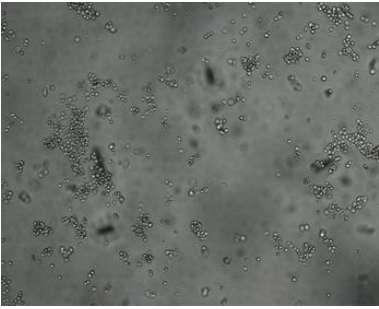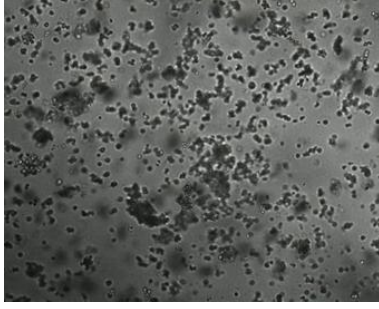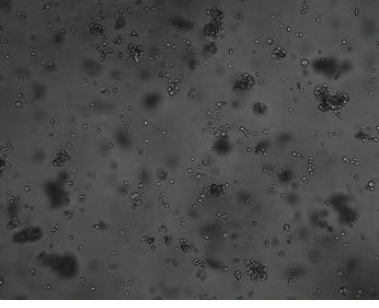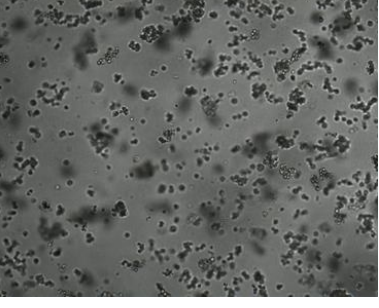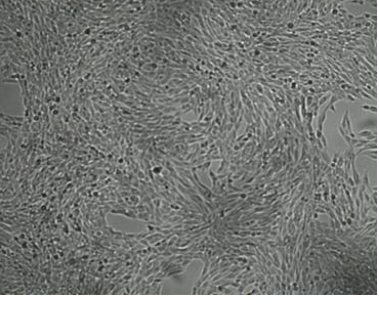
6.3 Recovery of infectious VPg donor viruses

Each of the Donor replicons was made into infectious clones by swapping the Pt.GFP coding region with the capsid coding region of O1K FMDV. *In vitro* transcribed RNA from each of the infectious clones (O1K 3A Donor, O1K 3C Donor and O1K No Donor) was transfected into BHK-21 and cells monitored for CPE as evidence for the production of infectious viruses.

Each of the viruses appeared to be recoverable with all producing CPE at passages 1 (BHKp1) and 2 (BHKp2) (See Figure 6.3.1). At passage 1 (Panel A), both the O1K 3A Donor and No Donor viruses produced extensive CPE at 48 hours post infection, whereas CPE was observed earlier in cell monolayers infected with O1K 3C Donor (28 hours). Of note, all of the Donor viruses produced CPE slower than the positive control O1K WT virus which produced total CPE by ~20 hours post infection. At passage 2 (panel B), CPE was observed at 18 hours post infection for each of the Donor viruses. Passage 2 viruses were titrated on BHK-21 cells by plaque assay (as described in Chapter 2 section 2.2.5.2); the results showed similar titres were obtained for each of the donor viruses (data not shown), although further work is required to clarify if the changes made to P3 impacted at all on viral growth kinetics.

A

Virus	Passage 1	Time post Infection
O1K WT		18 hours
O1K 3A Donor		48 hours
O1K 3C Donor		28 hours
O1K No Donor		48 hours
Cell only		18 hours

B	**Virus**	**Passage 2**	**Time post Infection**
	O1K WT		18 hours
	O1K 3A Donor		18 hours
	O1K 3C Donor		18 hours
	O1K No Donor		18 hours
	Cell only		18 hours

159

Figure 6.3.1: Recovery of the Donor viruses in BHK-21 cells. RNA was transcribed *in vitro* from each infectious clone (O1K 3A Donor, O1K 3C Donor and O1K No Donor) and transfected into BHK-21 cells. Infected cell lysates were passaged through BHK-21 cells. Cells were monitored for appearance of CPE. Shown is CPE for each virus at the indicated times post infection for passage 1 (A) and passage 2 (B). Data for O1K WT and uninfected cell monolayers are also shown.

At passages 1 and 2 in BHK-21 cells (BHKp1 and BHKp2), RNA was extracted from clarified cell-supernatants (as described in Chapter 2 section 2.2.5.3), reverse transcribed to make single stranded cDNA and the 3A to 3C coding region amplified by PCR. Sanger sequencing of the gel purified PCR products showed that at passage 1 and 2 (BHKp2), the O1K FMDV 3A Donor (which had TaV 2A between 3B3 and 3C) appeared to have reverted to the wildtype a.a sequence as no part of the TaV 2A sequence remained and the coding region of 3B3 was followed directly by that of 3C. However, careful inspection of the sequence traces revealed that at the nucleotide level the 3A donor virus showed twin peaks (Major and Minor) at 2 positions within the coding region for the C terminus of 3B3, and at 2 positions within the coding region for the N terminus of 3C (BHKp1 and BHKp2; Figure 6.3.2, panel A).

A
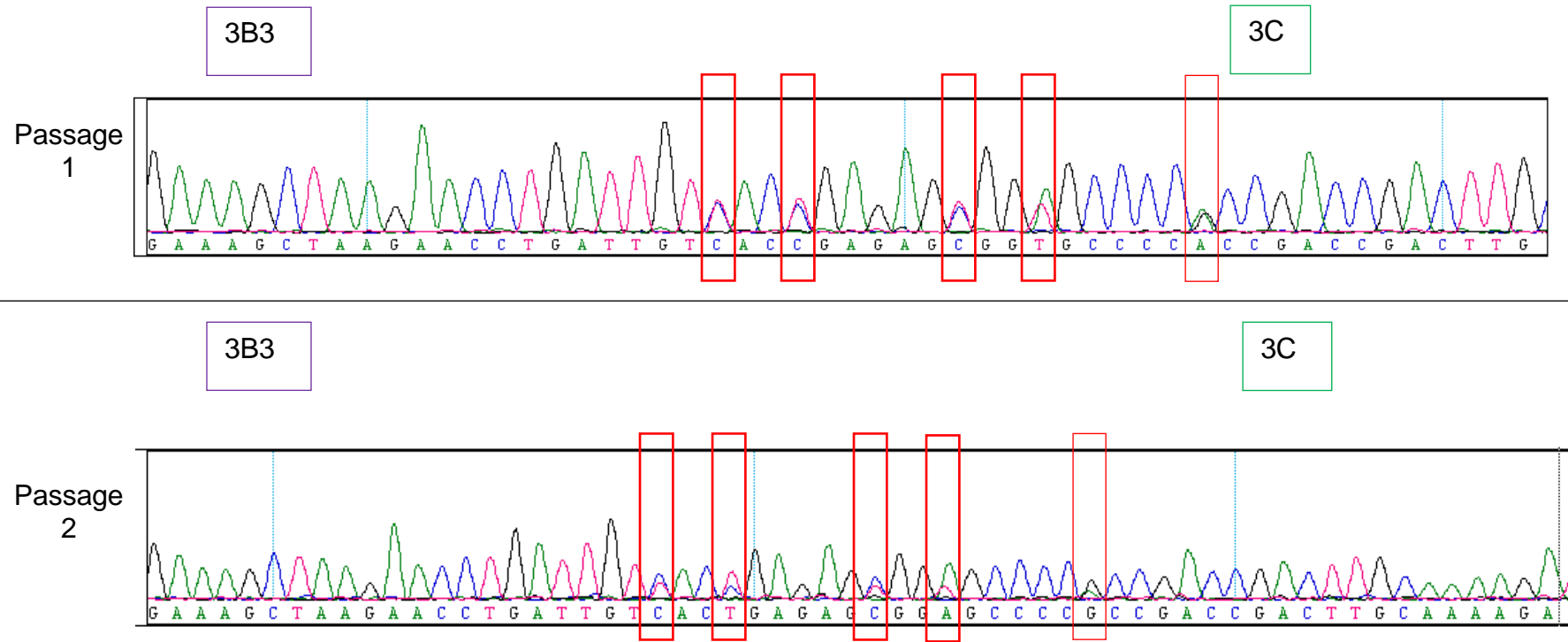
Amino acid and nucleotide sequence at the 3B3 and 3C boundary in the recovered O1K 3A Donor virus											
	3B3						3C					
aa	N	L	I	V	T	E	S	G	A	P	P	T
Wt	AAC	CTG	ATT	GTC	ACT	GAG	AGT	GGT	GCC	CCA	CCG	ACC
Mut	AAC	CT**C**	ATT	GT**T**	AC**C**	GAG	AG**C**	GG**A**	GCC	CC**G**	CC**C**	ACC
P1	AAC	CTG	ATT	GTC/**T**	ACT/**C**	GAG	AGT/**C**	GGT/**A**	GCC	CCA	CCG	ACC
P2	AAC	CTG	ATT	GTC/**t**	ACT/**c**	GAG	AGt/**C**	GGt/**A**	GCC	CCa/G	CCG	ACC
a.a = wt a.a sequence: Wt = wild-type sequence: Mut = mutations introduced into the short regions for 3B3 and 3C flanking TaV 2A in the original construct: P1 = sequence at the 3B3/3C boundary in the recovered virus at BHKp1: P2 = sequence at the 3B3/3C boundary in the recovered virus at BHKp2. Red font highlights the mutation sites. Lower case indicates the nucleotide was the minor peak.												

Figure 6.3.2: Chromatogram traces showing sequencing of RNA extracted from BHKp1 and BHKp2 recovered viruses for O1K 3A Donor. PCR products derived from RNA extracted from infected BHK-21 cells were Sanger sequenced using 3 different primers covering the P3 region. Chromatograms from one representative reaction are shown. Analysis revealed that the TaV 2A sequence was deleted at both passages suggesting possible reversion to wildtype virus. Two peaks were seen at some of the locations where silent mutations were made to limit recombination at the artificial 3C cleavage sites and additional proline residues that were present in the 3A donor cassette (Red boxes). The table (B) shows both the expected wildtype and mutated nucleotide sequences along with those observed from sequencing data of passages 1 and 2.

These peaks correspond to a mixture of the wildtype nucleotides and the third base mutations introduced into the coding region of the additional, short a.a sequences that were inserted to create artificial 3C cleavage sites either side of TaV 2A (i.e. residue 1-6 of 3C inserted between 3B3 and TaV 2A, and the last 6 residues of 3B3 inserted after TaV 2A and immediately before 3C; see Figure 6.3.2). Specifically, the twin peaks were at (i) the last 2 nucleotide positions (of 4) corresponding to where mutations were introduced into the short region encoding residue 1-6 of 3C and, (ii) at the first 2 nucleotide positions (of 3) corresponding to where mutations were introduced into the short region encoding the last 6 residues of 3B3. At the other sites where mutations were made only one peak was seen and this corresponded to the wildtype sequence. At BHKp1 (Figure 6.3.2, panel A upper trace), the major and minor peaks at these positions in 3B3 (C/T and C/T) and 3C (T/C and A/T) were of similar intensity while at BHKp2 (Figure 6.3.2, panel A lower trace), there were larger differences in peak intensity between the major and minor peaks. At the first position in 3B3 the C predominated over the T while at the second position a T predominated over the C; thus at these positions the wildtype nucleotide were predominant. In contrast, in 3C, at the first position the C predominated over the T while at the second position an A predominated over a T; consequently at these positions the mutations were the predominant nucleotides. The table in panel B of figure 6.3.2 shows the predicted nucleotide sequences of both the wildtype a.a codon and that of the mutation in addition to the codon sequences found in passages 1 and 2. The presence of twin peaks at these sites, and at the observed pattern, suggests that the recovered virus was a mixed population resulting from different deletions spanning the TaV 2A region and therefore a true reversion rather than contamination by a wildtype virus. Nevertheless, the results could also be explained by the presence of 2 main virus populations; one with a full wildtype sequence and the other with mutations in both 3B3 and 3C. However, given the design of the original construct it is difficult to explain how the latter virus could be generated by deletion or recombination which supports the conclusion that the sequencing results are best explained by 2

separate deletion events spanning the TaV 2A occurring on different RNA molecules.

In contrast to the 3A Donor virus, the sequence of the recovered O1K 3C Donor virus remained unchanged at passage 2 (Figure 6.3.3). The copy of TaV 2A and all other nucleotide changes present in the input RNA were faithfully retained. This virus was passaged on further to passage 4 (BHKp4) on BHK-21 cells and the sequenced of the PCR product (produced as above) showed that same result as no changes in the region of P3 sequenced were observed from the input RNA. A second experiment was carried out with new *in vitro* transcribed RNA derived from plasmid DNA that had been retransformed through bacteria and yielded similar results as the O1K 3A Donor virus appearing to revert to the wildtype a.a sequence at passage 1 (BHKp1)) but again 2 peaks were observed at positions where mutations had initially been introduced suggesting a possible mix of virus populations. The O1K FMDV 3C Donor recovered virus maintained the sequence of the input RNA as observed in the previous experiment.
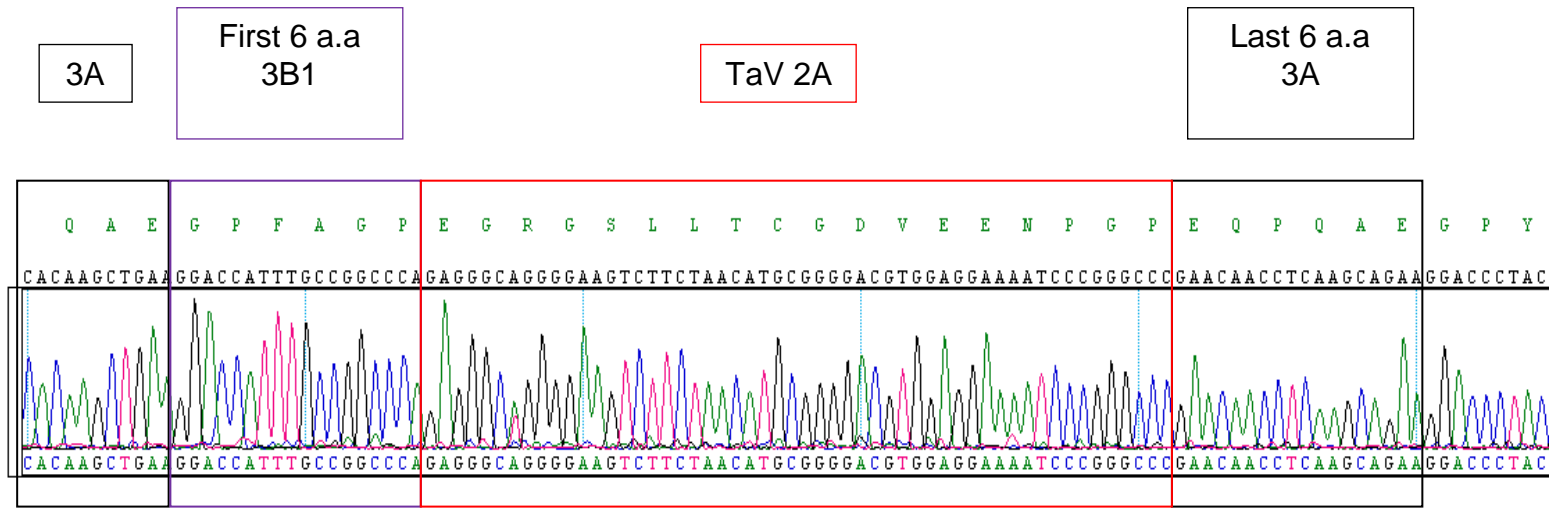
Figure 6.3.3 Recovery of O1K 3C Donor Virus: RNA extracted from passage 2 of the O1K 3C Donor virus (BHKp2) was reverse transcribed to produce single stranded cDNA which the P3 region was then used as a template in a PCR for the P3 region. The PCR products were sequenced by Sanger sequencing. The chromatogram produced from a single reaction is shown and indicates the changes made to the P3 region are still present at passage 2 in BHK -21 cells

The results of sequencing the O1K No Donor recovered viruses were less clear. Sequencing passage 2 (BHKp2) gave the wildtype FMDV nucleotide sequence with no TaV 2A sequence or mutations present. Therefore, the O1K FMDV No Donor plasmid was sequenced on the Miseq to obtain deep sequence data to look for possible contamination with wildtype FMDV at the plasmid level. An analysis of the data from the Miseq showed no evidence for a mixed population with a 99.5% confidence that the No Donor plasmid was correct. In addition, the earlier passage (BHKp1) was also sequenced along with the input RNA used for transfection and RNA extracted from the transfected cells. Analysis of the sequencing data from PCR products from both passage 1 and the transfection stage showed that the virus sequence exactly matched the wild-type O1K virus. In contrast, the PCR product derived from the input RNA showed that the sequence of the transcribed RNA appeared to be correct, matching that of the predicted O1K FMDV No Donor virus. This suggests, if the virus is reverting to wildtype it is doing so quickly and within the transfected cells. To see if this was possible a transfection time course (as described for O1K ALLA, Chapter 5 section 5.6) was carried out. Interestingly, when the PCR products were run on a gel, prior to sequencing, a clear size difference was observed between PCR products derived from the input RNA and the PCR products for all other time points investigated. This difference was approximately 150 base pairs which matched the expected size difference between the O1K No Donor and O1K wildtype virus (Figure 6.3.4). Sequencing of the PCR products showed that while the input RNA was correct and matched the expected O1K No Donor sequence, by 2 hours post transfection, and at all subsequent time points, the consensus sequence was that of O1K WT.
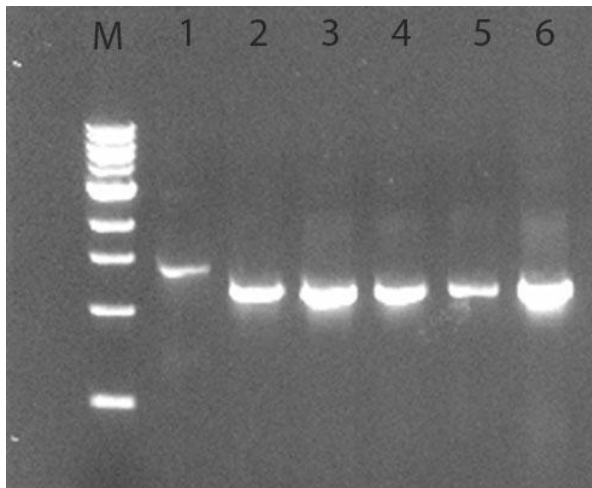
Lane M: 1Kb DNA marker
Lane 1: Input RNA
Lane 2: 2 hours post transfection
Lane 3: 4 hours post transfection
Lane 4: 6 hours post transfection
Lane 5: 8 hours post transfection
Lane 6: 10 hours post transfection

Time point	Consensus Sequence
Input RNA	O1K No Donor
2 hours post transfection	O1K WT
4 hours post transfection	O1K WT

Figure 6.3.4: Sequencing of O1K No Donor RNA in transfected cells: BHK-21 cells were transfected with the O1K FMDV No Donor RNA. Total RNA was extracted from the transfected cells at 2 hourly intervals post transfection. RT and PCR reactions spanning the P3 region of the genome were carried out using the extracted RNA as the starting template. PCR products were analysed by gel electrophoresis (upper panel) and sequenced by Sanger sequencing (lower Table). Input RNA used for the transfection was also used to generate a PCR product and sequenced. M indicates size markers. The PCR products for 2-10 hours post-transfection were ~150 base pairs smaller that the PCR for the input RNA. By 2 hours post transfection the PCR product had a sequence corresponding to a wildtype virus (O1K WT).

These results could be explained by the presence of a contaminating wildtype virus, which would be expected to out compete the O1K No Donor virus. However, if this were the case and wildtype and O1K No donor RNA were co-transfected then it might be expected that at 2h post-transfection two PCR products would be generated; one derived from the input O1K No donor RNA and the other from the contaminating wildtype RNA assuming there was enough of each type of RNA to be detected by running products on an agarose gel. Furthermore, the PCR product for the input O1K No donor RNA would likely persist in the transfected for longer and show a gradual replacement by the replication competent wildtype RNA. Although still to be confirmed this suggest that the apparent reversion to the wildtype sequence is more likely the result of an internal deletion within the input RNA that restores the wildtype sequence.

6.4 Investigating processing of the Donor Replicons and viruses

6.4.1 Investigating processing of Donor replicons and viruses by Western Blots

To ensure the addition of TaV 2A and the extra a.a included to generate artificial 3C cleavage sites had not affected P3 processing and therefore the ability of the Donor replicons to replicate, processing experiments were carried out using samples from both replicon transfected and infected cells. BHK-21 cells were transfected with *in vitro* transcribed replicon RNA or infected with the recovered donor viruses (MOI of 1). At 8 hours post transfection or 4 hours post infection, cells were lysed and supernatants boiled (see Chapter 2 section 2.2.6.1.). Samples were run on 12% SDS PAGE gels and western blots for both 3A and 3D proteins carried out as described in Chapter 2 section 2.2.6.2.

A
α3A (mAb 2C2)

B
α3D (Ab TC27)

C
β-actin
α3A (mAb 2C2)
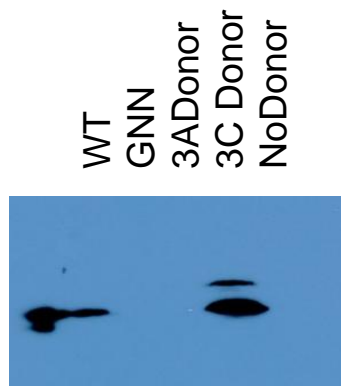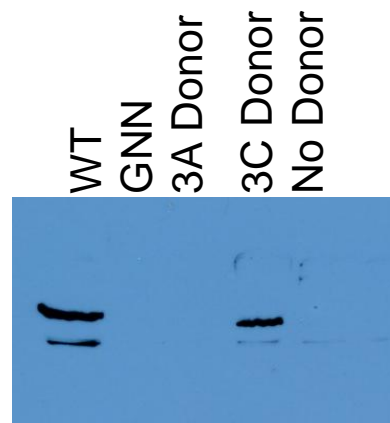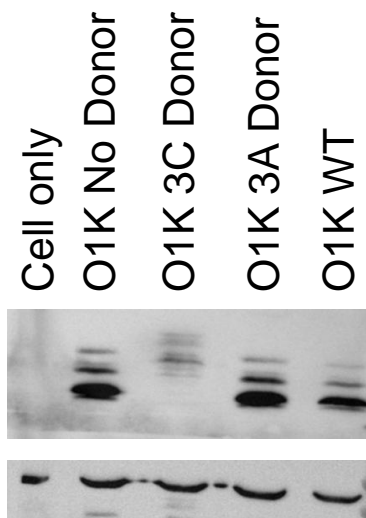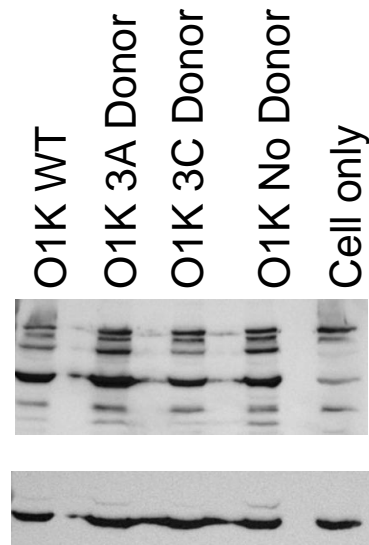
D
α3D (Ab TC27)

Protein	MW (KDa)
3A	17
3AB	19
3ABB	22
3ABBB	25
3ABBBC	48
3D	52

Figure 6.4.1: Western Blots for FMDV 3A and 3D in transfected and infected BHK-21 cells. Lysates were prepared from replicon (3A, 3C and No donor replicons) transfected cells at 8 hours post transfection or from cells infected with the Donor viruses (O1K FMDV 3A Donor, O1K FMDV 3C Donor and O1K FMDV No Donor) at 4 hours post infection and run on SDS-PAGE gels. Proteins were transferred to nitrocellulose membranes and probed with antibodies to the 3A (panels A and C) and 3D proteins (panels B and D). Panels A and B show blots using replicon transfected cell lysates while panels C and D show blots using lysates from infected cells.

Figure 6.4.1 (Panels A and B) shows results from western blots using samples from replicon transfected BHK-21 cells. Panel A shows that a band of approximately 20 KDa was detected with the antibody to 3A for the wildtype O1K Pt.GFP however for the O1K Pt.GFP 3C Donor replicons 2 bands of approximately 20 and 25 KDa were seen. For the O1K Pt.GFP replicon the band is likely to be 3A although it could be a 3A3B intermediate (3AB, 3ABB, or 3ABBB). In the O1K Pt.GFP 3C Donor, the lower band is similar in size to that observed in O1K Pt.GFP suggesting this could be mature 3A, which is possible as in O1K Pt.GFP 3C Donor, 3A is not covalently linked to 3B (assuming that the TaV 2A is working correctly). However, this band is slightly larger than the band for 3A seen for the wildtype replicon indicating the possibility that this band could be the 3A-TaV2A fusion protein (i.e. 3A3B1aa1-6+Y3F:TaV2A). This implies that the 3C Donor is unable to make mature 3A due to failure of 3C to process the artificial 3C cleavage site inserted between 3A and the TaV2A. This could possibly be due to the tyrosine to phenylalanine (Y3F) mutation created to prevent $3B_1$aa1-6+Y3F:TaV2A acting as a primer for replication. A second 3A positive band was also seen for the 3C Donor, which could be a higher-order precursor that contains 3A. For cells transfected with the No Donor or 3A Donor replicons, bands for 3A were not detected most likely as insufficient quantities of viral proteins are produced from replication-defective replicons.

Figure 6.4.1, Panel B shows western blots (using the same samples as used in panel A) with an antibody to 3D. Again bands were observed only for O1K Pt.GFP and O1K Pt.GFP 3C Donor. Of the two bands seen, the larger (approximately 50 KDa) is likely to be 3D (which has a molecular weight of 52

KDa), whereas the lower band is potentially a non-specific protein or a 3D degradation product picked up by the antibody. The above results are not surprising as the wildtype and 3C Donor replicons were the only replicons that showed evidence of replication and for the non-replicating replicons (O1K Pt.GFP 3A Donor, O1K Pt.GFP No Donor and O1K Pt.GFP GNN), it is possible that not enough of the 3A or 3D proteins are being produced to be detected by western blot.

Panels C and D of Figure 6.4.1 show western blots for detection of 3A (panel C) and 3D (panel D) proteins in supernatants from virally infected cells (BHKp2). In the blot for 3A (panel C) a similar banding pattern was observed for O1K WT, O1K 3A Donor and O1K No Donor viruses and multiple bands were seen corresponding in size to be 3A and 3AB intermediates. The similar banding patterns observed for the 3A and No Donor viruses to the wildtype O1K virus can be explained by the observation that by passage 2, the 3A and No donor viruses had restored the wildtype sequence (see section 6.3). In contrast, the O1K 3C Donor virus gave a different banding pattern to the other viruses, which could be the result of different processing of P3, as 3AB intermediates were not expected to be produced from this construct. However, there was also no evidence of a band of the correct size for 3A, which might have been expected. This supports the conclusion that the artificial 3C cleavage site inserted after 3A ($3B_1$aa1-6+Y3F) may not be processed correctly therefore leading to generation of $3A3B_1$aa1-6+Y3F:TaV2A as opposed to mature 3A. Nevertheless, the banding pattern of O1K 3C Donor virus appears to fit with the observation that it retained the original modifications made (see Figure 6.3.3).

Figure 6.4.1 Panel D shows a western blot for 3D and that similar patterns were produced by the wildtype and each of the Donor viruses. An intense band was seen at the correct size for 3D. In addition, a similar sized band of lesser intensity was seen in a cell only control lysate. However, the actin loading control shows that this difference in intensity is not due to loading less sample and suggests there may be a non-specific cellular protein of similar size to 3D that is detected. Despite this, it appears that all of the recovered Donor viruses generate processed 3D. In support of this conclusion, a band corresponding in

size to 3CD (~75kD) is only seen in the virus samples and not in the cells only control. These results can be explained by the observations that the O1K 3C Donor was replication competent as a replicon while the 3A and No Donor viruses had changed to the wildtype sequence by the passage used to infect cells (BHKp2).

6.4.2 Using TnT reactions to further investigate processing of the Donor replicons and viruses

P3 processing of the Donor constructs was investigated further using a TnT reaction (see Chapter 2 section 2.2.6.6). These experiments were carried out, with the help of Dr Joseph Newman. For this analysis, P3 templates were generated that included full-length 3A or the Donor changes (No, 3A or 3C) but 3C was truncated just before the coding region for the active site. This was done to clearly determine the functionality of the inserted TaV2A sequences and to help identify processing products. In addition, an aliquot of samples from each of the TnT reactions were treated with purified 3C to determine if the primary products from the TnT reaction could be further processed in trans by 3C.

PCR products, derived from each of the infectious clones, were generated using primers that incorporated a T7 promoter, an ATG start codon and a Kozak sequence upstream of the N terminus of 3A, and a second primer complementary to the mid region of 3C that included a translation stop codon (translation of this PCR would produce a truncated inactive 3C) (Full primer sequences are detailed in appendix 1). PCR products were confirmed to be correct size by gel electrophoresis before being used as templates in TnT reactions. Following incubation, samples were split into 2 and half of each sample treated with exogenous purified FMDV 3C protease (supplied by Dr Newman). An extensive list of the major predicted processing products that could be produced by these constructs with and without the addition of exogenous 3C is detailed in Table 6.4.2.

WT template: T7[met3A3B₁B₂B₃Δ3C]stop					

WT template: T7[met3A3B$_1$B$_2$B$_3$Δ3C]stop					
Products - added 3C	**KDa**	**On gel**	**Products + added 3C**	**KDa**	**On gel**
met3AB$_1$B$_2$B$_3$Δ3C	95.4	*	met3AB$_1$B$_2$B$_3$	25.2	*
			met3AB$_1$B$_2$	22.6	*
			met3AB$_1$	20	*
			met3A	17.4	*
			Δ3C	10.2	*
3A Donor: T7[met3A3B$_1$B$_2$B$_3$]-[3Caa1-6:TaV2A] // P-[3B$_3$aa19-24]-[Δ3C]stop					
Products - added 3C	**KDa**	**On gel**	**Products + added 3C**	**KDa**	**On gel**
met3AB$_1$B$_2$B$_3$-[3Caa1-6:TaV2A]	87.5	*	met3AB$_1$B$_2$B$_3$	25.2	*
			met3AB$_1$B$_2$	22.6	*
			met3AB$_1$	20	*
			met3A	17.4	*
			3Caa1-6:TaV2A	2.3	≠
P-[3B$_3$aa19-24]-Δ3C	10.9	*	P-[3B$_3$aa19-24]	0.7	≠
			Δ3C	10.2	*
3C Donor: **T7[met3A]-[3B$_1$aa1-6+Y3F:TaV2A] // P-[3Aaa148-153]-[3B$_1$B$_2$B$_3$3Δ3C]stop**					
Products - added 3C	**KDa**	**On gel**	**Products + added 3C**	**KDa**	**On gel**
met3A-[3B$_1$aa1-6+Y3F:TaV2A]	19.6	*	met3A	17.4	*
			3B$_1$aa1-6+Y3F:TaV2A	2.2	≠
P-[3Aaa148-153]-3B$_1$B$_2$B$_3$Δ3C]	65	*	P-[3Aaa148-153]	0.8	≠
			3B$_1$B$_2$B$_3$Δ3C	18.0	*
			B$_2$B$_3$Δ3C	15.4	*
			B$_3$Δ3C	12.8	*
			3B$_1$B$_2$B$_3$ (+ "free" 3B peptides)	7.8	≠
			Δ3C	10.2	*
No Donor: T7[met3A]-[3B$_1$aa1-6+Y3F:TaV2A] // **P-[3Aaa148-153]-[3B$_1$B$_2$B$_3$]-[3Caa1-6:TaV2A] // P-[3B$_3$aa19-24]-[Δ3C]stop**					
Products - added 3C	**KDa**	**On gel**	**Products + added 3C**	**KDa**	**On gel**
met3A-[3B$_1$aa1-6+Y3F:TaV2A]	19.6	*	met3A	17.4	*
			3B$_1$aa1-6+Y3F:TaV2A	2.2	≠
P-[3Aaa148-153]-[3B$_1$B$_2$B$_3$]-[3Caa1-6: TaV2A]	10.8	*	P-3Aaa148-153	0.7	≠
			3B$_1$B$_2$B$_3$ (+ "free" 3B peptides)	7.8	≠
			3Caa1-6:TaV2A	2.3	≠
P-[3B$_3$aa19-24]-[Δ3C]	10.9	*	P-3B$_3$aa19-24	0.7	≠
			Δ3C	10.2	*
* indicates position on gel; ≠ not visible on gel due to small size and/or insufficient Methionine residues					

Table 6.4.2 Potential processing products of the VPg Donor Cassettes:
The design of the wildtype and Donor templates used in the TnT is shown in blue. Predicted processing products produced without addition of exogenous 3C (-added 3C) are shown in left hand columns and those following further predicted processing with added 3c (added 3C) are shown on right hand columns. Predicted sizes (in KDa) and the corresponding symbol on the TnT gel of Figure 6.5.1are also indicated.
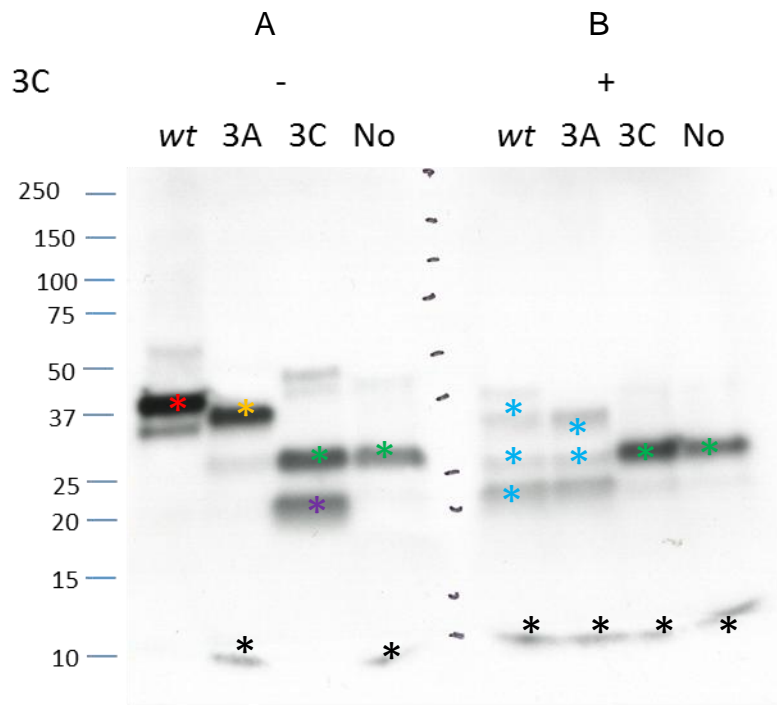
Protein product	Symbol
-3C = 3B3(19-24)∆3C +3C = ∆3C ∆	*
3ABBB∆3C	*
-3C = 3A(3B1aa1-6)TaV2A *+3C =3A(3B1aa1-6)TaV2A	*
(3A148-153)-3BBB∆3C	*
3A and 3AB precursors	*
3ABBB(3C1-6)TaV2A	*
* This product was not expected to still be present following treatment with exogenous 3C	

Figure 6.4.2: Investigating processing of VPg Donor constructs using Transcription and Translation coupled reactions: PCR products were made by amplifying the 3A to mid 3C region using infectious copy DNA for each of the donor constructs and he wildtype infectious clone plasmid. These products were then used in transcription and translation coupled reactions. Subsequently half of each reaction was treated with exogenous 3C protease. Samples were run on gradient SDS gels, which were soaked in salicylic acid and dried prior to exposing to X-ray film.

Figure 6.4.2. shows a representative result from one of two experimental repeats and the predicted products are marked with asterisks. In the samples that did not have active 3C added (panel A), the wildtype template produced a single major band at the expected size for unprocessed 3ABBBΔ3C (red asterisk). Both the 3A and No Donor templates showed a product of approximately 10 KDa which is likely to be the truncated Δ3C (black asterisk) (i.e. the last 6 residues of 3B3 + Δ3C; see primary processing products Figure 6.1.1) and suggests that the TaV 2A between 3B3 and 3C is self-cleaving correctly at its C terminus. Consistent with this conclusion, for the 3A donor template the most abundant band was seen at approximately 37 KDa, which is the correct size for the 3ABBBTaV2A fusion protein (3ABBB[3Caa1-6]TaV2A : orange asterisk). The No Donor template also gave a single major band at the expected size for the 3ATaV2A fusion protein (3A-(3B1aa1-6)TaV2A : green asterisk). The No Donor should also produce a third primary processing product (i.e. P-[3Aaa148-153]-[3B$_1$B$_2$B$_3$]-[3Caa1-6:TaV2A] which is similar in size but has less methionine residues and would therefore appear less intense. Alternatively the upper band in the No Donor lane could be a combination of each of the products (See Table 6.4.2).

As expected, in the absence of added 3C the 3C Donor template also gave a band for 3ATaV2A fusion protein (i.e. met3A-[3B$_1$aa1-6+Y3F:TaV2A] green asterisk) and a product of approximately 20KDa in size that matched the predicted size of the 3BBBΔ3C fusion protein (i.e. 3A148-153)-3BBBΔ3C (purple asterisk). These results show that in the absence of active 3C the products of the TnT reactions for each template are consistent with correct and

efficient self-cleavage at the inserted TaV 2A sequences (as shown in Table 6.4.2).

Upon addition of purified 3C (panel B) further processing events were seen for some of the constructs (predicted sizes are shown in the +3C column of Table 6.4.2). For each template (wildtype and all 3 Donor constructs), a products of ~10KDa (likely again to be Δ3C) was seen consistent with the presence of TaV 2A cleavage and further processing carried out by exogenous 3C. As expected the WT and 3A donor templates gave similar banding patterns with 3 additional products, most likely to be a combination of 3A and 3AB precursors (pale blue asterisks). The lower major-band in the untreated samples for the 3C donor template (purple asterisk) was not seen after the addition of purified 3C as this band corresponds to 3BBBΔ3C and would be extensively processed to yield Δ3C and the individual 3B peptides (which would be too small to be seen on this gel). However there was no bands visible to indicate mature 3A had been produced instead the larger band at the size expected for the 3A-TaV2A fusion protein (i.e. 3A-[3B$_1$aa1-6+Y3F:TaV2A]) was still visible. Taken together with the results seen for the western blot for 3A, carried out on a cell lysate from the 3C donor replicon (O1K Pt.GFP 3C Donor, Figure 6.4.1 panel A), this suggests that the 3C artificial cleavage site between 3A and TaV2A of the 3C donor construct is not able to be processed correctly. This is supported by the results of the No Donor construct which upon addition of 3C produced the same banding pattern to that of the 3C Donor and contains the same artificial 3C cleavage site between 3A and 3B as seen in the 3C Donor and would again if processed generated a smaller product similar in size to that of mature cleaved 3A.

6.4.3 Conclusions of VPg Donor experiments

The No Donor did not replicate as a replicon and could not be recovered as a virus. For the No Donor, the inability to replicate could be explained by four potential defects (see below), or by a combination of these.

1. The inability to form a covalent bond between 3A and 3B1.

2. The inability to form a covalent bond between 3B3 and 3C.

3. The artificial 3C cleavage site inserted between 3A and TaV2A (i.e. insertion of the first 6 a.a of 3B1 immediately after 3A) may not be cleaved resulting in a lack of mature 3A.

4. The artificial 3C cleavage site inserted between the second copy of TaV2A and 3C (i.e. insertion of the last 6 aa of 3B3 immediately before 3C) may not be cleaved resulting in a lack of mature 3C (i.e. an extension of 6 aa at the N terminus of 3C may inhibit 3C enzyme activity)

The first two explanations (1 and 2) suggest that the inability of the No Donor to construct to replicate (or be recovered as a virus) is a direct event resulting in reduced replication caused by the lack of 3B precursors (3ABBB or 3ABBBC). On the other hand the remaining two explanations (3 and 4) suggest the inability of the No Donor to replicate could be due to impacts from artificial insertions and mutations made to the genome which may interfere with the processing of the viral polyprotein and inhibit production of mature viral proteins.

The 3A Donor also did not replicate as a replicon and could not be recovered as a viable virus. In the 3A Donor cassette, as 3ABBB was the wt sequence two of the potential defects of the No Donor were restored. Therefore for the 3A Donor, the inability to replicate could be explained by the 2 remaining potential defects, or by a combination of these.

1. The inability to form a covalent bond between 3B3 and 3C

2. The artificial 3C cleavage site inserted between the second copy of TaV2A and 3C (i.e. insertion of the last 6 a.a of 3B3 immediately before

3C) may not be cleaved resulting in a lack of mature 3C (i.e. an extension of 6 aa at the N terminus of 3C may inhibit 3C enzyme activity).

As described above for the No Donor, the inability to replicate could be a direct effect on replication (defect 1) or due to indirect effects on processing of the polyprotein (defect 2), rather than the inability to replicate being solely due to 3B not being linked to 3A.

The 3C Donor was partially attenuated as a replicon and the virus based on this replicon was recovered with the 3C Donor cassette intact. In the 3C Donor, the other two potential defects of the No Donor were repaired, as 3BBBCD was restored to the wt sequence. Hence for the 3C Donor, the attenuation of replication could be explained by the 2 remaining potential defects, or by a combination of these.

1. The artificial 3C cleavage site inserted between 3A and TaV2A (i.e. insertion of the first 6 a.a of 3B1 immediately after 3A) may not be cleaved resulting in a lack of mature 3A. This may be the result of the Y3F mutation in the added 3B1 sequence and the TnT using the P3Δ3C template shows this site is not cleaved in trans by added 3C so it is unlikely to be cleaved in cis when 3C is part of a larger precursor (An artificial effect due to introduction of additional sequences)
2. The inability to form a covalent bond between 3A and 3B1.

As with the other Donor constructs, the negative impact on replication could be a result of the inclusion of artificial cleavage sites and other features influencing protein processing (as described in point 1), as opposed to a true effect seen due to preventing a covalent bond between 3A and 3B1.

Taken together, these observations support the conclusion that formation of 3ABBB is not essential for FMDV replication and that either 3C containing

precursors (or possibly "free" 3B peptides) are the preferred source of VPg for uridylation.

6.5 Discussion

The original models of picornavirus replication suggested that 3A was likely to be the donor of VPg (3B) to the replication complex (Liu et al., 2007, Murray and Barton, 2003); however, more recently it has been suggested that a 3C containing precursor is more likely to play this role (Pathak et al., 2008). A study by Pathak et al was carried out using PV, which encodes a single 3B; in comparison FMDV is unique among picornaviruses in that encodes three copies of 3B and therefore may use a different mechanism to deliver VPg to the RC (see Chapter 1 section 1.6.2 and 1.6.3). Each of the copies of 3B have been found linked to the genome although they are uridylated with different efficiency with 3B3 being the most efficient *in vitro* (Nayak et al., 2005), therefore changing the 3B donor source could have an effect on replication efficiency.

In this work FMDV replicons and recombinant viruses were used to investigate the impact of inserting copies of a '2A like' sequence (from the insect virus TaV) into the P3 encoding region of the FMDV genome to prevent 3B from being covalently linked either to 3A or 3C. Therefore, in these constructs 3B could only be donated to the replication complex as either a 3AB or 3BC precursor but never a combination of both. A third arrangement was also investigated where 3B was neither covalently linked to 3A or 3C (O1K No Donor).

Experimental data from replicon assays carried out as part of this work supports the conclusion that 3C is the preferred donor of 3B to a RC, as the 3C Donor replicon (O1K Pt.GFP 3C Donor) was the only Donor replicon that was replication competent, as both the 3A and No Donor replicons were completely attenuated. However in comparison to the wildtype O1K Pt.GFP replicon, replication of O1K Pt.GFP 3C Donor was partially attenuated, so it is possible a combination of both 3A and 3C and potentially free 3B is required for fully efficient replication of FMDV.

The above observations were made using BHK-21 cells but all 3 donor replicons appeared to be completely attenuated in MDBK and SK-RST cells, which derive from the natural bovine and porcine hosts of FMDV. It is not clear why the 3C donor replicon appeared attenuated in these cells (and not for BHK-21 cells) and suggests that there are subtle differences in the details of replication in BHK-21 in comparison to bovine and porcine cells. Nevertheless it appears BHK cells can be used to reveal the basic requirements for FMDV genome replication.

Furthermore, sequencing data derived from the recovered donor viruses also supports the conclusion that a 3BC containing precursor plays an important role in FMDV replication. Sequencing of the recovered O1K 3A Donor virus (in which 3B could only be covalently linked to 3A due to addition of a TaV 2A sequence between 3B3 and 3C), showed that the virus quickly reverted to a mixture of variants with deletions that removed the inserted TaV 2A but maintained the open reading frame of the genome. It is likely that this resulted from deletion events as third base changes that were included in additional a.a added at each terminus of the 2A protein remained. These results support the idea that a 3BC containing precursor is required as the source of 3B for replication as a virus where only 3AB, and not 3BBBC, is made (as in the case of the 3A Donor virus) was not able to be maintained when passaged in BHK-21 cells.

In contrast to the 3A donor, sequencing of a recovered virus in which 3B could only be covalently linked to 3C (O1K 3C Donor) maintained its additional copy of TaV 2A (and the mutations in the additional a.a residues included to create additional cleavage sites), without any apparent impact on the viruses ability to replicate in BHK-21 cells based on viral end point titre (data not shown). Although further investigations into growth kinetics of this virus are required. Additional passages and corresponding sequencing data showed that both the mutations and copy of TaV 2A were maintained up to passage 4, suggesting the virus is able to maintain these changes and utilise a 3BC precursor as a source of 3B for replication.

The O1K No Donor virus also appeared to be recoverable despite not replicating as a replicon (i.e. O1K Pt.GFP No Donor). However sequencing of the recovered virus (O1K No Donor) consistently came back showing the virus appeared to be wildtype, even at early stages post transfection of infectious copy derived RNA despite deep sequencing of the infectious copy DNA plasmid, which showed that there was no contamination by a wildtype plasmid. These results are similar to those observed from attempts to recover another virus in this study (O1K ALLA, chapter 5 section 5.6) that was not able to replicate as a replicon and attempts to recover it as a virus showed either rapid reversion to wildtype or contamination by a wildtype virus. Since the O1K FMDV No Donor virus has many changes in the P3 region (including two additional copies of a TaV 2A sequence and multiple additional a.a residues and single base mutations), and reverted to the wildtype FMDV sequence at 2 hours post transfection the reason behind recovery of the wildtype virus was not clear. However, the rapid disappearance in transfected cells of a PCR product for the No donor cassette (See Figure 6.3.4) coupled to the rapid appearance of a PCR product the correct size for the wildtype sequence spanning the cassette region, suggest that the recovered virus was generated by an internal deletion in the No donor virus that resulted in restoring the wildtype sequence as opposed to contamination with a replication competent wildtype virus.

Experiments investigating if the donor constructs were able to process P3 correctly were also carried out by both western blot and TnT reactions. The western blots showed that while each of the recovered Donor viruses were able to make the polymerase protein 3D (Note: the 3A and No donor viruses were recovered with the wildtype a.a sequence), O1K 3C Donor appeared to be compromised in its ability to process the 3A protein correctly. This lack of full-length 3A is one possible reason for the partial attenuated replication observed with O1K Pt.GFP 3C Donor particularly as 3A has been linked with other roles in replication. The similar banding patterns to the wildtype O1K virus seen for the 3A and No Donor recovered viruses in the blots to detect 3A can be explained as the lysates used were from the passage 2 viruses which had reverted to the wildtype FMDV sequence.

Western blots were also carried out using antibodies to detect the 3A and 3D proteins in samples from cells transfected with FMDV replicon RNA. These experiments showed that 3D was only expressed in detectable amounts, at 8 hours post transfection, in samples from O1K Pt.GFP and O1K Pt.GFP 3C Donor, both of which were replication competent based on GFP replicon assay data. Western blots to detect 3A within the replicon-transfected samples again only detected 3A for the O1K Pt.GFP and O1K Pt.GFP 3C Donor replicons. However, in contrast to the recovered 3C donor virus, where no 3A or 3A intermediate proteins were detected the blot from replicon transfected cells gave bands that could have been 3A and 3AB intermediates or potentially a 3ATaV2A fusion protein.

Further processing studies were carried out to confirm that the TaV 2A proteins were self-processing as expected at the C terminal end and to confirm they were being cleaved correctly by 3C. Results of TnT reactions suggested that the TaV 2A sequences were correctly and efficiently cleaving themselves in each construct at the C terminal as predicted for TaV 2A which has been shown to be 99.5% effective at cleaving itself from downstream proteins (Donnelly et al., 2001a). However results of TnT reactions where exogenous active 3C was added implied potential processing defects within the donor constructs. This could be explained by impaired cleavage of the inserted artificial 3C cleavage site inserted between 3A and TaV 2A, causing a lack of generation of mature 3A. This site also contained a mutation of tyrosine to phenylalanine which may have led to this deficiency.

Overall this chapter has shown that as in the 3C Donor a covalent bond is not formed between 3A and 3B1, 3ABBB may not be essential for replication and therefore that 3C could be the preferred donor of VPg (as a 3BC intermediate) for replication. Viruses with modifications that altered the covalent links between 3B, and 3A or 3C were recoverable. However, only the virus where 3B is linked to 3C (O1K FMDV 3C Donor) retained the modifications whereas the others (the 3A and No donor viruses) restored the link between 3B and 3C during recovery, thereby providing further evidence for the requirement for 3B to be covalently linked to 3C during replication. Together these observations support

the conclusion that the preferred donor of VPg is 3BC rather than 3AB. However, it is possible that 3B could be donated to a RC in multiple forms of precursory proteins 3AB, 3BC and free 3B for the most efficient replication.

Chapter 7: Final Discussion and Future Work

The *Picornaviridae* have been extensively studied although the majority of work has been carried out using the enteroviruses in particular PV. However FMDV differs from PV in a number of key aspects including having a longer 3A protein and encoding more than one copy of the 3B protein. Some of the non-structural proteins of picornaviruses have well characterised roles e.g. the 3D protein being the RNA-dependent RNA polymerase that of other non-structural proteins and processing intermediates (e.g. 3CD) have been shown to be functionally different across genera. This includes the non-structural protein 3A, which has been implicated as a determinant of viral host range and is thought to play a central role in vRNA replication but the exact role of 3A is still poorly understood in comparison to other viral proteins. Therefore this thesis focused on identifying possible roles of the FMDV 3A protein during replication.

As mentioned above, FMDV has a much longer 3A protein than other picornaviruses and has an extended C terminal domain. FMDV isolates from outbreaks in Asia have previously been identified that contain small deletions within the C terminal domain of 3A. These virus isolates replicated in porcine cells and were highly pathogenic for pigs but appeared to have attenuated growth in bovine cells *in vitro* and are significantly less virulent for cattle. This suggests that FMDV 3A may play a key role in determining viral host range (Pacheco et al., 2013, Pacheco et al., 2003, Beard and Mason, 2000). In this thesis, work carried out using GFP reporter, FMDV sub-genomic replicons (to allow quantification of replication) and recombinant viruses were used to investigate the effects of a much larger deletion (57 a.a in length) that was identified in viruses that existed as part of a mixed population within a vaccine strain of FMDV (Chapter 3). Results of replicon assays showed that the deletion had a negative impact on replication in a bovine kidney cell line (MDBK) whereas replication appeared to be enhanced in a porcine kidney cell line (SK-RST). Furthermore experimental results from assays using recombinant viruses were consistent with the replicon studies as the deletion in 3A appeared to

severely attenuate infection of MDBK cells and infection was slightly enhanced in porcine cells. However, the deletion had little effect on virus growth in primary bovine thyroid cells which appeared more susceptible to infection than MDBK cells. However, as described in the Discussion of Chapter 3, the virus with the 3A deletion was rapidly out competed in mixed infection studies by the wildtype virus with full-length 3A in BTY cells (C.Wright Personal Communication), thereby confirming that the deletion was detrimental to replication in bovine cells. These observations confirmed that the virus with the 57 aa deletion is able to replicate independently without the presence of a helper virus with full length 3A. These observations also suggest that the cell type (or cell line) could be a key factor in determining the effects of 3A deletions on replication and those deletions in the C terminal domain of 3A may enhance replication in porcine cells. Viruses with deletion in the C terminal domain of 3A are described as porcinophillic as they appear to replicate normally in porcine cells and cause classic FMD in pigs while they appear attenuated for bovine cells and are non-pathogenic for cattle. This information could be exploited for more host specific vaccine manufacture.

Part of the work for this thesis also examined the possibility that the extended C terminal domain of 3A in FMDV could be responsible for resistance to the fungal metabolite BFA. However when tested in replicon assays, the results showed that the same decrease in replication was observed in the wildtype, positive control replicon as that seen in the replicons with deletions in 3A. This inhibition in replication following pre-treated with BFA wasn't expected as previously little or no effect on virus yield has been observed in BFA treated cells. Previously, some studies had shown an increase in FMDV infection (i.e. the number of infected cells) for BFA treated cells (Martin-Acebes et al., 2008, Midgley et al., 2013, Monaghan et al., 2004, O'Donnell et al., 2001). Therefore the replicon assays in this study have shown that BFA may have multiple effects on FMDV including a negative impact on viral replication that could masked by other positive effects on infection.

In contrast to the deletions described above, a deletion that removed the last 5 a.a at the C terminal domain of 3A and majority of 3B1 had little impact on

replication in porcine or bovine cells when tested in replicon assays. This deletion effectively removed the first copy of 3B (i.e. 3B1) and was originally identified in a natural isolate during and outbreak of FMD in pigs in South Korea. The previous study that identified this isolate showed they were virulent for pigs but did not investigate infection in cattle, therefore it was undetermined if the removal of the last 5 a.a influenced replication in cattle (Park et al., 2016). Interestingly, results from the studies with recombinant virus (Chapter 3) showed that effects on replication differed slightly depending on if the remainder of the 3A sequence was based on O1K (where little difference was seen in viral titre between the wildtype and deleted virus) or on the original South Korean virus isolate, where there was a clear decrease in viral titre between the virus with full length 3A and that with the deletion (Chapter 3 section 3.7). This suggests that other regions, outside of the deletion could influence host range, partially agreeing with a previous study by Ma *et al* (Ma et al., 2014, Ma et al., 2016). It is also interesting to speculate that deletions in 3A may be occurring in pigs in Asia due to the introduction of intensive pig farming in that region and that variants containing such deletions (in 3A and 3B1) could be linked with evolution of the viruses within one host (Knowles et al., 2001).

Future work to determine the effects of the deletion studied here on host range could involve investigation of virus replication in additional bovine and porcine cell lines (to those tested here) and in addition to characterising the innate immune status of the various cell lines used. This could determine if the deletions in 3A are restricting replication in specific cells or if the differences seen are due to altered immune status of the cell lines. Additional experiments the growth kinetics of the different viruses with deletions should also be carried out in multiple cell lines. In addition, further work investigating the effects of the MOI and BFA concentration on both replication and infection levels could determine if BFA does act on FMDV at different stages of the viral lifecycle.

The 3A protein of picornaviruses interacts with a number of cellular proteins and appears to be involved in generating replication complexes and replication organelles. The other main aim of this thesis was to identify and investigate potential interaction partners of FMDV 3A. To achieve this 3A-GFP fusion

proteins were used in immunoprecipitation reactions to pull out cellular proteins that interacted with 3A. Mass spectrometry of the IP samples produced a large number of potential hits (possible interaction partners) which was then searched for previously identified partners of picornavirus 3A proteins (Lanke et al., 2009, Teterina et al., 2011, Wessels et al., 2006, Greninger et al., 2012, Klima et al., 2017). Despite a number of these not being present (e.g. GBF1, ACBD3 and PI4K), a high number of Rab proteins were identified including Rab7L1 (Rab29), which had previously been identified in a Y2H screen (carried out by collaborators at Edinburgh) as potential interaction partner for the precursor protein 3ABB. Rab7L1 has previously been identified in maintaining the structural integrity of the TGN (Wang et al., 2014) and shown to interact with the NS5 protein of HCV (Sklan et al., 2007b). The role of Rab 7L1 was investigated using siRNA designed to target the porcine Rab7L1 gene and appeared to show that levels of infection were lower in siRNA treated cells when compared to the untreated cells. Unfortunately a non-target siRNA control appeared to have a similar effect to the Rab7L1 specific siRNA with both leading to a reduction in the number of infected cells when compared to levels in untreated infected cells. Therefore it was not possible to determine if the effect of the specific siRNA was directly due to knockdown of expression of Rab7L1. Furthermore, due to a lack of a reliable antibody to Rab7L1 it was not possible to confirm the efficiency of Rab7L1 knockdown and further investigations are required to establish if Rab7L1 is a true interaction partner of FMDV 3A and if depleting its expression directly impacts on FMDV infection.

Experiments were also carried out on a second protein, TBC1D20, which was also identified as a potential interacting partner of 3A in the mass spectrometry, experiment. Using TBC1D20 knockout cell lines revealed that FMDV infection levels were reduced in the knockout cell lines when compared to the parental cell lines suggesting TBC1D20 availability may aid viral infection but that it is not essential as infection still occurred within the knockout cell lines. This was confirmed in replicon assays as replication (based on GFP expression) was detected in the knockout cells but at a decreased level in comparison to that seen in the parent cell line, suggesting TBC1D20 may act as a co-factor to

improve efficiency of replication and infection. However, it should be noted that the knockout cell lines were Hela cells and therefore not derived from a natural host of FMDV, so the effect of TBC1D20 depletion may differ for cells derived from the natural hosts of FMDV. Future work could include the use of siRNA to knockdown TBC1D20 in cells derived from natural hosts of FMDV to gain a more realistic result of effects on infection levels.

A major opportunity for future study is to maximise use of the information from the 3A mass spectroscopy experiments. A number of proteomic pipelines for post-acquisition data analysis are available including various tools to analyses potential protein interactions. This could also include network analysis to identify the broader biological context and pathways that could be expected to negatively impact on FMDV replication; this could also include the potential relevance of the identified pathways to epithelial cells (the preferred cell type infected by FMDV). Such analysis could be used to develop testable models how FMDV 3A binding to cellular proteins could enhance virus replication.

Other potential roles played by FMDV 3A were also investigated as part of the work conducted for this thesis. A conserved sequence located in the N terminal domain of FMDV 3A was found to have the characteristics of a previously described VAP binding motif known as a FFAT-like domain (Loewen and Levine, 2005, Loewen et al., 2003). Introduction of mutations within this motif of FMDV 3A was found to have a variety of effects on replication, dependent on position of the mutation and the replacement a.a residue, suggesting VAP binding may have been impaired in some cases. In addition, these studies showed that certain positions can tolerate a.a substitutions that do not appear to affect replication which is in agreement with observations from other studies that characterised the FFAT motif (Mikitova and Levine, 2012, Murphy and Levine, 2016, Kaiser et al., 2005). In particular, position 5 of FFAT motifs has been shown to tolerate some variation (Mikitova and Levine, 2012), and in this study results from experiments with different substitutions at this position of the predicted FFAT-like motif in FMDV 3A also showed varying effects on replication. Substitution of the glycine at position 5 in the motif of FMDV 3A to

alanine had no impact on replication, whereas changing to a serine led to partial attenuation of replication suggesting a potential partial inhibition of VAP binding, agreeing with a study by Mikitova *et al* (Mikitova and Levine, 2012). Moreover this was the only mutation (of three selected to make into recombinant viruses) that was maintained by the virus when passaged in culture, suggesting FMDV can tolerate substitutions that lead to partial attenuation but not those that are lethal to replication. Interestingly the substitution of glycine to glutamic acid had no effect on FMDV replication, and therefore potentially interaction of 3A with VAP, whereas Mikitova *et al* had found this mutation led to a major reduction of VAP binding by proteins (Mikitova and Levine, 2012). This difference could be due to the highly flexible nature of FFAT-like domains as described by Murphy *et al* (Murphy and Levine, 2016).

Taken together these results suggest it is highly likely that 3A could interact with the ER via VAP proteins expressed on its surface through a FFAT-like motif to allow efficient replication. However further work is required to confirm a direct interaction between the VAP proteins and FMDV 3A, and confocal microscopy could be used to investigate co-localisation of 3A and the VAP proteins in FMDV infected cells.

This thesis also investigated the possibility that 3ABBB could act as the donor of VPg to a RC (possibly as substrate for uridylation of 3B) during replication (Chapter 6). Previously it was suggested that 3AB was the primary source of 3B for this reaction (Liu et al., 2007) although more recently studies with PV observed that a 3C containing intermediate was the more likely substrate (Pathak et al., 2008). However key differences between FMDV and PV is that FMDV encodes 3 copies of 3B within its genome (all of which can be uridylated) (Nayak et al., 2005) thereby potentially increasing the number of 3B containing precursors that could donate VPg to a RC.

Results from experiments with replicons and recombinant viruses, in which 3B could only be covalently linked to either 3A or 3C or produced as a free peptide, provided support for a 3BC precursor as being the template utilised for uridylation of 3B. This agrees with the studies on PV of Oh *et al* and Pathak *et al* (Oh et al., 2009, Pathak et al., 2008). However although the construct in

which 3B was only covalently linked to 3C was the only one seen to be replication competent and recoverable as a virus it was partially attenuated compared to the wildtype suggesting a combination of precursors may be required for efficient replication. However, evidence was found that suggested that impaired processing of 3A may have contributed to attenuation of replication of the 3C Donor virus. Therefore it is not possible to precisely define the exact product utilised for uridylation of 3B during replication, nevertheless, from the results presented in Chapter 6 it can be concluded that 3ABBB is not essential for FMDV replication.

Future work could include investigation into the growth kinetics of the O1K 3C Donor (in comparison to the O1K wildtype virus) to establish the effects of restricting the number of 3B-containing precursors on replication. In addition, it would be interesting to extend the observations made by Nayak *et al* (Nayak et al., 2006), to look to see if 3ABBB is a substrate for uridylation in vitro.

Recovery of the No Donor virus and viruses with mutations in the FFAT domain of 3A were affected by potential contamination by low levels of wildtype virus that appeared to out -compete the viruses that had mutations that appeared to cause attenuation of replication. This stresses the importance of including marker mutations, outside of the regions where changes are made to allow clear differentiation between contamination with a replication competent wild type virus and reversion events. Key evidence of the usefulness of this approach was seen in the case of sequencing the O1K 3A donor viruses where third base changes that were initially included to prevent recombination were still present following reversion of the virus to the wildtype sequence (Chapter 6).

In summary this thesis provides new insights into the roles of 3A in FMDV infection. Evidence supporting previous theories that deletions within 3A enhance infection in porcine cells was found, as were results suggesting that attenuation of replication in one bovine cell line could not be fully restored by supplying wildtype 3A in trans. However further work is required to investigate this effect due to variations observed in different types of bovine derived cells.

Potential interaction partners were also identified and investigated including VAP, TBC1D20 and Rab7L1. Interactions between the flavivirus HCV and VAP have previously been described (Gupta et al., 2012, Gupta and Song, 2016, Hamamoto et al., 2005) and results from this work suggest potential for interaction between FMDV 3A and VAP is also highly likely, particularly as mutations that were likely to have inhibited this interaction were not maintained in viruses and totally attenuated replication. Assays TBC1D20 knockout cells showed that it could be a cellular factor that aids FMDV infection. Investigations into the possible interaction of FMDV 3A with Rab7L1 however require further optimisation and investigation as these experiments were highly impacted by a lack of reliable antibodies to Rab7L1.

Finally key results from Chapter 6 provided evidence that a 3BC containing precursor is the preferred donor of 3B for uridylation. Previously this was unknown for FMDV as previous studies were conducted using PV and the number of FMDV potential precursors being much larger due to FMDV encoding 3 copies of 3B in its genome. Although not possible to define which exact precursor is the most utilised for this reaction, the results show that 3ABBB is not essential for FMDV replication.

In conclusion FMDV remains an important pathogen globally and gaining greater understanding of key aspects involved in replication, including that of the 3A protein, is vital for development of new and safer therapeutics, vaccinations and control methods to prevent and reduce the impacts of FMD outbreaks worldwide. Although this thesis presents a number of findings related to roles of FMDV 3A there is still a number of gaps remaining with regards to understanding of FMDV replication. The roles in replication of number of the non-structural proteins are still poorly understood particularly those of the P2 proteins. Furthermore it is still not understood why FMDV 3A is so much longer in comparison to other picornaviruses and the potential roles of 3A in subverting immune pathways have not yet been investigated in detail.

References

ALDABE, R., IRURZUN, A. & CARRASCO, L. 1997. Poliovirus protein 2BC increases cytosolic free calcium concentrations. *Journal of Virology,* 71**,** 6214-6217.

ALEXANDERSEN, S. & DONALDSON, A. I. 2002. Further studies to quantify the dose of natural aerosols of foot-and-mouth disease virus for pigs. *Epidemiology and Infection,* 128**,** 313-323.

AMARILIO, R., RAMACHANDRAN, S., SABANAY, H. & LEV, S. 2005. Differential regulation of endoplasmic reticulum structure through VAP-Nir protein interaction. *Journal of Biological Chemistry,* 280**,** 5934-5944.

AO, D., GUO, H.-C., SUN, S.-Q., SUN, D.-H., FUNG, T. S., WEI, Y.-Q., HAN, S.-C., YAO, X.-P., CAO, S.-Z., LIU, D. X. & LIU, X.-T. 2015. Viroporin Activity of the Foot-and-Mouth Disease Virus Non-Structural 2B Protein. *PLoS One,* 10**,** e0125828.

ARIAS, A., PERALES, C., ESCARMIS, C. & DOMINGO, E. 2010. Deletion mutants of VPg reveal new cytopathology determinants in a picornavirus. *PLoS One,* 5**,** e10735.

ARITA, M., KOJIMA, H., NAGANO, T., OKABE, T., WAKITA, T. & SHIMIZU, H. 2013. Oxysterol-Binding Protein Family I Is the Target of Minor Enviroxime-Like Compounds. *Journal of Virology,* 87**,** 4252-4260.

BARAJAS, D., XU, K., SHARMA, M., WU, C. Y. & NAGY, P. D. 2014. Tombusviruses upregulate phospholipid biosynthesis via interaction between p33 replication protein and yeast lipid sensor proteins during virus replication in yeast. *Virology,* 471-473**,** 72-80.

BARANOWSKI, E., RUIZ-JARABO, C. M., SEVILLA, N., ANDREU, D., BECK, E. & DOMINGO, E. 2000. Cell Recognition by Foot-and-Mouth Disease Virus That Lacks the RGD Integrin-Binding Motif: Flexibility in Aphthovirus Receptor Usage. *Journal of Virology,* 74**,** 1641-1647.

BARTON, D. J. & FLANEGAN, J. B. 1997. Synchronous replication of poliovirus RNA: initiation of negative-strand RNA synthesis requires the guanidine-inhibited activity of protein 2C. *Journal of Virology,* 71**,** 8482-9.

BARTON, D. J., O'DONNELL, B. J. & FLANEGAN, J. B. 2001. 5′ cloverleaf in poliovirus RNA is a cis-acting replication element required for negative-strand synthesis. *The EMBO Journal,* 20**,** 1439-1448.

BEARD, C. W. & MASON, P. W. 2000. Genetic Determinants of Altered Virulence of Taiwanese Foot-and-Mouth Disease Virus. *Journal of Virology,* 74**,** 987-991.

BEHURA, M., MOHAPATRA, J. K., PANDEY, L. K., DAS, B., BHATT, M., SUBRAMANIAM, S. & PATTNAIK, B. 2016. The carboxy-terminal half of nonstructural protein 3A is not essential for foot-and-mouth disease virus replication in cultured cell lines. *Archives of Virology,* 161**,** 1295-1305.

BELNAP, D. M., FILMAN, D. J., TRUS, B. L., CHENG, N., BOOY, F. P., CONWAY, J. F., CURRY, S., HIREMATH, C. N., TSANG, S. K., STEVEN, A. C. & HOGLE, J. M. 2000. Molecular Tectonic Model of Virus Structural Transitions: the Putative Cell Entry States of Poliovirus. *Journal of Virology,* 74**,** 1342-1354.

BELOV, G. A., ALTAN-BONNET, N., KOVTUNOVYCH, G., JACKSON, C. L., LIPPINCOTT-SCHWARTZ, J. & EHRENFELD, E. 2007. Hijacking Components of the Cellular Secretory Pathway for Replication of Poliovirus RNA. *Journal of Virology,* 81**,** 558-567.

BELOV, G. A., FENG, Q., NIKOVICS, K., JACKSON, C. L. & EHRENFELD, E. 2008. A critical role of a cellular membrane traffic protein in poliovirus RNA replication. *PLoS Pathogens,* 4**,** e1000216.

BELSHAM, G. J. 2013. Influence of the Leader protein coding region of foot-and-mouth disease virus on virus replication. *Journal General Virology,* 94**,** 1486-1495.

BELSHAM, G. J. & BRANGWYN, J. K. 1990. A region of the 5' noncoding region of foot-and-mouth disease virus RNA directs efficient internal initiation of protein synthesis within cells: involvement with the role of L protease in translational control. *Journal of Virology,* 64**,** 5389-5395.

BELSHAM, G. J., MCINERNEY, G. M. & ROSS-SMITH, N. 2000. Foot-and-Mouth Disease Virus 3C Protease Induces Cleavage of Translation Initiation Factors eIF4A and eIF4G within Infected Cells. *Journal of Virology,* 74**,** 272-280.

BELSHAM, G. J. & SONENBERG, N. 1996. RNA-protein interactions in regulation of picornavirus RNA translation. *Microbiological Reviews,* 60**,** 499-511.

BERNARDS, A. & SETTLEMAN, J. 2004. GAP control: regulating the regulators of small GTPases. *Trends in Cell Biology,* 14**,** 377-385.

BERRYMAN, S., CLARK, S., MONAGHAN, P. & JACKSON, T. 2005. Early events in integrin alphavbeta6-mediated cell entry of foot-and-mouth disease virus. *Journal of Virology,* 79**,** 8519-8534.

BERRYMAN, S., MOFFAT, K., HARAK, C., LOHMANN, V. & JACKSON, T. 2016. Foot-and-mouth disease virus replicates independently of phosphatidylinositol 4-phosphate and type III phosphatidylinositol 4-kinases. *Journal of General Virology,* 97**,** 1841-1852.

BOROS, Á., KISS, T., KISS, O., PANKOVICS, P., KAPUSINSZKY, B., DELWART, E. & REUTER, G. 2013. Genetic characterization of a novel picornavirus distantly related to the marine mammal-infecting aquamaviruses in a long-distance migrant bird species, European roller (Coracias garrulus). *Journal of General Virology,* 94**,** 2029-2035.

BURMAN, A., CLARK, S., ABRESCIA, N. G. A., FRY, E. E., STUART, D. I. & JACKSON, T. 2006. Specificity of the VP1 GH Loop of Foot-and-Mouth Disease Virus for αv Integrins. *Journal of Virology,* 80**,** 9798-9810.

CARIDI, F., VÁZQUEZ-CALVO, A., SOBRINO, F. & MARTÍN-ACEBES, M. A. 2015. The pH Stability of Foot-and-Mouth Disease Virus Particles Is Modulated by Residues Located at the Pentameric Interface and in the N Terminus of VP1. *Journal of Virology,* 89**,** 5633-5642.

CARRILLO, C., TULMAN, E. R., DELHON, G., LU, Z., CARRENO, A., VAGNOZZI, A., KUTISH, G. F. & ROCK, D. L. 2005. Comparative genomics of foot-and-mouth disease virus. *Journal of Virology,* 79**,** 6487-6504.

CHAMBERLAIN, K., FOWLER, V. L., BARNETT, P. V., GOLD, S., WADSWORTH, J., KNOWLES, N. J. & JACKSON, T. 2015. Identification

of a novel cell culture adaptation site on the capsid of foot-and-mouth disease virus. *Journal of General Virology,* 96**,** 2684-2692.

CHANG, P.-C., CHEN, S.-C. & CHEN, K.-T. 2016. The Current Status of the Disease Caused by Enterovirus 71 Infections: Epidemiology, Pathogenesis, Molecular Epidemiology, and Vaccine Development. *International Journal of Environmental Research and Public Health,* 13**,** e890.

CHASE, A. J., DAIJOGO, S. & SEMLER, B. L. 2014. Inhibition of Poliovirus-Induced Cleavage of Cellular Protein PCBP2 Reduces the Levels of Viral RNA Replication. *Journal of Virology,* 88**,** 3192-3201.

CUCONATI, A., MOLLA, A. & WIMMER, E. 1998. Brefeldin A Inhibits Cell-Free, De Novo Synthesis of Poliovirus. *Journal of Virology,* 72**,** 6456-6464.

CURRY, S., ABRAMS, C. C., FRY, E., CROWTHER, J. C., BELSHAM, G. J., STUART, D. I. & KING, A. M. 1995. Viral RNA modulates the acid sensitivity of foot-and-mouth disease virus capsids. *Journal of Virology,* 69**,** 430-438.

DAIJOGO, S. & SEMLER, B. L. 2011. Mechanistic intersections between picornavirus translation and RNA replication. *Advances in Virus Research,* 80**,** 1-24.

DESTEFANO, J. J. & TITILOPE, O. 2006. Poliovirus Protein 3AB Displays Nucleic Acid Chaperone and Helix-Destabilizing Activities. *Journal of Virology,* 80**,** 1662-1671.

DEVANEY, M. A., VAKHARIA, V. N., LLOYD, R. E., EHRENFELD, E. & GRUBMAN, M. J. 1988. Leader protein of foot-and-mouth disease virus is required for cleavage of the p220 component of the cap-binding protein complex. *Journal of Virology,* 62**,** 4407-4409.

DODD, D. A., GIDDINGS, T. H. & KIRKEGAARD, K. 2001. Poliovirus 3A Protein Limits Interleukin-6 (IL-6), IL-8, and Beta Interferon Secretion during Viral Infection. *Journal of Virology,* 75**,** 8158-8165.

DOEDENS, J. R., GIDDINGS, T. H. & KIRKEGAARD, K. 1997. Inhibition of endoplasmic reticulum-to-Golgi traffic by poliovirus protein 3A: genetic and ultrastructural analysis. *Journal of Virology,* 71**,** 9054-9064.

DOEL, T. R. 2003. FMD vaccines. *Virus Research,* 91**,** 81-99.

DOMINGO, E., ESCARMíS, C., BARANOWSKI, E., RUIZ-JARABO, C. M., CARRILLO, E., NÚÑEZ, J. I. & SOBRINO, F. 2003. Evolution of foot-and-mouth disease virus. *Virus Research,* 91**,** 47-63.

DONNELLY, M. L. L., HUGHES, L. E., LUKE, G., MENDOZA, H., TEN DAM, E., GANI, D. & RYAN, M. D. 2001a. The 'cleavage' activities of foot-and-mouth disease virus 2A site-directed mutants and naturally occurring '2A-like' sequences. *Journal of General Virology,* 82**,** 1027-1041.

DONNELLY, M. L. L., LUKE, G., MEHROTRA, A., LI, X., HUGHES, L. E., GANI, D. & RYAN, M. D. 2001b. Analysis of the aphthovirus 2A/2B polyprotein 'cleavage' mechanism indicates not a proteolytic reaction, but a novel translational effect: a putative ribosomal 'skip'. *Journal of General Virology,* 82**,** 1013-1025.

DOROBANTU, C. M., ALBULESCU, L., HARAK, C., FENG, Q., VAN KAMPEN, M., STRATING, J. R. P. M., GORBALENYA, A. E., LOHMANN, V., VAN DER SCHAAR, H. M. & VAN KUPPEVELD, F. J. M. 2015a. Modulation

of the Host Lipid Landscape to Promote RNA Virus Replication: The Picornavirus Encephalomyocarditis Virus Converges on the Pathway Used by Hepatitis C Virus. *PLoS Pathogens,* 11**,** e1005185.

DOROBANTU, C. M., ALBULESCU, L., LYOO, H., VAN KAMPEN, M., DE FRANCESCO, R., LOHMANN, V., HARAK, C., VAN DER SCHAAR, H. M., STRATING, J. R. P. M., GORBALENYA, A. E. & VAN KUPPEVELD, F. J. M. 2016. Mutations in Encephalomyocarditis Virus 3A Protein Uncouple the Dependency of Genome Replication on Host Factors Phosphatidylinositol 4-Kinase IIIα and Oxysterol-Binding Protein. *mSphere,* 1**,** e00068.

DOROBANTU, C. M., FORD-SILTZ, L. A., SITTIG, S. P., LANKE, K. H. W., BELOV, G. A., VAN KUPPEVELD, F. J. M. & VAN DER SCHAAR, H. M. 2015b. GBF1- and ACBD3-Independent Recruitment of PI4KIIIβ to Replication Sites by Rhinovirus 3A Proteins. *Journal of Virology,* 89**,** 1913-1918.

DOROBANTU, C. M., VAN DER SCHAAR, H. M., FORD, L. A., STRATING, J. R., ULFERTS, R., FANG, Y., BELOV, G. & VAN KUPPEVELD, F. J. 2014. Recruitment of PI4KIIIbeta to coxsackievirus B3 replication organelles is independent of ACBD3, GBF1, and Arf1. *Journal of Virology,* 88**,** 2725-2736.

DUKE, G. M., HOFFMAN, M. A. & PALMENBERG, A. C. 1992. Sequence and structural elements that contribute to efficient encephalomyocarditis virus RNA translation. *Journal of Virology,* 66**,** 1602-1609.

DUNN, C. S. & DONALDSON, A. I. 1997. Natural adaption to pigs of a Taiwanese isolate of foot-and-mouth disease virus. *Veterinary Record,* 141**,** 174-175.

ELLARD, F. M., DREW, J., BLAKEMORE, W. E., STUART, D. I. & KING, A. M. Q. 1999. Evidence for the role of His-142 of protein 1C in the acid-induced disassembly of foot-and-mouth disease virus capsids. *Journal of General Virology,* 80**,** 1911-1918.

ETCHISON, D., MILBURN, S. C., EDERY, I., SONENBERG, N. & HERSHEY, J. W. 1982. Inhibition of HeLa cell protein synthesis following poliovirus infection correlates with the proteolysis of a 220,000-dalton polypeptide associated with eucaryotic initiation factor 3 and a cap binding protein complex. *Journal of Biological Chemistry,* 257**,** 14806-1410.

ETTAYEBI, K. & HARDY, M. E. 2003. Norwalk Virus Nonstructural Protein p48 Forms a Complex with the SNARE Regulator VAP-A and Prevents Cell Surface Expression of Vesicular Stomatitis Virus G Protein. *Journal of Virology,* 77**,** 11790-11797.

FALK, M. M., SOBRINO, F. & BECK, E. 1992. VPg gene amplification correlates with infective particle formation in foot-and-mouth disease virus. *Journal of Virology,* 66**,** 2251-2260.

FERRER-ORTA, C., ARIAS, A., PEREZ-LUQUE, R., ESCARMÍS, C., DOMINGO, E. & VERDAGUER, N. 2004. Structure of Foot-and-Mouth Disease Virus RNA-dependent RNA Polymerase and Its Complex with a Template-Primer RNA. *Journal of Biological Chemistry,* 279**,** 47212-47221.

FERRIS, N. P., HUTCHINGS, G. H., MOULSDALE, H. J., GOLDING, J. & CLARKE, J. B. 2002. Sensitivity of primary cells immortalised by oncogene transfection for the detection and isolation of foot-and-mouth disease and swine vesicular disease viruses. *Veterinary Microbiology,* 84**,** 307-316.

FICHTNER, D., PHILIPPS, A., GROTH, M., SCHMIDT-POSTHAUS, H., GRANZOW, H., DAUBER, M., PLATZER, M., BERGMANN, S. M., SCHRUDDE, D., SAUERBREI, A. & ZELL, R. 2013. Characterization of a Novel Picornavirus Isolate from a Diseased European Eel (Anguilla anguilla). *Journal of Virology,* 87**,** 10895-10899.

FRASA, M. A. M., KOESSMEIER, K. T., AHMADIAN, M. R. & BRAGA, V. M. M. 2012. Illuminating the functional and structural repertoire of human TBC/RABGAPs. *Nature Reviews Molecular Cell Biology,* 13**,** 67-73.

FURUITA, K., JEE, J., FUKADA, H., MISHIMA, M. & KOJIMA, C. 2010. Electrostatic Interaction between Oxysterol-binding Protein and VAMP-associated Protein A Revealed by NMR and Mutagenesis Studies. *Journal of Biological Chemistry,* 285**,** 12961-12970.

GALAN, A., LOZANO, G., PIÑEIRO, D. & MARTINEZ-SALAS, E. 2017. G3BP1 interacts directly with the FMDV IRES and negatively regulates translation. *The FEBS Journal,* 284**,** 3202-3217.

GAO, L., AIZAKI, H., HE, J.-W. & LAI, M. M. C. 2004. Interactions between Viral Nonstructural Proteins and Host Protein hVAP-33 Mediate the Formation of Hepatitis C Virus RNA Replication Complex on Lipid Raft. *Journal of Virology,* 78**,** 3480-3488.

GAZINA, E. V., MACKENZIE, J. M., GORRELL, R. J. & ANDERSON, D. A. 2002. Differential Requirements for COPI Coats in Formation of Replication Complexes among Three Genera of Picornaviridae. *Journal of Virology,* 76**,** 11113-11122.

GEORGES, A. A. & FRAPPIER, L. 2015. Proteomics methods for discovering viral-host interactions. *Methods,* 90**,** 21-27.

GERONDOPOULOS, A., BASTOS, R. N., YOSHIMURA, S.-I., ANDERSON, R., CARPANINI, S., ALIGIANIS, I., HANDLEY, M. T. & BARR, F. A. 2014. Rab18 and a Rab18 GEF complex are required for normal ER structure. *The Journal of Cell Biology,* 205**,** 707-720.

GIRAUDO, A. T., BECK, E., STREBEL, K., DE MELLO, P. A., LA TORRE, J., SCODELLER, E. A. & BERGMANN, I. E. 1990. Identification of a nucleotide deletion in parts of polypeptide 3A in two independent attenuated aphthovirus strains. *Virology,* 177**,** 780-783.

GLADUE, D. P., O'DONNELL, V., BAKER-BRANSETTER, R., PACHECO, J. M., HOLINKA, L. G., ARZT, J., PAUSZEK, S., FERNANDEZ-SAINZ, I., FLETCHER, P., BROCCHI, E., LU, Z., RODRIGUEZ, L. L. & BORCA, M. V. 2014. Interaction of foot-and-mouth disease virus nonstructural protein 3A with host protein DCTN3 is important for viral virulence in cattle. *Journal of Virology,* 88**,** 2737-2747.

GONZÁLEZ-MAGALDI, M., MARTÍN-ACEBES, M. A., KREMER, L. & SOBRINO, F. 2014. Membrane Topology and Cellular Dynamics of Foot-and-Mouth Disease Virus 3A Protein. *PLoS One,* 9**,** e106685.

GONZALEZ-MAGALDI, M., POSTIGO, R., DE LA TORRE, B. G., VIEIRA, Y. A., RODRIGUEZ-PULIDO, M., LOPEZ-VINAS, E., GOMEZ-PUERTAS, P., ANDREU, D., KREMER, L., ROSAS, M. F. & SOBRINO, F. 2012. Mutations that hamper dimerization of foot-and-mouth disease virus 3A protein are detrimental for infectivity. *Journal of Virology,* 86**,** 11013-11023.

GONZALEZ-MAGALDI, M., VAZQUEZ-CALVO, A., DE LA TORRE, B. G., VALLE, J., ANDREU, D. & SOBRINO, F. 2015. Peptides Interfering 3A Protein Dimerization Decrease FMDV Multiplication. *PLoS One,* 10**,** e0141415.

GOODFELLOW, I., CHAUDHRY, Y., RICHARDSON, A., MEREDITH, J., ALMOND, J. W., BARCLAY, W. & EVANS, D. J. 2000. Identification of a cis-Acting Replication Element within the Poliovirus Coding Region. *Journal of Virology,* 74**,** 4590-4600.

GRADI, A., SVITKIN, Y. V., IMATAKA, H. & SONENBERG, N. 1998. Proteolysis of human eukaryotic translation initiation factor eIF4GII, but not eIF4GI, coincides with the shutoff of host protein synthesis after poliovirus infection. *Proceedings of the National Academy of Sciences of the United States of America,* 95**,** 11089-11094.

GRAFF, J., NORMANN, A., FEINSTONE, S. M. & FLEHMIG, B. 1994. Nucleotide sequence of wild-type hepatitis A virus GBM in comparison with two cell culture-adapted variants. *Journal of Virology,* 68**,** 548-554.

GRENINGER, A. L., KNUDSEN, G. M., BETEGON, M., BURLINGAME, A. L. & DERISI, J. L. 2012. The 3A protein from multiple picornaviruses utilizes the golgi adaptor protein ACBD3 to recruit PI4KIIIbeta. *Journal of Virology,* 86**,** 3605-3616.

GRENINGER, A. L., KNUDSEN, G. M., BETEGON, M., BURLINGAME, A. L. & DERISI, J. L. 2013. ACBD3 interaction with TBC1 domain 22 protein is differentially affected by enteroviral and kobuviral 3A protein binding. *MBio,* 4**,** e00098-13.

GREVE, J. M., DAVIS, G., MEYER, A. M., FORTE, C. P., YOST, S. C., MARLOR, C. W., KAMARCK, M. E. & MCCLELLAND, A. 1989. The major human rhinovirus receptor is ICAM-1. *Cell,* 56**,** 839-847.

GROPPELLI, E., TUTHILL, T. J. & ROWLANDS, D. J. 2010. Cell Entry of the Aphthovirus Equine Rhinitis A Virus Is Dependent on Endosome Acidification. *Journal of Virology,* 84**,** 6235-6240.

GRUBMAN, M. J. 1980. The 5′ end of foot-and-mouth disease virion RNA contains a protein covalently linked to the nucleotide pUp. *Archives of Virology,* 63**,** 311-315.

GRUBMAN, M. J. & BAXT, B. 2004. Foot-and-Mouth Disease. *Clinical Microbiology Reviews,* 17**,** 465-493.

GUPTA, G., QIN, H. & SONG, J. 2012. Intrinsically Unstructured Domain 3 of Hepatitis C Virus NS5A Forms a "Fuzzy Complex" with VAPB-MSP Domain Which Carries ALS-Causing Mutations. *PLoS One,* 7**,** e39261.

GUPTA, G. & SONG, J. 2016. C-Terminal Auto-Regulatory Motif of Hepatitis C Virus NS5B Interacts with Human VAPB-MSP to Form a Dynamic Replication Complex. *PLoS One,* 11**,** e0147278.

HAAS, A. K., YOSHIMURA, S.-I., STEPHENS, D. J., PREISINGER, C., FUCHS, E. & BARR, F. A. 2007. Analysis of GTPase-activating proteins: Rab1 and Rab43 are key Rabs required to maintain a functional Golgi complex in human cells. *Journal of Cell Science,* 120**,** 2997-3010.

HAMAMOTO, I., NISHIMURA, Y., OKAMOTO, T., AIZAKI, H., LIU, M., MORI, Y., ABE, T., SUZUKI, T., LAI, M. M., MIYAMURA, T., MORIISHI, K. & MATSUURA, Y. 2005. Human VAP-B is involved in hepatitis C virus replication through interaction with NS5A and NS5B. *Journal of Virology,* 79**,** 13473-13482.

HANDLEY, M. T., CARPANINI, S. M., MALI, G. R., SIDJANIN, D. J., ALIGIANIS, I. A., JACKSON, I. J. & FITZPATRICK, D. R. 2015. Warburg Micro syndrome is caused by RAB18 deficiency or dysregulation. *Open Biology,* 5**,** 150047.

HANSEN, J. L., LONG, A. M. & SCHULTZ, S. C. 1997. Structure of the RNA-dependent RNA polymerase of poliovirus. *Structure,* 5**,** 1109-1122.

HARAK, C. & LOHMANN, V. 2015. Ultrastructure of the replication sites of positive-strand RNA viruses. *Virology,* 479**,** 418-433.

HARRIS, J. R. & RACANIELLO, V. R. 2005. Amino acid changes in proteins 2B and 3A mediate rhinovirus type 39 growth in mouse cells. *Journal of Virology,* 79**,** 5363-5373.

HARRIS, K. S., XIANG, W., ALEXANDER, L., LANE, W. S., PAUL, A. V. & WIMMER, E. 1994. Interaction of poliovirus polypeptide 3CDpro with the 5' and 3' termini of the poliovirus genome. Identification of viral and cellular cofactors needed for efficient binding. *Journal of Biological Chemistry,* 269**,** 27004-27014.

HE, Y., BOWMAN, V. D., MUELLER, S., BATOR, C. M., BELLA, J., PENG, X., BAKER, T. S., WIMMER, E., KUHN, R. J. & ROSSMANN, M. G. 2000. Interaction of the poliovirus receptor with poliovirus. *Proceedings of the National Academy of Sciences,* 97**,** 79-84.

HEROD, M. R., LOUNDRAS, E. A., WARD, J. C., TULLOCH, F., ROWLANDS, D. J. & STONEHOUSE, N. J. 2015. Employing transposon mutagenesis to investigate foot-and-mouth disease virus replication. *Journal of General Virology,* 96**,** 3507-3518.

HEROLD, J. & ANDINO, R. 2000. Poliovirus Requires a Precise 5′ End for Efficient Positive-Strand RNA Synthesis. *Journal of Virology,* 74**,** 6394-6400.

HOGLE, J., CHOW, M. & FILMAN, D. 1985. Three-dimensional structure of poliovirus at 2.9 A resolution. *Science,* 229**,** 1358-1365.

HOLLISTER, J. R., VAGNOZZI, A., KNOWLES, N. J. & RIEDER, E. 2008. Molecular and phylogenetic analyses of bovine rhinovirus type 2 shows it is closely related to foot-and-mouth disease virus. *Virology,* 373**,** 411-425.

HOPE, D. A., DIAMOND, S. E. & KIRKEGAARD, K. 1997. Genetic dissection of interaction between poliovirus 3D polymerase and viral protein 3AB. *Journal of Virology,* 71**,** 9490-9498.

HSU, N.-Y., ILNYTSKA, O., BELOV, G., SANTIANA, M., CHEN, Y.-H., TAKVORIAN, P. M., PAU, C., VAN DER SCHAAR, H., KAUSHIK-BASU, N., BALLA, T., CAMERON, C. E., EHRENFELD, E., VAN KUPPEVELD,

F. J. M. & ALTAN-BONNET, N. 2010. Viral Reorganization of the Secretory Pathway Generates Distinct Organelles for RNA Replication. *Cell,* 141**,** 799-811.

JACKSON, T., ELLARD, F. M., GHAZALEH, R. A., BROOKES, S. M., BLAKEMORE, W. E., CORTEYN, A. H., STUART, D. I., NEWMAN, J. W. & KING, A. M. 1996. Efficient infection of cells in culture by type O foot-and-mouth disease virus requires binding to cell surface heparan sulfate. *Journal of Virology,* 70**,** 5282-5287.

JACKSON, T., MOULD, A. P., SHEPPARD, D. & KING, A. M. Q. 2002. Integrin αβ1 Is a Receptor for Foot-and-Mouth Disease Virus. *Journal of Virology,* 76**,** 935-941.

JACKSON, T., SHEPPARD, D., DENYER, M., BLAKEMORE, W. & KING, A. M. Q. 2000. The Epithelial Integrin αβ6 Is a Receptor for Foot-and-Mouth Disease Virus. *Journal of Virology,* 74**,** 4949-4956.

JAMAL, S. M. & BELSHAM, G. J. 2013. Foot-and-mouth disease: past, present and future. *Veterinary Research,* 44**,** 116-130.

KAFASLA, P., LIN, H., CURRY, S. & JACKSON, R. J. 2011. Activation of picornaviral IRESs by PTB shows differential dependence on each PTB RNA-binding domain. *RNA,* 17**,** 1120-1131.

KAISER, S. E., BRICKNER, J. H., REILEIN, A. R., FENN, T. D., WALTER, P. & BRUNGER, A. T. 2005. Structural basis of FFAT motif-mediated ER targeting. *Structure,* 13**,** 1035-1045.

KAWANO, M., KUMAGAI, K., NISHIJIMA, M. & HANADA, K. 2006. Efficient trafficking of ceramide from the endoplasmic reticulum to the Golgi apparatus requires a VAMP-associated protein-interacting FFAT motif of CERT. *Journal of Biological Chemistry,* 281**,** 30279-30288.

KING, A. M., SANGAR, D. V., HARRIS, T. J. & BROWN, F. 1980. Heterogeneity of the genome-linked protein of foot-and-mouth disease virus. *Journal of Virology,* 34**,** 627-634.

KITCHING, R. P. & HUGHES, G. 2003. *Clinical variation in foot and mouth disease: Sheep and goats.*

KLEIN, M., EGGERS, H. J. & NELSEN-SALZ, B. 1999. Echovirus 9 strain Barty non-structural protein 2C has NTPase activity. *Virus Research,* 65**,** 155-160.

KLIMA, M., CHALUPSKA, D., ROZYCKI, B., HUMPOLICKOVA, J., REZABKOVA, L., SILHAN, J., BAUMLOVA, A., DUBANKOVA, A. & BOURA, E. 2017. Kobuviral Non-structural 3A Proteins Act as Molecular Harnesses to Hijack the Host ACBD3 Protein. *Structure,* 25**,** 219-230.

KNIGHT-JONES, T. J. D. & RUSHTON, J. 2013. The economic impacts of foot and mouth disease – What are they, how big are they and where do they occur? *Preventive Veterinary Medicine,* 112**,** 161-173.

KNOWLES, N. J., DAVIES, P. R., HENRY, T., O'DONNELL, V., PACHECO, J. M. & MASON, P. W. 2001. Emergence in Asia of foot-and-mouth disease viruses with altered host range: characterization of alterations in the 3A protein. *Journal of Virology,* 75**,** 1551-1556.

KNOWLES, N. J. & SAMUEL, A. R. 2003. Molecular epidemiology of foot-and-mouth disease virus. *Virus Research,* 91**,** 65-80.

KNOWLES, N. J., SAMUEL, A. R., DAVIES, P. R., MIDGLEY, R. J. & VALARCHER, J.-F. 2005. Pandemic Strain of Foot-and-Mouth Disease Virus Serotype O. *Emerging Infectious Diseases,* 11**,** 1887-1893.

KONDRATOVA, A. A., NEZNANOV, N., KONDRATOV, R. V. & GUDKOV, A. V. 2005. Poliovirus Protein 3A Binds and Deregulates LIS1, Causing Block of Membrane Protein Trafficking and Deregulation of Cell Division. *Cell Cycle,* 4**,** 1403-1410.

KUKIHARA, H., MORIISHI, K., TAGUWA, S., TANI, H., ABE, T., MORI, Y., SUZUKI, T., FUKUHARA, T., TAKETOMI, A., MAEHARA, Y. & MATSUURA, Y. 2009. Human VAP-C Negatively Regulates Hepatitis C Virus Propagation. *Journal of Virology,* 83**,** 7959-7969.

LAMA, J., SANZ, M. A. & CARRASCO, L. 1998. Genetic analysis of poliovirus protein 3A: characterization of a non-cytopathic mutant virus defective in killing Vero cells. *Journal of General Virology,* 79**,** 1911-1921.

LANKE, K. H. W., VAN DER SCHAAR, H. M., BELOV, G. A., FENG, Q., DUIJSINGS, D., JACKSON, C. L., EHRENFELD, E. & VAN KUPPEVELD, F. J. M. 2009. GBF1, a Guanine Nucleotide Exchange Factor for Arf, Is Crucial for Coxsackievirus B3 RNA Replication. *Journal of Virology,* 83**,** 11940-11949.

LEE, F., JONG, M.-H. & YANG, D.-W. 2006. Presence of antibodies to non-structural proteins of foot-and-mouth disease virus in repeatedly vaccinated cattle. *Veterinary Microbiology,* 115**,** 14-20.

LI, D., LEI, C., XU, Z., YANG, F., LIU, H., ZHU, Z., LI, S., LIU, X., SHU, H. & ZHENG, H. 2016. Foot-and-mouth disease virus non-structural protein 3A inhibits the interferon-beta signaling pathway. *Nature Scientific Reports,* 6**,** e21888.

LIU, Y., FRANCO, D., PAUL, A. V. & WIMMER, E. 2007. Tyrosine 3 of poliovirus terminal peptide VPg(3B) has an essential function in RNA replication in the context of its precursor protein, 3AB. *Journal of Virology,* 81**,** 5669-5684.

LOEWEN, C. J. & LEVINE, T. P. 2005. A highly conserved binding site in vesicle-associated membrane protein-associated protein (VAP) for the FFAT motif of lipid-binding proteins. *Journal of Biological Chemistry,* 280**,** 14097-14104.

LOEWEN, C. J. R., GASPAR, M. L., JESCH, S. A., DELON, C., KTISTAKIS, N. T., HENRY, S. A. & LEVINE, T. P. 2004. Phospholipid Metabolism Regulated by a Transcription Factor Sensing Phosphatidic Acid. *Science,* 304**,** 1644-1647.

LOEWEN, C. J. R., ROY, A. & LEVINE, T. P. 2003. A conserved ER targeting motif in three families of lipid binding proteins and in Opi1p binds VAP. *The EMBO Journal,* 22**,** 2025-2035.

LOGAN, D., ABU-GHAZALEH, R., BLAKEMORE, W., CURRY, S., JACKSON, T., KING, A., LEA, S., LEWIS, R., NEWMAN, J. & PARRY, N. 1993. Structure of a major immunogenic site on foot-and-mouth disease virus. *Nature,* 362**,** 566-568.

MA, X., LI, P., BAI, X., SUN, P., BAO, H., LU, Z., CAO, Y., LI, D., CHEN, Y., QIAO, Z. & LIU, Z. 2014. Sequences outside that of residues 93-102 of 3A protein can contribute to the ability of foot-and-mouth disease virus

(FMDV) to replicate in bovine-derived cells. *Virus Research,* 191**,** 161-171.

MA, X., LI, P., SUN, P., LU, Z., BAO, H., BAI, X., FU, Y., CAO, Y., LI, D., CHEN, Y., QIAO, Z. & LIU, Z. 2016. Genome sequence of foot-and-mouth disease virus outside the 3A region is also responsible for virus replication in bovine cells. *Virus Research,* 220**,** 64-69.

MACLEOD, D. A., RHINN, H., KUWAHARA, T., ZOLIN, A., DI PAOLO, G., MCCABE, B. D., MARDER, K. S., HONIG, L. S., CLARK, L. N., SMALL, S. A. & ABELIOVICH, A. 2013. RAB7L1 interacts with LRRK2 to modify intraneuronal protein sorting and Parkinson's disease risk. *Neuron,* 77**,** 425-439.

MARTIN-ACEBES, M. A., GONZALEZ-MAGALDI, M., ROSAS, M. F., BORREGO, B., BROCCHI, E., ARMAS-PORTELA, R. & SOBRINO, F. 2008. Subcellular distribution of swine vesicular disease virus proteins and alterations induced in infected cells: a comparative study with foot-and-mouth disease virus and vesicular stomatitis virus. *Virology,* 374**,** 432-443.

MASON, P. W., BEZBORODOVA, S. V. & HENRY, T. M. 2002. Identification and Characterization of a cis-Acting Replication Element (cre) Adjacent to the Internal Ribosome Entry Site of Foot-and-Mouth Disease Virus. *Journal of Virology,* 76**,** 9686-9694.

MASON, P. W., GRUBMAN, M. J. & BAXT, B. 2003. Molecular basis of pathogenesis of FMDV. *Virus Research,* 91**,** 9-32.

MASSILAMANY, C., GANGAPLARA, A., BASAVALINGAPPA, R. H., RAJASEKARAN, R. A., VU, H., RIETHOVEN, J.-J., STEFFEN, D., PATTNAIK, A. K. & REDDY, J. 2015. Mutations in the 5' NTR and the Non-Structural Protein 3A of the Coxsackievirus B3 Selectively Attenuate Myocarditogenicity. *PLoS ONE,* 10**,** e0131052.

MCKNIGHT, K. L. & LEMON, S. M. 1998. The rhinovirus type 14 genome contains an internally located RNA structure that is required for viral replication. *RNA,* 4**,** 1569-1584.

MENDELSOHN, C. L., WIMMER, E. & RACANIELLO, V. R. 1989. Cellular receptor for poliovirus: Molecular cloning, nucleotide sequence, and expression of a new member of the immunoglobulin superfamily. *Cell,* 56**,** 855-865.

MENEGHETTI, M. C. Z., HUGHES, A. J., RUDD, T. R., NADER, H. B., POWELL, A. K., YATES, E. A. & LIMA, M. A. 2015. Heparan sulfate and heparin interactions with proteins. *Journal of the Royal Society Interface,* 12**,** 20150589.

MESSACAR, K., ABZUG, M. J. & DOMINGUEZ, S. R. 2016. The Emergence of Enterovirus-D68. *Microbiology Spectrum,* 4**,** EI10-0018.

MIDGLEY, R. 2011. *The Role of the Early Secretory Pathway in Foot-and Mouth Disease Virus Replication.* PhD, Imperial College London.

MIDGLEY, R., MOFFAT, K., BERRYMAN, S., HAWES, P., SIMPSON, J., FULLEN, D., STEPHENS, D. J., BURMAN, A. & JACKSON, T. 2013. A role for endoplasmic reticulum exit sites in foot-and-mouth disease virus infection. *The Journal of General Virology,* 94**,** 2636-2646.

MIKITOVA, V. & LEVINE, T. P. 2012. Analysis of the Key Elements of FFAT-Like Motifs Identifies New Proteins That Potentially Bind VAP on the ER, Including Two AKAPs and FAPP2. *PLoS One,* 7**,** e30455.

MILLER, S. & KRIJNSE-LOCKER, J. 2008. Modification of intracellular membrane structures for virus replication. *Nature Reviews Microbiology,* 6**,** 363-374.

MINSKAIA, E., NICHOLSON, J. & RYAN, M. D. 2013. Optimisation of the foot-and-mouth disease virus 2A co-expression system for biomedical applications. *BMC Biotechnology,* 13**,** 67-67.

MOFFAT, K., HOWELL, G., KNOX, C., BELSHAM, G. J., MONAGHAN, P., RYAN, M. D. & WILEMAN, T. 2005. Effects of foot-and-mouth disease virus nonstructural proteins on the structure and function of the early secretory pathway: 2BC but not 3A blocks endoplasmic reticulum-to-Golgi transport. *Journal of Virology,* 79**,** 4382-4395.

MOFFAT, K., KNOX, C., HOWELL, G., CLARK, S. J., YANG, H., BELSHAM, G. J., RYAN, M. & WILEMAN, T. 2007. Inhibition of the secretory pathway by foot-and-mouth disease virus 2BC protein is reproduced by coexpression of 2B with 2C, and the site of inhibition is determined by the subcellular location of 2C. *Journal of Virology,* 81**,** 1129-1139.

MONAGHAN, P., COOK, H., JACKSON, T., RYAN, M. & WILEMAN, T. 2004. The ultrastructure of the developing replication site in foot-and-mouth disease virus-infected BHK-38 cells. *Journal of General Virology,* 85**,** 933-946.

MOSSESSOVA, E., CORPINA, R. A. & GOLDBERG, J. 2003. Crystal Structure of ARF1•Sec7 Complexed with Brefeldin A and Its Implications for the Guanine Nucleotide Exchange Mechanism. *Molecular Cell,* 12**,** 1403-1411.

MURPHY, S. E. & LEVINE, T. P. 2016. VAP, a Versatile Access Point for the Endoplasmic Reticulum: Review and analysis of FFAT-like motifs in the VAPome. *Biochimica et Biophysica Acta,* 1861**,** 952-961.

MURRAY, K. E. & BARTON, D. J. 2003. Poliovirus CRE-Dependent VPg Uridylylation Is Required for Positive-Strand RNA Synthesis but Not for Negative-Strand RNA Synthesis. *Journal of Virology,* 77**,** 4739-4750.

NACHMIAS, D., SKLAN, E. H., EHRLICH, M. & BACHARACH, E. 2012. Human immunodeficiency virus type 1 envelope proteins traffic toward virion assembly sites via a TBC1D20/Rab1-regulated pathway. *Retrovirology,* 9**,** 7-14.

NAYAK, A., GOODFELLOW, I. G. & BELSHAM, G. J. 2005. Factors Required for the Uridylylation of the Foot-and-Mouth Disease Virus 3B1, 3B2, and 3B3 Peptides by the RNA-Dependent RNA Polymerase (3Dpol) In Vitro. *Journal of Virology,* 79**,** 7698-7706.

NAYAK, A., GOODFELLOW, I. G., WOOLAWAY, K. E., BIRTLEY, J., CURRY, S. & BELSHAM, G. J. 2006. Role of RNA Structure and RNA Binding Activity of Foot-and-Mouth Disease Virus 3C Protein in VPg Uridylylation and Virus Replication. *Journal of Virology,* 80**,** 9865-9875.

NEFF, S., SÁ-CARVALHO, D., RIEDER, E., MASON, P. W., BLYSTONE, S. D., BROWN, E. J. & BAXT, B. 1998. Foot-and-Mouth Disease Virus Virulent

for Cattle Utilizes the Integrin α(v)β(3) as Its Receptor. *Journal of Virology,* 72**,** 3587-3594.

NISHIMURA, A. L., MITNE-NETO, M., SILVA, H. C. A., RICHIERI-COSTA, A., MIDDLETON, S., CASCIO, D., KOK, F., OLIVEIRA, J. R. M., GILLINGWATER, T., WEBB, J., SKEHEL, P. & ZATZ, M. 2004. A Mutation in the Vesicle-Trafficking Protein VAPB Causes Late-Onset Spinal Muscular Atrophy and Amyotrophic Lateral Sclerosis. *American Journal of Human Genetics,* 75**,** 822-831.

NIU, T.-K., PFEIFER, A. C., LIPPINCOTT-SCHWARTZ, J. & JACKSON, C. L. 2005. Dynamics of GBF1, a Brefeldin A-Sensitive Arf1 Exchange Factor at the Golgi. *Molecular Biology of the Cell,* 16**,** 1213-1222.

NUNEZ, J. I., BARANOWSKI, E., MOLINA, N., RUIZ-JARABO, C. M., SANCHEZ, C., DOMINGO, E. & SOBRINO, F. 2001. A single amino acid substitution in nonstructural protein 3A can mediate adaptation of foot-and-mouth disease virus to the guinea pig. *Journal of Virology,* 75**,** 3977-3983.

O'DONNELL, V., LAROCCO, M. & BAXT, B. 2008. Heparan Sulfate-Binding Foot-and-Mouth Disease Virus Enters Cells via Caveola-Mediated Endocytosis. *Journal of Virology,* 82**,** 9075-9085.

O'DONNELL, V., LAROCCO, M., DUQUE, H. & BAXT, B. 2005. Analysis of foot-and-mouth disease virus internalization events in cultured cells. *Journal of Virology,* 79**,** 8506-18.

O'DONNELL, V. K., PACHECO, J. M., HENRY, T. M. & MASON, P. W. 2001. Subcellular distribution of the foot-and-mouth disease virus 3A protein in cells infected with viruses encoding wild-type and bovine-attenuated forms of 3A. *Virology,* 287**,** 151-162.

OH, H. S., PATHAK, H. B., GOODFELLOW, I. G., ARNOLD, J. J. & CAMERON, C. E. 2009. Insight into poliovirus genome replication and encapsidation obtained from studies of 3B-3C cleavage site mutants. *Journal of Virology,* 83**,** 9370-9387.

PACHECO, J. M., GLADUE, D. P., HOLINKA, L. G., ARZT, J., BISHOP, E., SMOLIGA, G., PAUSZEK, S. J., BRACHT, A. J., O'DONNELL, V., FERNANDEZ-SAINZ, I., FLETCHER, P., PICCONE, M. E., RODRIGUEZ, L. L. & BORCA, M. V. 2013. A partial deletion in non-structural protein 3A can attenuate foot-and-mouth disease virus in cattle. *Virology,* 446**,** 260-267.

PACHECO, J. M., HENRY, T. M., O'DONNELL, V. K., GREGORY, J. B. & MASON, P. W. 2003. Role of Nonstructural Proteins 3A and 3B in Host Range and Pathogenicity of Foot-and-Mouth Disease Virus. *Journal of Virology,* 77**,** 13017-13027.

PACHECO, J. M., PICCONE, M. E., RIEDER, E., PAUSZEK, S. J., BORCA, M. V. & RODRIGUEZ, L. L. 2010. Domain disruptions of individual 3B proteins of foot-and-mouth disease virus do not alter growth in cell culture or virulence in cattle. *Virology,* 405**,** 149-156.

PANJWANI, A., STRAUSS, M., GOLD, S., WENHAM, H., JACKSON, T., CHOU, J. J., ROWLANDS, D. J., STONEHOUSE, N. J., HOGLE, J. M. & TUTHILL, T. J. 2014. Capsid Protein VP4 of Human Rhinovirus Induces

Membrane Permeability by the Formation of a Size-Selective Multimeric Pore. *PLoS Pathogens,* 10**,** e1004294.

PARK, J. H., TARK, D., LEE, K. N., LEE, S. Y., KO, M. K., LEE, H. S., KIM, S. M., KO, Y. J., SEO, M. G., CHUN, J. E., LEE, M. H. & KIM, B. 2016. Novel foot-and-mouth disease virus in Korea, July-August 2014. *Clin Exp Vaccine Res,* 5**,** 83-87.

PATEL, M. & COCHI, S. 2017. Addressing the Challenges and Opportunities of the Polio Endgame: Lessons for the Future. *The Journal of Infectious Diseases,* 216**,** S1-S8.

PATHAK, H. B., OH, H. S., GOODFELLOW, I. G., ARNOLD, J. J. & CAMERON, C. E. 2008. Picornavirus genome replication: roles of precursor proteins and rate-limiting steps in oriI-dependent VPg uridylylation. *Journal of Biological Chemistry,* 283**,** 30677-30688.

PAUL, A. V., RIEDER, E., KIM, D. W., VAN BOOM, J. H. & WIMMER, E. 2000. Identification of an RNA Hairpin in Poliovirus RNA That Serves as the Primary Template in the In Vitro Uridylylation of VPg. *Journal of Virology,* 74**,** 10359-10370.

PAUL, A. V. & WIMMER, E. 2015. Initiation of protein-primed picornavirus RNA synthesis. *Virus Research,* 206**,** 12-26.

PERERA, R., DAIJOGO, S., WALTER, B. L., NGUYEN, J. H. C. & SEMLER, B. L. 2007. Cellular Protein Modification by Poliovirus: the Two Faces of Poly(rC)-Binding Protein. *Journal of Virology,* 81**,** 8919-8932.

PERETTI, D., DAHAN, N., SHIMONI, E., HIRSCHBERG, K. & LEV, S. 2008. Coordinated lipid transfer between the endoplasmic reticulum and the Golgi complex requires the VAP proteins and is essential for Golgi-mediated transport. *Molecular Biology of the Cell,* 19**,** 3871-3884.

PFISTER, T., JONES, K. W. & WIMMER, E. 2000. A Cysteine-Rich Motif in Poliovirus Protein 2CATPaseIs Involved in RNA Replication and Binds Zinc In Vitro. *Journal of Virology,* 74**,** 334-343.

PLUTNER, H., COX, A. D., PIND, S., KHOSRAVI-FAR, R., BOURNE, J. R., SCHWANINGER, R., DER, C. J. & BALCH, W. E. 1991. Rab1b regulates vesicular transport between the endoplasmic reticulum and successive Golgi compartments. *The Journal of Cell Biology,* 115**,** 31-43.

PROSSER, D. C., TRAN, D., GOUGEON, P. Y., VERLY, C. & NGSEE, J. K. 2008. FFAT rescues VAPA-mediated inhibition of ER-to-Golgi transport and VAPB-mediated ER aggregation. *Journal of Cell Science,* 121**,** 3052-3061.

RACANIELLO, V. R. 2006. One hundred years of poliovirus pathogenesis. *Virology,* 344**,** 9-16.

REUTER, G., BOROS, Á., KISS, T., DELWART, E. & PANKOVICS, P. 2014. Complete genome characterization of mosavirus (family Picornaviridae) identified in droppings of a European roller (Coracias garrulus) in Hungary. *Archives of Virology,* 159**,** 2723-2729.

REUTER, G., BOROS, Á., TÓTH, Z., GIA PHAN, T., DELWART, E. & PANKOVICS, P. 2015. A highly divergent picornavirus in an amphibian, the smooth newt (Lissotriton vulgaris). *The Journal of General Virology,* 96**,** 2607-2613.

RICHARDS, A. L., SOARES-MARTINS, J. A. P., RIDDELL, G. T. & JACKSON, W. T. 2014. Generation of Unique Poliovirus RNA Replication Organelles. *mBio,* 5**,** e00833-13.

RIEDER, E., BUNCH, T., BROWN, F. & MASON, P. W. 1993. Genetically engineered foot-and-mouth disease viruses with poly(C) tracts of two nucleotides are virulent in mice. *Journal of Virology,* 67**,** 5139-5145.

RODRIGUEZ, L. L. & GAY, C. G. 2011. Development of vaccines toward the global control and eradication of foot-and-mouth disease. *Expert Review of Vaccines,* 10**,** 377-387.

ROMANOVA, L. I., LIDSKY, P. V., KOLESNIKOVA, M. S., FOMINYKH, K. V., GMYL, A. P., SHEVAL, E. V., HATO, S. V., VAN KUPPEVELD, F. J. M. & AGOL, V. I. 2009. Antiapoptotic Activity of the Cardiovirus Leader Protein, a Viral "Security" Protein. *Journal of Virology,* 83**,** 7273-7284.

ROSAS, M. F., VIEIRA, Y. A., POSTIGO, R., MARTIN-ACEBES, M. A., ARMAS-PORTELA, R., MARTINEZ-SALAS, E. & SOBRINO, F. 2008. Susceptibility to viral infection is enhanced by stable expression of 3A or 3AB proteins from foot-and-mouth disease virus. *Virology,* 380**,** 34-45.

ROULIN, PASCAL S., LÖTZERICH, M., TORTA, F., TANNER, LUKAS B., VAN KUPPEVELD, FRANK J. M., WENK, MARKUS R. & GREBER, URS F. 2014. Rhinovirus Uses a Phosphatidylinositol 4-Phosphate/Cholesterol Counter-Current for the Formation of Replication Compartments at the ER-Golgi Interface. *Cell Host & Microbe,* 16**,** 677-690.

ROYSTON, L. & TAPPAREL, C. 2016. Rhinoviruses and Respiratory Enteroviruses: Not as Simple as ABC. *Viruses,* 8.

RYAN, M. D. & DREW, J. 1994. Foot-and-mouth disease virus 2A oligopeptide mediated cleavage of an artificial polyprotein. *The EMBO Journal,* 13**,** 928-933.

SAITA, S., SHIRANE, M., NATUME, T., IEMURA, S. & NAKAYAMA, K. I. 2009. Promotion of neurite extension by protrudin requires its interaction with vesicle-associated membrane protein-associated protein. *Journal of Biological Chemistry,* 284**,** 13766-13777.

SÁIZ, M., GÓMEZ, S., MARTíNEZ-SALAS, E. & SOBRINO, F. 2001. Deletion or substitution of the aphthovirus 3′ NCR abrogates infectivity and virus replication. *Journal of General Virology,* 82**,** 93-101.

SASAKI, J., ISHIKAWA, K., ARITA, M. & TANIGUCHI, K. 2012. ACBD3-mediated recruitment of PI4KB to picornavirus RNA replication sites. *The EMBO Journal,* 31**,** 754-766.

SASAKI, J., NAGASHIMA, S. & TANIGUCHI, K. 2003. Aichi Virus Leader Protein Is Involved in Viral RNA Replication and Encapsidation. *Journal of Virology,* 77**,** 10799-10807.

SEAN, P., NGUYEN, J. H. C. & SEMLER, B. L. 2008. The linker domain of poly(rC) binding protein 2 is a major determinant in poliovirus cap-independent translation. *Virology,* 378**,** 243-253.

SERRANO, P., PULIDO, M. R., SÁIZ, M. & MARTÍNEZ-SALAS, E. 2006. The 3′ end of the foot-and-mouth disease virus genome establishes two distinct long-range RNA–RNA interactions with the 5′ end region. *Journal of General Virology,* 87**,** 3013-3022.

SKEHEL, P. A., FABIAN-FINE, R. & KANDEL, E. R. 2000. Mouse VAP33 is associated with the endoplasmic reticulum and microtubules. *Proceedings of the National Academy of Sciences of the United States of America,* 97**,** 1101-1106.

SKLAN, E. H., SERRANO, R. L., EINAV, S., PFEFFER, S. R., LAMBRIGHT, D. G. & GLENN, J. S. 2007a. TBC1D20 is a Rab1 GTPase-activating protein that mediates hepatitis C virus replication. *Journal of Biological Chemistry,* 282**,** 36354-36361.

SKLAN, E. H., STASCHKE, K., OAKES, T. M., ELAZAR, M., WINTERS, M., AROETI, B., DANIELI, T. & GLENN, J. S. 2007b. A Rab-GAP TBC domain protein binds hepatitis C virus NS5A and mediates viral replication. *Journal of Virology,* 81**,** 11096-11105.

SPANÒ, S., LIU, X. & GALÁN, J. E. 2011. Proteolytic targeting of Rab29 by an effector protein distinguishes the intracellular compartments of human-adapted and broad-host Salmonella. *Proceedings of the National Academy of Sciences of the United States of America,* 108**,** 18418-18423.

SPEAR, A. R., OGRAM, S. A., MORASCO, B. J., SMERAGE, L. E. & FLANEGAN, J. B. 2015. Viral Precursor Protein P3 and its Processed Products Perform Discrete and Essential Functions in the Poliovirus RNA Replication Complex. *Virology,* 485**,** 492-501.

STENMARK, H. 2009. Rab GTPases as coordinators of vesicle traffic. *Nature Reviews Molecular Cell Biology,* 10**,** 513-525.

STRATING, JEROEN R. P. M., VAN DER LINDEN, L., ALBULESCU, L., BIGAY, J., ARITA, M., DELANG, L., LEYSSEN, P., VAN DER SCHAAR, HILDE M., LANKE, KJERSTIN H. W., THIBAUT, HENDRIK J., ULFERTS, R., DRIN, G., SCHLINCK, N., WUBBOLTS, RICHARD W., SEVER, N., HEAD, SARAH A., LIU, JUN O., BEACHY, PHILIP A., DE MATTEIS, MARIA A., SHAIR, MATTHEW D., OLKKONEN, VESA M., NEYTS, J. & VAN KUPPEVELD, FRANK J. M. 2015. Itraconazole Inhibits Enterovirus Replication by Targeting the Oxysterol-Binding Protein. *Cell Reports,* 10**,** 600-615.

SUHY, D. A., GIDDINGS, T. H. & KIRKEGAARD, K. 2000. Remodeling the Endoplasmic Reticulum by Poliovirus Infection and by Individual Viral Proteins: an Autophagy-Like Origin for Virus-Induced Vesicles. *Journal of Virology,* 74**,** 8953-8965.

SUTMOLLER, P., BARTELING, S. S., OLASCOAGA, R. C. & SUMPTION, K. J. 2003. Control and eradication of foot-and-mouth disease. *Virus Research,* 91**,** 101-144.

SWEENEY, T. R., CISNETTO, V., BOSE, D., BAILEY, M., WILSON, J. R., ZHANG, X., BELSHAM, G. J. & CURRY, S. 2010. Foot-and-mouth disease virus 2C is a hexameric AAA+ protein with a coordinated ATP hydrolysis mechanism. *Journal of Biological Chemistry,* 285**,** 24347-24359.

TANG, B. L. 2017. Rabs, Membrane Dynamics, and Parkinson's Disease. *Journal of Cellular Physiology,* 232**,** 1626-1633.

TANG, F., XIA, H., WANG, P., YANG, J., ZHAO, T., ZHANG, Q., HU, Y. & ZHOU, X. 2014. The identification and characterization of nucleic acid

chaperone activity of human enterovirus 71 nonstructural protein 3AB. *Virology,* 464**,** 353-364.

TEN HAVE, S., BOULON, S., AHMAD, Y. & LAMOND, A. I. 2011. Mass spectrometry-based immuno-precipitation proteomics - the user's guide. *Proteomics,* 11**,** 1153-1159.

TETERINA, N. L., GORBALENYA, A. E., EGGER, D., BIENZ, K. & EHRENFELD, E. 1997. Poliovirus 2C protein determinants of membrane binding and rearrangements in mammalian cells. *Journal of Virology,* 71**,** 8962-8972.

TETERINA, N. L., PINTO, Y., WEAVER, J. D., JENSEN, K. S. & EHRENFELD, E. 2011. Analysis of poliovirus protein 3A interactions with viral and cellular proteins in infected cells. *Journal of Virology,* 85**,** 4284-4296.

TILEY, L., KING, A. M. Q. & BELSHAM, G. J. 2003. The Foot-and-Mouth Disease Virus cis-Acting Replication Element (cre) Can Be Complemented in trans within Infected Cells. *Journal of Virology,* 77**,** 2243-2246.

TISDALE, E. J., BOURNE, J. R., KHOSRAVI-FAR, R., DER, C. J. & BALCH, W. E. 1992. GTP-binding mutants of rab1 and rab2 are potent inhibitors of vesicular transport from the endoplasmic reticulum to the Golgi complex. *The Journal of Cell Biology,* 119**,** 749-761.

TOWNER, J. S., MAZANET, M. M. & SEMLER, B. L. 1998. Rescue of Defective Poliovirus RNA Replication by 3AB-Containing Precursor Polyproteins. *Journal of Virology,* 72**,** 7191-7200.

TRINKLE-MULCAHY, L., BOULON, S., LAM, Y. W., URCIA, R., BOISVERT, F. M., VANDERMOERE, F., MORRICE, N. A., SWIFT, S., ROTHBAUER, U., LEONHARDT, H. & LAMOND, A. 2008. Identifying specific protein interaction partners using quantitative mass spectrometry and bead proteomes. *Journal of Cell Biology,* 183**,** 223-239.

TULLOCH, F., PATHANIA, U., LUKE, G. A., NICHOLSON, J., STONEHOUSE, N. J., ROWLANDS, D. J., JACKSON, T., TUTHILL, T., HAAS, J., LAMOND, A. I. & RYAN, M. D. 2014. FMDV replicons encoding green fluorescent protein are replication competent. *Journal of Virological Methods,* 209**,** 35-40.

VAN DER SCHAAR, H. M., VAN DER LINDEN, L., LANKE, K. H. W., STRATING, J. R. P. M., PÜRSTINGER, G., DE VRIES, E., DE HAAN, C. A. M., NEYTS, J. & VAN KUPPEVELD, F. J. M. 2012. Coxsackievirus mutants that can bypass host factor PI4KIIIβ and the need for high levels of PI4P lipids for replication. *Cell Research,* 22**,** 1576-1592.

VIKTOROVA, E. G., NCHOUTMBOUBE, J., FORD-SILTZ, L. A. & BELOV, G. A. 2015. Cell-specific establishment of poliovirus resistance to an inhibitor targeting a cellular protein. *Journal of Virology,* 89**,** 4372-4386.

WANG, J., DU, J., WU, Z. & JIN, Q. 2013. Quinacrine Impairs Enterovirus 71 RNA Replication by Preventing Binding of Polypyrimidine-Tract Binding Protein with Internal Ribosome Entry Sites. *PLoS One,* 8**,** e52954.

WANG, S., MA, Z., XU, X., WANG, Z., SUN, L., ZHOU, Y., LIN, X., HONG, W. & WANG, T. 2014. A role of Rab29 in the integrity of the trans-Golgi network and retrograde trafficking of mannose-6-phosphate receptor. *PLoS One,* 9**,** e96242.

WASMEIER, C., ROMAO, M., PLOWRIGHT, L., BENNETT, D. C., RAPOSO, G. & SEABRA, M. C. 2006. Rab38 and Rab32 control post-Golgi trafficking of melanogenic enzymes. *The Journal of Cell Biology,* 175**,** 271-281.

WESSELS, E., DUIJSINGS, D., NIU, T.-K., NEUMANN, S., OORSCHOT, V. M., DE LANGE, F., LANKE, K. H. W., KLUMPERMAN, J., HENKE, A., JACKSON, C. L., MELCHERS, W. J. G. & VAN KUPPEVELD, F. J. M. 2006. A Viral Protein that Blocks Arf1-Mediated COP-I Assembly by Inhibiting the Guanine Nucleotide Exchange Factor GBF1. *Developmental Cell,* 11**,** 191-201.

WUTZ, G., AUER, H., NOWOTNY, N., GROSSE, B., SKERN, T. & KUECHLER, E. 1996. Equine rhinovirus serotypes 1 and 2: relationship to each other and to aphthoviruses and cardioviruses. *Journal of General Virology,* 77**,** 1719-1730.

WYLES, J. P. & RIDGWAY, N. D. 2004. VAMP-associated protein-A regulates partitioning of oxysterol-binding protein-related protein-9 between the endoplasmic reticulum and Golgi apparatus. *Exp Cell Res,* 297**,** 533-547.

XIA, H., WANG, P., WANG, G.-C., YANG, J., SUN, X., WU, W., QIU, Y., SHU, T., ZHAO, X., YIN, L., QIN, C.-F., HU, Y. & ZHOU, X. 2015. Human Enterovirus Nonstructural Protein 2C(ATPase) Functions as Both an RNA Helicase and ATP-Independent RNA Chaperone. *PLoS Pathogens,* 11**,** e1005067.

XU, G., XIN, X. & ZHENG, C. 2013. GPS2 is required for the association of NS5A with VAP-A and hepatitis C virus replication. *PLoS One,* 8**,** e78195.

YUAN, T., WANG, H., LI, C., YANG, D., ZHOU, G. & YU, L. 2017. T135I substitution in the nonstructural protein 2C enhances foot-and-mouth disease virus replication. *Virus Genes***,** 840-847.

ZELL, R., DELWART, E., GORBALENYA, A. E., HOVI, T., KING, A. M. Q., KNOWLES, N. J., LINDBERG, A. M., PALLANSCH, M. A., PALMENBERG, A. C., REUTER, G., SIMMONDS, P., SKERN, T., STANWAY, G., YAMASHITA, T. & CONSORTIUM, I. R. 2017. ICTV Virus Taxonomy Profile: Picornaviridae. *Journal of General Virology***,** 2421-2422.

ZHOU, Z., MOGENSEN, M. M., POWELL, P. P., CURRY, S. & WILEMAN, T. 2013. Foot-and-Mouth Disease Virus 3C Protease Induces Fragmentation of the Golgi Compartment and Blocks Intra-Golgi Transport. *Journal of Virology,* 87**,** 11721-11729.

ZIBERT, A., MAASS, G., STREBEL, K., FALK, M. M. & BECK, E. 1990. Infectious foot-and-mouth disease virus derived from a cloned full-length cDNA. *Journal of Virology,* 64**,** 2467-2473.

Appendix

A1 Primers used for construction of Fusion Proteins and PCR products for use in TnT reactions

Primer Name	Sequence 5' to 3'	Description
TnTFor	TAATATTAATACGACTCACTATAGG GATATGCCGCCACCATGATCTCAA TTCCTTCTCA	Forward primer used to produce PCR product for use in TnT reaction Including T7 promoter (red), Kozak sequence (yellow) and methionine start codon (Green)
TnTΔ3C Rev	TTTTTTTTTTTTTTTTTTTTTTTCATTAG TGGAGCACCATGAGCGC	Reverse primer used to produce PCR product for TnTs where 3C was truncated upstream of active site
N1-3A F	AGCGAGCTCGCCACCATGGGTATC TCAATTCCTTCTCAAAAATCT	Forward primer to amplify 3A or 3ABBB regions to create fusion proteins
N1-3A R	ATGACCGGTCCTTCAGCTTGTGGT TGCTCCTC	Reverse primer to amplify 3A region to create fusion proteins
N1-3AB R	ATGACCGGTCCCTCAGTGACAATC AGGTTCTTAGC	Reverse primer to amplify 3ABBB region to create fusion proteins

Table A1 Primers used in this study: PCR primers used to amplify the 3A to mid 3C region for use in TnT coupled reactions are shown. The forward primer incorporated a T7 promoter, Kozak sequence and start codon upstream of 3A sequence. Primers used to amplify 3A or 3ABBB regions from O1K FMDV to allow cloning into the pEGFP-N1 vector to create fusion proteins are also shown.

A2 Complete sequences of Donor Cassettes:

3A only possible donor →3A, 3B1, 3B2, 3B3, 1-6(3C)-2A // Proline -last 6 aa 3B3, 3C
490nt

3A (XbaI)
```
T CTA GAG ACC AGC GGC GCC AGC ACC GTT GGC TTT AGA GAG AGA ACT CTC CCA GGT CAA
  L   E   T   S   G   A   S   T   V   G   F   R   E   R   T   L   P   G   Q

AAG GCA TGC GAT GAC GTG AAC TCC GAG CCT GCC CAA CCT GTT GAG GAG CAA CCA CAA
 K   A   C   D   D   V   N   S   E   P   A   Q   P   V   E   E   Q   P   Q
```

              3B1
```
GCT GAA GGA CCC TAC GCC GGA CCA CTC GAG CGT CAG AAA CCT CTG AAA GTG AGA GCC
 A   E   G   P   Y   A   G   P   L   E   R   Q   K   P   L   K   V   R   A
```

                      3B2
```
AAG CTC CCA CAG CAG GAG GGG CCT TAC GCT GGT CCG ATG GAG AGA CAA AAA CCG CTA
 K   L   P   Q   Q   E   G   P   Y   A   G   P   M   E   R   Q   K   P   L
```

                              3B3
```
AAA GTG AAA GCA AAA GCC CCG GTC GTG AAG GAA GGA CCT TAC GAG GGA CCG GTG AAG
 K   V   K   A   K   A   P   V   V   K   E   G   P   Y   E   G   P   V   K
```

                                          aa 1-6 3C
```
AAG CCT GTC GCT TTG AAA GTG AAA GCT AAG AAC CTG ATT GTC ACT GAG AGC GGA GCC
 K   P   V   A   L   K   V   K   A   K   N   L   I   V   T   E   S   G   A
```

              2A TaV
```
CCG CCC ACC GAG GGC AGG GGA AGT CTT CTA ACA TGC GGG GAC GTG GAG GAA AAT CCC
 P   P   T   E   G   R   G   S   L   L   T   C   G   D   V   E   E   N   P
```

              PRO   last 6 aa 3B3   3C
```
GGG CCC AAC CTC ATT GTT ACC GAG AGT GGT GCC CCA CCG ACC GAC TTG CAA AAG ATG
 G   P   N   L   I   V   T   E   S   G   A   P   P   T   D   L   Q   K   M
```

                                  SacI
```
GTC ATG GGC AAC ACA AAG CCT GTT GAG CTC
 V   M   G   N   T   K   P   V   E   L
```

3C is the only possible donor

3A, aa 1-6 3B1 with Y3F sub-2A // Proline -last 6 aa of 3A, 3B1, 3B2, 3B3, 3C
490nt

```
T CTA GAG ACC AGC GGC GCC AGC ACC GTT GGC TTT AGA GAG AGA ACT CTC CCA GGT CAA
  L   E   T   S   G   A   S   T   V   G   F   R   E   R   T   L   P   G   Q

AAG GCA TGC GAT GAC GTG AAC TCC GAG CCT GCC CAA CCT GTT GAG GAG CAA CCA CAA
 K   A   C   D   D   V   N   S   E   P   A   Q   P   V   E   E   Q   P   Q

GCT GAA GGA CCA TTT GCC GGC CCA GAG GGC AGG GGA AGT CTT CTA ACA TGC GGG GAC
 A   E   G   P   F   A   G   P   E   G   R   G   S   L   L   T   C   G   D

GTG GAG GAA AAT CCC GGG CCC GAA CAA CCT CAA GCA GAA GGA CCC TAC GCC GGA CCA
 V   E   E   N   P   G   P   E   Q   P   Q   A   E   G   P   Y   A   G   P

CTC GAG CGT CAG AAA CCT CTG AAA GTG AGA GCC AAG CTC CCA CAG CAG GAG GGG CCT
 L   E   R   Q   K   P   L   K   V   R   A   K   L   P   Q   Q   E   G   P

TAC GCT GGT CCG ATG GAG AGA CAA AAA CCG CTA AAA GTG AAA GCA AAA GCC CCG GTC
 Y   A   G   P   M   E   R   Q   K   P   L   K   V   K   A   K   A   P   V

GTG AAG GAA GGA CCT TAC GAG GGA CCG GTG AAG AAG CCT GTC GCT TTG AAA GTG AAA
 V   K   E   G   P   Y   E   G   P   V   K   K   P   V   A   L   K   V   K

GCT AAG AAC CTG ATT GTC ACT GAG AGT GGT GCC CCA CCG ACC GAC TTG CAA AAG ATG
 A   K   N   L   I   V   T   E   S   G   A   P   P   T   D   L   Q   K   M

GTC ATG GGC AAC ACA AAG CCT GTT GAG CTC
 V   M   G   N   T   K   P   V   E   L
```

3B ONLY EVER "FREE" **no donor**

3A, aa 1-6 3B1 with Y3F sub-2A // Proline -last 6 aa of 3A, 3B1, 3B2, 3B3, 1-6(3C)-2A // 2A-last 6 aa 3B3, 3C

580nt

T CTA GAG ACC AGC GGC GCC AGC ACC GTT GGC TTT AGA GAG AGA ACT CTC CCA GGT CAA
  L   E   T   S   G   A   S   T   V   G   F   R   E   R   T   L   P   G   Q

AAG GCA TGC GAT GAC GTG AAC TCC GAG CCT GCC CAA CCT GTT GAG GAG CAA CCA CAA
  K   A   C   D   D   V   N   S   E   P   A   Q   P   V   E   E   Q   P   Q

GCT GAA GGA CC**A** TTT GCC GG**C** CCA GAG GGC AGG GGA AGT CTT CTA ACA TGC GGG GAC
  A   E   G   P   F   A   G   P   E   G   R   G   S   L   L   T   C   G   D

GTG GAG GAA AAT CCC GGG CCC GA**A** CAA CC**T** CAA GC**A** GAA GGA CCC TAC GCC GGA CCA
  V   E   E   N   P   G   P   E   Q   P   Q   A   E   G   P   Y   A   G   P

CTC GAG CGT CAG AAA CCT CTG AAA GTG AGA GCC AAG CTC CCA CAG CAG GAG GGG CCT
  L   E   R   Q   K   P   L   K   V   R   A   K   L   P   Q   Q   E   G   P

TAC GCT GGT CCG ATG GAG AGA CAA AAA CCG CTA AAA GTG AAA GCA AAA GCC CCG GTC
  Y   A   G   P   M   E   R   Q   K   P   L   K   V   K   A   K   A   P   V

GTG AAG GAA GGA CCT TAC GAG GGA CCG GTG AAG AAG CCT GTC GCT TTG AAA GTG AAA
  V   K   E   G   P   Y   E   G   P   V   K   K   P   V   A   L   K   V   K

GCT AAG AAC CTG ATT GTC ACT GAG AG**C** GG**A** GCC CC**G** CC**A** ACC GAG GG**A** AGG GG**C** AGT
  A   K   N   L   I   V   T   E   S   G   A   P   P   T   E   G   R   S

CT**A** CT**T** ACA TGC GG**A** GAC GT**T** GAG GA**G** AAT CC**A** GGG CCC AAC CT**C** ATT GT**T** AC**C** GAG
  L   L   T   C   G   D   V   E   E   N   P   G   P   N   L   I   V   T   E

AGT GGT GCC CCA CCG ACC GAC TTG CAA AAG ATG GTC ATG GGC AAC ACA AAG CCT GTT
  S   G   A   P   P   T   D   L   Q   K   M   V   M   G   N   T   K   P   V

GAG CTC
  E   L